AUBURN

SAMUEL GINN
COLLEGE OF ENGINEERING

Final Report

HURRICANE SURGE/SURFACE WAVE FORCES ON DECK-GIRDER BRIDGES AND DESIGN/RETROFIT OPTIONS FOR THESE BRIDGES

Submitted to

Alabama Department of Transportation
Research Project 930-687

Prepared by

G. Ed Ramey
Alvin Sawyer, III
Joel G. Melville

April 2008

Highway Research Center

Final Report

on

Alabama Department of Transportation
Research Project 930-687

HURRICANE SURGE/SURFACE WAVE FORCES ON DECK-GIRDER BRIDGES AND DESIGN/RETROFIT OPTIONS FOR THESE BRIDGES

Prepared by

G. Ed Ramey
Alvin Sawyer, III
Joel G. Melville

Highway Research Center
and
Department of Civil Engineering
at
Auburn University

April 2008

TABLE OF CONTENTS

ABSTRACT

An increasingly common occurrence when strong hurricanes come ashore along the Gulf of Mexico is that the hurricane surge/surface waves lift and push the superstructures of coastline bridges from their support bents into the water. It appears that the superstructures of many of these coastal bridges are not positively connected, or only minimally connected, to the supporting pile bent caps. This lack of adequate connection may be due to anticipation that the hurricane surge/surface waves will not reach the elevation of the superstructure, or it may be that the anticipated surge/surface wave forces are considered to be too great to economically design to resist. However, based on the performances of some closely adjacent bridges across Lake Pontchartrain when Hurricane Katrina came ashore in August 2005, it appears that it should be very feasible to connect new bridge components, or to take retrofit action for existing bridges, in a manner to avoid having hurricane surge/surfaces waves dump the bridge superstructure into the water.

Determining what is the appropriate design hurricane sea state at the I-10 bridges across the north end of Mobile Bay and the surge/surface wave forces that this sea state would apply to the bridge superstructure and substructure was the purpose of this research. The investigation was limited to a review of the literature, discussions with state DOT bridge engineers and discussions with coastal engineering experts to determine the mode and sequence of failure of coastal bridges as hurricane surge/surface waves pass through these bridges. Using these same sources of information, a design hurricane sea state and its associated design storm surge/surface wave forces were estimated for the I-10 bridges. An analytical assessment of the

adequacy of the as-is I-10 Mobile Bay bridge as well as an appropriately retrofitted I-10 bridge for the estimated design hurricane passing directly through the bridge was performed. Conclusions and recommendation resulting from the analyses and assessment are presented.

ACKNOWLEDGEMENTS

I. INTRODUCTION

1.1 Statement of Problem

An increasingly common occurrence when strong hurricanes come ashore along the Gulf of Mexico is that the hurricane surge/surface waves lift and push the superstructures of coastline bridges from their support bents into the water as shown in Figs. 1.1 and 1.2. It appears that the superstructures of many of these coastal bridges are not positively connected, or only minimally connected, to the supporting pile bent caps. This lack of adequate connection may be due to probability-based anticipation that the hurricane surge/surface waves will not reach the elevation of the superstructure, or it may be that the anticipated surge/surface wave forces are considered to be too great to economically design to resist. Some recent discussions seem to indicate that the latter may be the case. However, based on the performances of some closely adjacent bridges across Lake Pontchartrain when Hurricane Katrina came ashore in August 2005, it appears that it should be very feasible to connect new bridge components, or to take retrofit action for existing bridges in a manner to avoid having hurricane surge/surfaces waves dump the bridge superstructure into the water. Exploring these actions in greater detail was the impetus and purpose of this research.
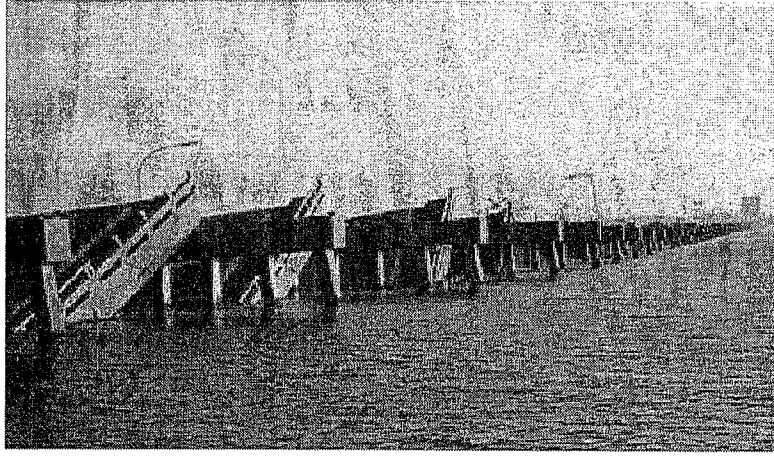
Figure 1.1 Looking west toward Biloxi from the east shore, many superstructure spans of US-90 Biloxi-Ocean Springs bridge were displaced north off their piers (photo credit: J. O'Connor, MCEER) [8].
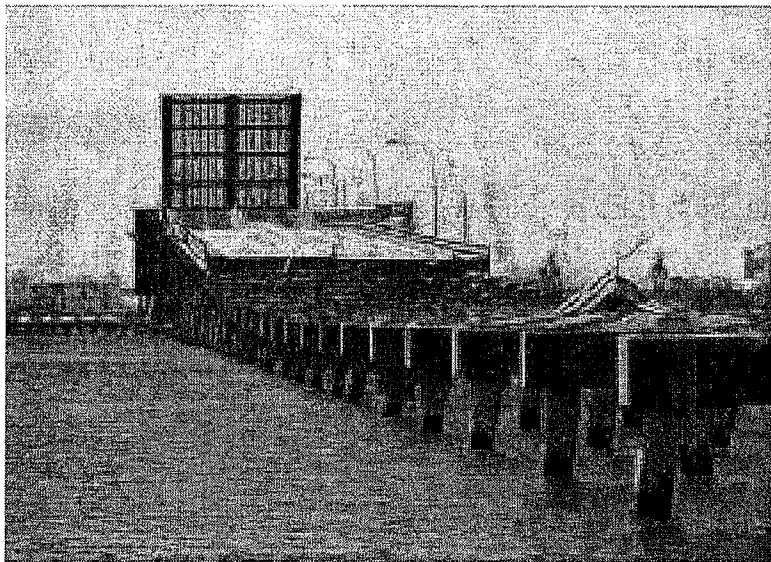
Figure 1.2 Looking west toward Biloxi, spans above the surge line near the navigation channel survived, but the superstructure in the foreground was dropped off the piers (photo credit: J. O'Connor, MCEER) [8].

1.2   Research Objectives

Determining what are the hurricane surge wave forces that coastal bridge superstructures and substructures need to be designed for, or retrofit for, to prevent them from being dumped in the water when hit by a hurricane; and to determine the behavior and performance of ALDOT's I-10 bridges across Mobile Bay if so retrofitted are the objectives of this research. More specifically, the objectives of this research are as follows:

1. Identify and quantify the primary hurricane surge/surface wave-induced forces on coastal deck-girder bridge superstructures and substructures.

2. Identify appropriate bridge venting actions to take on retrofitting existing bridges to minimize hurricane induced surge/surface wave buoyant forces on bridge superstructures and substructures.

3. Identify and develop appropriate existing bridge retrofit systems to adequately connect bridge super-and sub-structures to resist hurricane surge/surface wave forces.

4. Determine the behavior and performances of coastal deck-girder bridge superstructures supported on single-row pile bent substructures, i.e., I-10 bridges, retrofitted as indicated in (3) above, as hurricane surge/surface waves pass through the bridges.

1.3   Work Plan

A brief work plan to accomplish the research objectives is given below.

1. Locate and study video documentation of hurricane surge waves approaching, inundating, and displacing coastal bridge superstructures. Questions that such videos would help answer are:

   - What is the approximate rate of water elevation rise on the bridges?

- What is the feasibility of venting bridge superstructures to avoid the enlarged buoyant force due to entrapped air between the girders and underside of the deck, and above the deck for bridges with solid guard rails?

- What are the differences in performances of bridges with solid and open guard rails?

- When does the superstructure begin to lift off of the bent caps?

- What is the likelihood that hydrodynamic water forces are significant contributors to moving the bridge superstructure?

2. Study the literature on water wave forces on fixed and water-surrounded structures and determine what wave actions and forces are applicable for cases of hurricane surge/surface waves passing through coastline bridges. Then, quantify these wave forces on the superstructures of deck-girder bridges for various surge/surface wave heights, surface wave breaking conditions, bridge heights, and depth-of-water conditions.

3. Secure and analyze hurricane surge wave historical data from the National Hurricane Center and from ALDOT'S 9th Division to ascertain hurricane surge wave heights along the Alabama coast and anticipated worst case hurricane surge wave scenarios for Alabama.

4. Secure and study superstructure drawings of I-10 and US-11 bridges over Lake Pontchartrain and the I-10 bridge ramp across Mobile Bay to better compare the designs, connection details, and performances of these bridges as Hurricane Katrina came ashore.

5. Identify appropriate new bridge design connections between the bridge superstructure and pile bent/cap substructure.

6. Identify appropriate retrofit actions to take to vent existing bridge superstructure decks and solid guard rails in order that the surge wave buoyant forces on the bridge superstructure would be minimized.

7. Identify appropriate retrofit systems for existing coastal deck-girder bridges to adequately connect the bridge super-and substructures to resist the anticipated maximum hurricane surge wave forces.

8. Determine the behavior and performance of the I-10 deck-girder bridge across Mobile Bay retrofitted as indicated in (6) and (7) above, as a major hurricane surge/surface wave passes through the bridge.

9. Prepare final report.

1.4   Scope of Work

This investigation was limited to a review of the literature, discussions with state DOT bridge engineers, discussions with coastal engineering researchers, etc. to determine the state of the art procedures for determining the magnitudes of hurricane surge/surface wave forces on coastal bridges and appropriate design actions to mitigate and/or sustain these forces. Qualitative analyses were performed to identify the primary hurricane surge/surface wave forces acting on coastal bridge superstructures and these were followed by quantitative analyses to determine the magnitudes of the primary surge/surface wave forces. Bridge superstructure venting to reduce the wave forces as well as bridge component connectivity to sustain the forces were investigated.

An analytical assessment of the adequacy of the as-is I-10 bridge across Mobile Bay as well as an appropriately retrofitted I-10 bridge for a projected major hurricane passing directly through the bridge were performed. No laboratory or field structural testing or wave basin testing were performed in the investigation to verify or refute the results of the analytical analyses.

2. BACKGROUND AND LITERATURE REVIEW

2.1   Background

As indicated in Section 1.1, an increasingly common problem as strong hurricanes come ashore along the Gulf of Mexico coastline is for the hurricane storm surge and surface waves to lift and push the superstructures of coastal bridges into the water. On many of these bridges a positive connection of the superstructure to the substructure is nonexistent or only minimal, and in many cases this is by design because it is felt that the wave induced forces are too great to resist. However, the performances of some closely adjacent bridges across Lake Pontchartrain in Louisiana when Hurricane Katrina came ashore in August 2005 were documented in Reference [8] and this documentation seems to refute the idea that hurricane storm surge/surface wave forces are too large to resist. Figure 2.1 and 2.2 shows three closely positioned and aligned bridges (I-10 Twin Bridges, US-11 Bridge, Norfolk Southern Railroad Bridge) across the eastern end of Lake Pontchartrain in New Orleans, LA. The following description and performance of each of these bridges, as well as the Lake Pontchartrain Causeway bridge ramp during Hurricane Katrina was extracted from Reference [8].

> **I-10 twin span bridges.** The I-10 twin span bridges (two separate bridges, nominally eastbound and westbound) over Lake Pontchartrain connect New Orleans and Slidell, Louisiana to the north. Each bridge is two lanes wide and 5.4 miles long. According to the Louisiana Department of Transportation and Development (LA DOTD), the deck level stands at 14 feet above mean sea level. The bridges were built in the early 1960's using prefabricated construction. The superstructure is comprised of 65-foot-long prestressed concrete spans weighing
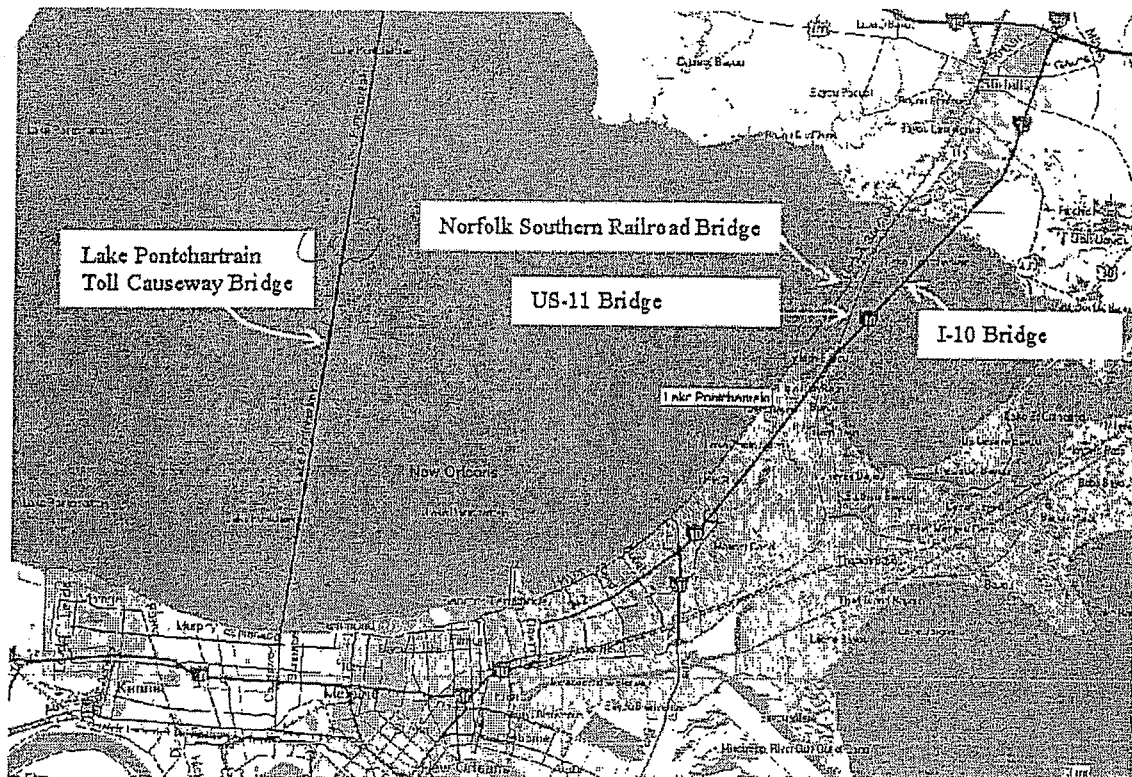
Fig. 2.1 Major bridges over Lake Pontchartrain in Louisiana [8].
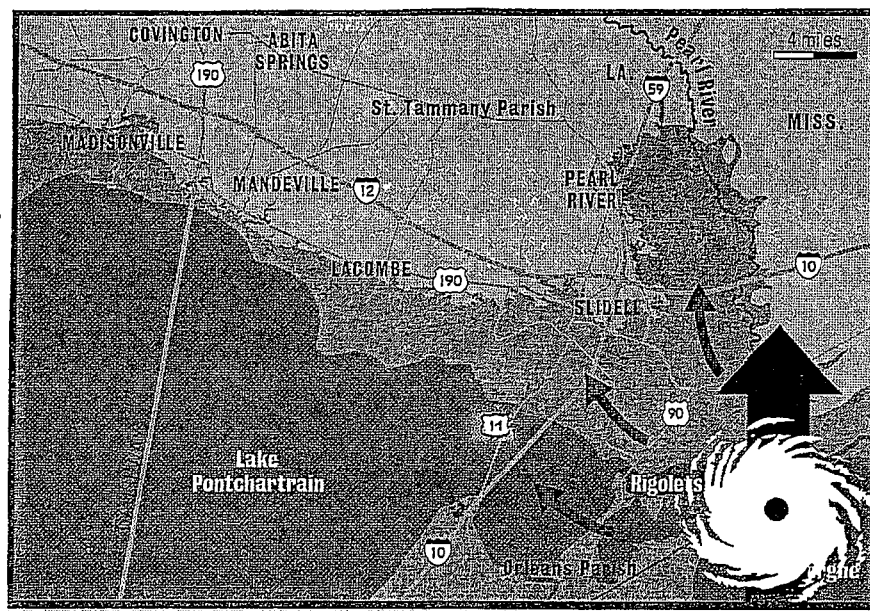
Fig. 2.2 Katrina makes landfall near Slidell, LA – storm surge is 15 feet at the Lake Pontchartrain north shoreline [8].

approximately 285 tons each. Each superstructure span is a monolithically cast concrete system comprising a concrete deck, fascia section (safety walk curbs with vertical solid parapet), and six concrete girders with I-cross section. The span was cast at a factory offsite and transported by barge for erection on the piers. Each span was simply supported and seated on the piers through steel bearing plates that provide little restraint against lateral displacement. The steel bearing plates were bolted into the cap beam of the pier on top of low risers (or pedestals). This connection design facilitates easy replacement of the superstructure spans but provides no provision for restraint against uplift (aside from the span dead weight) or lateral displacement.

The I-10 twin span bridges sustained extensive damage, primarily due to high storm surges and associated surface wave forces caused by Hurricane Katrina. Surge/surface wave forces (lateral and uplift forces), combined with the lack of restraint against uplift and lateral displacement of the superstructure spans, caused many spans of both the eastbound and westbound bridges to be uplifted and displaced laterally in a southerly direction. According to a damage summary by the LA DOTD, a total of 38 eastbound spans and 26 westbound spans were displaced and dropped completely into the water. In addition, 170 eastbound spans and 303 westbound spans were shifted out of alignment. In most cases, the misaligned superstructure spans displaced less than 5 feet in the transverse direction (one riser spacing) due to the fascia girder making contact with the adjacent riser. Wave forces also broke more than 14,000 ft of the concrete

railings along the base of the curb line, leaving them dangling and connected to the bridge deck only by the reinforcing bars. Surge damage to the superstructures of the I-10 bridges established the surge height at this location to be at least 14 feet. Figure 2.3 shows a view looking north of the westbound I-10 bridge with missing spans and broken curb rails.
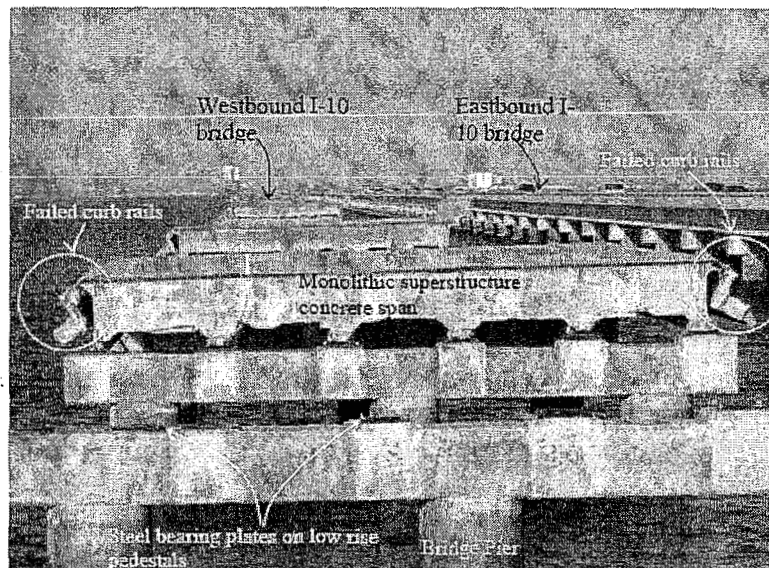
Fig. 2.3   View looking north from west abutment of I-10 twin span bridges over Lake Pontchartrain (photo credit: NIST) [8].

US-11 bridge. The two-lane US-11 bridge is just to the west of the I-10 bridges (see Figure 2.1), and carries vehicular traffic of US-11 between Slidell and New Orleans over Lake Pontchartrain. Its superstructure is a series of reinforced concrete girders (three per span) with a concrete deck. The bridge deck, girders, and piers were cast in place and the connections between the girders and the bridge piers were monolithic, thus providing positive connection between the bridge superstructure and the supporting piers. According to the bridge tender, a new concrete deck was cast over the length of the bridge in 2001. This provides continuity between the individual spans and likely contributed to the good performance of the bridge. The deck level of this bridge stands at 11 feet above mean sea level.

Despite being 3 feet lower in elevation compared with the adjacent I-10 twin span bridges, and thus likely subjected to the same surge and wave actions from Hurricane Katrina that affected the twin span bridges due to their close proximity, the US-11 bridge sustained very minor damage. The damage was nonstructural and was limited to a few sections of the concrete bridge rails and the approach guard rail from the west side shore being torn off by surge-induced wave forces, and the bascule lift span (drawbridge) was damaged by flooding and rendered inoperable. The extent of damage to the bridge rails of this bridge was also much more limited compared to damage to the bridge curb rails of the I-10 twin span bridge. This is likely due to the difference in the construction of the curb rails. The I-10 bridges have solid parapet curb rails which resulted in larger wave

forces due to the larger surface, while the US-11 bridge has open-face curb rails with less surface area and smaller wave forces.

Unlike the twin span bridges, none of the superstructure spans of the US-11 bridge was lost or misaligned during Hurricane Katrina. This can likely be attributed to the fact that the superstructure is continuous and positively connected to the supporting piers through cast-in-place construction methods. Figure 2.4 shows a view looking north along the intact US-11 bridge.

Norfolk Southern Railroad bridge. The Norfolk Southern railroad bridge is a 5.8-mile long concrete bridge that is also in close proximity to the US-11 bridge and the I-10 twin span bridges (see Figure 2.1). Thus, it was likely subjected to the same surge and wave actions that affected the I-10 and US-11 bridges. The bridge's superstructure consists of a concrete deck supported by pre-stressed concrete box girders. The superstructure is supported by concrete piers with shear block detailing at each end to provide restraint against lateral displacement (see Figure 2.5). This restraint probably contributed substantially to its successful performance during Hurricane Katrina. Surge-induced wave forces swept the railroad tracks and ties off the structure, but the bridge itself sustained no structural damage and was able to be returned to service just a few weeks after the storm.

Also extracted from Reference [8] and presented below is a report on the performance of the Lake Pontchartrain Toll Causeway Bridge (see Fig. 2.1) during Hurricane Katrina.
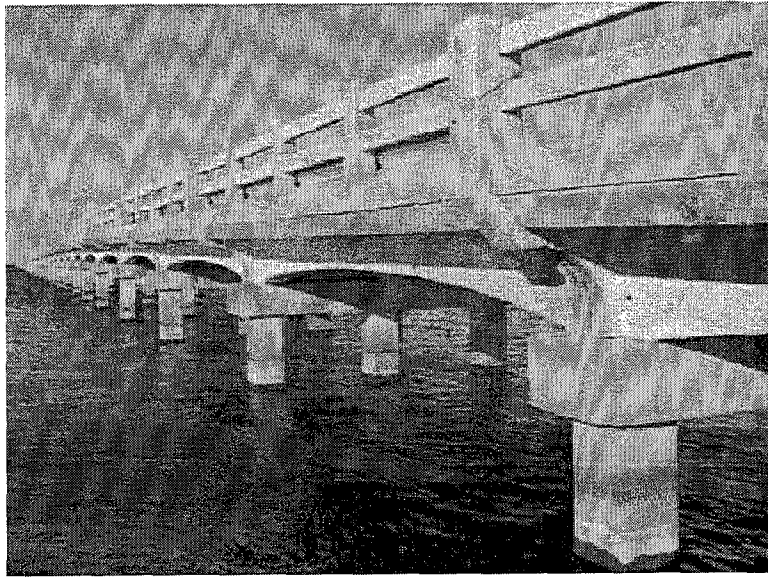
Figure 2.4   Cast-in-place concrete bridge carries the traffic of US-11 over Lake Pontchartrain (photo credit: J. O'Connor, MCEER) [8].
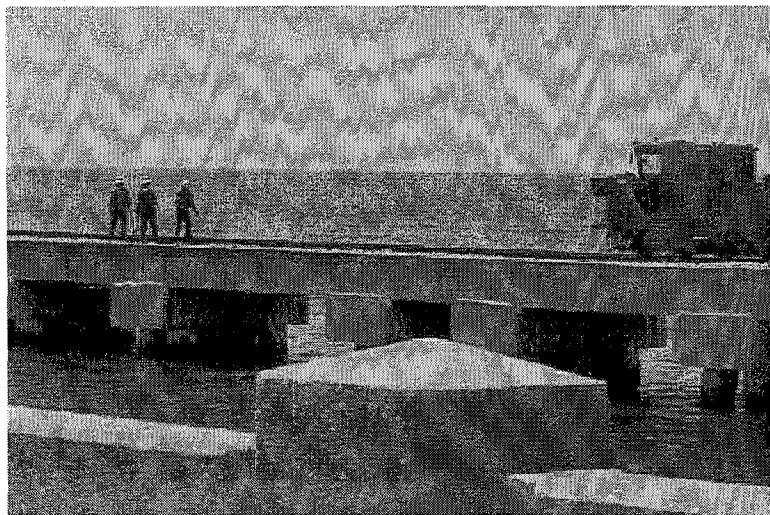
Figure 2.5   The Norfolk Southern Railroad bridge over Lake Pontchartrain had its tracks stripped from the superstructure but otherwise remained intact (photo credit: J. O'Connor, MCEER) [8].

Lake Pontchartrain Toll Causeway. The Toll Causeway is a 24-mile long concrete bridge that runs across the middle of Lake Pontchartrain in a north-south direction and carries vehicular traffic into the City of New Orleans from the areas north of the lake. Similar to the I-10 twin span bridges, the Toll Causeway is comprised of two separate bridges, each carrying one-way traffic. In addition, there are turn-around ramps, which are separate bridges (supported by a separate set of piers) that run between the two main bridges to allow traffic to change direction midway on the bridge. The deck surfaces of the main bridges stand at 20 feet above mean sea level, making them the tallest bridges over Lake Pontchartrain. The superstructures are comprised of simply supported concrete spans. Similar to the I-10 twin bridges, each span was monolithically cast in a factory offsite. Each is comprised of a concrete deck, fascia section, and I-section concrete girders. Each span was connected to the piers by steel bearing plates, which provide only restraint against displacement in the longitudinal direction, not in the lateral or vertical directions. The steel bearing plates were bolted into the concrete piers. The superstructure of the turn-around ramp was similarly constructed and supported, but has progressively lower elevation, with the lowest span being only a few feet above mean sea level.

Due to their high elevation (20 feet) and the observed surge height at their location (about 9 feet), the superstructures of the main Toll Causeway bridges were not subjected to surge-induced wave actions and sustained no damage. However, several superstructure spans of the turn-around ramps, being at lower

elevation and not restrained against lateral and uplift displacements, were subjected to the lateral and uplift wave forces and were either dropped into the lake or misaligned. As in the cases of the other bridges over Lake Pontchartrain, the substructures of the Toll Causeway bridges sustained no damage. Figures 2.6 and 2.7 show the turn-around ramp with missing and misaligned superstructure spans.

In summary, the above discussions and figures/photographs document that the best solution to avoiding lost of coastal bridges from hurricane surge wave forces is to elevate them sufficiently to allow the surge/surface wave to pass under the bridge superstructure. However, if this is too costly and/or the bridge is already in existence, it appears that it should be very feasible to connect the bridge components in a manner, or to take retrofit action, to avoid having the hurricane surge/surface wave dump the superstructure into the water.
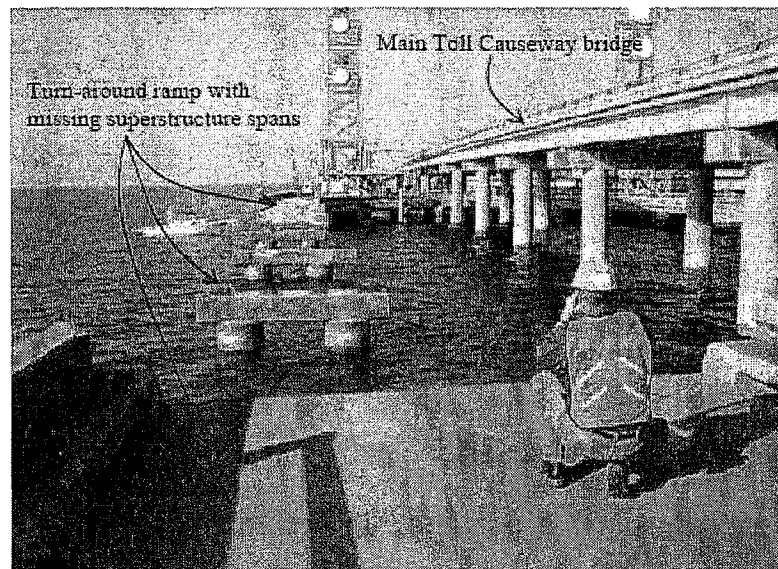
Figure 2.6   Toll Causeway turnaround bridge ramp failures (photo credit: Ron T. Eguchi, ImageCat) [8].

Figure 2.7   Misaligned spans of the Toll Causeway's turn around ramp (photo credit: Ron T. Eguchi, ImageCat) [8].

2-10

2.2 Literature Review

Since hurricanes are the source/cause of surge and surface wave damage to coastal bridges, it behooves us to examine the features and characteristics of these disastrous coastal storms. It should be noted that the hurricane storm surge causes a "wind tide" water build up which raises the water surface to a level where significant hydrostatic/buoyant water forces can act on a bridge; but more importantly, it raises the water surface to a level where large high wind generated surface waves can batter a bridge superstructure.

2.2.1 Hurricanes. A hurricane (or tropical cyclone) is a large weather system consisting of a system of spiraling winds rotating counterclockwise (in the northern hemisphere) and converging with increasing speed toward a low pressure center where they rise vertically around an area of relative calm (the eye). Spreading over an area between 50 and 600 miles in diameter, the hurricane travels over the ocean at speeds from 10 to 25 mph while tangential wind speed varies from 40 to 200 mph. The track and wind system of a typical hurricane as it moves in the Atlantic Ocean adjacent to the eastern coast of the U.S. is shown in Fig. 2.8. Hurricane damage is caused not just by high winds. Surges of the sea (storm surges) and the action of strong waves also pose severe threat to lives and properties in low areas along coastlines, as does flooding from torrential rains that come with a hurricane.

The National Hurricane Center defines storm surge as *"An abnormal rise in sea level accompanying a hurricane or other intense storm, and whose height is the difference between the observed level of the sea surface and the level that would have*

occurred in the absence of the cyclone. Storm surge is usually estimated by subtracting the normal or astronomic high tide from the observed storm tide." On top of storm surge and astronomical tide, are surface waves generated by powerful storm winds. Hurricanes also bring torrential rain which often causes severe flooding problems. Therefore, design against hurricanes must consider not only high winds but also the hurricane-generated surge/surface waves and floods.
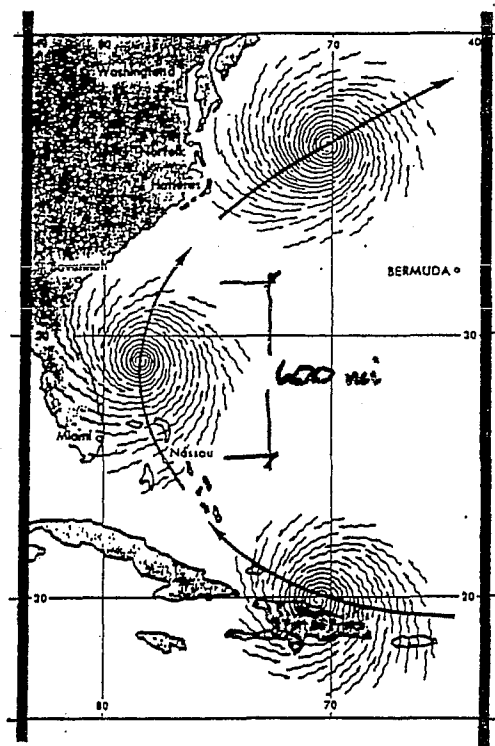
Fig. 2.8   Track and wind system of a typical hurricane

Hurricanes are rated in intensity and damage potential on the Saffir-Simpson Hurricane Scale. This scale rates a hurricane at a given time in its life as a Category I, II, III, IV, or V, with each category having an associated range of central barometric pressure, windspeed, surge height, and damage potential as shown in Table 2.1 and Fig. 2.9.

Table 2.1   Saffir-Simpson Hurricane Scale

Category	Central Pressure		Windspeed (mph)		Surge (ft)	Damage Potential
	millibars	inches of Hg	1-min.	3-sec.		
I	>980	>28.9	74-95	94-121	4-5	Minimal
II	965-979	28.5-28.9	96-110	122-140	6-8	Moderate
III	945-964	27.9-28.5	111-130	141-165	9-12	Extensive
IV	920-944	27.2-27.9	131-155	166-197	13-18	Extreme
V	<920	<27.2	>155	>198	>18	Catastrophic

Saffir-Simpson Hurricane Scale
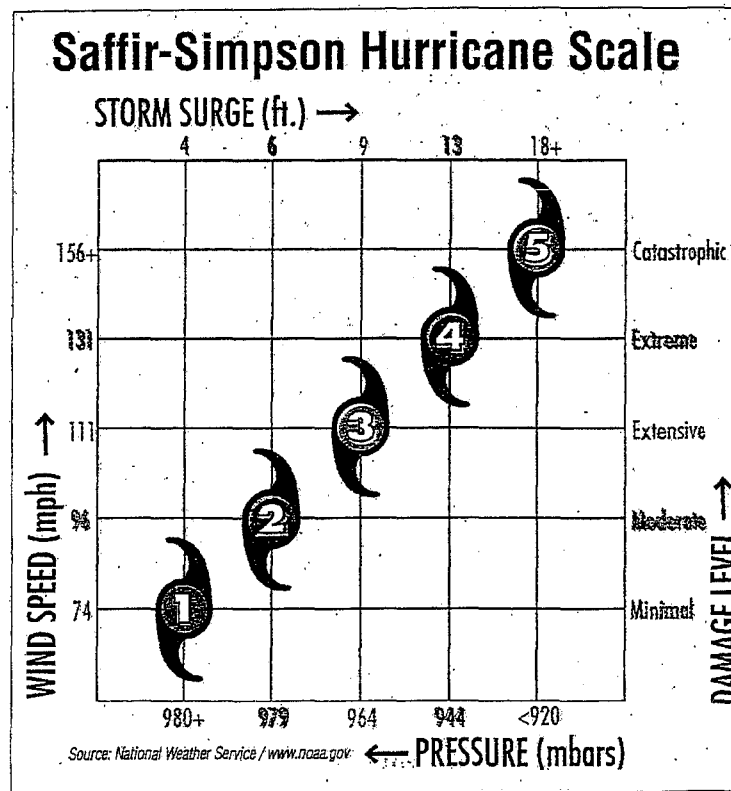
Fig. 2.9   Saffir-Simpson Hurricane Scale shown graphically

Figure 2.10 shows qualitative sketches of the windfield, wind generated waves and surge bubble in the eye of a hurricane. Figure 2.11 shows the storm surge build-up or setup prior to a hurricane making landfall and as the hurricane makes landfall. The setup or wind tide (also sometimes called the forerunner) is a characteristic rise in the water level near the coast, which precedes the actual arrival of the center of a hurricane. This can be explained by the fact that water is actually being transported and accumulated toward the shore. The forerunner extends for long distance along the shore, whereas the surge bubble covers only a small portion of the shoreline. The forerunner elevation is the greatest just to the right of the storm centerline where the rotational and the forward translational winds are parallel and additive. The surge bubble adds its action to that of the forerunner in further raising the water level.

Figure 2.12 shows a qualitative sketch of a hurricane surge wave approaching and making landfall. Note in that figure the much larger surge wave height and lateral extension on the right-hand side of the hurricane due to the hurricane tangential and translational winds being in the same direction. It should be noted that a fairly rapid rise in water surface elevation occurs near the center of the hurricane due to a barometric pressure drop in the eye and due to the radial component of the hurricane windfield as it spirals inward to the eye. The rise in water level due to the barometric pressure drop is only about 3 ft and its extension along the coastline is somewhat less than the diameter of the hurricane eye.

SWELL RADIATING OUT FROM INTENSE WIND REGION TO THE RIGHT OF THE STORM CENTER

CALM EYE OF THE STORM

COUNTER-CLOCKWISE WIND DIRECTION

80 Knots

980 mbar

a

a

WAVES GENERATED IN THIS REGION PROPAGATE IN THE OPPOSITE DIRECTION TO THE STORM AND HAVE A SHORT FETCH

WAVES GENERATED IN THIS REGION PROPAGATE FORWARD WITH THE STORM AND EXPERIENCE AN EXTENDED FETCH
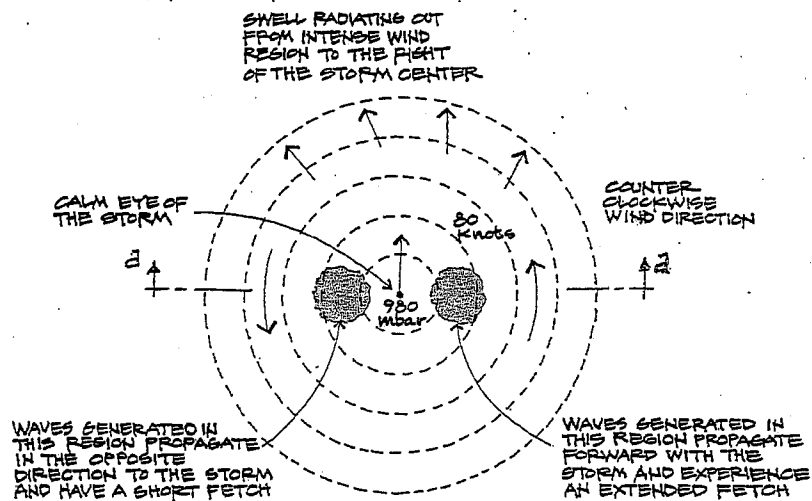
a. Plan view of windfield and resulting wind generated waves

Hurricane area

Lower than atmospheric pressure

Atmospheric pressure

Atmospheric pressure
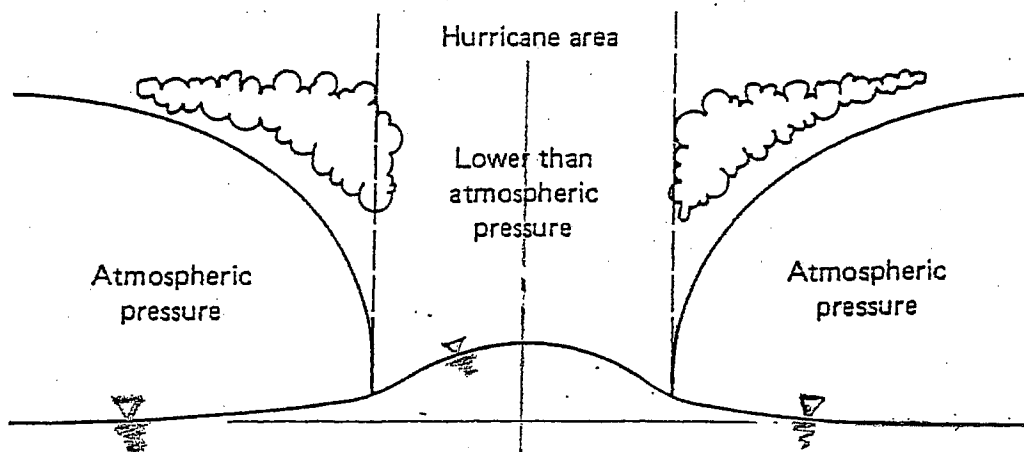
b. Elevation view along diameter a-a of surge bubble in "eye" due to reduced atmospheric pressure and radial inward component of hurricane windfield

Fig. 2.10   Approximate hurricane windfield and radiating waves and surge bubble in "eye"

2-15

Wind →

Rise of sea level produced by hurricane wind

Setup (*Wind Tide*)

Astronomical Tide

Original sea level
(*Worst case is when this is high tide*)
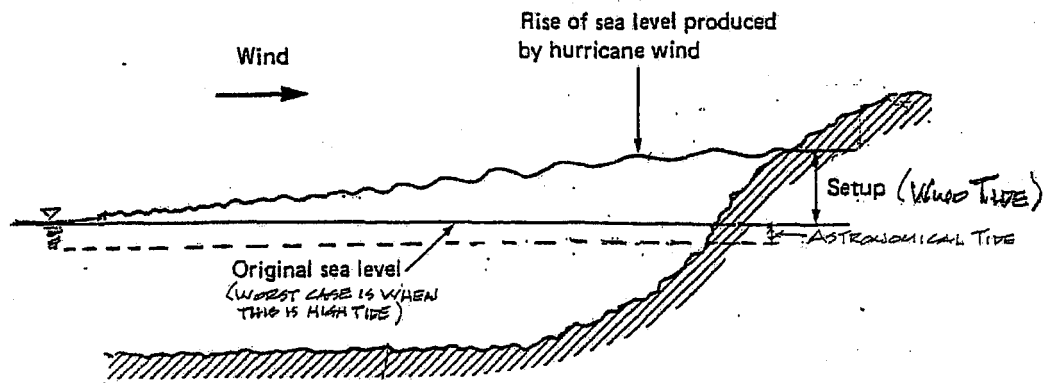
a. Prior to hurricane making landfall

Wind →

Wind induced surface waves

Surge caused by low atmospheric pressure in "eye" (3-4') and the radial inward component of hurricane windfield

Rise of sea level produced by hurricane wind

Setup (*Wind Tide*)

Astronomical Tide

Original sea level
(*Worst case is when this is high tide*)
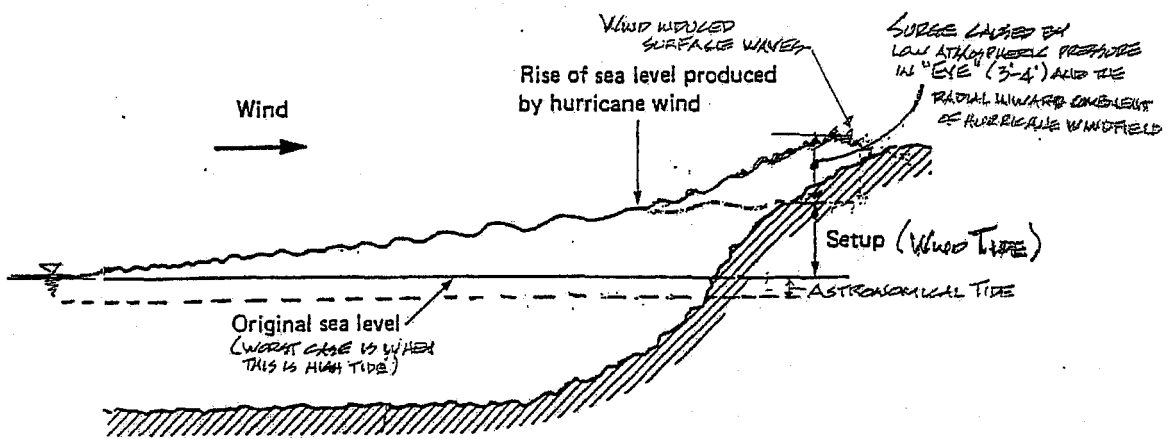
b. As center of hurricane makes landfall

Fig. 2.11 Surface waves and wind tide generated by hurricane

2-16
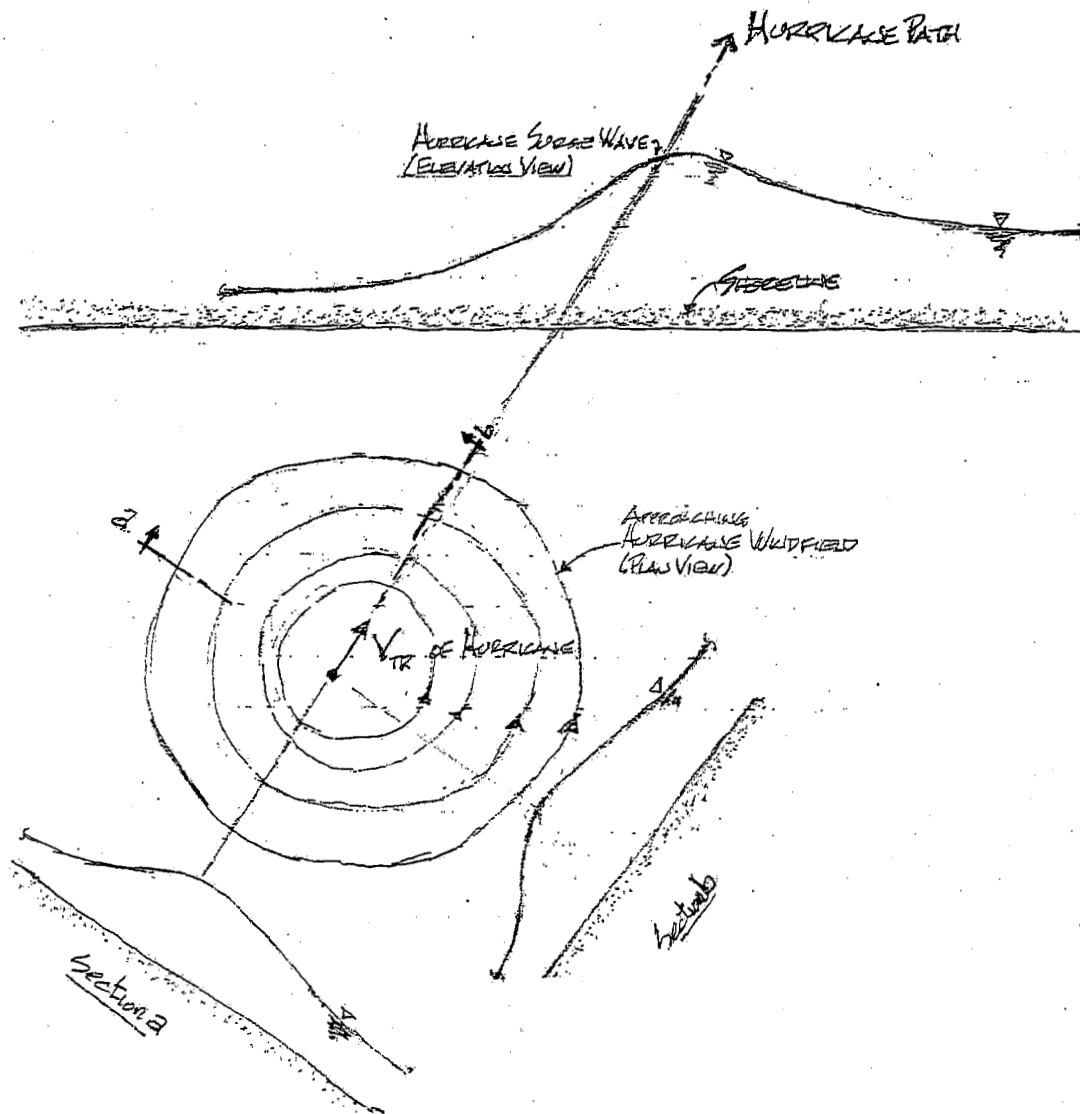
Fig. 2.12   Qualitative sketch of hurricane surge wave approaching and making landfall

It should be noted in Fig. 2.11b that the setup or wind tide is superimposed on the ordinary (astronomical) tide, the hurricane eye bubble is superimposed on the setup, and the wind generated surface waves are superimposed on the setup and eye bubble. This combination of ordinary tide, wind tide, and eye bubble many times results in the water level at a bridge site being raised by the storm surge to a level where the 8-9 ft high surface waves inundate or partially inundate a bridge superstructure and create large buoyant forces as well as slam the superstructure with large horizontal and vertical pressures as implied in Fig. 2.13.

For coastal bridges, hurricane peak storm surge and surface wave heights at the location of the bridge are the primary storm parameters of interest in assessing the impact of a hurricane on a bridge. Ideally, one would like to have storm surge and surface wave information as shown in Fig. 2.14. However, having just the peak surge elevation and the significant wave height would suffice. Immediately after Hurricane Katrina, a post-storm survey by FEMA field teams allowed FEMA to map coastal surge heights in 1-foot intervals using documented coastal High Water Marks (HWMs) data caused by Katrina's storm surge. Field personnel deployed by FEMA collected detailed information about each HWM, including the physical basis of the mark, e.g., a mud line inside a building, a mud line on the outside of a building, or debris. Figure 2.15 shows these contours along the Mississippi coastline. A storm surge contour map was also created for the New Orleans area of southeastern Louisiana. Figure 2.16 depicts surge elevation contours calculated from post-Katrina HWMs collected along the Gulf of Mexico, Lake Borgne, and Lake Pontchartrain coastlines of Louisiana. Figures 2.17 and 2.18 show Katrina making landfall near Slidell, LA to allow correlations between the

hurricane path and the mapped storm surge contours, and to provide a perspective of the lateral dimensions of the storm surge. It should be noted that at the I-10/Mobile Bay On-Ramp, the surge level was approximately 12 ft. Note in these figures the much larger height and lateral extension of the storm surge on the right-hand side of the hurricane (this was indicated qualitatively in Fig. 2.12).
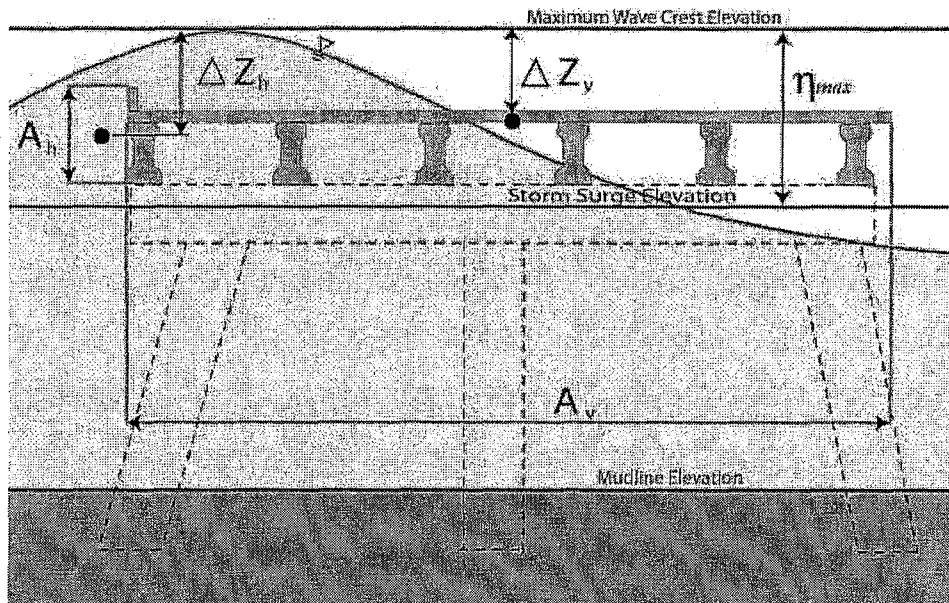
Fig. 2.13 Partial inundation of bridge superstructure by storm surface wave due to rise in water surface by the storm surge [1].
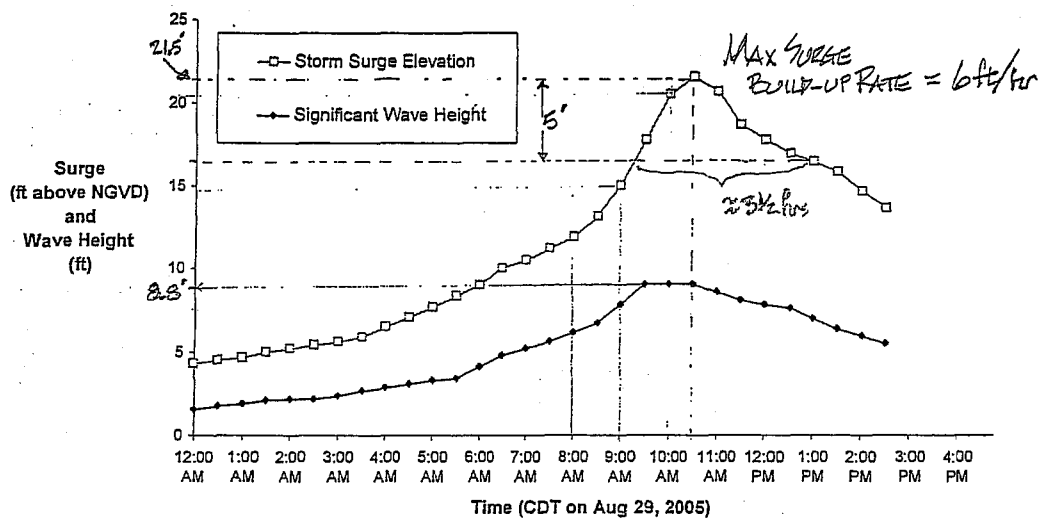
Fig. 2.14 Estimated storm surge and wave heights at bridge as Katrina made landfall [1].
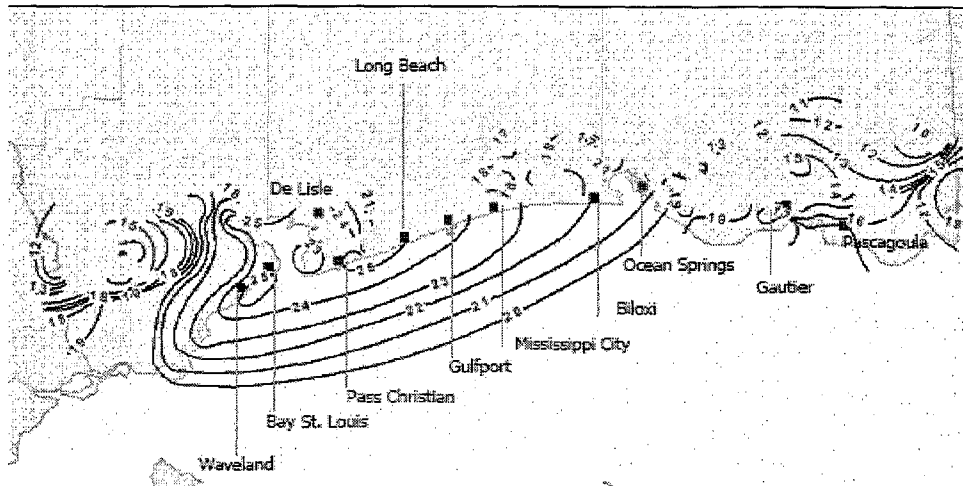
Fig. 2.15   Storm surge contours for Mississippi, as mapped by FEMA (heights measured in feet). (Source: FEMA, enhanced by Ron T. Eguchi, ImageCat) [8].
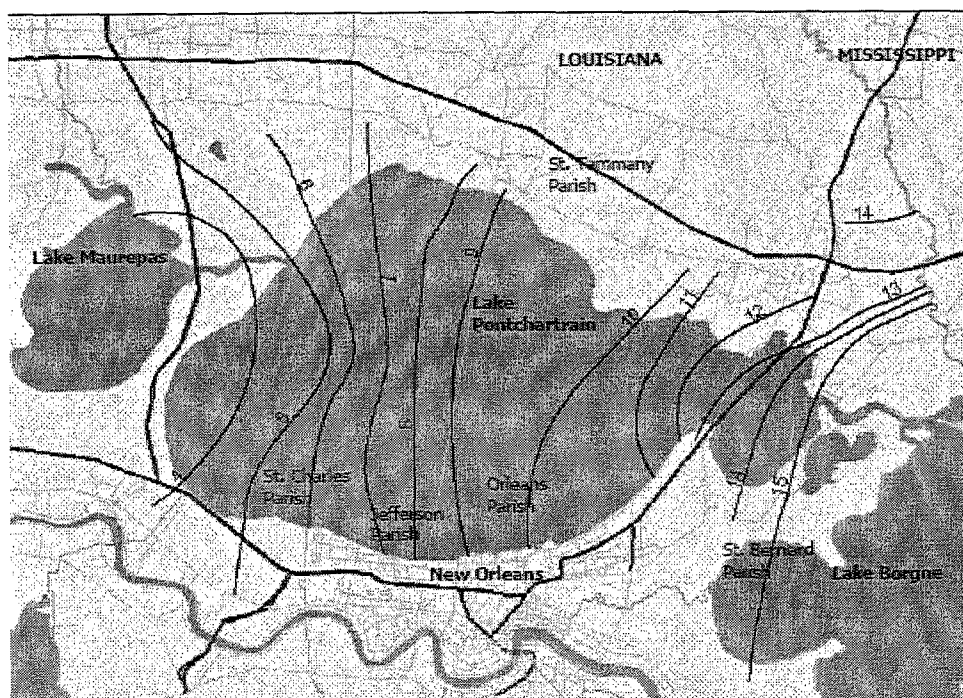
Fig. 2.16   Storm surge contours (heights measured in feet) for the New Orleans area of southeastern Louisiana, as mapped by FEMA (Source: FEMA, enhanced by Ron T. Eguchi, ImageCat) [8].
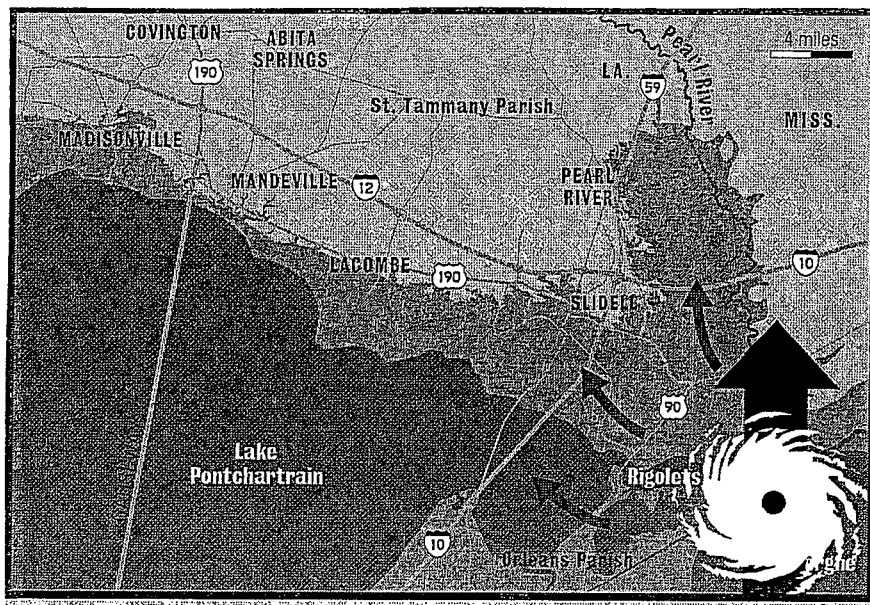
Fig. 2.17   Katrina makes landfall near Slidell, LA – storm surge is 15 feet at the Lake Pontchartrain north shoreline [8].
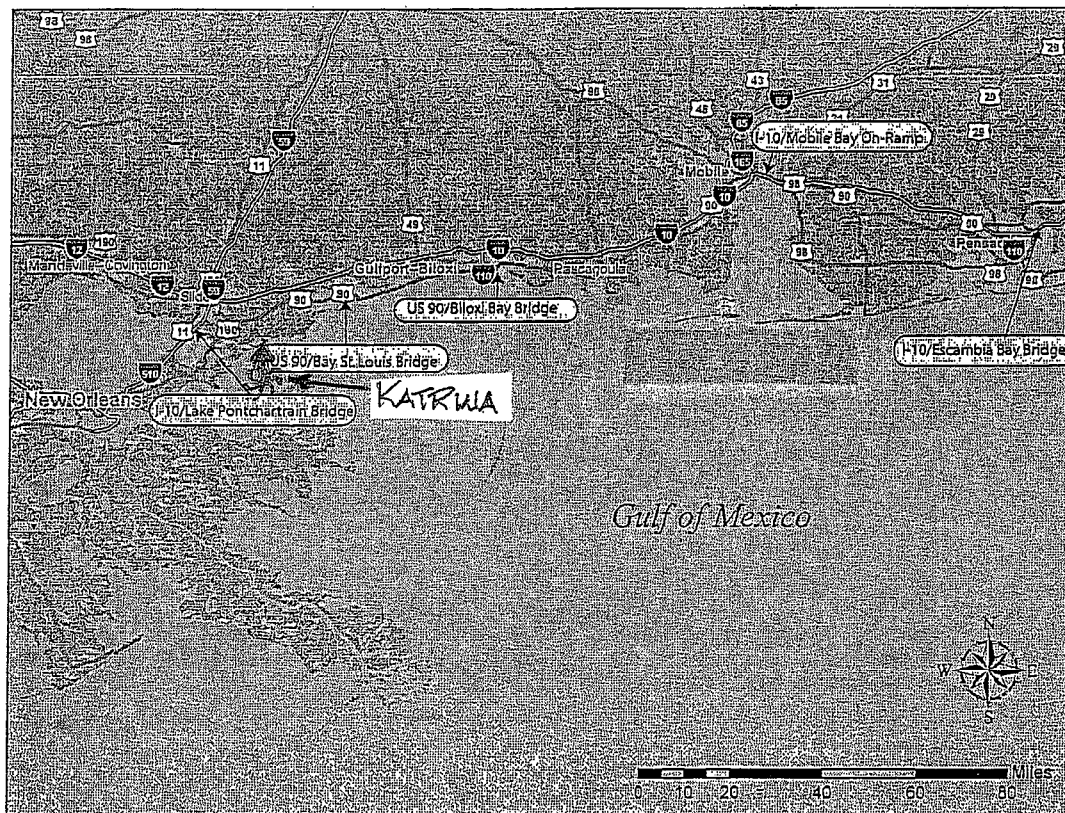
Fig. 2.18   Location map of coastal highway bridges damaged by Hurricane Katrina [8].

It should be noted that NOAA/FEMA personnel conduct preliminary storm surge modeling when a weather system develops to the point of being a hurricane and gets close enough to the U.S. to estimate the vicinity of striking the U.S. (i.e., the Gulf of Mexico coast, Atlantic Ocean coast, etc). At that point they conduct real-time forecasts of potential storm surge for approaching hurricanes using the computer software SLOSH (Sea, Lake, and Overland Surges from Hurricanes) and include these forecasts in periodic hurricane advisories. NOAA forecasts, evacuation plans and real-time decisions of the emergency management community for storm surge are based on SLOSH. In real-time, NOAA runs storm surge simulations and considers the associated output in its operational text and graphical products.

Results of a preliminary storm surge hindcast performed by NOAA using SLOSH for the Mississippi coast for Hurricane Katrina is shown in Fig. 2.19. A comparison of storm surge predictions using SLOSH with preliminary high water marks observed by FEMA in Mississippi and Louisiana is shown in Fig. 2.20, and indicates that the SLOSH program did a good job of predicting storm surge levels. This is important as it indicates that NOAA/FEMA can accurately predict maximum surge water levels at an existing or planned coastal bridge site. These water levels are needed if the bridge is to be designed with an "air gap" procedure, or to properly estimate surge/surface wave loadings on the bridge if the "air gap" procedure is not used.
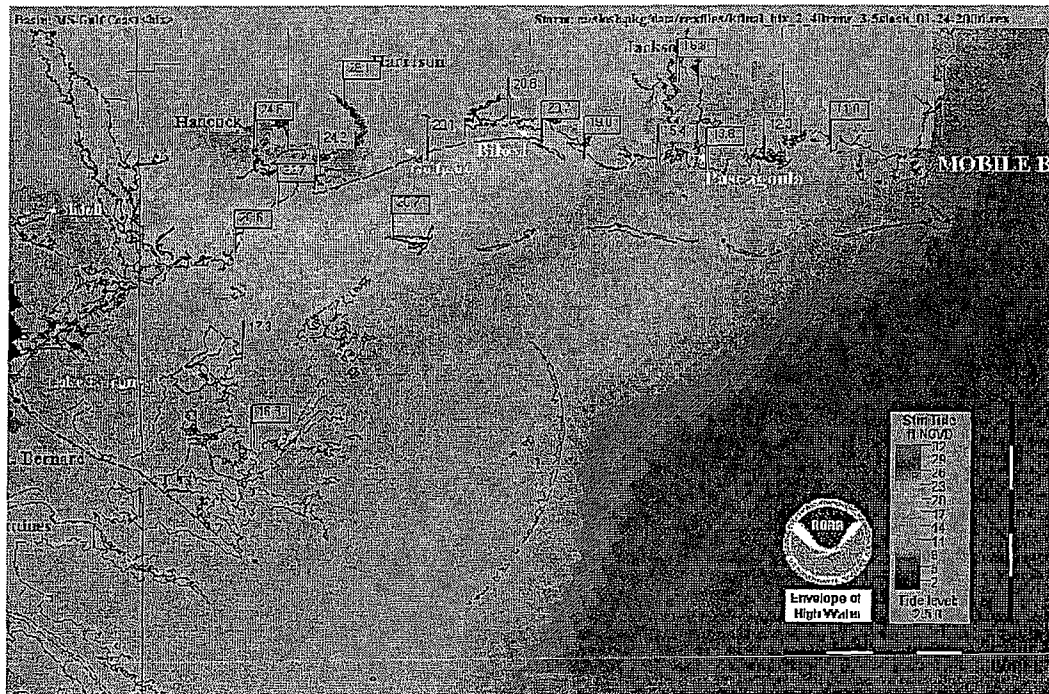
Fig. 2.19 Preliminary storm surge hindcast results for Mississippi Gulf Coast for Hurricane Katrina using SLOSH (Source: NOAA/Ref. [8])
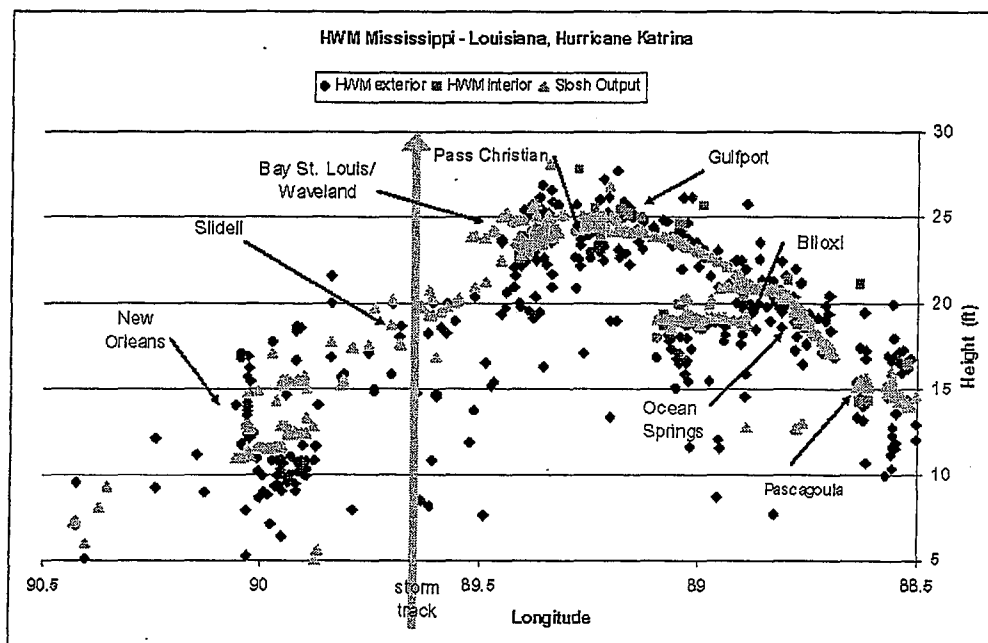
Fig. 2.20 Comparison of storm surge predictions using SLOSH with preliminary high water marks observed by FEMA in Mississippi and Louisiana (Source:NOAA/Ref. [8])

2.2.2 Hurricane Katrina Damage to Coastal Bridges. In Section 2.1 photos of damages to some bridges across Lake Pontchartrain caused by Hurricane Katrina were presented and discussed. However, to the east of Katrina's landfall location near Slidell, LA, there was much coastal bridge damage as indicated in Fig. 2.21 and the photos of Fig. 2.22. For coastal bridges, hurricane induced surge/surface waves are the primary cause of damage as evident in Fig. 2.22.
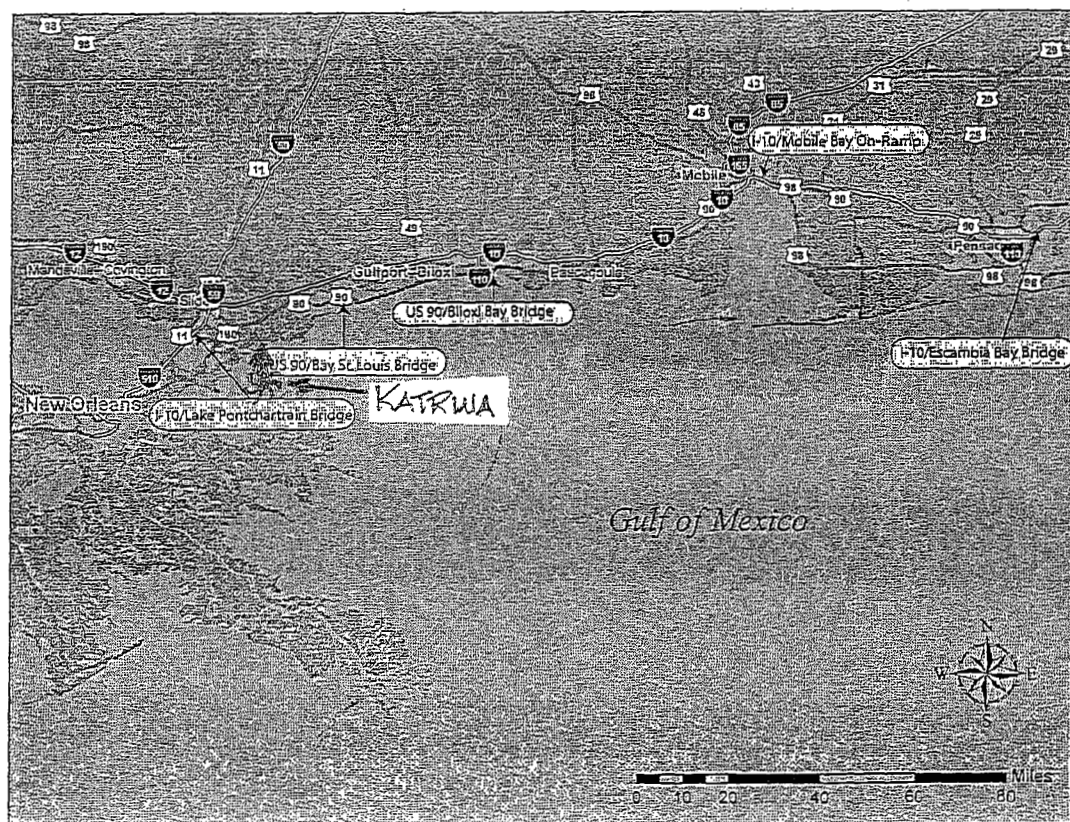
Fig. 2.21   Location map coastal highway bridges damaged by Hurricane Katrina.

2-25
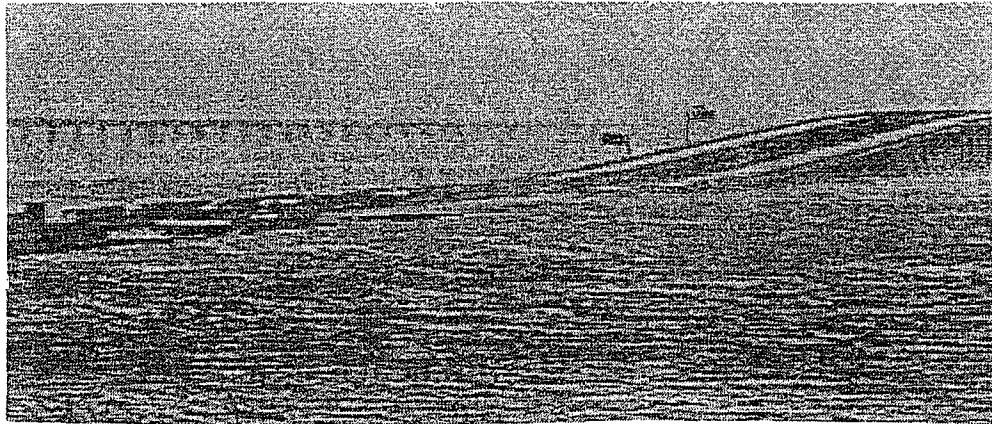
a. Partially inundated bridge
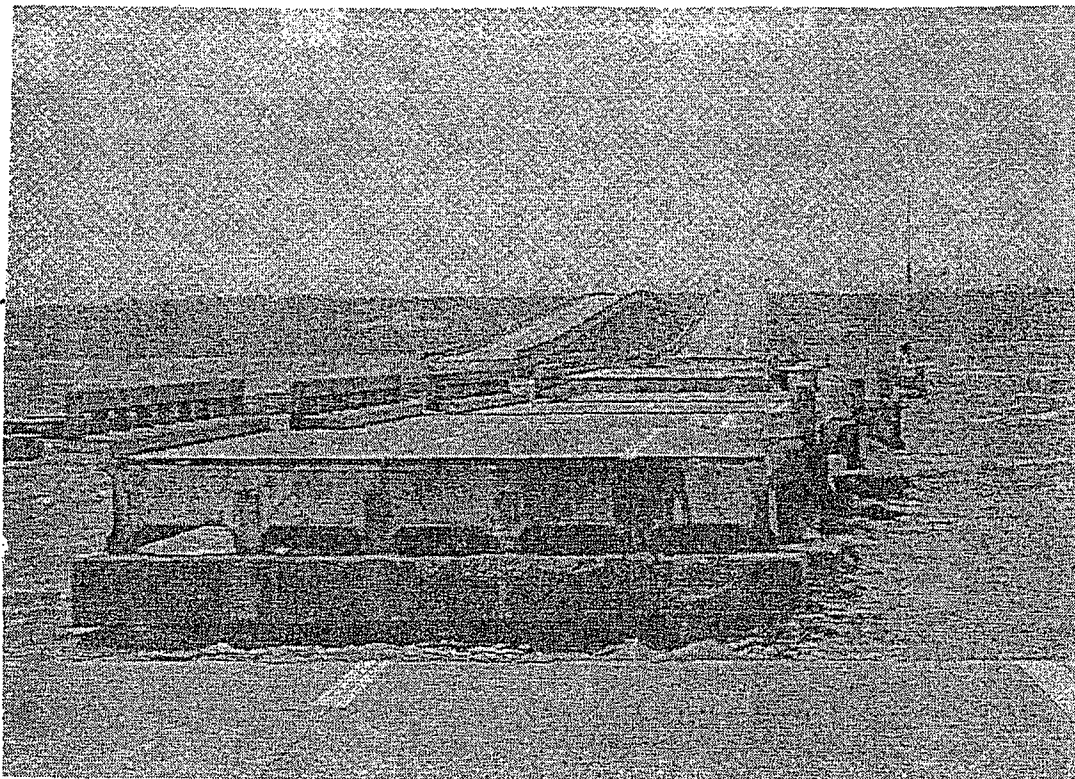
b. Close-up of bridge superstructure failure

Fig. 2.22 Hurricane surge/surface wave induced bridge superstructure failure near Pensacola, FL in Hurricane Katrina [8].

Hurricane Katrina's storm surge/surface waves virtually destroyed the U.S. Hwy 90 Biloxi Bay Bridge, Biloxi, Mississippi, and the U.S. 90 Bay St. Louis Bridge, Bay St. Louis, Mississippi. Figures 2.23 and 2.24 show the state of the Biloxi Bay Bridge after Katrina. After Katrina, the Mississippi Department of Transportation (MSDOT) contracted with the Parsons Corp. and URS Corp. for the Biloxi Bay Bridge, and with HNTB Corp. and URS Corp. for the Bay St. Louis Bridge, for the engineering design of the new replacement bridges. The MSDOT design changes on these two bridges to mitigate future hurricane storm surge/surface wave damage were as follows:

1. Used much higher vertical clearances. At the highest point the vertical clearance is 95ft on the Biloxi bridge and 85 ft on the Bay St. Louis Bridge. These clearances are controlled by navigation requirements. On both bridges at other locations the clearances are controlled by storm wave elevations and these clearances were increased substantially (to approximately 35ft).

2. Used longer and heavier spans to provide greater dead load resistance.

3. Used continuous spans to better distribute any wave loads.

4. Used shallower superstructure diaphragms to reduce entrapped air.

5. Used shear keys to lock the spans to the support bents.

6. Used seawalls around the abutments to prevent wave loading and scour at the abutments.
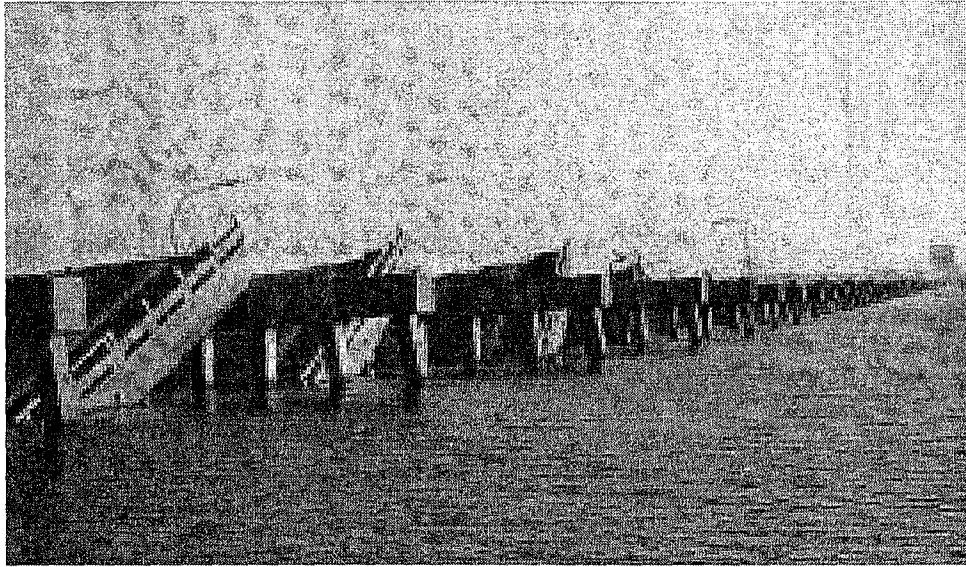
Fig. 2.23 Looking west toward Biloxi from the east shore, many superstructure spans of US-90 Biloxi-Ocean Springs bridge were displaced north off their piers (photo credit: J. O'Connor, MCEER) [8].
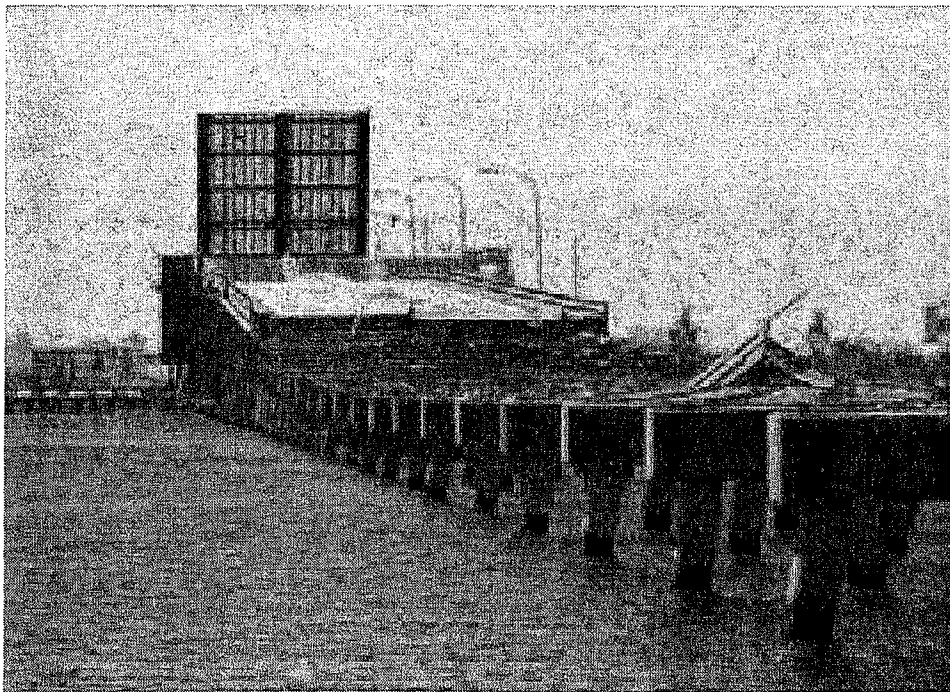
Fig. 2.24 Photo looking west toward Biloxi of Hurricane Katrina damage to U.S. 90 Bridge over Biloxi Bay [1].

Figure 2.25 shows the new Biloxi Bay Bridge under construction and scheduled for completion in April 2008. Figure 2.26 shows the new Bay St. Louis Bridge under construction; it was scheduled for completion in November 2007.

Fig. 2.25 U.S. 90 Biloxi Bay Bridge under construction
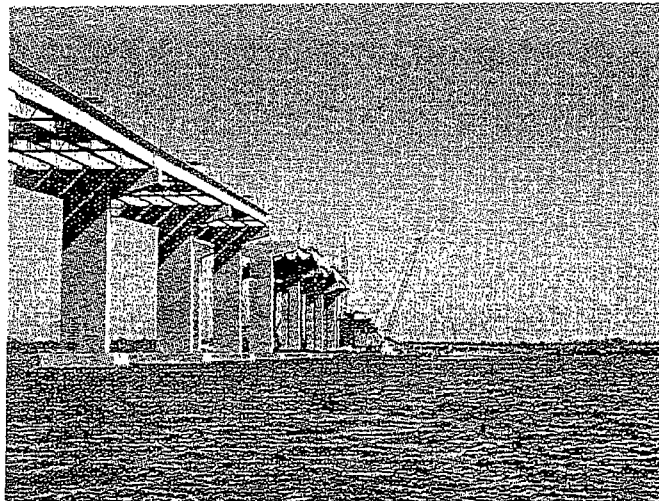
Fig. 2.26 U.S. 90 Bay St. Louis Bridge under construction

As discussed in Section 2.1, Hurricane Katrina's high storm surge/surface waves did tremendous damage to the twin I-10 bridges across the east end of Lake Pontchartrain near New Orleans, as evident in Fig. 2.27. The damage, and probability of a future repeat incident were so great that the bridges are now being replaced by two new I-10 twin bridges which are scheduled to be completed in August 2011. Volkert Construction Services Inc. is performing the engineering design and construction inspection for the twin bridges. Volkert's primary design changes from the original bridges include

- an elevated bridge height (21 ft higher than the old bridge)

- greater weather resistant concrete

- reinforced attachments between the decks and girders and girders and substructure to prevent uplift and lateral movement from storm surge/surface waves.

Figure 2.28 shows the repaired old twin bridges with pile driving underway for the adjacent new bridges.

Damage to I-10 Ramp in Mobile Bay. Although Hurricane Katrina made landfall nearly 100 miles away (see Fig. 2.21), the storm surge and surface waves at the north end of Mobile Bay caused significant damage to an I-10 on-ramp at that location as reported by Douglass, et al [1]. The peak storm surge at the I-10 on-ramp was estimated to be 12 ft based on high water data at the nearby USS Alabama Battleship Park, with a corresponding significant wave height of $H_s = 5.6$ ft. The storm surge/waves caused movement to the north in the direction of wave propagation of the lowest five simply-supported ramp spans as can be seen in Fig. 2.29. It should be noted that some of the spans that moved would have probably continued to move and perhaps fallen from the support bents had they not been somewhat pie-shaped and
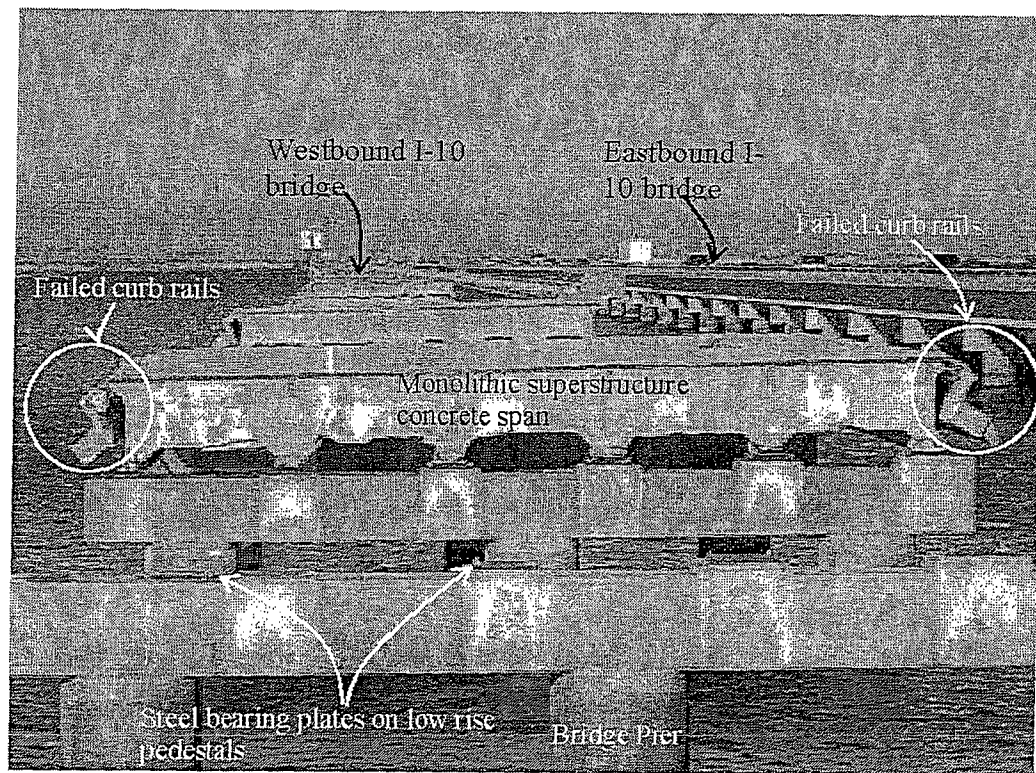
Fig. 2.27 Katrina damage to I-10 twin bridges on Lake Pontchartrain – view looking north from west abutment (photo credit: NIST) [1].
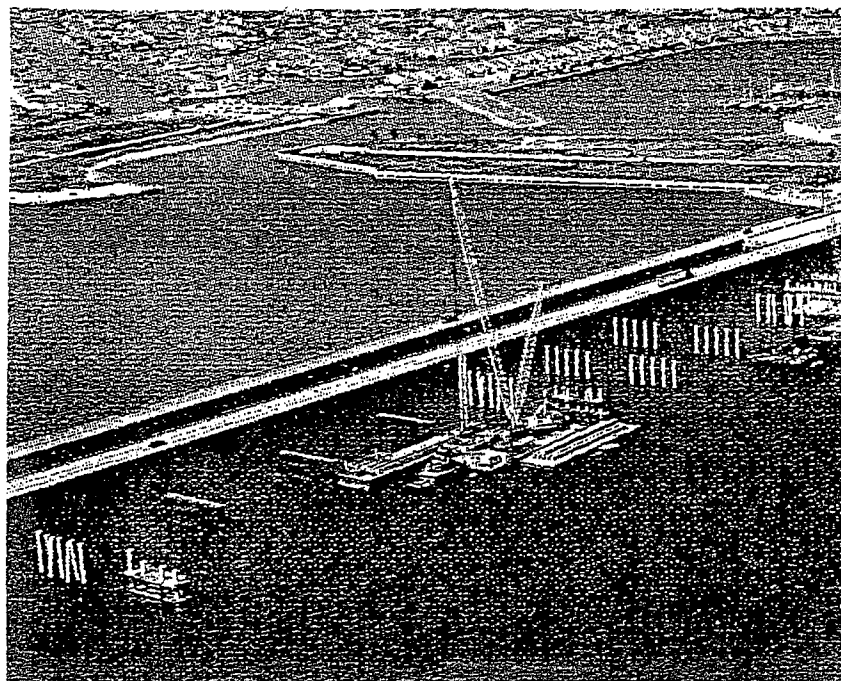
Fig. 2.28 New twin I-10 bridges just beginning construction/pile driving adjacent to old twin I-10 bridges across Lake Pontchartrain

wedged themselves in place. Also, it should be noted in Fig. 2.29 that the lower

elevation spans which did not move were continuous spans with the superstructure cast

monothically with the piles and pile cap, and the higher elevation spans (going up the

ramp) were sufficiently high to partially miss the large wave loadings.
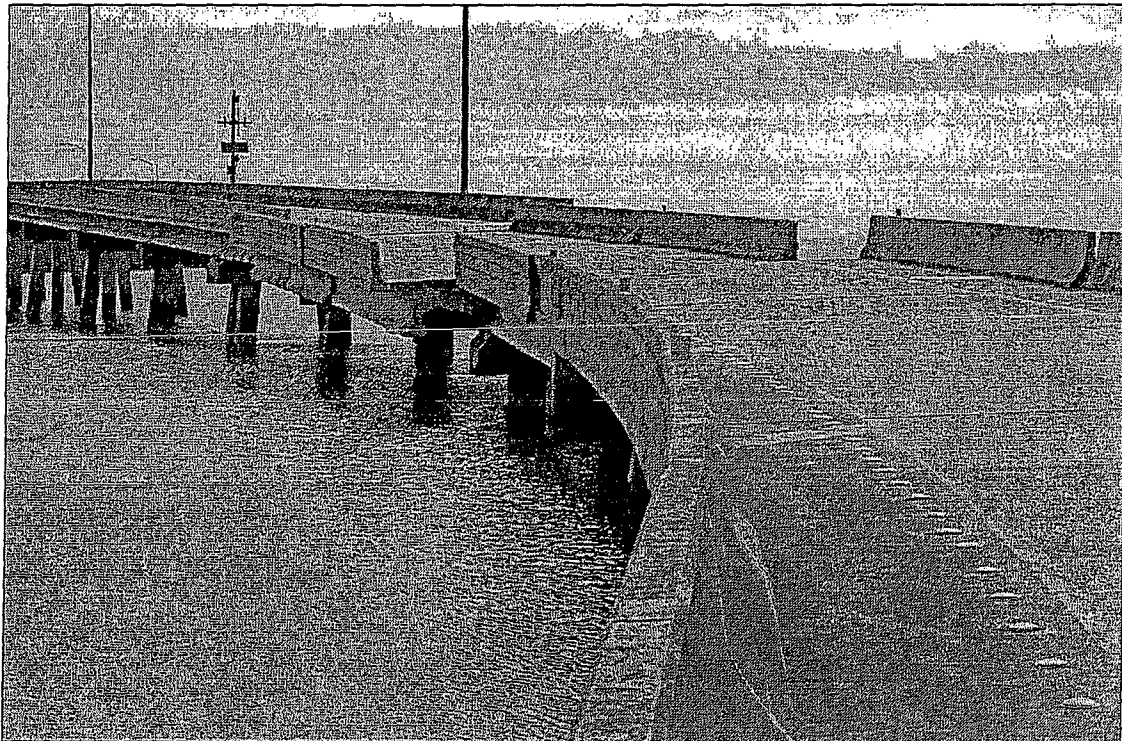
**Fig. 2.29 Damage to I-10 on-ramp near Mobile, Alabama,
caused by Hurricane Katrina [1].**

Douglass et al. report [1] that the five moved spans had low-chord elevations at

or below the peak of the storm surge. The sixth simply-supported span up the ramp

(span #14), i.e., the first one not damaged, had an elevation with about 1.4 feet of

clearance between the low-chord elevation and the surge elevation. Thus, it was being

hit by waves at the peak of the storm. The elevations and dimensions of the on-ramp

spans were obtained from the ALDOT from their engineering plans. The ramp slopes up as well as on a horizontal curve to the left with a superelevation that sets the south side higher. The five ramp spans that moved had top-of-deck elevations of between 8.0 and 13.7 feet as measured at the center of the span. The corresponding "low-chord" elevations at the mid-point of the south side of the spans was typically about 3.7 feet lower than the top-of-deck elevation.

The connection of the simply-supported span superstructure to the pile bent substructure consisted of eight sets of bolts in each span placed at the inside and the outside of the girders in each corner of the span. Inspection indicated that the bolts did not shear but rather the bent cap or girder concrete failed as can be seen in Figs. 2.30-2.31. Figure 2.32 shows one of the connections on a higher elevation span that survived the storm. Based on estimated values of the concrete tensile strength and failure area, Douglass, et al. estimated the total resistance to movement of each span to be approximately $200^k - 400^k$.

Using the known dimensions of the ramp spans (from the ALDOT) and the equations and procedure for estimating wave loadings that they recommended, Douglass, et al., estimated the wave loading on the five on-ramp spans that moved (spans #9 - #13) and the next span up the ramp which did not move, i.e., span #14. The results of their analyses are shown graphically in Fig. 2.33. Douglass, et al. point out the good correlation between the estimated applied loads and the estimated span connection resistance ($200^k - 400^k$), i.e., spans #9 - #13 had estimated applied loads larger than the estimated resistance and they broke their connections and moved, while span #14 had an estimated resistance that was adequate for the loading and did not move.

this girder moved this way
off the pile cap and pulled 4
bolts out
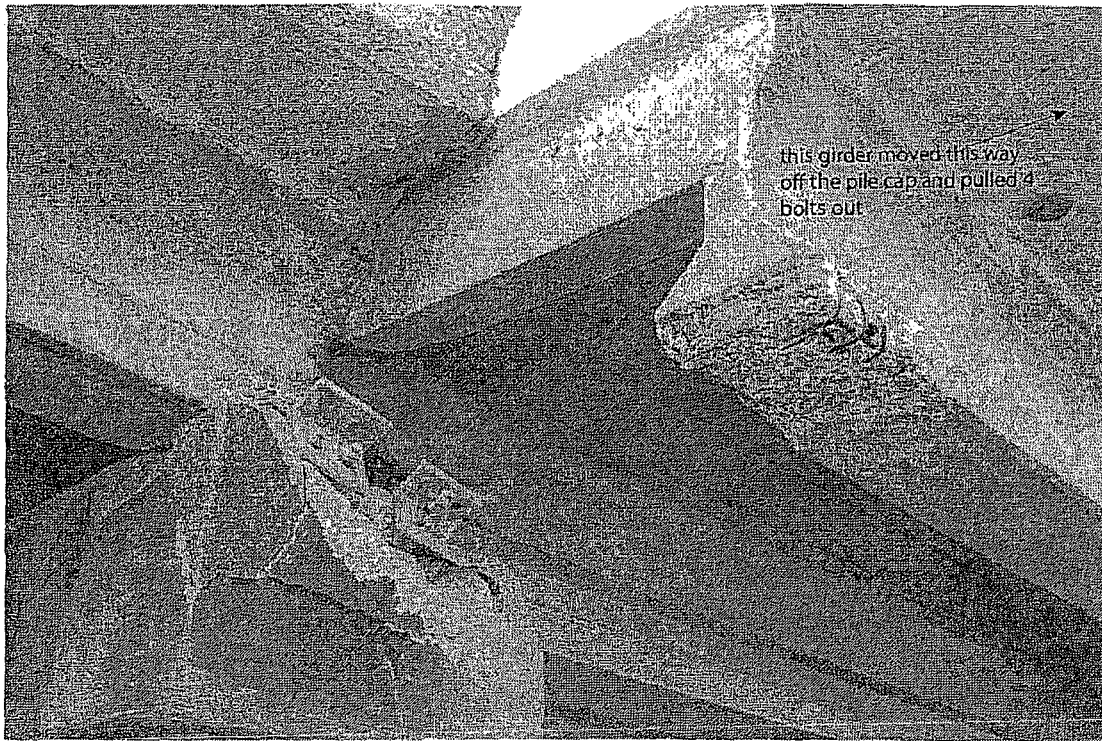
Fig. 2.30   Photo of northeast corner of span #11 of I-10 on-ramp near
Mobile, AL [1].
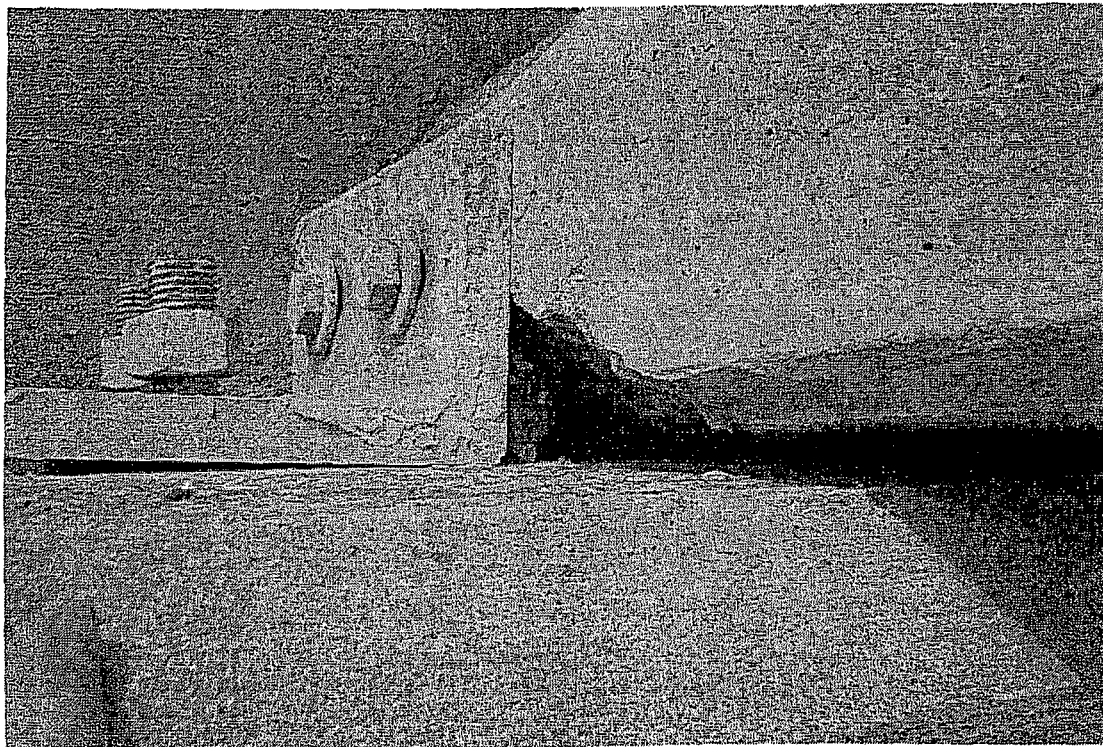
Fig. 2.31   Photo of typical slip angle connection of I-10 on-ramp near
Mobile showing failure of concrete around bolts but without
subsequent span displacement [1].

2-34
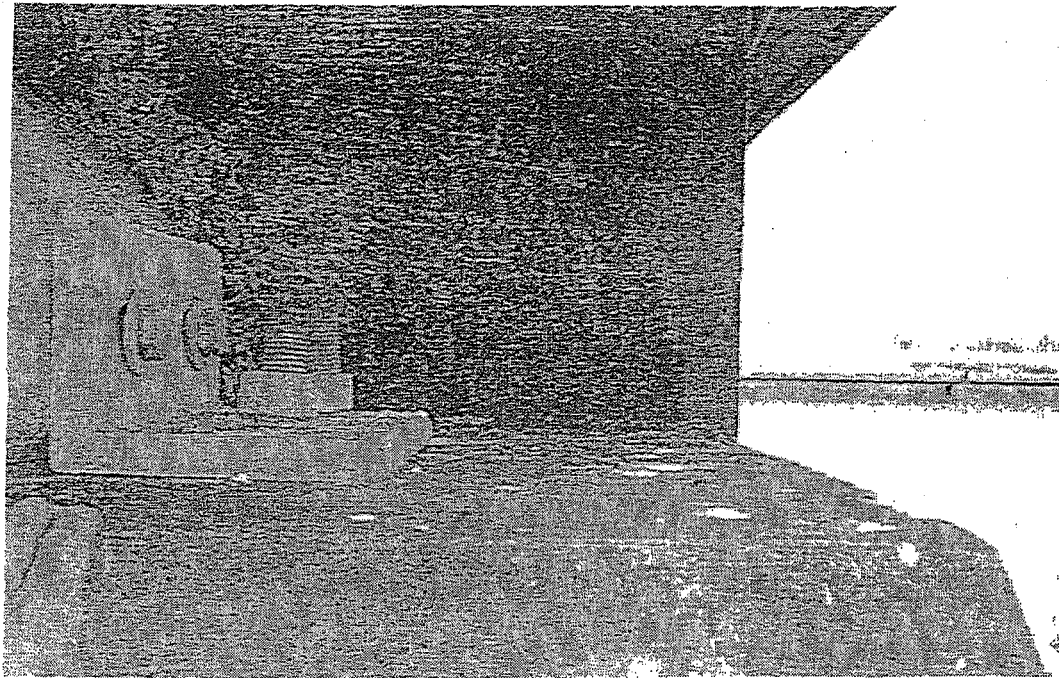
Fig. 2.32 Photo of clip angle connection that did not fail on another part of I-10 on-ramp near Mobile [1].
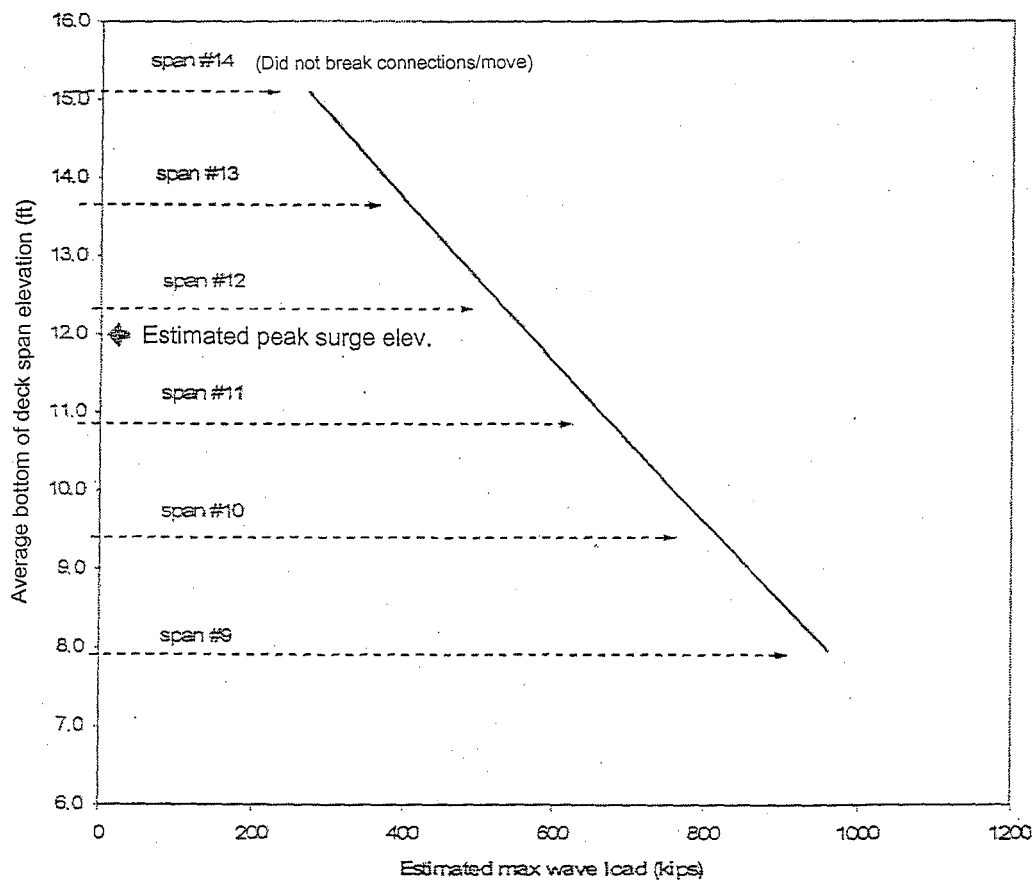
Fig.2.33   Reduction in estimated wave loads on I-10 on-ramp near Mobile with elevation (modified from [1]).

2-35

2.2.3 Hurricane Frederic Storm Surge Heights and Bridge Damages

Hurricane Frederic (rated as a high category 3 hurricane) approached the Alabama Coast with a forward speed of about 15 mph. The eye of the storm measured 50 miles east to west, and 40 miles north to south. In the opinion of some weather forecasters Frederic had the largest storm center ever recorded. The storm center crossed over the western end of Dauphin Island at about 10 p.m. CDT on 12 September 1979. At Dauphin Island Bridge a 145 mph peak gust of wind was recorded. The hurricane continued on a course slightly west of due north with its center striking the mainland in Alabama near the Alabama-Mississippi border about an hour later (see Figs. 2.34 and 2.35).
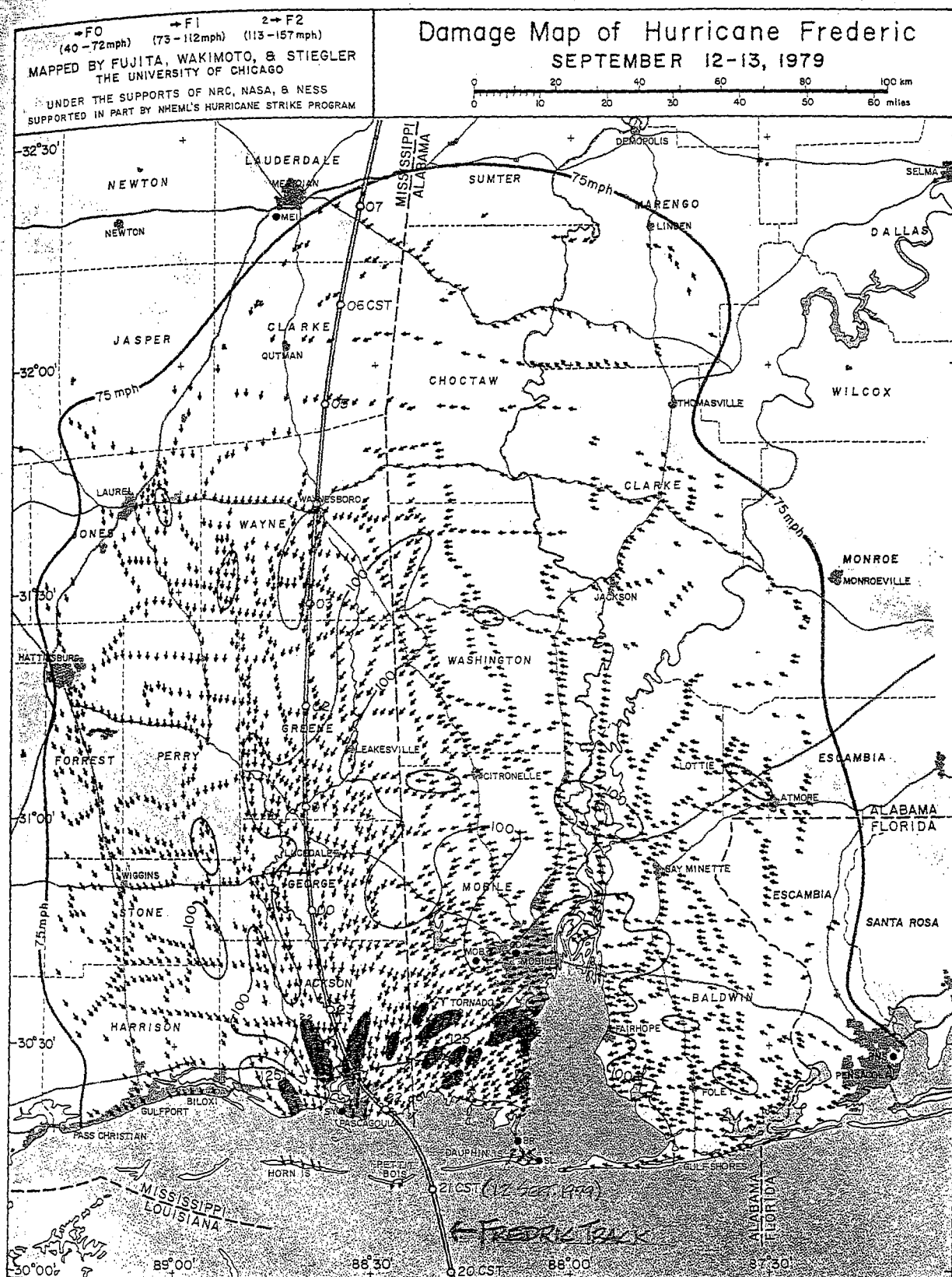
Fig. 2.34 Damage Map of Hurricane Frederic [12].
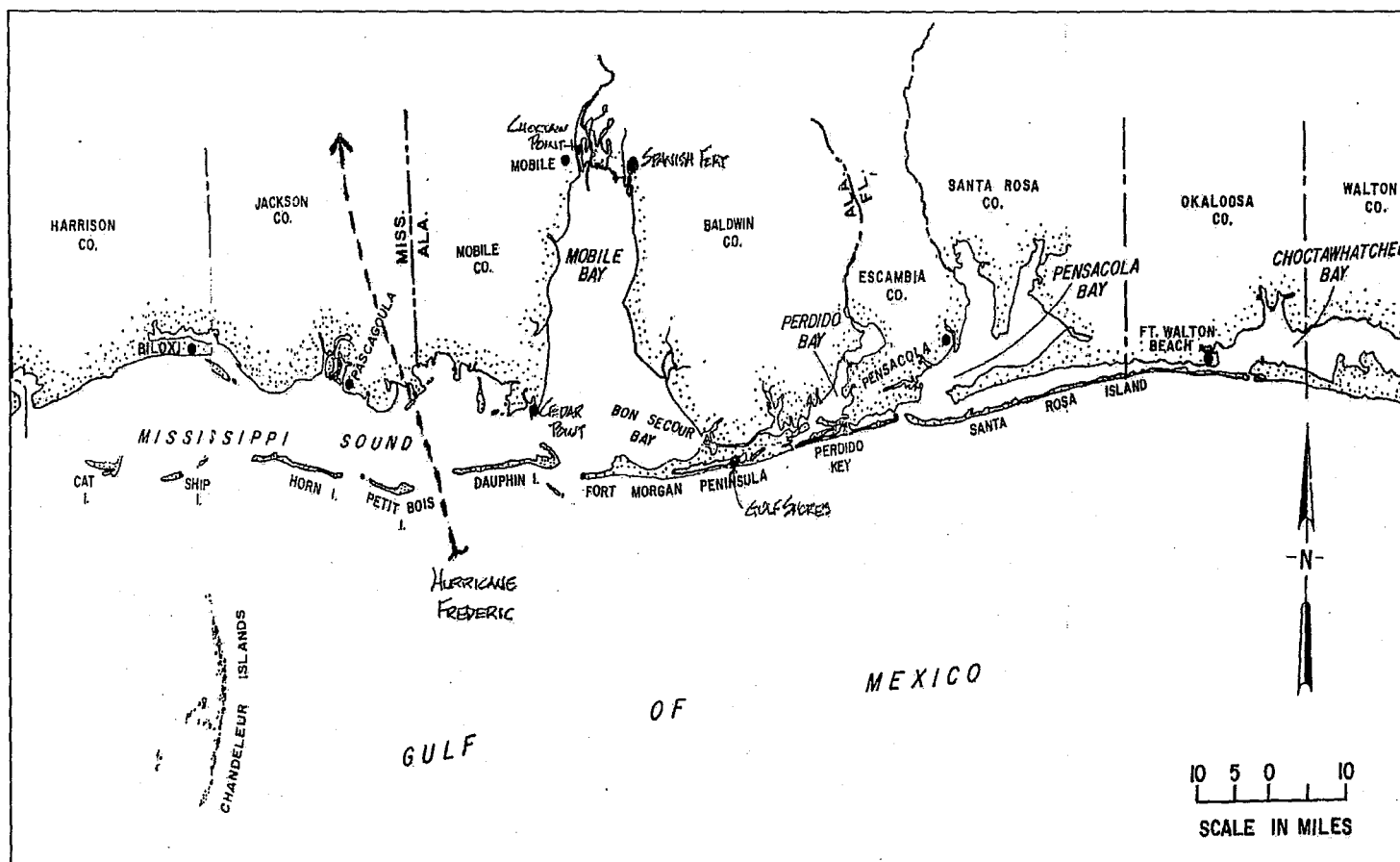
Fig. 2.35 Gulf Coastal Area Affected by Hurricane Frederic [12].

Storm Surge. As the storm struck the coast, the storm surge was greatest in its north-eastern quadrant, which swept along the Alabama Gulf Coast near the Alabama-Florida State line. On Dauphin Island the astronomical low tide occurred at 1:05 p.m. on 12 September, and the high tide occurred at 1:53 a.m. on 13 September. The tide variation from low to high was about 1.1 feet. Some storm surge heights and damages the surge and associated surface waves caused are given below.

- On the Alabama beaches in Baldwin County, from Fort Morgan (at Mobile Bay) east to Alabama Point (at Perdido Pass), storm surge high water elevations ranged from 10 feet to more than 15 feet above the National Geodetic Vertical Datum, NGVD (formerly mean sea level). One of the higher water marks (HWM) was measured at 15.79 feet, along a driftline at the northwest corner of the main building at Gulf State Park, Gulf Shores, Alabama (see Figs. 2.34 and 2.35 for site locations).

- A wave height was measured at elevation 16.93 feet NGVD, and its associated wave runup of 23.88 feet, on the coast about three miles west of Perdido Bay.

- High water elevations on the Gulf Coast of Perdido Key, Florida were about 11 to 15 feet.

- On Dauphin Island, Alabama, high water elevations ranged from 9 feet on the eastern end near Fort Gaines, to over 13 feet NGVD on the Gulf

(south) side, about midway of the island. The western end of the island, for a distance of about 11 miles, was over-topped by the storm surge and no high water elevations were available. On the north side, at the eastern end of the island, the high water elevations ranged from 6 to 8 feet in Dauphin Island Bay, between Dauphin Island and Little Dauphin Island.

- In Alabama, along the eastern shore of Mobile Bay from Bon Secour north to Spanish Fort, the high water elevations were 6 to 8 feet. The causeway, which crosses the delta at the northern end of Mobile Bay, had high water elevations of 8 to 10 feet and most of the buildings along that portion of Highway US 90, 98, and 31 were destroyed or severely damaged.

- The Alabama State Docks gage at Mobile, Alabama on the Mobile River, recorded a high water elevation of 8.05 feet NGVD. Choctaw Point, at the mouth of Mobile River had a high of 12.0 feet.

- The western shore of Mobile Bay had high water elevations ranging from 7 to 12 feet. Near Cedar Point, at the junction of Mobile Bay and Mississippi Sound, a high water mark of 13.5 feet was recorded at the Cut-Off Bridge on Alabama Highway 163. The high water elevations along the western Alabama coast near Bayou La Batre and Coden were 9 to 10 feet.

- On the extreme southern tip of mainland Mobile County, known as Cedar Point, State Highway 163 sustained considerable damage from erosion. A section of the road about 200 feet in length was washed away (see Fig. 2.36). The Heron Bay Cut-Off Bridge was destroyed (see Fig. 2.37).

- The Dauphin Island Bridge from Cedar Point south to the island was destroyed by the 145 mph wind and storm surge. The road on the causeway portion of bridge sustained major damage, and 135 spans of the bridge were forced into the water on the east side of the bridge. The remainder of the bridge was so severely damaged that it had to be demolished (see Fig. 2.38).

- At the north end of Mobile Bay, two spans of the I-10 eastbound entrance ramp at highway US 90 were lifted and moved on their support bents over six feet as shown in Fig. 2.39.

- Frederic's storm surge at the Mobile Bay I-10 Bridge was approximately 11.7 ft which is the second largest (only Katrina's at 12.4 ft was higher) in recorded history.
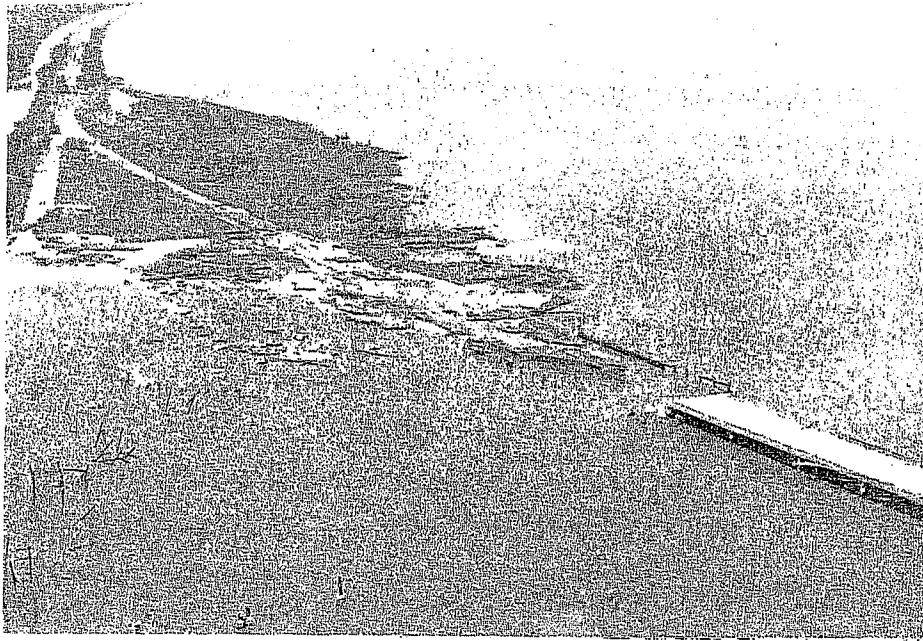
Fig. 2.36 A Section of the Dauphin Island Bridge, South from the Mainland at
Cedar Point, was Destroyed and the Road Washed Away [12].
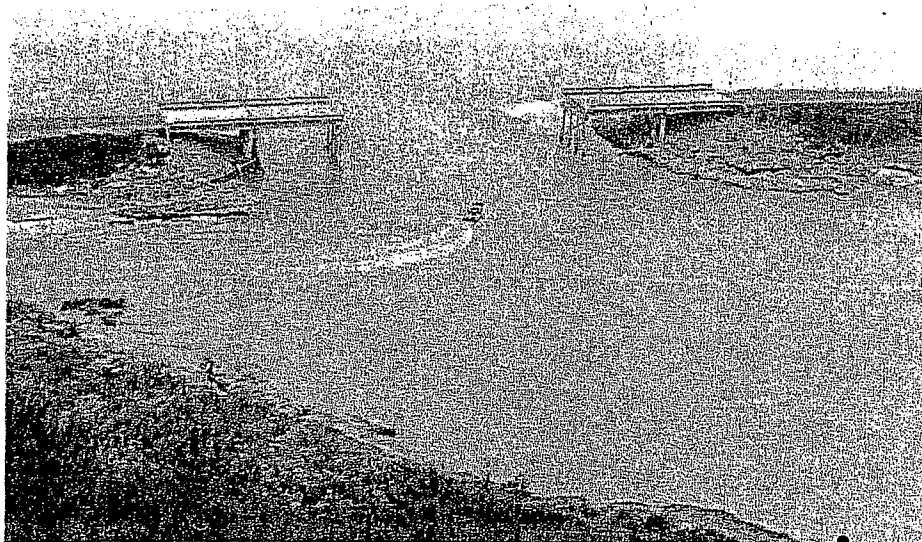
Fig. 2.37 The Midspan of the Cut-Off Bridge Near Cedar Point on Ala. Hwy. 163
was Destroyed by a 13 Foot Storm Surge [12].
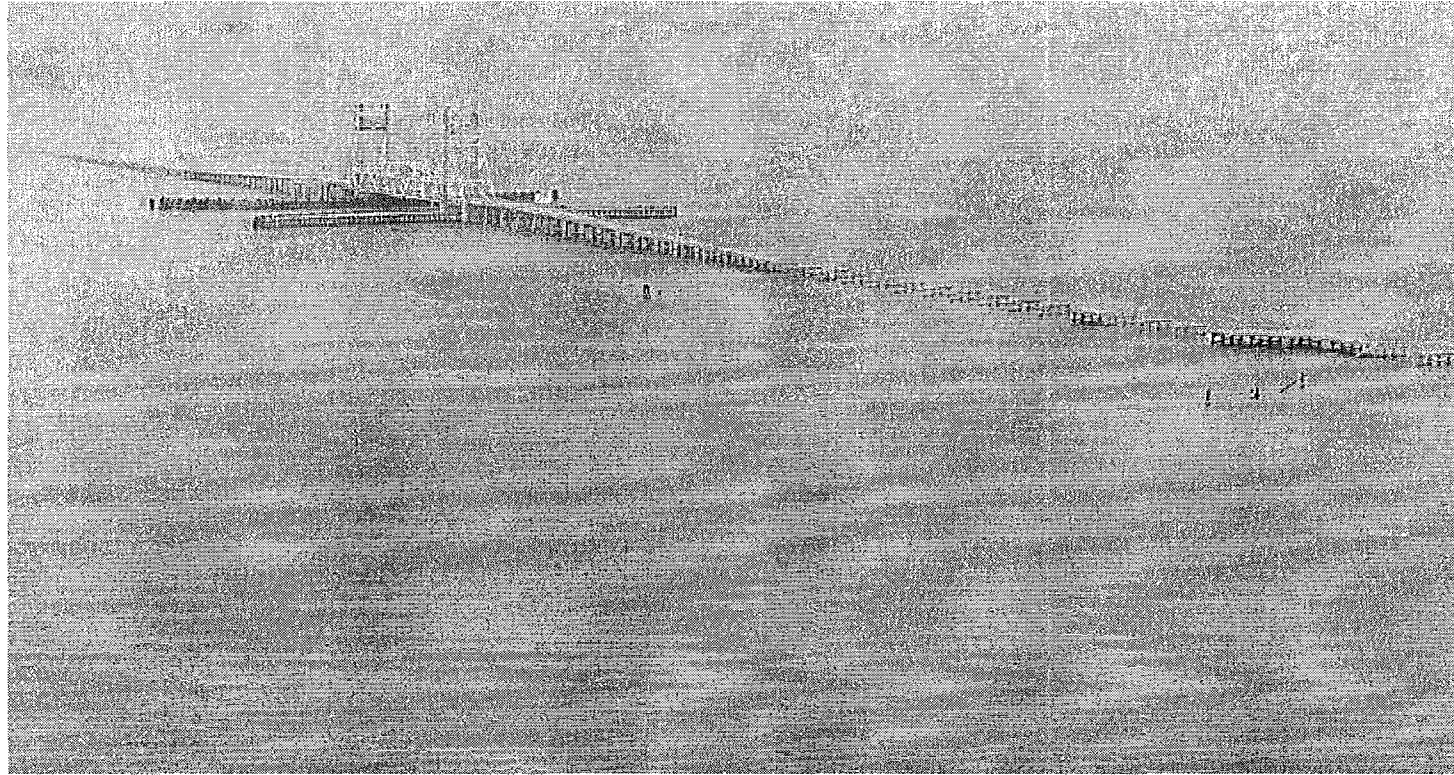
Fig. 2.38 Aerial View of Dauphin Island Bridge Showing Damage Near Lift Span
at Intersection of Gulf Intracoastal Waterway Channel [12].
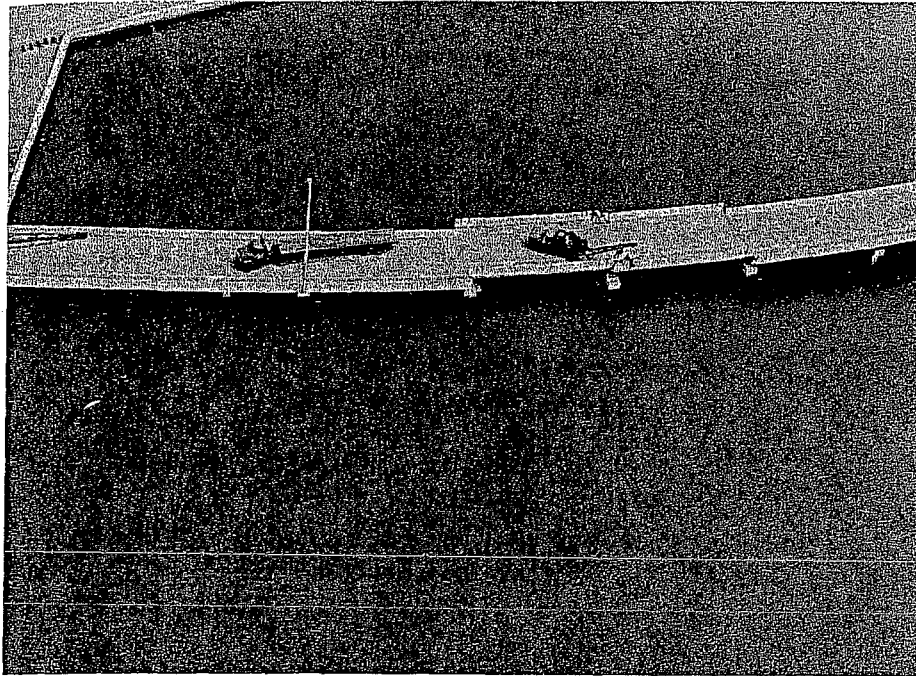
Fig. 2.39 Spans of I-10 Eastbound Entrance Ramp at Hwy. U.S. 90 were Lifted and Displaced over Six Feet on their Support Bents [12].

2.2.4 Basic Definitions and Characteristics of Ocean Waves.

A full description of surface waves requires consideration of many physical aspects such as bottom conditions, surface conditions, and flow and fluid conditions. As a result, there is no single analytic solution that fully describes all wave conditions. Rather, there are a number of solutions that are applicable over certain ranges of conditions.

The primary variables used to describe waves are the wave height H, which is the crest to trough vertical distance; the wave period T, which is the time between the passage of successive wave crests; the wave length L, which is the horizontal distance between wave crests; and the still water depth h or d, which is the vertical distance from the bottom to the free surface if no waves are present. A dimensionless ratio commonly used to express wave profile characteristics is the wave steepness, defined as H/L. The speed at which the wave crest moves is the wave celerity c. A definition sketch of these primary surface wave parameters is presented in Fig. 2.40.

A more general and descriptive surface wave sketch is shown in Fig. 2.41. In this figure, the free surface profile η is the vertical distance measured from the still water level (SWL). The simplest and probably the most widely used wave analytic representation/theory for surface waves is linear wave theory (LWT). For LWT, the height of the crest a_c and the depth of the trough a_t in Fig. 2.41 are both equal to $H/2$ and are centered on the SWL. In other wave theories and often in nature, this is not necessarily the case and the crest height is greater than the trough depth, and the average position of the free surface is not the same as the still water level. In LWT, the wave free water surface is assumed to be a simple sinusoidal function as shown below:

$$\eta = \frac{H}{2}\cos(kx - \omega t)$$

- **Height, Length, Period:**

MEAN SEA LEVEL

H = HEIGHT
L = WAVELENGTH
T = PERIOD
d = DEPTH

Properties of an ideal wave.
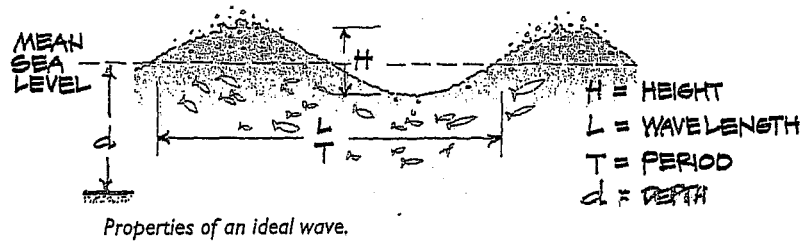
- **Speed of Propagation (Celerity, c):**

$$c = \frac{L}{T} \qquad \text{(in deep water)}$$

$$c = \sqrt{gd} \qquad \text{(in shallow water)}$$

- **Energy (E):**

$$E \propto H^2$$

For wave heights of

$$H = 5 \text{ ft}$$

$$H = 10 \text{ ft}$$

the 10 ft wave has 4 times the destructive potential of the 5 ft wave.

Fig. 2.40   Primary surface wave properties

Thus, the wave celerity is

$$c = \frac{L}{T} = \frac{\omega}{k}$$

where k is the wave number and is $k = 2\pi/L$.

For LWT to be valid, $H/L \ll 1$ or, in other words, the wave height must be nearly zero with respect to the wave length. This is a very severe assumption, but is invoked because it allows the development of a rather simple analytical description of the waves. It should be noted that the near-shore sea state during hurricane conditions is such that LWT is not valid.

As waves become steeper, the crests become higher and more peaked and the troughs become shallower and longer as shown by the dashed line in Fig. 2.42. The amplitude of the crest may be much larger than the amplitude of the trough. As a result, the forces associated with the crest are much larger. Also, for extreme wind conditions with resulting extreme wave conditions (such as hurricane conditions), the wave H/L is no longer small since H gets larger and L gets smaller near the shore. For these conditions, more sophisticated (and more complicated) wave theories must be employed. The two most common nonlinear analytical wave theories are the Stokes and cnoidal theories.

Coastal engineers and researchers have found cnoidal wave theory to be most applicable for steep waves in shallow water. Figure 2.43 shows a sketch of cnoidal waves in shallow water and this basically fits the profile of waves at the beach in stormy weather, and is the condition that exists at most coastal bridges during hurricane storm conditions. Figure 2.44 illustrates LWT, Stokes 5th order, and 3rd-order cnoidal wave
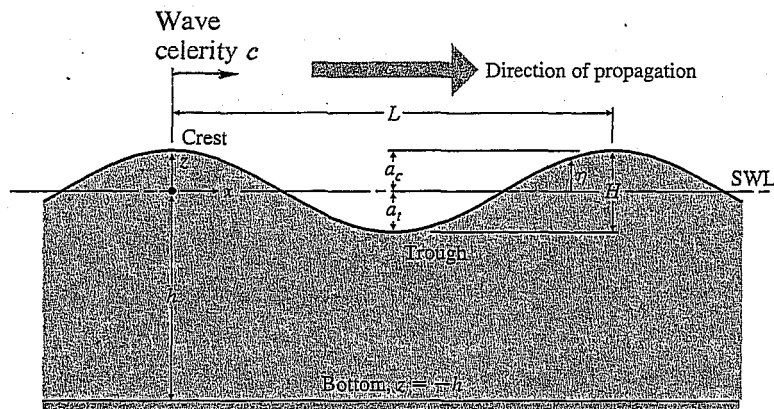
Fig. 2.41 Surface wave definition sketch
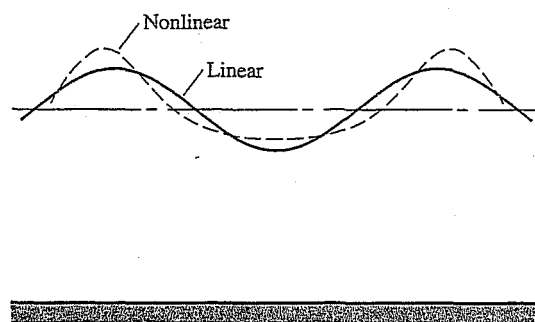
Fig.2.42 Comparison of linear and nonlinear free-surface profiles
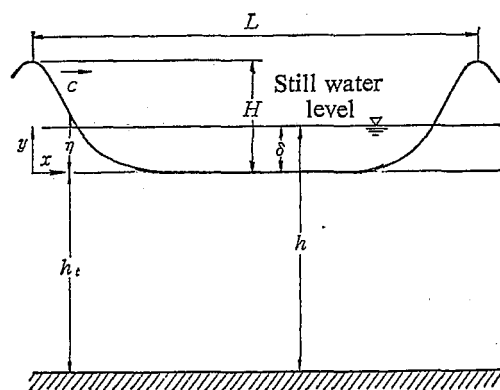
Fig. 2.43 Sketch of cnoidal wave

theory free surface profiles for H = 1 m, T = 10 sec, and h = 6.5 m. For shallow water, Stokes theory overpredicts the wave amplitude. In fact, in shallow water, LWT may yield more accurate estimates than Stokes. Figure 2.45 indicates the regions in which these three analytical theories provide the best estimate, based on errors in the dynamic free surface boundary condition. This curve is for reasonably steep waves with H/H_B > 1/4, where H_B is the breaking wave height. For shallow conditions, cnoidal wave theory provides the best estimates, and for deep water Stokes 5th yields the more accurate results. Note, however, that over a range of intermediate water depth, LWT provides the best estimates.
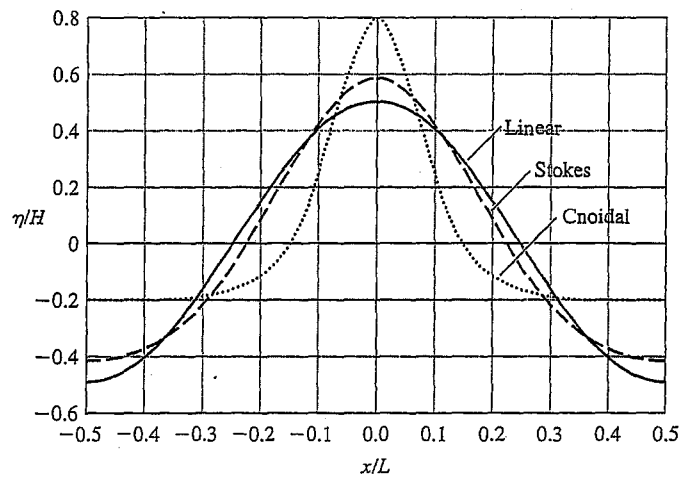
Fig. 2.44 Comparison of LWT, Stokes 5th order, and 3rd-order cnoidal wave theories for H = 1m, T = 10 sec, and h = 6.5 m
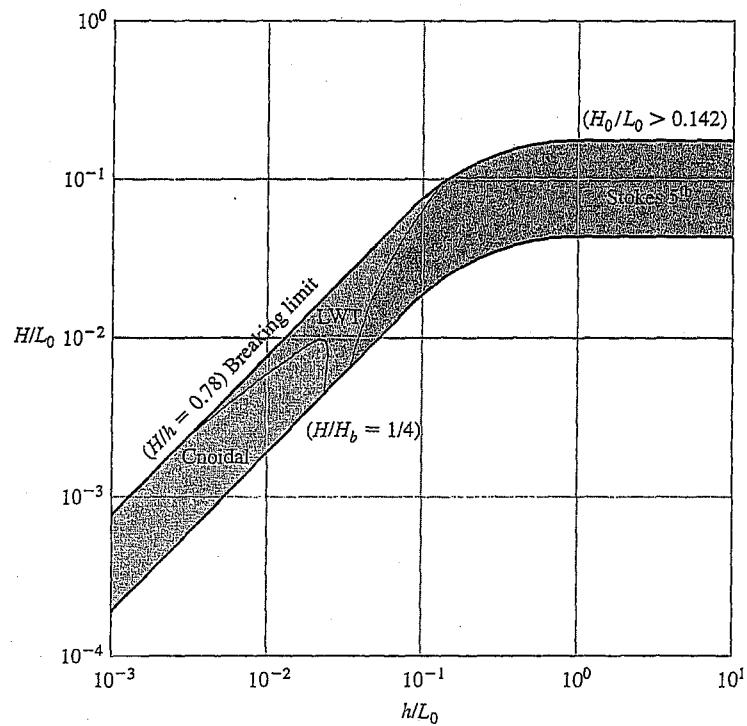
Fig. 2.45 Periodic analytic wave theories providing the best fit to the dynamic free-surface boundary condition. Adapted from *Evaluation and Development of Water Wave Theories for Engineering Applications* by R.G. Dean, courtesy of U.S. Corps of Engineers, Vols. I and II, 1974.

The free surface profile of wind-generated water waves is rarely, if ever, simple sinusoidal with constant amplitude/height and period as in LWT. Actual wave observations include many different wave heights, periods, and directions that are superimposed to yield the local wave conditions as shown in Fig. 2.46. However, for design some simplifying assumptions are required.

A common way of treating actual or irregular waves is to express them by representative wave characteristics in a statistical sense. To do this, it is necessary to define the wave height and period from a series of wave records such as those shown in Fig. 2.46. The zero-up crossing method is the one generally employed and this method uses the time when the surface wave profile crosses the zero (still water) level in the upward direction. An individual wave height is defined by the vertical difference between the maximum and minimum levels with adjacent zero-up cross points, and the corresponding wave period is defined by the interval of the two crossing points.

To determine the statistically representative wave by using the height and period data obtained by the above procedure, four methods are normally used to define the representative wave:

1) The maximum wave (H_{max}, T_{max}), which corresponds to the maximum height in a given wave group;

2) The one-tenth highest wave ($H_{1/10}$, $T_{1/10}$), which corresponds to the average of the heights and periods of the one-tenth highest waves of a given wave group;

3) The significant wave (H_s, T_s or $H_{1/3}$, $T_{1/3}$), which corresponds to the average of the heights and periods of the one-third highest waves of a given wave group;

4) The mean wave ($\overline{H}$, $\overline{T}$), which corresponds to the mean wave height and period of a given wave group.
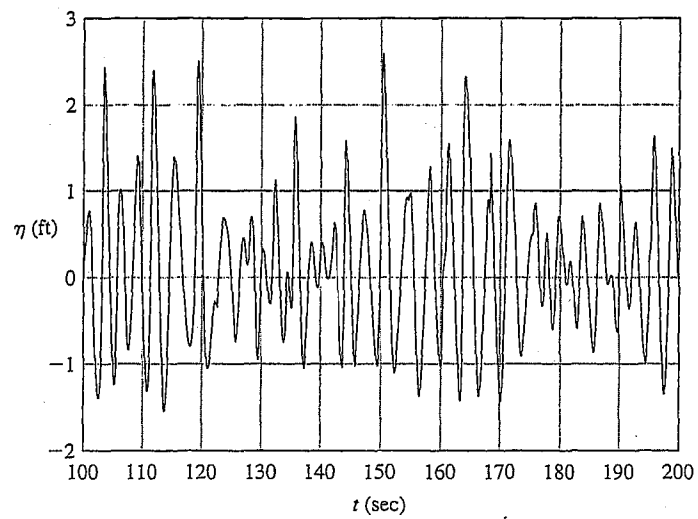
a. Measured free-water surface profile
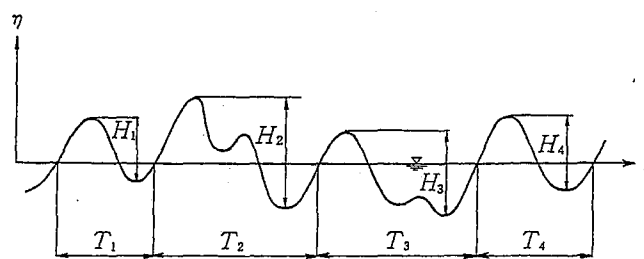
b. Definition sketch of surface profile

Fig. 2.46 Measured and schematic of a free-water surface profile
of ocean waves

Among these statistically representative waves, the significant wave with wave height, H_s, is most frequently used in the coastal engineering field.

Assuming a Rayleigh wave height distribution, H_s may be further defined in approximate relation to other height parameters of the statistical wave height distribution in deep water as follows:

$H_{10} \approx 1.27\ H_s$ = average of highest 10 percent of all waves

$H_5 \approx 1.37\ H_s$ = average of highest 5 percent of all waves

$H_1 \approx 1.67\ H_s$ = average of highest 1 percent of all waves

The maximum wave height, H_{max}, cannot be determined as a definite value, but a most probable value can be estimated. However, to directly design for this value would be compounding too many low probability events, e.g., the probability of a major hurricane hitting the bridge site, the waves moving perpendicular to the bridge, the height of wave being at H_{max} over a full span length, etc. Also, the bridge, if properly designed and/or retrofitted, will have inherent ductility and/or be able to move somewhat to withstand the super H_{max} wave. Thus, for design, it is recommended that coastal bridges be designed/retrofitted for wave forces corresponding to

$$\tilde{H}_{max} = 1.4\ H_s$$

and incorporate ductility, small movement capability, and some venting in the design/retrofit to allow the bridge to withstand the superwaves and some wave impact loadings. In so doing, we are designing for approximately the average of the highest 4 to 5 percent of all of a hurricane's waves.

Regarding wave period, Horikawa (13), indicates that observation data at

Nagoya Harbor give the results $T_{1/10} / T_{1/3} = 0.99 \pm 0.06$ and $T_{1/3} / \bar{T} = 1.07 \pm 0.08$.

Thus, we can assume statistically that

$$T_{1/10} \approx T_{1/3} \text{ and } T_{1/3} \approx 1.1 \bar{T}$$

Or,

$$\bar{T} \approx \text{constant.}$$

A cork in the path of an ocean wave moves forward with the crest of the wave,

but then moves *backward* in the trough until it rises and moves forward with the next

crest. Waves move water particles up and down in circular orbits (deep water) or

elliptical orbits (shallow water) as the wave itself moves forward with a speed/celerity, c.

Figure 2.41 shows the pressure fields and water particle movement in and with the

passage of a deep water wave. Note in Fig. 2.47a that the pressure at a particular point

and time is essentially hydrostatic, i.e.,

$$p_p = \gamma d_p$$

where d_p is the depth of the point from the free
water surface at the particular time

where γ is the unit weight of water

The arrowed vectors on the free water surface in Fig. 2.47b show the direction of select

surface particle movements at the time of the surface profile snapshot. Figure 2.48

shows the transition of the water surface profile and water particle orbits as a surface

wave moves from deep to shallow water (shore).
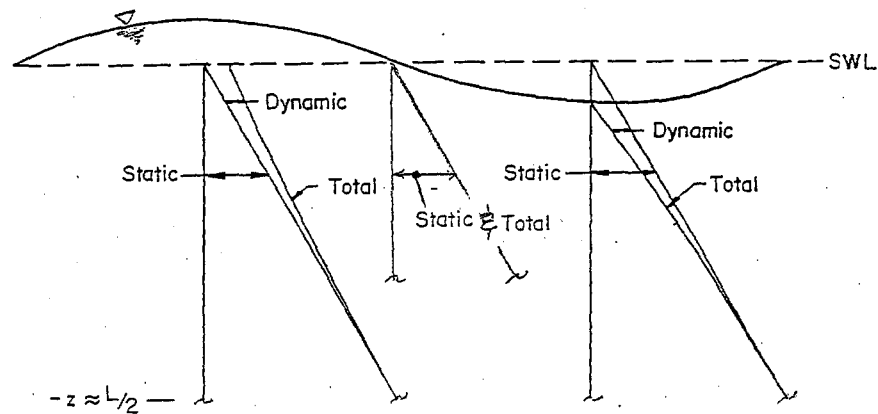
a. Pressure fields
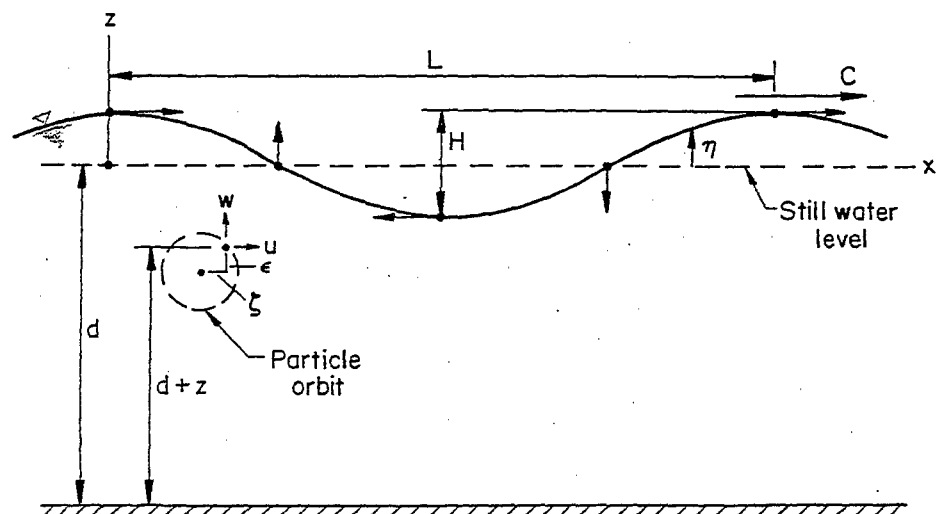
b. Definition of wave parameters and water particle movements

Fig. 2.47 Deep water waves, pressure fields, and water particle movements

2-55
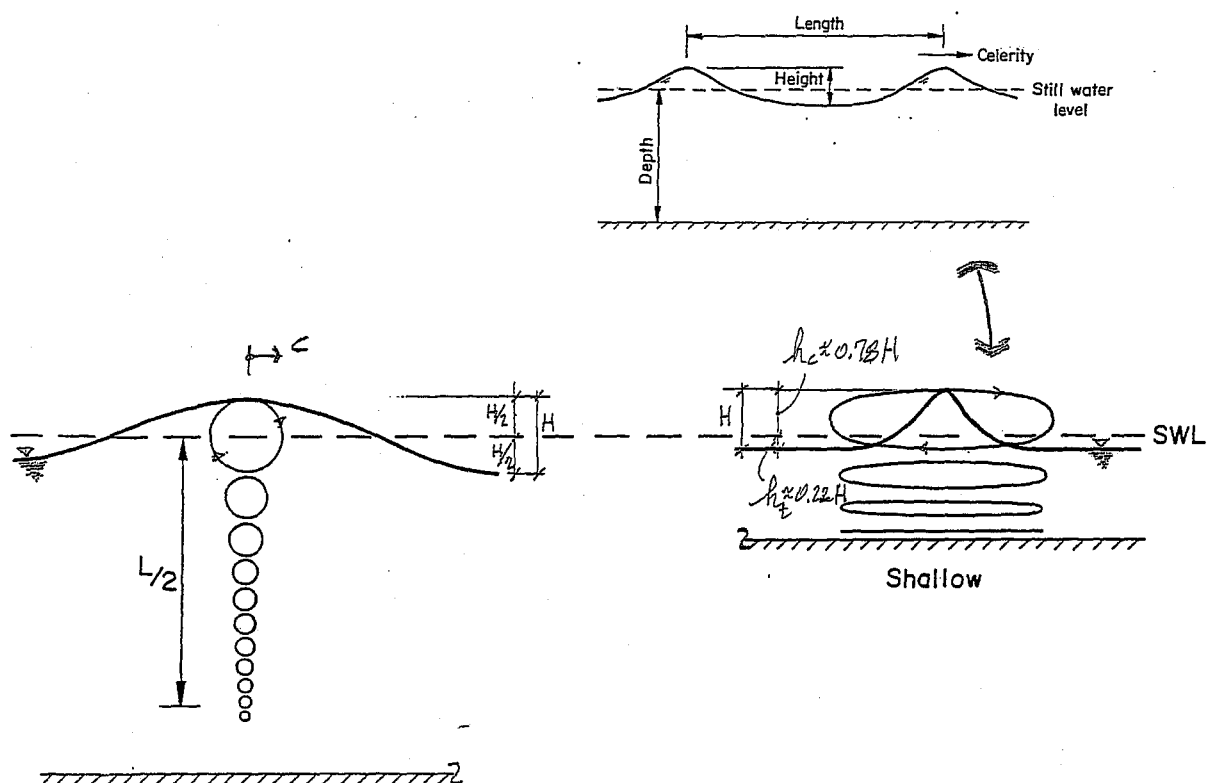
Fig. 2.48   Transition of surface profile and particle orbits in going from deep to shallow water

Wave Transformation due to Water Depth Shoaling. Important wave transformations and relationships as waves move into shallow water (where coastal bridges are typically located) are presented below. These equations and relationships were extracted from Ref [13]. When a wave enters shallow water, the height, length, and celerity change. If we assume that the ocean bottom slope has a negligible effect on the wave characteristics, then the waves at any location on a sloping bottom can be described by small amplitude wave theory, (LWT), from which the wave length and celerity are

$$L = \frac{gT^2}{2\pi}\tanh\frac{2\pi h}{L} \qquad (2.1a)$$

or for deep water,

$$L_0 = \frac{gT^2}{2\pi} \quad \Longrightarrow \quad L_0 = 5.12T^2 \text{ (in ft.)} \qquad (2.1b)$$

and,

$$c = \frac{L}{T} = \frac{gT}{2\pi}\tanh\frac{2\pi h}{L} \qquad (2.1c)$$

or for deep water,

$$c_0 = \frac{gT}{2\pi} \quad \Longrightarrow \quad c_0 = 5.12T \text{ (in fps)} \qquad (2.1d)$$

The subscript 0 in Eqns (2.1b) and (2.1d) indicates values in deep water. From Eqs. (2.1) we obtain

$$\frac{L}{L_0} = \frac{c}{c_0} = \tanh\frac{2\pi h}{L} \qquad (2.2)$$

Equation (2.2) can be rewritten in the form

$$\frac{h}{L_0} = \frac{h}{L} \tanh \frac{2\pi h}{L}$$

(2.3)

from which the relative water depth with respect to the deep water wave length h/L_0 is correlated with the relative water depth h/L. That is to say, the wave length L at the water depth h is determined from the water depth and deep water wave length, where the latter can be calculated from the wave period.

Equation (2.1a) above is called the dispersion equation and defines the relationship among the wave frequency, wave number, and water depth. It may be written using either the wave number $k = 2\pi/L$ and wave frequency or the wave length and wave period, i.e.,

$$\omega^2 = gk \tanh(kh) \quad \text{or} \quad L = \frac{gT^2}{2\pi} \tanh\left(\frac{2\pi h}{L}\right)$$

(2.4)

If the argument of the tanh term in Eq. (2.4) is large (which corresponds to h/L being large), then tanh $\rightarrow$ 1. This is referred to as a deep water wave (which is usually characterized by $h/L > 0.5$) for which the wave length is given by Eqn (2.1b).

If the argument of the tanh term in Eqn (2.4) is small (which corresponds to h/L being small), then tanh (x) $\rightarrow$ x. For this case,

$$L = \frac{gT^2}{2\pi}\left(\frac{2\pi h}{L}\right) \quad \Longrightarrow \quad L^2 = ghT^2 \quad \Longrightarrow \quad L = \sqrt{gh}\, T$$

(2.5)

This is referred to as a shallow water wave which is usually characterized by $h/L < 0.05$.

Between the above extreme conditions, i.e., $0.05 < h/L < 0.5$, the depth is considered to be intermediate and a trial-and-error solution must be performed on the transcendental equation (Eqn (2.1a)) to determine the wave length.

In the literature (15), a simple approximate analytical equation for L is given as

$$L = (2\pi h L_0)^{1/2}\left(1 - \frac{\pi h}{3L_0}\right)$$

(2.6)

This equation has a relative error of less than 2% when $h/L_0 < 0.3$ (Tedesco) and this should always be the case for coastal bridge sites.

It can be noted from the above equations that as a wave propagates into shallow water, its wave length and celerity decrease. For example, a wave with a period of 10 sec has the wave lengths and celerities ($c = L/T$) shown in Table 2.2 as it propagates into shallow water.

Table 2.2 Approximate Changes in *L* and *c* with Water Depth

Water Depth (ft)	Water Length (ft)	Celerity (fps)	*h/L*
256	512	51.2	0.50
100	451	45.1	0.22
50	360	36.0	0.14
20	243	24.3	0.082
10	176	17.6	0.057
5	125	12.5	0.04

Note in Table 2.2, that only the 5 ft water depth would be characterized as shallow water, i.e., *h/L* <0.05. It should be noted that in linear wave theory (and most other wave theories) the period is assumed to remain constant, which is consistent with observations. For hurricane storm conditions wave periods are usually in the range of 3s < *T* < 10s.

Horikawa (13) gives the following empirical relationship for estimating shallow water wave periods:

$$T_{1/3} = 3.86\sqrt{H_{1/3}} \qquad \text{(units in m and sec)} \qquad (2.7)$$

where $H_{1/3}$ and $T_{1/3}$ are the significant wave height and period respectively.

Let's now determine the wave height at a given water depth. The average wave energy transported through a vertical section with unit crest width per unit time, $\overline{\dot{W}}$, is given by

$$\overline{\dot{W}} = \overline{E}c_g = \overline{E}cn \qquad (2.8a)$$

where c_g is the speed at which a group of waves propagate and $n = c_g/c$ and is less than 1.0.

Assuming that $\overline{\dot{W}}$ is conserved in the process of wave propagation, we take the reference section in deep water, and hence, $\overline{\dot{W}} = \overline{\dot{W}}_0$, that is,

$$\frac{1}{8}\rho g H^2 c n = \frac{1}{8}\rho g H_0^2 c_0 n_0 \qquad (2.8b)$$

From Eq. (2.8b), the following important relations are obtained,

$$\left.\begin{array}{l} \dfrac{H}{H_0} = \sqrt{\dfrac{1}{2n}\dfrac{c_0}{c}} = K_s \\[4mm] n = \dfrac{1}{2}\left[1 + \dfrac{4\pi h/L}{\sinh{(4\pi h/L)}}\right] \end{array}\right\} \qquad (2.9)$$

where K_s is called the shoaling coefficient. The parameters K_s and n are also functions of h/L, hence h/L_0. Figure 2.49 shows the variations of L/L_0, c/c_0, K_s, n, and h/L with change of h/L_0. In the range of $h/L_0 < 0.01$, the following approximations to the above equations and relationships can be used:

$$\left.\begin{array}{l} \dfrac{H}{H_0} \approx \left(8\pi\dfrac{h}{L_0}\right)^{-1/4} \\[4mm] n \approx 1 \\[4mm] \dfrac{c}{c_0} \approx \left(2\pi\dfrac{h}{L_0}\right)^{1/2} \\[4mm] \dfrac{h}{L} \approx \left(\dfrac{1}{2\pi}\dfrac{h}{L_0}\right)^{1/2} \end{array}\right\} \qquad (2.10)$$

It should be noted that the above equations and relationships are based on small amplitude wave theory (LWT) and should not be directly applied to relatively steep waves which normally occur near the coastline in hurricane conditions. However, the equations can be used to obtain quick first estimates of the wave parameter values and for determining deep water values which are sometimes used in shallow water empirical equations. The variations of wave height with water depth in shallow water for cnoidal waves, which are the typical near-shore wave types, where determined by Iwagaki and are shown in Fig. 2.50. The $H_0/L_0 = 0$ wave in Fig. 2.44 corresponds to the relation given in Eqn (2.9).
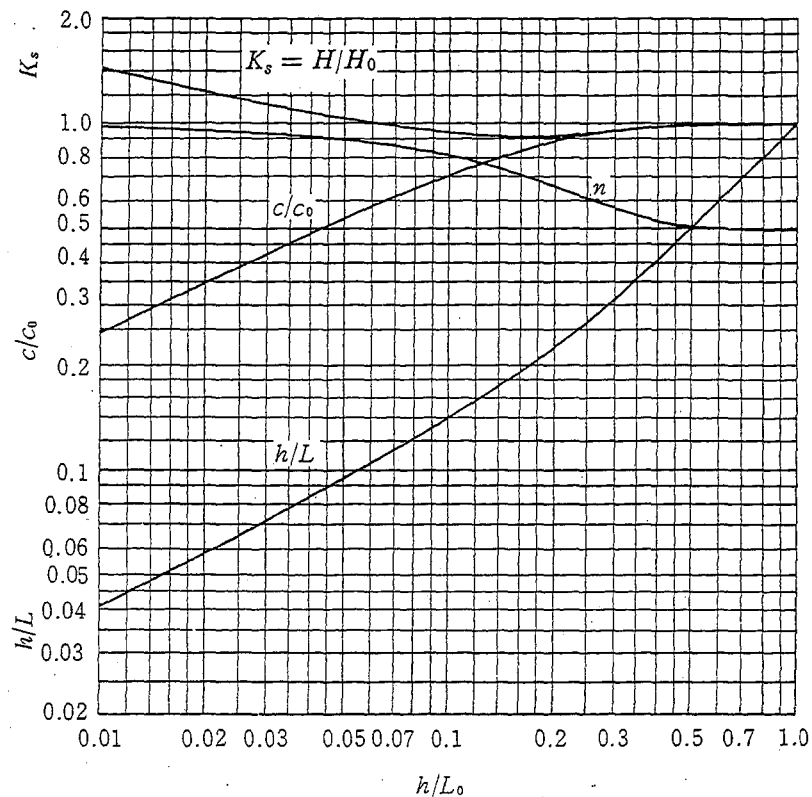
Fig. 2.49 Wave properties in shallow water (after *Hydraulic Formulae*, JSCE, 1971).
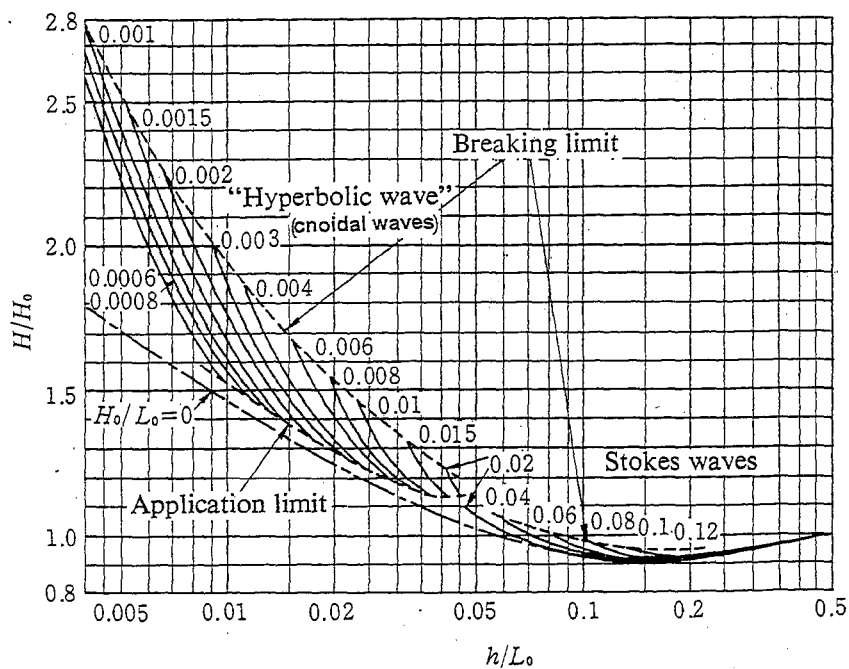
Fig. 2.50 Variation of wave height due to water depth change, where "hyperbolic wave" means an approximate expression of cnoidal waves obtained by Iwagaki (after Iwagaki, 1968).

Breaking Waves. The literature and our experiences at coastal beaches tell us that breaking waves exert very large forces on objects in their path including coastal bridges. Thus, let us discuss and examine these waves in a little more detail. Waves proceeding from deep to shallow water gradually decrease in length, and increase in height, and therefore their steepness (H/L) increases. At some point, primarily determined by their steepness and the sea bottom slope, they break at a certain water depth.

Breaking waves are classified into spilling breakers, plunging breakers, and surging breakers, as illustrated by two different authors in Figs. 2.51 and 2.52. The type of breaker is primarily determined by the wave steepness and the sea bottom slope as shown in Fig. 2.53. Figures 2.54 and 2.55 show diagrams developed by Goda from extensive field and laboratory data for estimating breaking water depth, h_b, and breaking wave height, $'H_b$, respectively based on deep water wave steepness, H_0/L_0, and sea bottom slope.
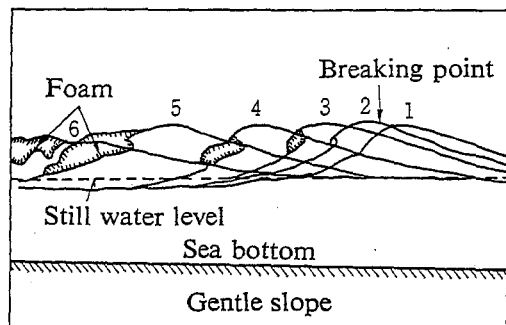
(a) Spilling breakers
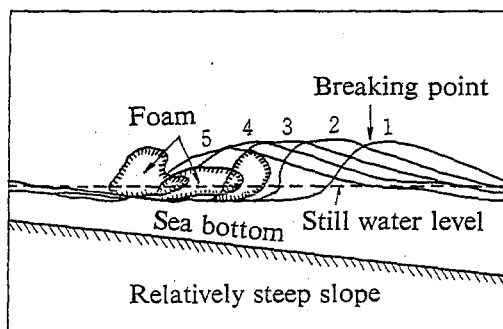
(b) Plunging breakers
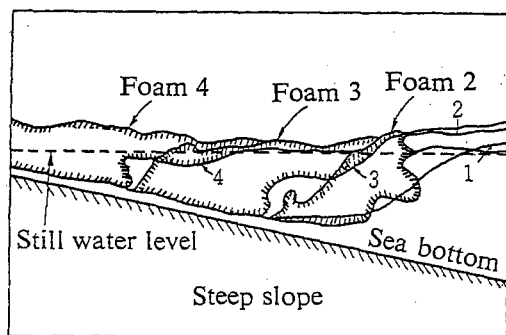
(c) Surging breakers

Fig. 2.51 Classification of breaking wave patterns (after Wiegel, 1953).
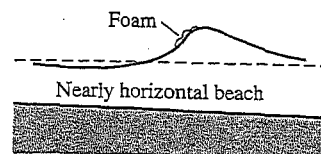
(a) spilling
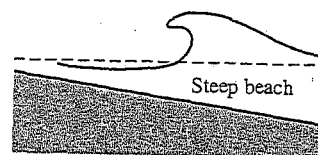
(b) plunging
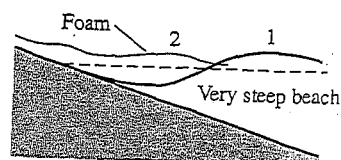
(c) surging

Fig. 2.52 Common types of breaking waves (from Ref. [13])
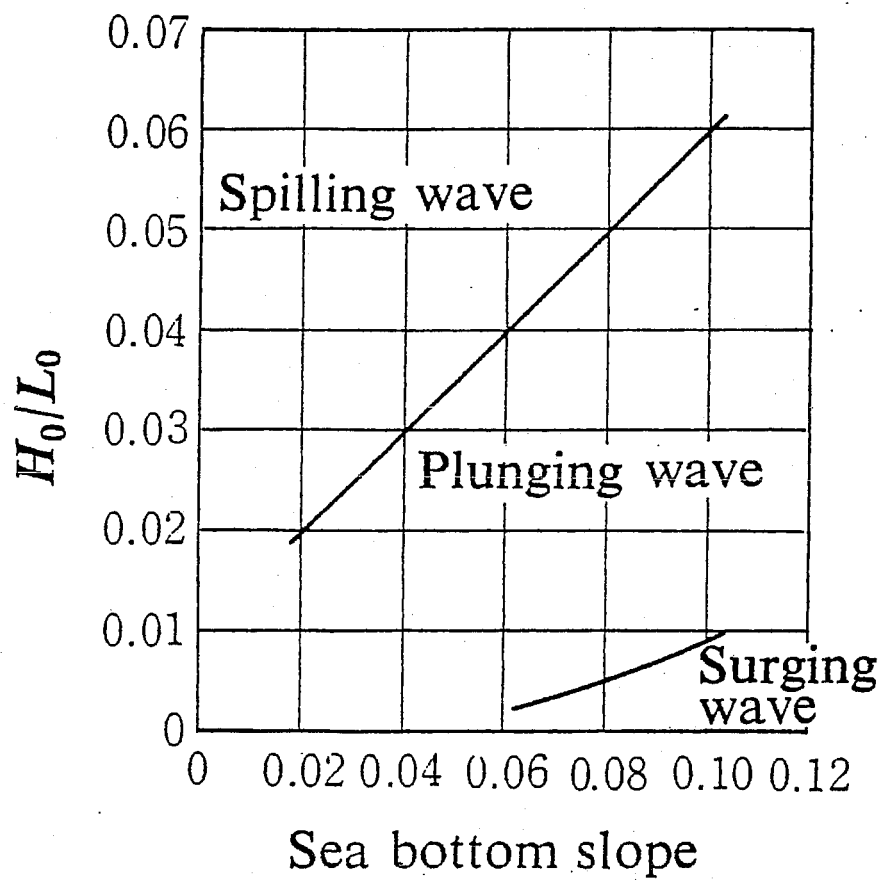
Fig. 2.53 Classification of breaking patterns
(after *Hydraulic Formulae*, JSCE, 1971).
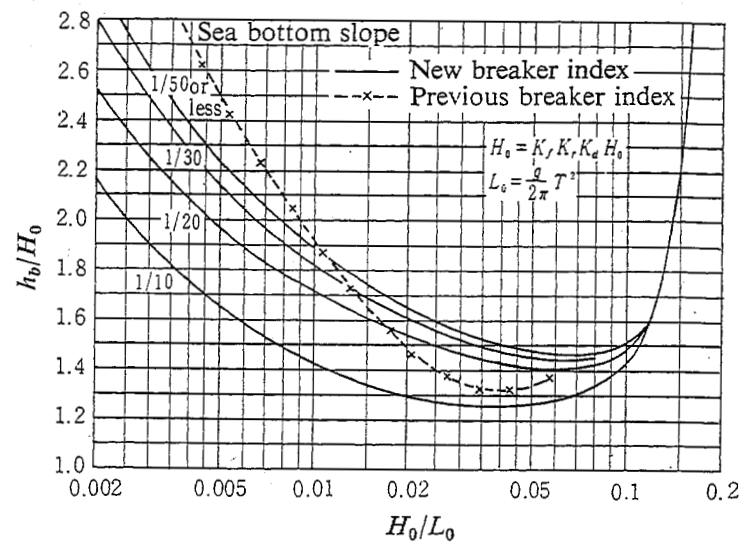
Fig. 2.54 Wave breaking depth (after Goda, 1970).
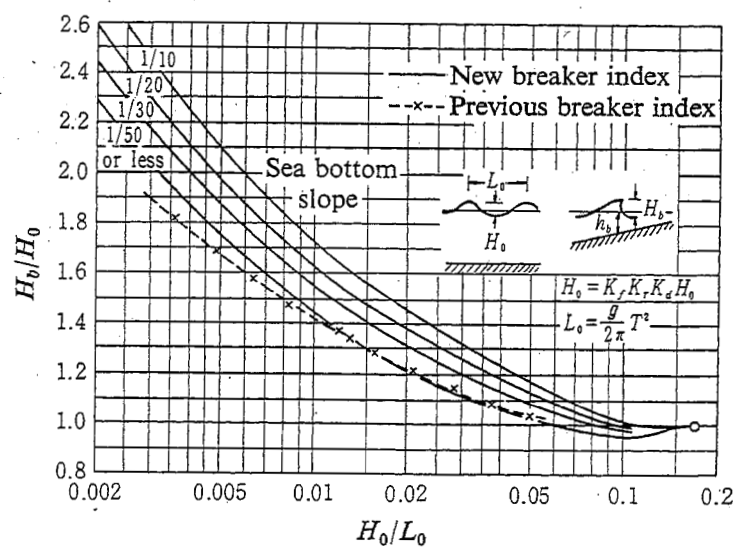
Fig. 2.55 Wave breaking height (after Goda, 1970).

Waves normally break when the water depth gets shallow enough to significantly slow the propagation speed and the trailing waves "over-run" those in front and/or high winds act on the back of the upper portion of the wave and topples it forward. However, waves can also break in water of intermediate depth and in deep water. This is important because a coastal bridge that was initially in shallow water will probably later be in intermediate depth water due to a hurricane's storm surge.

In an analysis of wave forces on structures, a distinction is made between the action of *nonbreaking, breaking,* and *broken* waves.

- Nonbreaking waves are seaward of surf zone

- Breaking waves are in surf zone

- Broken waves are shoreward of surf zone

- Forces due to nonbreaking waves are primarily hydrostatic and can easily be assessed.

- Forces due to broken waves are hydrostatic forces plus the forces due to dynamic pressure exerted by water particles now moving forward/shoreward (rather than in orbits) with the approximate velocity of the wave propagation as of when the wave broke.

- Forces due to breaking waves are primarily from dynamic pressures/inertia forces of a mass of water slamming into a structure and the hydrostatic forces may be negligible in comparison with these forces.

Figure 2.56 shows two breaking waves as they are breaking. Note in the figure that the wave doesn't break all along its length at the same time, the significant variation in wave height along the length of the wave, and the obvious sizable force that the waves could exert on a structure. Wave forces on structures and coastal bridges will be discussed more fully in later chapters of the report.

2-68
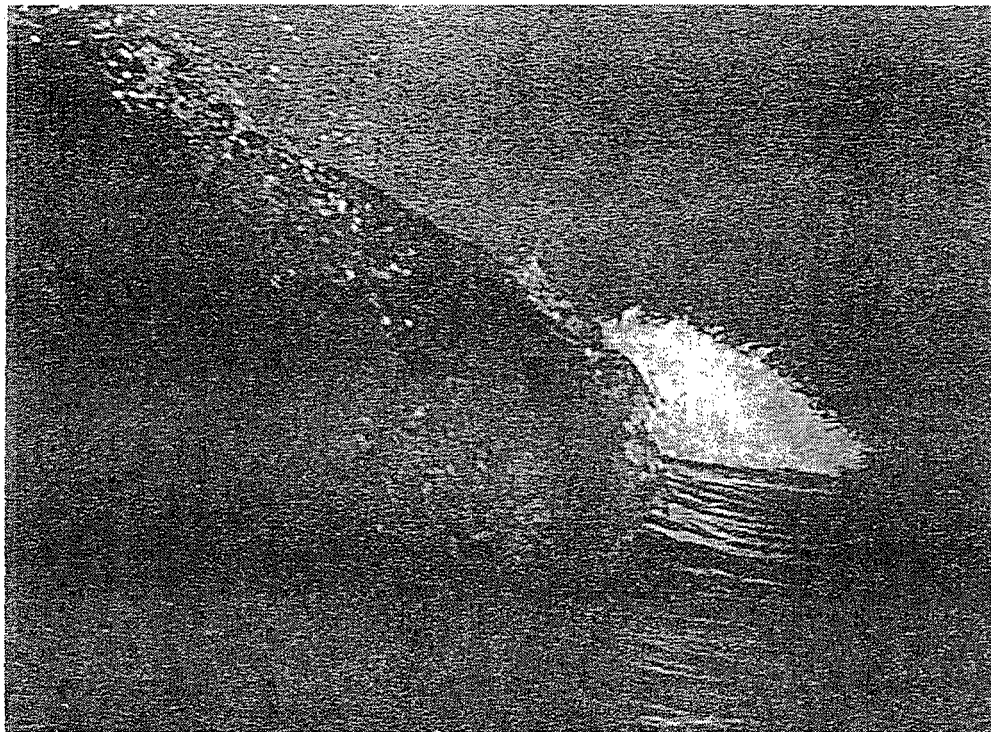
a. Large breaking wave at Dam Neck, Virginia

b. Large breaking wave at unknown coastline

Fig. 2.56   Photographs of two large breaking waves

2-69

Tidal Phenomena. The sea surface rises and falls quite regularly once or twice a day. This phenomenon is called tidal motion and is caused by the continuous change in the position of the sun and the moon with respect to the earth. The sea level reaches its maximum height at high tide and its lowest height at low tide. The vertical distance between high and low tide sea levels is called the tidal range. Because the tide is generated by the motion of the earth-moon-sun system, and is completely independent of sea level changes induced by meteorological conditions, the tide is sometimes referred to as the astronomical tide. It should be noted that a hurricane's storm surge is caused by meteorological factors such as atmospheric pressure drops and high winds and can be referred to as a meteorological tide.

To understand the tide-generating mechanism, consider the earth-moon system shown in Fig. 2.57. In this figure, the magnitude and direction of the tide-generating forces are defined as the difference between the attractive and centrifugal forces at given points on the surface of the earth. The relative distribution of the tide-generating forces along a meridian is shown in Fig. 2.58. The semi-diurnal tidal effect of the sun is only about one-half as large as that of the moon (due to its far greater distance from the earth).

⟹ attractive forces

⟹ centrifugal forces

⟹ tide generating forces
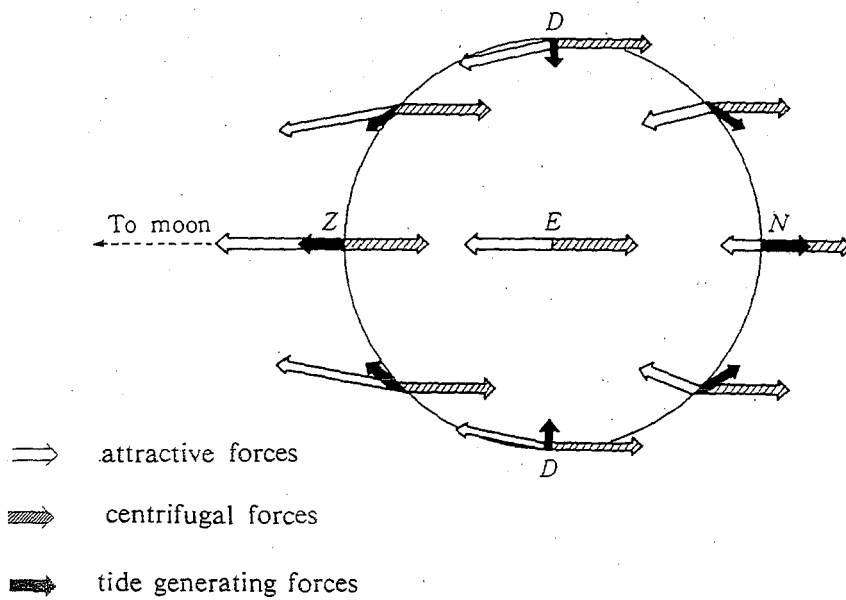
Fig. 2.57 Intensity and Direction of Earth-Moon System
Tide-Generating Forces [13].
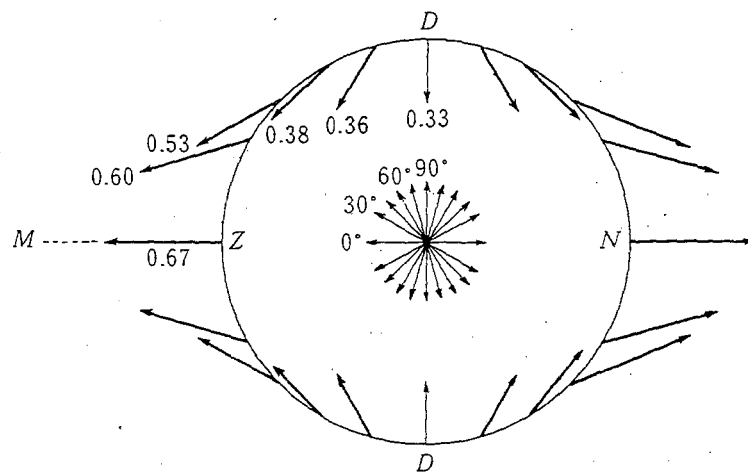
Fig. 2.58 Relative Distribution of Tide-Generating Forces Along a Meridian
Section of the Earth [13].

Most tidal ranges around the world are considered semi-diurnal, meaning there are two high and two low tides per tidal day. The tidal range for Mobile Bay is classified as diurnal, meaning there is only one high and one low tide in a tidal day. Diurnal tides are found only in certain parts of the world, one of which being along the northern coast of the Gulf of Mexico. Diurnal tides are known for producing higher tidal ranges than that of semi-diurnal tides. In addition to these higher than normal tidal ranges, spring and neap tides occur along with the normal tidal cycle. Spring tides are formed during the new and full moon phases (the earth, moon, and sun form a straight line with one another) therefore enhancing the tidal forces produced by each. This phenomenon produces a greater than average tidal range. Neap tides are formed during the first and third-quarter phases of the moon (the moon and sun are at right angles to the earth). The tidal forces of each are partially cancelling and therefore produce lower tidal ranges. Figures 2.59 and 2.60 show graphical representations of the occurrence of spring and neap tides respectively. A general spring and neap tide range for the location around the Mobile Bay I-10 Bridge site are 1.5 ft. and 1.0 ft respectively relative to Mean Sea Level.
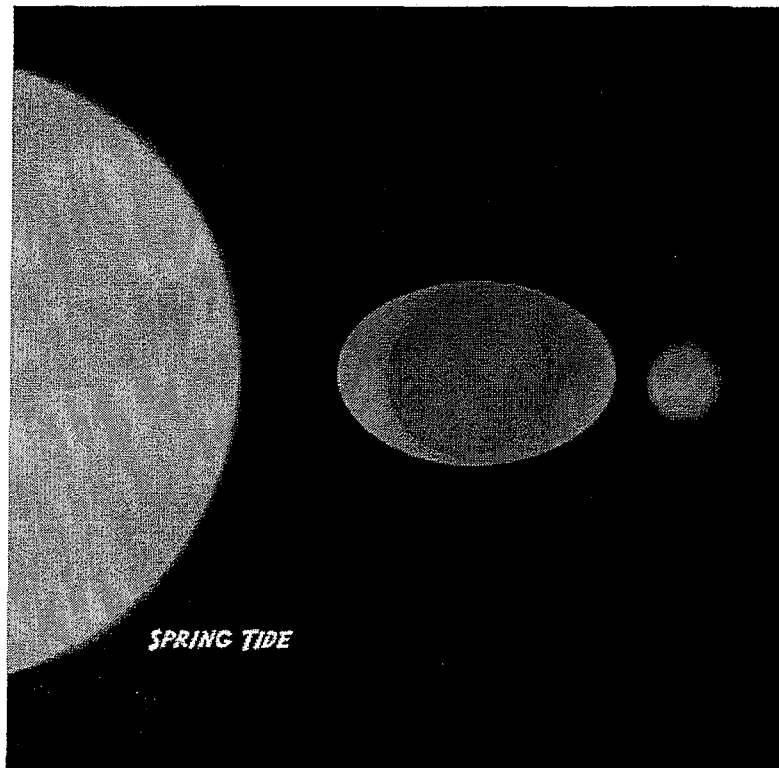
Fig. 2.59 Depiction of Spring Tide
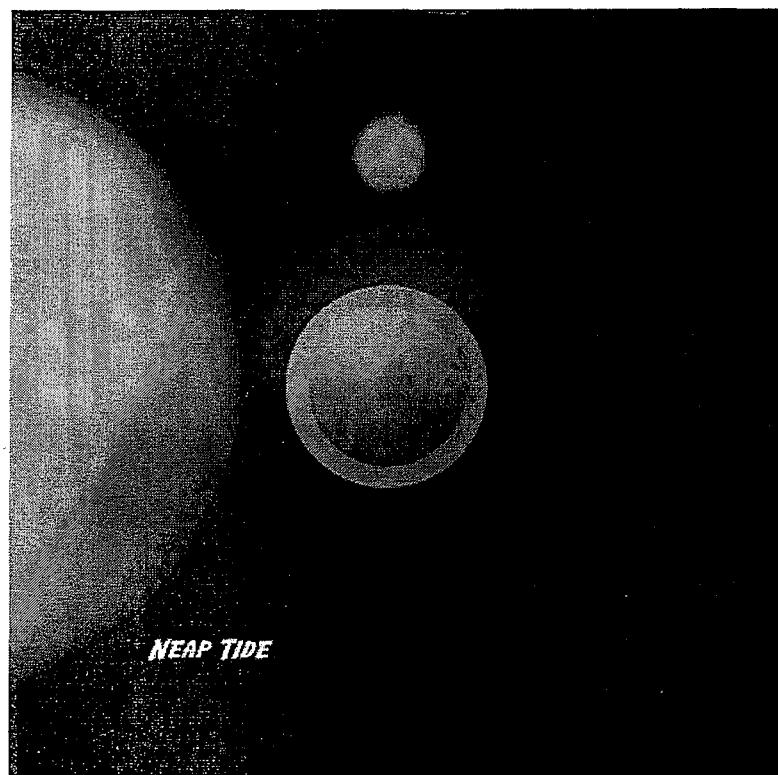
Fig. 2.60 Depiction of Neap Tide

The mean sea level at a particular location along the coastline is determined by averaging the observed heights of the tide w.r.t. a certain datum. The observations should extend over a sufficient period of time to eliminate the effect of meteorological disturbances. In addition to varying with location on the earth's surface, the mean sea level varies with time of the year. Thus the mean sea level of interest in this study is that at Daphne Island or Mobile, AL during the period of the year of August 1 - October 31. Figure 2.61 shows the mean sea level and tidal range near Mobile, AL during the time period August 1 - October 31.

The mean sea level and tidal range at a particular location and time of year are important in predicting hurricane storm surge/surface wave forces on coastal bridges. The mean seal level plus half of the tidal range plus the storm surge height establishes the temporary still water level (SWL) at a coastal bridge site. Superimposed on this SWL will be the hurricane wind induced surface waves. All of these affect the buoyancy force and/or venting requirements for a bridge superstructure, and the dynamic surface wave forces (vertical and horizontal) on the superstructure.
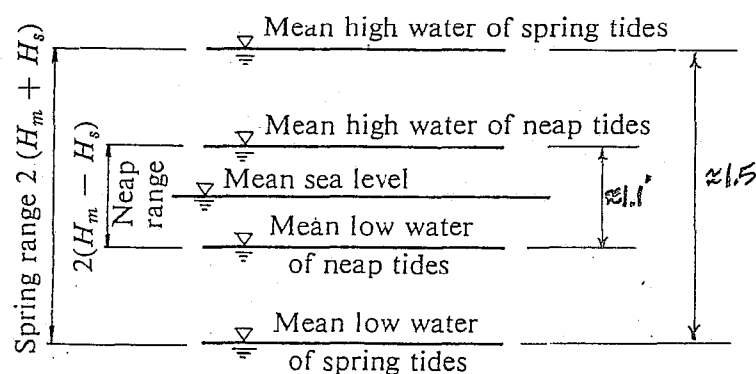
Fig. 2.61   Mean Sea Level and Tidal Levels Near Mobile, AL
in August 1 - October 31 Time Period (Modified from [13]).

Wave Forces on Coastal Structures. A review of the literature revealed that there were no equations that are directly applicable to predicting surface wave forces (both horizontal and vertical forces) on coastal bridges. However, there are some equations that may be adaptable to predicting these forces as a first order estimate and/or as limiting values. The equations and procedures in the literature that appear to best fall into this category are the following:

1. Corps of Engineers Coastal Design Manual – Unbroken Wave Equation

2. Corps of Engineers Coastal Design Manual – Broken Wave Equation

3. Corps of Engineers Coastal Design Manual – Breaking Wave Equation

4. FEMA Coastal Construction Manual Breaking Wave Load Equations

5. McConnell, et al. equations from laboratory wave flume testing

6. Douglass, et al. bridge-specific simplification of McConnell's equations

7. Modified Douglass, et al. equations as per Ramey and Sawyer

8. AASHTO/FHWA Pooled Fund equations

These equations are presented and discussed in detail in the following chapter. Each equation is also applied to the same example bridge problem in Chapter 3.

3. HURRICANE SURGE/SURFACE WAVE FORCE PREDICTION EQUATIONS

3.1 General

The part that the hurricane storm surge plays in the damage to coastal bridges is simply that it raises the sea state water level, or still water level (SWL), to an elevation where, firstly, vertical buoyant forces may act on the bridge superstructure. These forces may be due to the SWL being higher than parts of the superstructure, or may be from surface waves on top of the SWL being higher than all or part of the superstructure. Secondly, and more importantly, the storm surge raises the SWL to a height where storm surface waves begin to apply large periodic hydrodynamic, and sometimes slamming forces, to the superstructure. In this chapter, we will focus on the forces applied to bridge superstructures by the storm surface waves.

From the literature review, the Corps of Engineers Coastal Design Manual equations for forces on vertical walls being hit by storm waves which are unbroken, breaking, or broken, and the Federal Emergency Management Agency (FEMA) breaking wave force equation, all adjusted as needed for coastal bridge structures, are reasonable candidate force prediction equations for application to coastal bridges. The McConnell, et al. equations, which are based on wave tank experimental testing for jetty heads/docks facilities and the Douglass, et al. equations which are based on McConnell's equations, adjusted for coastal highway bridge applications, are also reasonable candidate force prediction equations. These equations and approaches are discussed and applied to the same example application problem in the following sections and this is followed by a comparison of the analysis results.

3.2 Corps of Engineers Unbroken Wave Forces

When coastal bridges are loaded by unbroken waves in a hurricane sea state such as shown in Fig. 3.1, the pressure distribution on the bridge seaward vertical face will be approximately hydrostatic as indicated in Fig. 3.2. The local SWL at the bridge will probably be slightly elevated due to some wave reflection and will thus slightly raise the top of the hydrostatic pressure distribution; however, in our load evaluation we will assume the freewater surface elevation to be the top of the guard rail independent of the level of the SWL if the SWL is at an elevation higher than the top of guard rail. Note in Fig. 3.1 that the maximum horizontal wave force will occur for wave position ②and that hydrostatic pressure only acts on the vertical projection of the seaward face of the bridge. For this wave position, there will also be a significant upward vertical force on the seaward deck overhang and the seaward girder and a significant overturning moment from the vertical forces.

For wave position ①, the net resultant horizontal force is approximately zero as the horizontal pressures tend to cancel each other. However, for this wave position, the vertical uplift force will be at a maximum and the overturning moment will be zero. It should be noted that if wave position ① is "backed-up" a distance equal to the girder spacing, s_g, then the vertical uplift force will still be at a maximum value, but there will also be an overturning moment equal to $F_v^{max} \times s_g$.

The values of the wave forces and moments for the above wave positions for an I-10 ramp span in Mobile Bay during Hurricane Katrina are shown in the following example.
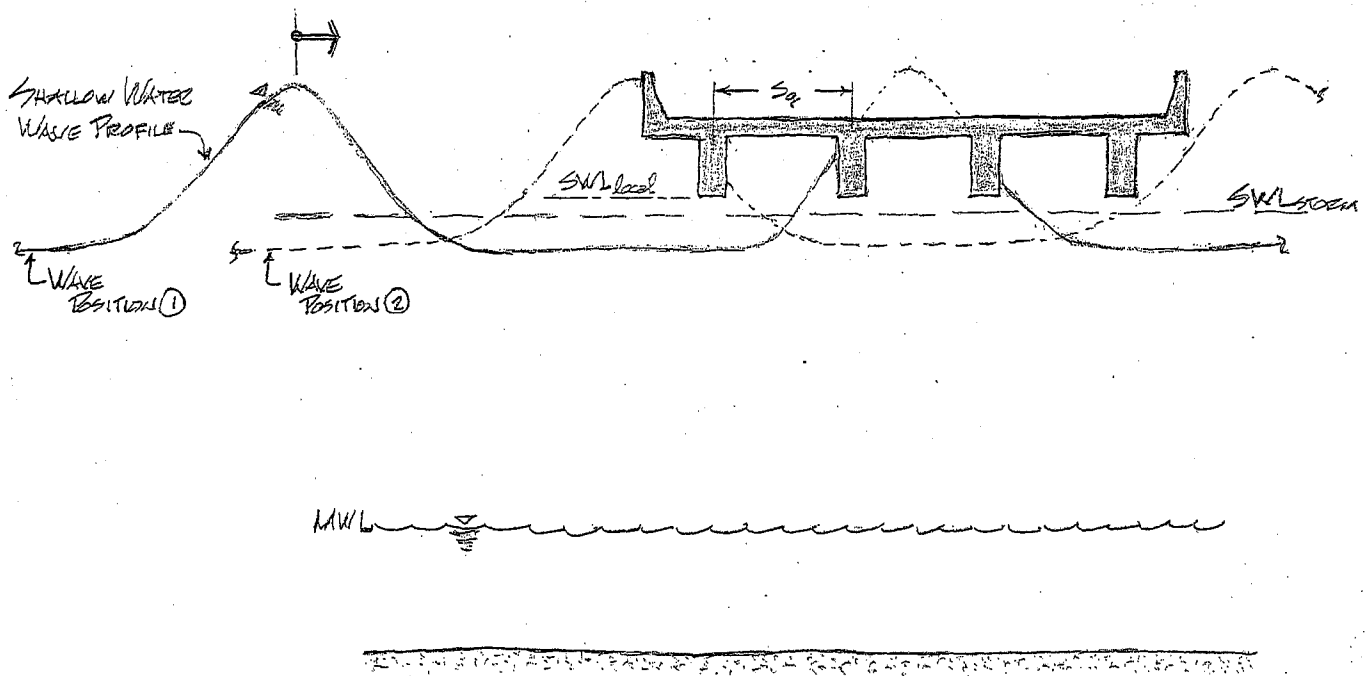
Fig. 3.1   Unbroken shallow-water wave passing through a coastal bridge
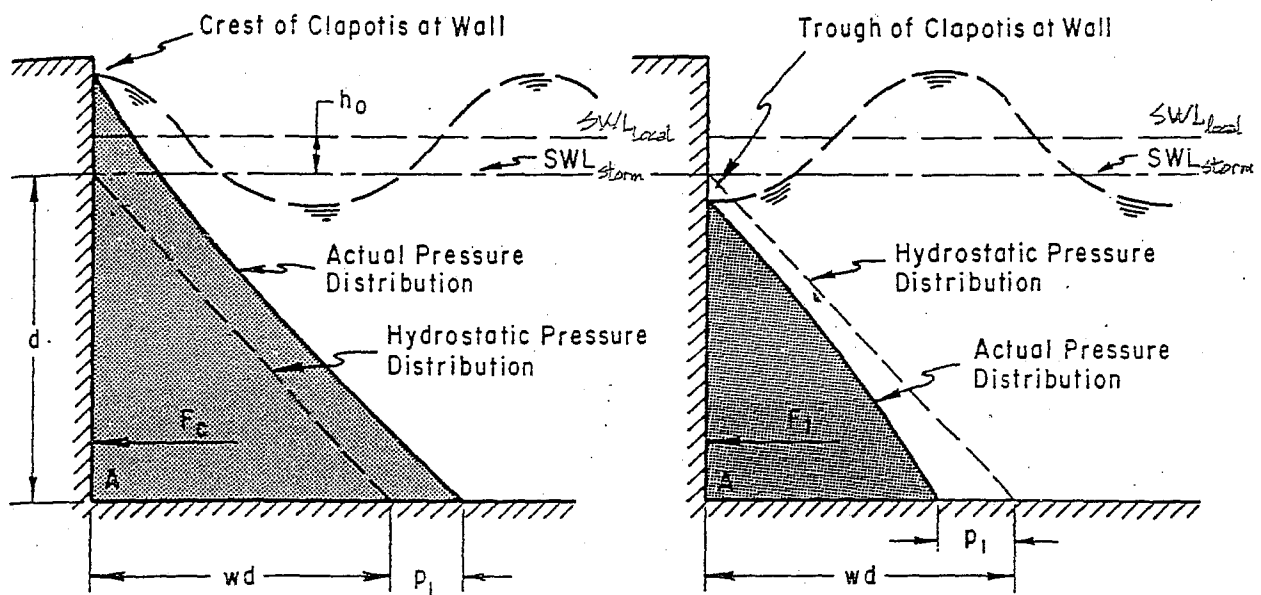
Fig. 3.2   Approximate hydrostatic pressure distribution from freewater surface
(modified from (11))

Example Application – Determine the maximum wave forces and moment from unbroken waves on a 52 ft long I-10 ramp span in Mobile Bay when Hurricane Katrina hit.

A partial sketch of the ramp span geometry and elevations and the maximum sea state at the ramp when Katrina hit are shown in Fig. 3.3.
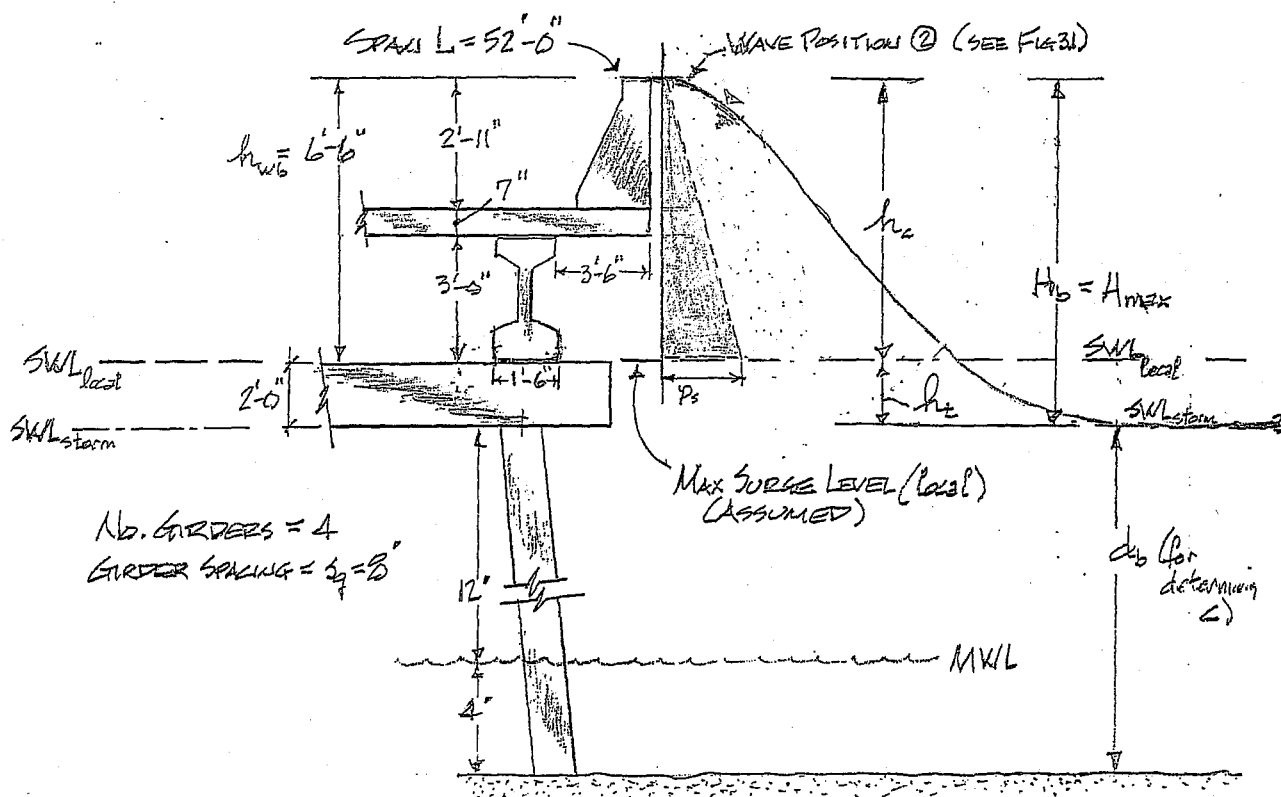
Fig. 3.3 Partial sketch of Mobile, AL I-10 ramp span geometry and sea state during Hurricane Katrina

In performing the analysis the following pertinent parameter values were extracted from the storm data or were assumed:

SWL_{local} = at top of bent cap = SWL_{storm} + 2' (assumed)

SWL_{storm} = at bottom of bent cap

$h_c = 0.78H_b$

$h_t = 0.22H_b$

Significant Wave Ht. = H_s = 6.1'

Max Wave Ht. = H_b = 1.4H_s = 8.5'

h_c = 0.78 x 8.5' = 6.6' $\Longrightarrow$ Use 6.5' (top of rail)

d_b = Initial Depth + Max Storm Surge = Elev. Of Bottom of Bent Cap

d_b = 4' +12' = 16'

Span Length = 52'

Elev Bay Bottom = 0'

Elev MWL = 4'

Elev. Bottom of Bent Cap = 16'

Elev. Top of Bent Cap = 18'

Elev. Bottom of Girders = 18'

Elev. Top of Guardrail = 24.5'

Girder Spacing = s_g = 8.0'

Analysis:

Max Horizontal Force:
(see wave position ②
In Fig. 3.1)

$p_s = wh_{vp}$ = 64 x 6.5' = 416psf

$R_s = \dfrac{1}{2}p_s h_{vp} = \dfrac{1}{2}$ x 416 x 6.5' = 1352 lb/ft

$F_h^{max} = R_s$ x L = 1352 x 52' = 70.3^k

3-5

Vertical Force and
Moment acting with
F_h^{max} and Wave
Position ② :
(see Figs. 3.1 and 3.3)

$p_{bd} = wh_{bd} = 64 \times 3.5' = 224$ psf

$R_{dv} = p_{bd} \times w_{do} = 224 \times 3.5' = 784$ lb/ft

$R_{gv} = p_{bg} \times w_g = 64 \times 6.5' \times 1.5' = 624$ lb/ft

$F_v = (R_{dv} + R_{gv})L = (784 + 624)52' = 73.2^k$

$M_{cg} = (R_{dv} \times h_{dv} + R_{gv} \times h_{gv})L$
$\qquad (h_{gv} + 2.5')$

$M_{cg} = (784 \times 14.5' + 624 \times 12')52'$

$M_{cg} = (11.4^k + 7.5^k)52' = 983$ ft-kips

Max Vertical Force:
(see Wave Position ①
In Fig. 3.1)

$p_{bg} = wh_{bg} = 64 \times 6.5' = 416$ psf

Assume entrapped air between girders

$R_v = p_{bg} (w_g +$ girder spacing$)$

$\quad = 416(1.5' + 8.0') = 3952$ lb/ft

$F_v^{max} = R_v \times L = 3952 \times 52 = 206^k$

Horizontal Force and
Moment acting with
F_v^{max} and Wave
Position ① :
(see Figs. 3.1 and 3.3)

$F_h \approx 0$

$M \approx 0$

The above resulting maximum forces for the worst case unbroken wave loading conditions, i.e., wave positions ① and ② in Fig. 3.1, are shown in Fig. 3.4. It should be noted that a worst case condition for a combination of maximum F_v and M acting simultaneously would be when a wave is positioned so that its crest is centered on the most seaward cell between girders as shown by wave position ③ in Fig. 3.4b. For this case,

$F_v^{max} \approx 206^k$

$M^{max} \approx 206^k \times s_g = 206^k \times 8.0' = 1648$ ft-kips

$F_h \approx 0$
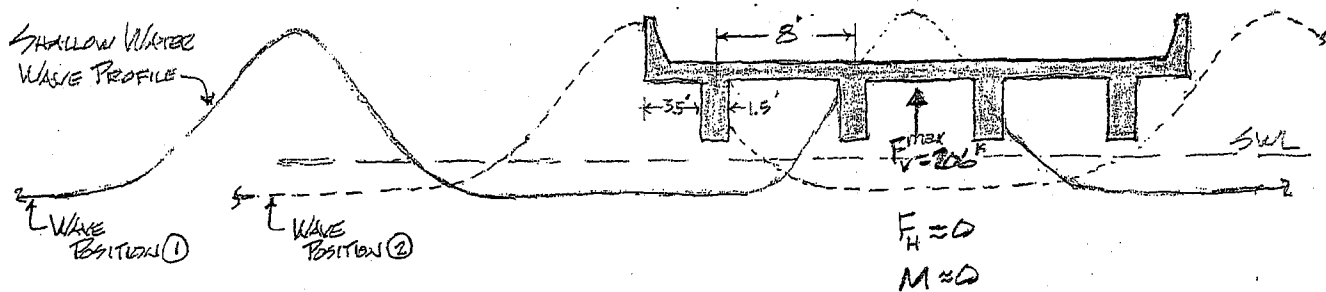
a. Resultant wave forces on bridge for wave position ①
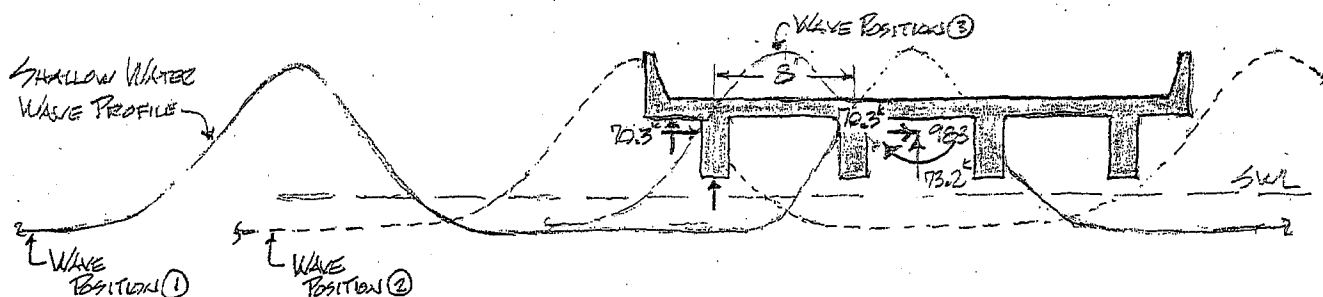
b. Wave forces on seaward faces and resultant wave forces for wave position ②

Fig. 3.4 Unbroken wave resultant forces for worst case loading conditions

3-7

3.3   Corps of Engineers Broken Wave Forces

Coastal bridges may be located so that even under severe storm and tide conditions surface waves will break before striking the bridge. Also, for bridges further out from shore, reflection waves from the bridge may result in the incoming waves being broken waves. It is assumed for broken waves that, immediately after breaking, the water mass in the wave moves forward with the velocity of wave propagation attained before breaking. That is, upon breaking, the water particle motion changes from oscillatory to translational motion. For a conservative estimate of wave force (from broken waves), it is assumed that neither the wave height nor wave velocity decreases from the breaking point to the point where the wave strikes the coastal bridge or structure.

Model tests have shown that, for waves breaking at or near the shore, approximately 78 percent of the breaking wave height H_b is above the stillwater level (SWL) as indicated in Fig. 3.5. Walls or coastal bridges hit by broken waves are subjected to wave pressures that are partly dynamic and partly hydrostatic as indicated in Fig. 3.5. In Fig. 3.5 the SWL should be a local SWL (i.e., SWL_{local}) which will be somewhat higher than the storm SWL due to waves reflecting off the wall and raising the SWL as indicated in Fig. 3.6. This would also be the case for coastal bridges where the level of wave reflection and raising of the SWL will primarily depend on the shape/geometry of the seawall/bridge "vertical face", the depth of openness on the underside of the bridge, and the angle of incidence of the approaching waves relative to the bridge. The wave reflection coefficient, x, in Fig. 3.6 is equal to 1.0 (complete reflection) when the wall is solid to the bottom, flat and smooth, and is perpendicular to the direction of wave propagation. Since coastal bridges are open below the
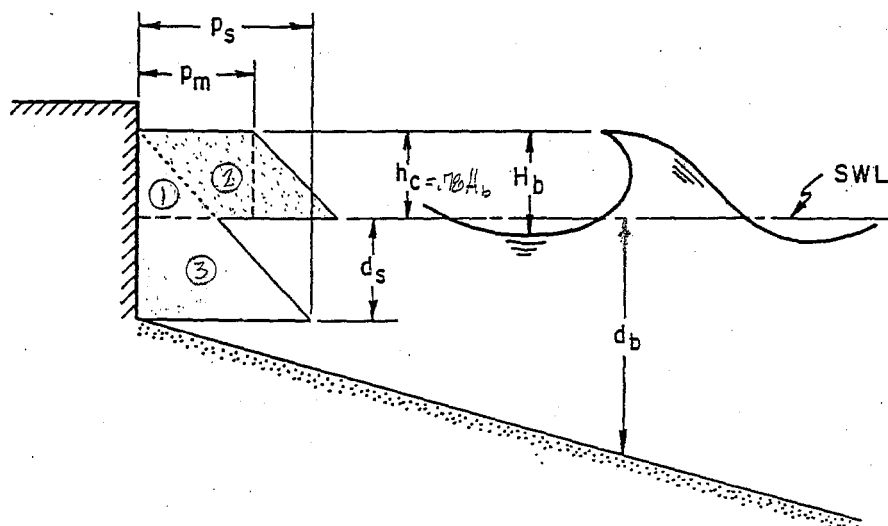
Fig 3.5 Wave Pressures from Broken Waves (Modified from (11))
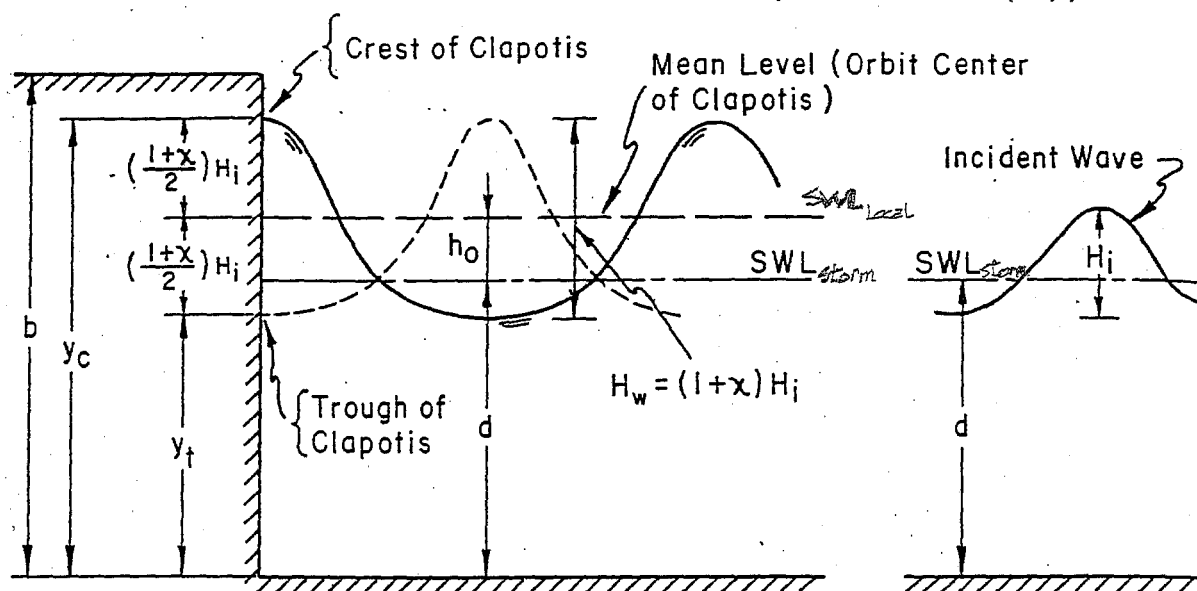
b = Height of Wall

d = Depth from Stillwater Level

H_i = Height of Original Free Wave (In Water of Depth, d)

x = Wave Reflection Coefficient

h_o = Height of Clapotis Orbit Center (Mean Water Level at Wall) Above the Stillwater Level (See Figures 7-90 and 7-93)

y_c = Depth from Clapotis Crest = $d + h_o + \left(\frac{1+x}{2}\right) H_i$

y_t = Depth from Clapotis Trough = $d + h_o - \left(\frac{1+x}{2}\right) H_i$

Fig. 3.6 Nonbreaking Wave Hitting Wall and Term Definitions (Modified from (11)).

approximate 6'-6" girder-deck-guardrail vertical projection and the "vertical face" is quite

irregular, the wave reflection coefficient, x, will be much less than 1.0. A reasonable

estimate is probably x ≈0.2.

To determine broken wave maximum pressures and forces on the seawall of

Fig. 3.5 one would proceed as follows:

- Use the shallow water equation

$$c = \sqrt{gd_b}$$

where g = gravitational acceleration constant

d_b = depth of water at breaking (use depth of SWL$_{storm}$)

c = celerity or velocity of wave propagation

to determine the velocity of wave propagation.

- The maximum dynamic component of the pressure will be

$$p_m = \frac{wc^2}{2g} = \frac{wd_b}{2}$$

where w is the unit weight of water.

- Assume the dynamic pressure is uniformly distributed from the still-

water level to a height h_c above SWL (as indicated in Fig. 3.5), where

h_c is given as

$$h_c = 0.78H_b$$

and thus the dynamic component of the maximum wave force per

unit length of wall is given as

$$R_m = p_m h_c = \frac{wd_b h_c}{2}$$

3-10

- The hydrostatic component of pressure will vary from zero at a height h_c above SWL to a maximum p_s at the wall base. This maximum will be given as,

$$p_s = w\left(d_s + h_c\right)$$

The hydrostatic pressure varies with time just as the dynamic pressure does. However, the variation of pressure with depth remains approximately hydrostatic as indicated in Fig. 3.7.

- The hydrostatic force component per unit length of wall will therefore be

$$R_s = \frac{w\left(d_s + h_c\right)^2}{2}$$

- The total force per unit length on the wall is the sum of the dynamic and hydrostatic components,

$$R_t = R_m + R_s$$

For coastal bridges, part ③ of the pressure distribution shown in Fig. 3.5, would not be present due to openness on the underside of the bridges. The hydrostatic part ① should be included as the water level on the shore side of the bridge would probably be at an elevation between SWL_{local} and SWL_{storm}, which would be below the elevation of the bottom of the girders. Also, for coastal bridges, the maximum value of h_c in Fig. 3.5 would be as indicated in Fig. 3.8, and the height of the hydrostatic and dynamic pressure

3-11
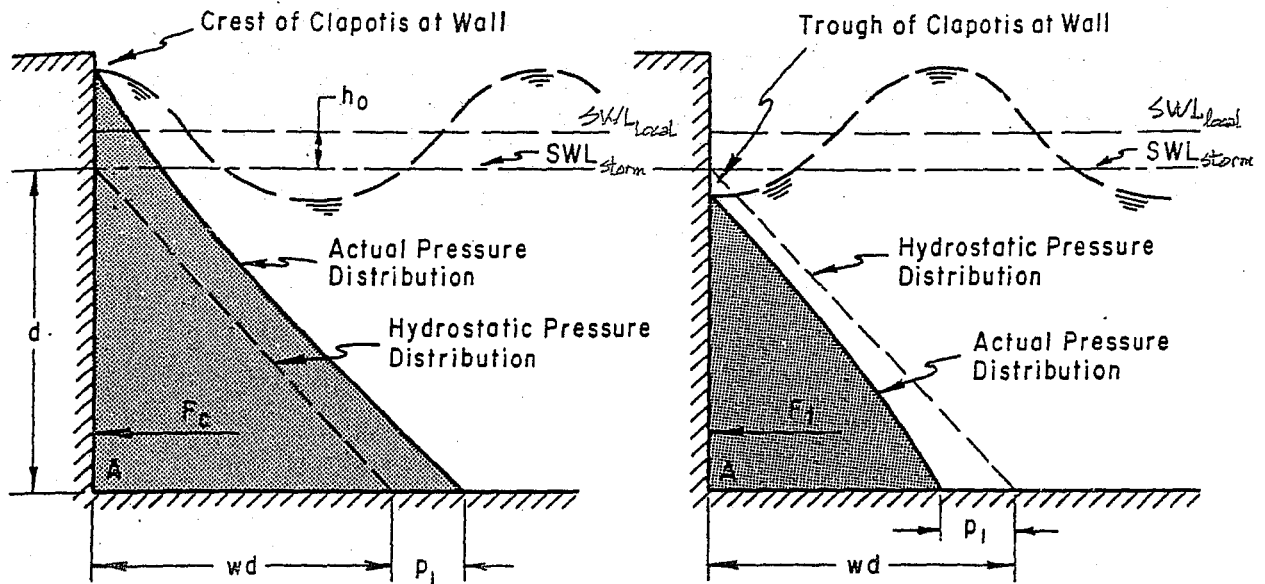
Fig. 3.7 Approximate Hydrostatic Pressure Distribution From Freewater Surface
(Modified from (11))
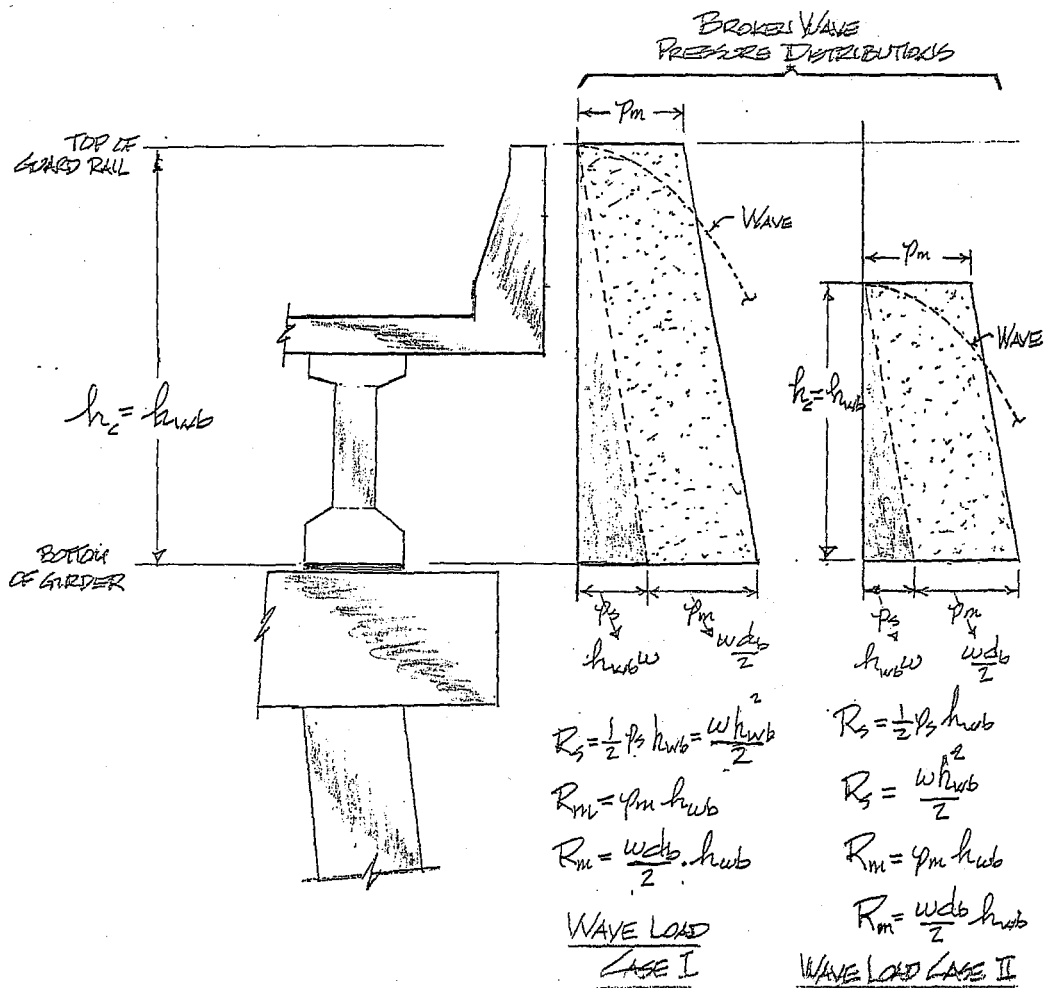
Fig. 3.8 Broken Wave Horizontal Load on Coastal Bridges

distributions (1) and (2) respectively in Fig. 3.5 would be as shown in Fig. 3.8. For the sea state at the bridge location, assume the following:

Height of Wave Crest $= H_b = H_{max} = 1.4H_s$
(at breaking)

Height of H_{max} above SWL_{local} $= h_c = 0.78\ H_{max} = 1.1H_s$

$SWL_{local} = SWL_{storm} + h_o$

where $h_o \approx 0.2H_{max}$ $\Longrightarrow$ Assume $h_o = 2'$

$\therefore SWL_{local} \approx SWL_{storm} + 2'$

Elevation of Wave Crest $= SWL_{storm} + h_o + h_c \approx SWL_{storm} + 2' + 1.1H_s$
(at breaking)

h_{wb} = Elevation of Wave Crest $-$ Elevation of Bottom of Girders (see Fig. 3.8)
(at breaking)

If Elevation of Wave Crest > Elevation of Top of Bridge $\Longrightarrow$ Use Wave
(at breaking)   Guard Rail   Load Case I
                                                              in Fig. 3.8

If Elevation of Wave Crest < Elevation of Top of Bridge $\Longrightarrow$ Use Wave
(at breaking)   Guard Rail   Load Case II
                                                              in Fig. 3.8

Thus, the procedure to determine broken wave maximum pressures and horizontal forces on the seaward face of a coastal bridge via modifying the equations for a seawall are as follows:

- Determine the shallow water velocity of wave propagation as before, i.e.,

$$c = \sqrt{gd_b}$$

- Determine the maximum dynamic component of the pressure as before, i.e.,

$$p_m \frac{wc^2}{2g} = \frac{wd_b}{2}$$

- Determine the elevation of the wave crest at breaking (EWC) from

$$EWC = SWL_{storm} + 2' + 1.1H_s$$

- Determine the elevations of the bottom of girders (EBG) and top of guardrail (ETR)

- Determine h_{wb} in Fig. 3.8 from $h_{wb} = EWC - EBG$

- Determine if $EWC \geq ETR \Longrightarrow$ If it is, use Wave Load Case I in Fig. 3.8 with $h_c = h_{wb} = 6.67\text{ft}$

  If it is not, use Wave Load Case II in Fig. 3.8 with $h_{wb} = EWC - EBG$

- Determine the dynamic component of the maximum horizontal wave force per unit length of bridge from

$$R_m = p_m h_{wb} \text{ for Load Cases I and II}$$

where h_{wb} is defined for each Load Case in Fig. 3.8

- Determine the hyrdrostatic component of the maximum horizontal wave force per unit length of bridge from

$$R_s = \frac{w h_{wb}^2}{2} \text{ for Load Cases I and II}$$

where h_{wb} is defined for each Load Case in Fig. 3.8

- Determine the maximum total horizontal wave force per unit length of bridge from

$$R_t = R_m + R_s$$

Application of the above procedure to a 52ft long ramp span on the I-10 bridge over Mobile Bay is presented in an Example Application on the following pages to illustrate the wave load analysis procedure.

Example Application - Determine the horizontal wave loading from broken waves on the seaward face of an I-10 ramp span in Mobile Bay when Hurricane Katrina hit.

A partial sketch of the ramp span geometry and elevations and the maximum sea state at the ramp when Katrina hit are shown in Fig. 3.9.

Fig. 3.9 Partial Sketch of Mobile, AL I-10 Ramp Span Geometry and Sea State During Hurricane Katrina

In performing the analysis the following pertinent parameter values were extracted from the storm data or were assumed:

SWL_{local} = at top of bent cap = SWL_{storm} + 2' (assumed for Example)

SWL_{storm} = at bottom of bent cap

$h_c = 0.78 H_b$

$h_t = 0.22 H_b$

Significant Wave Ht. = H_s = 6.1'

Max Wave Ht. = H_b = 1.4H_s = 8.5'

h_c = 0.78 x 8.5' = 6.6' $\implies$ Use 6.5' (top of rail)

d_b = Initial Depth + Max Storm Surge = Elev. Of Bottom of Bent Cap

d_b = 4' +12' = 16'

Span Length = 52'

Elev Bay Bottom = 0'

Elev MWL = 4'

Elev. Bottom of Bent Cap = 16'

Elev. Top of Bent Cap = 18'

Elev. Bottom of Girders = 18'

Elev. Top of Guardrail = 24.5'

Girder Spacing = s_g = 8'

Analysis:

$$c = \sqrt{gd_b} = \sqrt{32.2 \text{ ft/s}^2 \times 16'} = 22.7\text{fps} = 15.5\text{mph}$$

$$p_m = \frac{wc^2}{2g} = \frac{wgd_b}{2g} = \frac{wd_b}{2} = \frac{64 \times 16}{2} = 512\text{psf}$$

Elev. of Wave Crest (EWC) = SWL_{local} + 1.1H_s = 18' + 1.1(6.1') = 24.7ft (at breaking)

EWC $\geq$ ETR $\implies$ 24.7' > 24.5' $\implies$ Use Wave Load Case I

For Load Case I (see Fig. 3.8),

$$R_m = \frac{wd_b}{2} \times h_{wb} = p_m \times h_c = 512\text{psf} \times 6.5' = 3328 \text{ lb/ft}$$

$p_s = wh_{wb} = 64 \times 6.5' = 416 psf$

$R_s = \dfrac{1}{2} p_s h_{wb} = \dfrac{1}{2} \times 416 \times 6.5' = 1352 \text{ lb/ft}$

Total Horiz Force $= R_t = R_m + R_s = 3328 + 1352 = 4680 \text{ lb/ft}$

For 1-span $\implies F_{max}^{horiz} = R_t \times L = 4680 \times 52' = 243^k$

Note that the above value of F_{max}^{horiz} is the force on the seaward face of the bridge span. This will be a lower bound load on the span as no wave impact was considered and no additional load from dynamic pressure drag on other span girders were considered. An increase in F_{max}^{horiz} should be made for these contributions as the increase could be as large as 100%.

Simultaneous Vertical Upward Force on Deck Overhang:

$p_m = 512 \text{ psf}$

$p_s^{bd} = wh_{bd} = 64 \times 3.5' = 224 \text{ psf}$

$p_t = p_m + p_s^{bd} = 512 + 224 = 736 \text{ psf}$

$R_v = p_t \times w_{do} = 736 \times 3.5 = 2576 \text{ lb/ft}$

$F_v^{max} = R_v \times L = 2576 \times 52 = 134^k$

Simultaneous Overturning Moment From F_v^{max}:

$M^{max} = F_v^{max} \times h_{do} = 134^k \times 14.5' = 1943 \text{ ft-kips}$

3.4 Corps of Engineers Breaking Wave Forces

Waves breaking directly against vertical-face structures exert high, short duration, dynamic pressures that act near the region where the wave crests hit the structure. These impact or shock pressures have been observed and reported by several researchers as indicated by the impact force, F_{max}, shown in Fig. 3.10 and by $F_{slamming}$ shown in Fig. 3.11. Fortunately these high impact/slamming pressures are of short duration (approximately $0.03 < t_{duration} < 0.1s$). They have been studied in the laboratory to some extent, and wave tank experiments by Bagnold led to the following explanation of breaking wave impact/slamming loadings:

- The impact pressures occur at the instant that the vertical front face of a breaking wave hits a wall and only when a plunging wave entraps a cushion of air against a wall.

- Because of their critical dependence/sensitivity to wave geometry, high impact pressures are infrequent against coastal structures. However, the possibility of high impact pressures should be recognized and possibly considered in design.

- Since the high impact pressures are short in duration (on the order of hundredths of a second), their importance in the design of coastal bridge super and substructures is questionable; however, lower dynamic forces of longer durations are important.
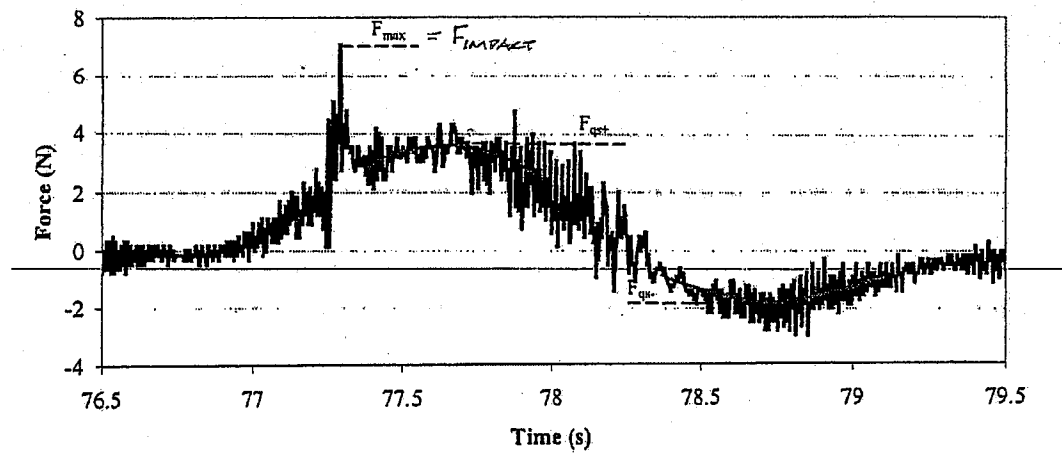
Fig. 3.10   Definition of force parameters (model units)
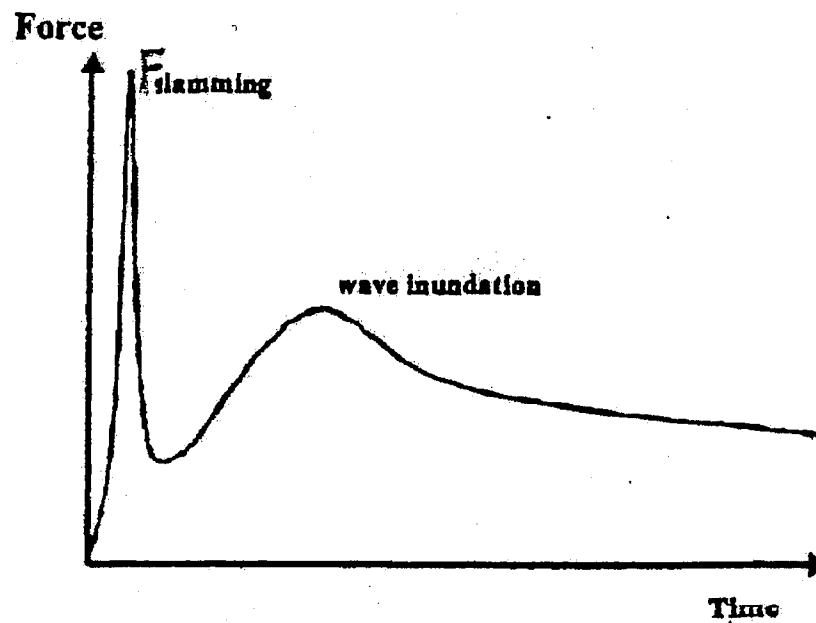
Fig. 3.11   Idealized force development on platform deck

Based on Bagnold's results and observations of full-scale breakwaters, Minikin recommended the following equation for maximum impact pressure from breaking waves

$$p_m = 101w\frac{H_b}{L_D}\frac{d_s}{D}(D + d_s) \tag{3.1}$$

where,

p_m = the maximum dynamic pressure

H_b = the breaker height

d_s = the depth at the toe of the wall

D = the depth one wavelength in front of the wall

L_D = the wavelength in water of depth D

The distribution of dynamic pressure is assumed to be symmetric about the SWL as shown in Fig. 3.12. The pressure decreases parabolically from p_m at the SWL to zero at a distance of $H_b/2$ above and below the SWL.

The final design forces recommended by Minikin are as follows:

- The resultant dynamic force per unit length of wall is represented by the area under the dynamic pressure distribution curve in Fig. 3.12 and is

$$R_m = \frac{p_m H_b}{3} \tag{3.2}$$
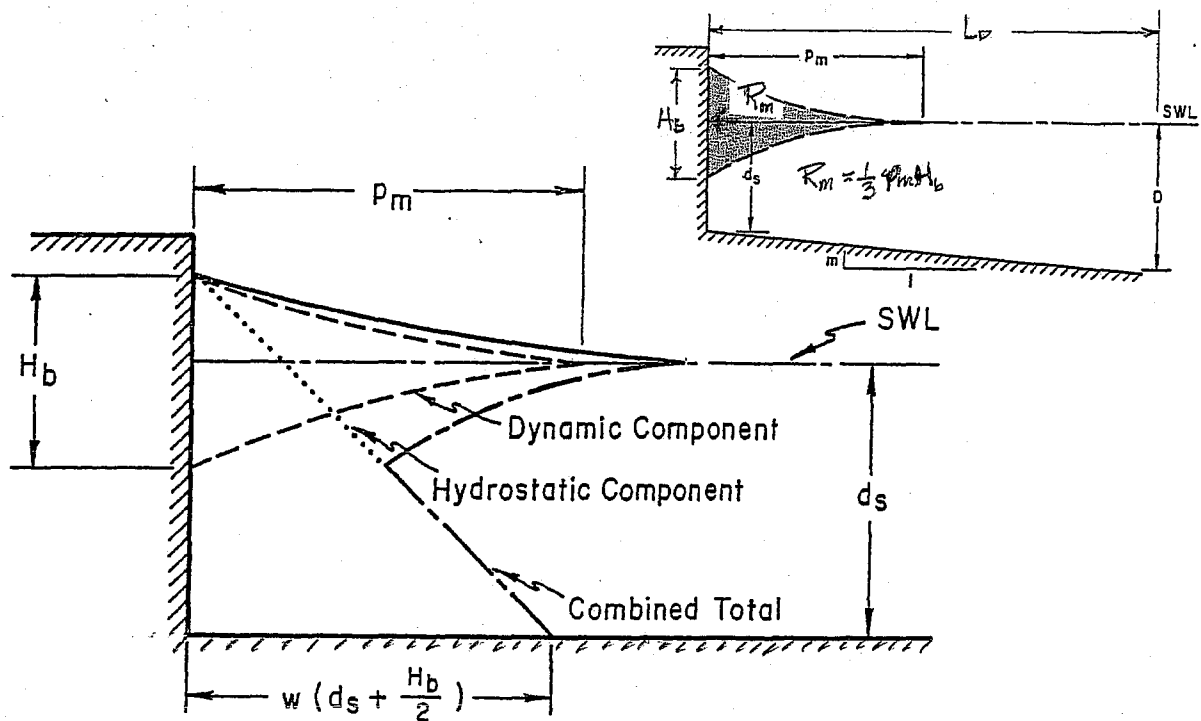
Fig. 3.12 Minikin breaking wave pressure diagram

- The hydrostatic contribution to the force must be added to the dynamic component, R_m, to determine total force. Thus, the total breaking wave force on a wall per unit wall length is

$$R_t = R_m + R_s = R_m + \frac{w\left(d_s + \dfrac{H_b}{2}\right)^2}{2} \qquad (3.3)$$

It should be noted that Minikin's method can give wave forces that are extremely high, as much as 15 to 18 times those calculated for nonbreaking waves. Because the dynamic pressure, p_m, and dynamic force, R_m, presented above are impact loadings of very short duration ($\approx 0.03s < t < 0.1s$), and because of their infrequent application due to their extreme sensitivity to wave and wall geometry, and because wave height and breaking

3-22

status vary considerably along the length of a wave, the assumption that the maximum p_m and R_m values occur, and that they occur simultaneously along the length of a bridge span is felt to be too conservative. Thus, it is recommended that Minikin's recommended p_m equation, when used for design of a bridge span, be reduced by a factor of 10, i.e., it is recommended that the following equations be used for design:

$$\tilde{p}_m = \frac{1}{10}p_m^{Minikin} = \frac{101}{10}w\frac{H_b}{L_D}\frac{d_s}{D}(D + d_s) \tag{3.4a}$$

$$\tilde{R}_m = \frac{\tilde{p}_m H_b}{3} \tag{3.4b}$$

An Example Application determining breaking wave forces on a bridge deck is given on the following pages using the above $\tilde{p}_m$ and $\tilde{R}_m$ equations and later compared with results using an unbroken wave loading and a broken wave loading.

Example Application - Determine the horizontal wave loading from breaking waves on the seaward face of a 52 ft long I-10 ramp span in Mobile Bay when Hurricane Katrina hit.

A partial sketch of the ramp span geometry and elevations and the maximum sea state at the ramp when Katrina hit are shown in Fig. 3.13.

Fig. 3.13 Partial sketch of Mobile, AL I-10 ramp span geometry and sea state during Hurricane Katrina

In performing the analysis the following pertinent parameter values were extracted from the storm data or were assumed:

SWL_{local} = at top of bent cap = SWL_{storm} + 2' (assumed for Example)

SWL_{storm} = at bottom of bent cap

$h_c = 0.78 H_b$

$h_t = 0.22 H_b$

Significant Wave Ht. = H_s = 6.1'

Max Wave Ht. = H_b = $1.4 H_s$ = 8.5'

h_c = 0.78 x 8.5' = 6.6' $\Longrightarrow$ Use 6.5' (top of rail)

d_b = Initial Depth + Max Storm Surge = Elev. Of Bottom of Bent Cap

d_b = 4' +12' = 16'

Span Length = 52'

Elev Bay Bottom = 0'

Elev MWL = 4'

Elev. Bottom of Bent Cap = 16'

Elev. Top of Bent Cap = 18'

Elev. Bottom of Girders = 18'

Elev. Top of Guardrail = 24.5'

Girder Spacing = s_g = 8'

Analysis:

$$\tilde{p}_m = 10.1w \, \frac{H_b}{L_D} \frac{d_s}{D} (D + d_s)$$

where $L_D = (2\pi h L_0)^{1/2} \left(1 - \frac{\pi h}{3L_0}\right)$

$L_0 \approx 5.12T^2$ (in ft.)

Assume $T = 7\text{sec} \Longrightarrow L_0 = 5.12(7)^2 = 250'$

$$L_D = (2\pi \times 16' \times 250')^{1/2} \left(1 - \frac{\pi \times 16'}{3 \times 250'}\right)$$

$L_D = (158.5)(0.933) = 148 \text{ ft}$

$$\tilde{p}_m^{T=7s} = 10.1 \times 64 \times \frac{8.5}{148} \times \frac{16}{16} (16 + 16) = 1188 \text{ psf}$$

for $T = 4\text{sec} \Longrightarrow L_0 = 5.12(4)^2 = 82'$

$$L_D = (2\pi \times 16' \times 82') \left(1 - \frac{\pi \times 16'}{3 \times 82}\right)$$

$L_D = (90.79)(0.7957) = 72 \text{ ft}$

$$\tilde{p}_m^{T=4s} = 10.1 \times 64 \times \frac{8.5}{72} \times \frac{16}{16} (16 + 16) = 2442 \text{ psf}$$

$\therefore$ Use larger value, $\tilde{p}_m = 2442 \text{ psf}$

$$\tilde{R}_m = \frac{1}{3} \tilde{p}_m h_{wb} = \frac{1}{3} \times 2442 \times 6.5' = 5291 \text{ lb/ft}$$

$$p_s = w h_{wb} = 64 \times 6.5' = 416 \text{ psf}$$

$$R_s = \frac{1}{2} p_s h_{wb} = \frac{1}{2} \times 416 \times 6.5' = 1352 \text{ lb/ft}$$

Total Horiz Force = $R_t = \tilde{R}_m + R_s = 5291 + 1352 = 6643 \text{ lb/ft}$

For 1-span $\Longrightarrow$ $F_{max}^{horiz} = R_t \times L = 6643 \times 52' = 345^k$

3-26

Note that the above value of F_{max}^{horiz} is the force on the seaward face of the bridge span. This will probably be a lower bound load on the span as no additional load from dynamic pressure drag on other span girders were considered.

Simultaneous Vertical Upward Force on Deck Overhang:

See Parabolic $\tilde{p}_m$ Distribution at Right.

$$\tilde{p}_m^{bd} = \left(\frac{3.5}{6.5}\right)^2 \tilde{p}_m = 0.29\,\tilde{p}_m = 0.29 \times 2442 = 708 \text{ psf}$$

$$p_s^{bd} = wh_{bd} = 64 \times 3.5 = 224 \text{ psf}$$

$$\tilde{R}_v^{bd} = \tilde{R}_{mv}^{bd} + R_{sv}^{bd}$$

$$= 708 \times 3.5' + 224 \times 3.5'$$

$$= 2478 + 784 = 3262 \text{ lb/ft}$$

$$F_v^{bd} = \tilde{R}_v^{bd} \times L$$

$$F_v^{bd} = 3262 \times 52' = 170^k$$
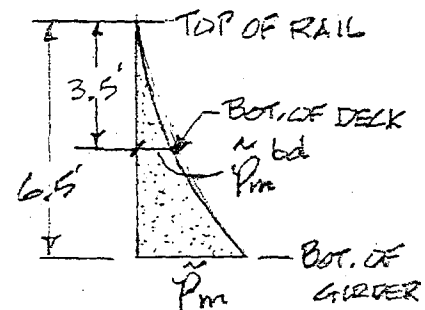
Simultaneous Overturning Moment From F_v^{bd}:

$$M^{max} = F_v^{bd} \times 14.5'$$

$$M^{max} = 170^k \times 14.5' = 2465 \text{ ft-kips}$$

3.5   FEMA Manual Wave Forces

The FEMA Coastal Construction Manual (3) recommends for structures subjected to coastal flood and storm events and located below the storm wave crest elevation that they be designed for breaking wave loads as determined by FEMA Manual Formula 11.6 which is shown in Fig. 3.14. It should be noted in using Formula 11.6 that Case 2 would be the applicable case for coastal bridges, and that the f_{brkw} formula gives breaking wave load per unit length of wall. The FEMA Manual provides values of the dynamic pressure coefficient in their Table 11.1 and the location of the resultant force in their Figure 11-7 (both of these are also shown in Fig. 3.14). Also, for Case 2, the FEMA manual provides a graphical solution for the dynamic force component in Formula 11.6 (the first term in the formula) as well as a relationship between still water depth and wave height in their Fig. 11-8 which is reproduced in Fig. 3.15. Note in Fig. 3.15 that the dynamic force component is very large; however, the duration of this component is quite brief (i.e., a fraction of a second).

—

Example Application: Determine the maximum horizontal force on I-10 Ramp Span seaward face using – FEMA Formula 11.6 Breaking Wave Force on Vertical Walls.

Note in Fig. 3.14 from the FEMA Coastal Construction Manual, that FEMA Formula 11.6 is for a vertical wall which extends from the top of a breaking wave down to the ocean bottom and thus would not be applicable to our coastal bridge situation. However, to gain an estimation of what the FEMA wave load equations might yield, we assumed a vertical wall the height of the vertical plane projection of our bridge superstructure as shown in Fig. 3.16. In this modified case, we assumed the SWL to be at the bottom of the bridge deck/top of girders and the ocean bottom to be at the

bottom of the vertical plane projection, i.e., at the bottom of the bridge girders as shown in Fig. 3.16. Note for this case that the d_s and $1.2d_s$ vertical dimensions shown in Fig. 3.16 were about those shown in Fig. 3.14. From Fig. 3.14, the applicable FEMA force prediction equation is

$$F_{brkw} = f_{brkw} \times L$$

where $f_{brkw} = 1.1 C_p \gamma \, d_s^2 + 1.91 \gamma \, d_s^2$

where C_p will be taken as $C_p = 2.4$

Thus,

$$f_{brkw} = 1.1 \times 2.4 \times 64 \times 3.0^2 + 1.91 \times 64 \times 3.0^2$$

$$= 1520 \text{ lb/ft} + 1100 \text{ lb/ft}$$

$$F_{brkw} = 2620 \text{ lb/ft}$$

and,

$$F_{brkw} = 2620 \times 52 = 136^k$$

√ƒ **ormula**

Breaking Wave Load
on Vertical Walls

Formula 11.6 Breaking Wave Load on Vertical Walls

Case 1 (enclosed dry space behind wall):

$$f_{brkw} = 1.1C_p\gamma d_s^2 + 2.41\gamma d_s^2$$

← HYDROSTATIC COMPONENT

For Coastal Bridges → Case 2 (equal stillwater level on both sides of wall):

$$f_{brkw} = 1.1C_p\gamma d_s^2 + 1.91\gamma d_s^2$$

← DYNAMIC COMPONENT

where: f_{brkw} = total breaking wave load per unit length of wall (lb/ft) acting at the stillwater level

F_{brkw} = total breaking wave load (lb) acting at the stillwater level = f_{brkw} w, where w = width of wall in feet

C_p = dynamic pressure coefficient from Table 11.1

γ = specific weight of water (62.4 lb/ft³ for fresh water and 64.0 lb/ft³ for saltwater)

d_s = design stillwater flood depth in feet

Note: Formula 11.6 includes the hydrostatic component calculated by Formula 11.3
If Formula 11.6 is used, do not add a lateral hydrostatic force from Formula 11.3.

Table 11.1
Value of Dynamic Pressure
Coefficient, Cp, as a Function
of Probability of Exceedance
(from Walton, et al. 1989)

C_p	Building Type	Probability of Exceedance
1.6	accessory structure, low hazard to human life or property in the event of failure	0.5
2.8	coastal residential building	0.01
3.2	high-occupancy building or critical facility	0.001

Figure 11-7
Dynamic, static, and total
pressure distributions
against a vertical wall.
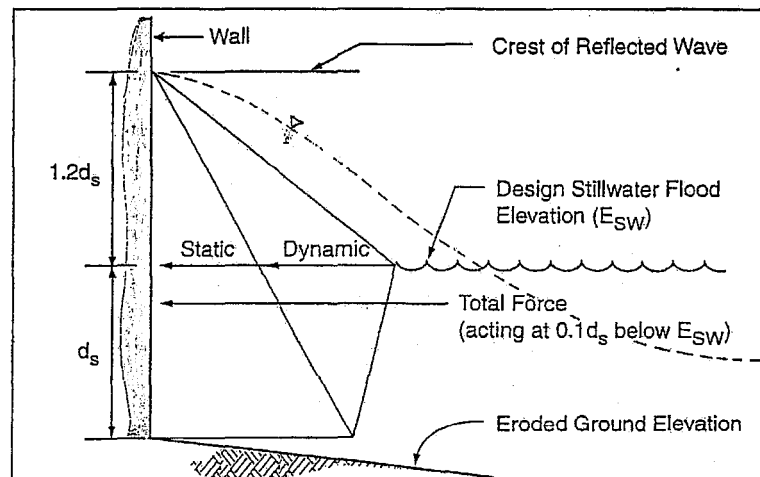
Fig. 3.14 Breaking Wave Force Formula, Pressure Coefficient Table, and Pressure Distribution Figure (from FEMA Coastal Construction Manual)
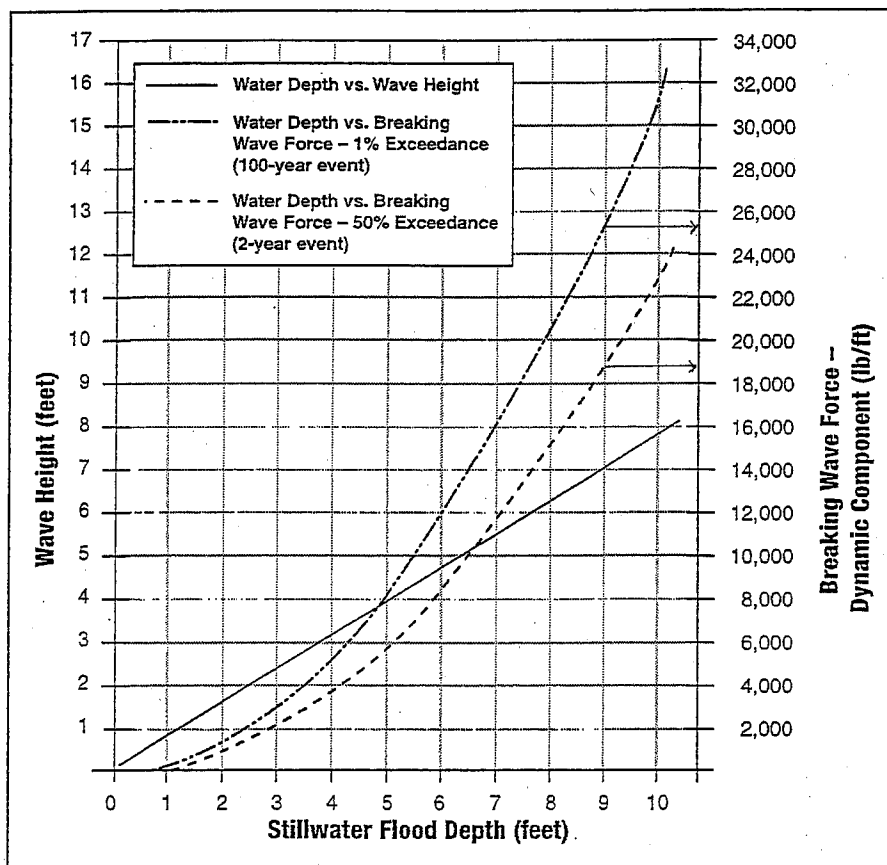
Figure 11-8
Water depth vs. wave height, and water depth vs. breaking wave force against a vertical wall (for Case 2, with stillwater behind the wall) for the 1-percent and 50-percent exceedance interval events.

Fig. 3.15 Storm Wave Height vs. Water Depth Relationship and Dynamic Wave Force Component vs. Water Depth Relationship Figure (from FEMA Coastal Construction Manual).
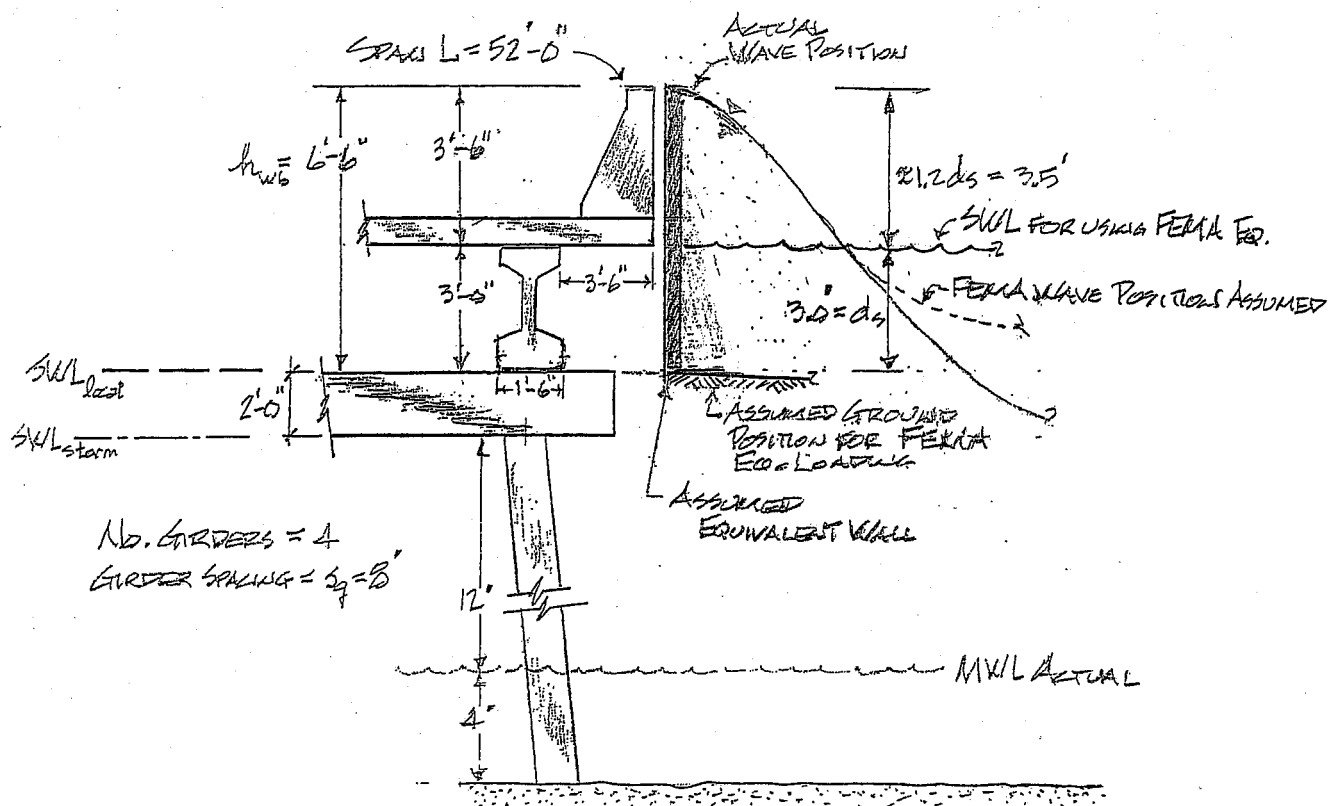
Fig. 3.16 Partial sketch of Mobile, AL I-10 ramp span geometry and sea state during Hurricane Katrina and assumed situation for applying FEMA equations for breaking wave loading.

3.6   McConnell et al. Equations for Wave Forces on Jetty Heads/Docks

Trade activities of many coastal countries make use of jetties for berthing of ocean vessels for the loading and discharge of cargo. Liquid natural and petroleum gas producers commonly make use of such industrial terminals for loading and unloading their cargo. Figures 3.17 and 3.18 show a typical approach trestle and jetty head for an industrial gas terminal. A concern at these locations is the risk of occurrence of wave forces on the jetty superstructure and the magnitude of such forces should they occur.

Existing guidance on such loadings are mainly derived from the offshore gas/oil industry, and in this industry an approach termed the 'air gap' approach is normally adopted for the platform design. In this approach, the maximum wave crest elevation is predicted for the design condition and the deck (or soffit) level is located at an allowance or 'air gap' above this elevation to ensure a low probability of occurrence of wave forces on the superstructure. The 'air gap' approach is often adopted in the design of shore-connected trestles and jetties as well. However, for some of these terminals, elevation constraints may prevent adoption of the air gap approach, and in these cases, there may be a risk of wave loads on the structure.

Because of limited information and guidance on the magnitude of such potential wave loadings, the UK government funded an experimental wave flume research project in the early 2000's to develop more quantitative guidance on the appropriate design forces for these facilities. Figures 3.19 and 3.20 show a jetty head deck model out-of and in the wave flume, respectively. The primary force parameters monitored/measured in the wave flume testing are identified and defined below, and in Fig. 3.21.

F_{max} Impact force (short duration, high magnitude)

$F_{qs+, v\,or\,h}$ Maximum positive (upward or landward) quasi-static (pulsating) force

$F_{qs-, v\,or\,h}$ Maximum negative (downward or seaward) quasi-static (pulsating) force

Figure 3.17   Typical exposed jetty (from McConnell, et al.)
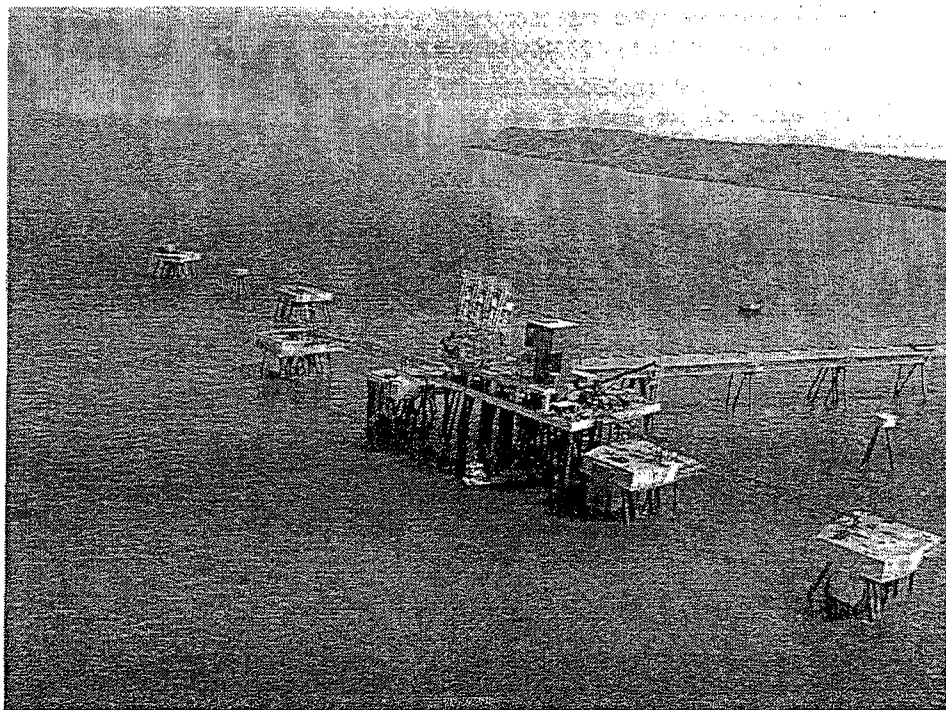
Figure 3.18   Typical jetty head (courtesy Kier) (from McConnell, et al.)
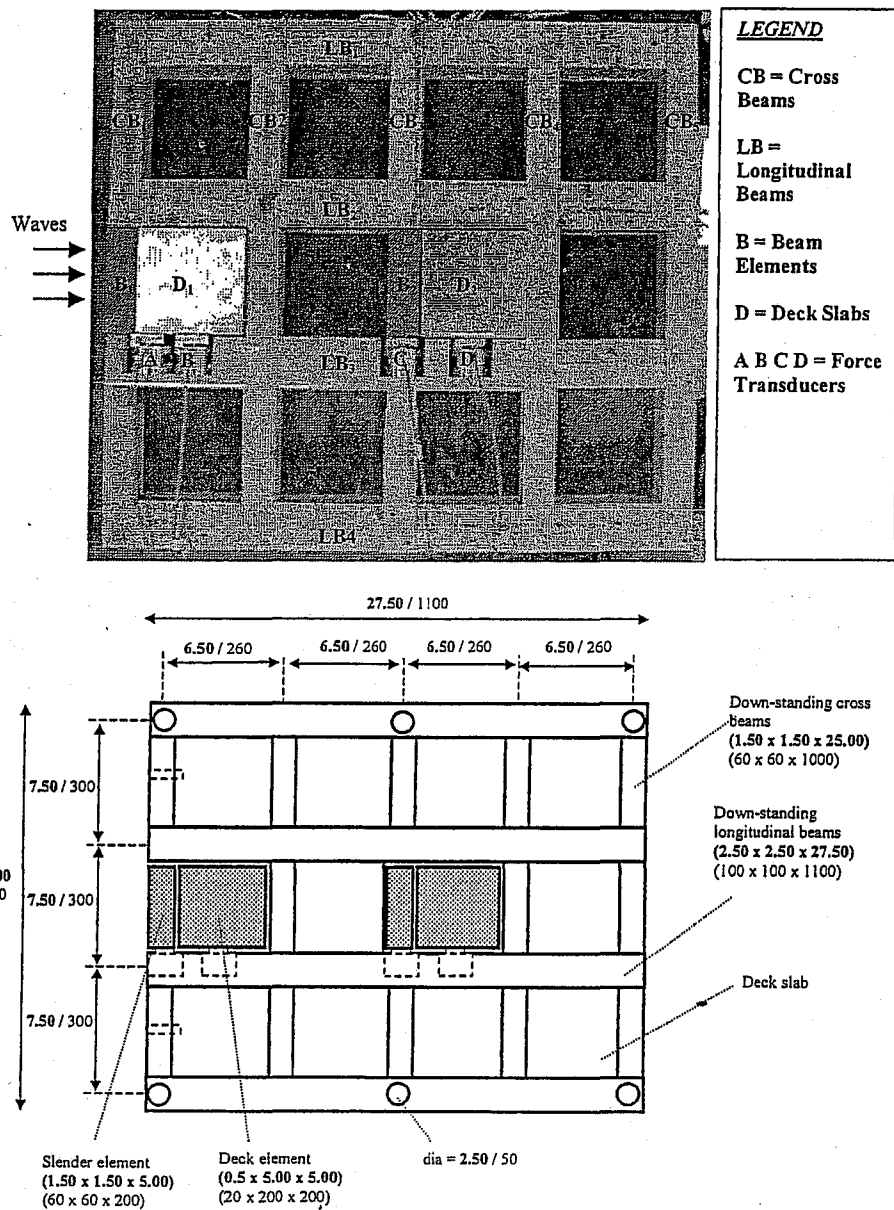
Figure 3.19 Underside of model deck showing measurement elements
Note: dimensions given as prototype (model)
(from McConnell, et al.)

Figure 3.20   Physical model in wave flume (McConnell et al., 2004)
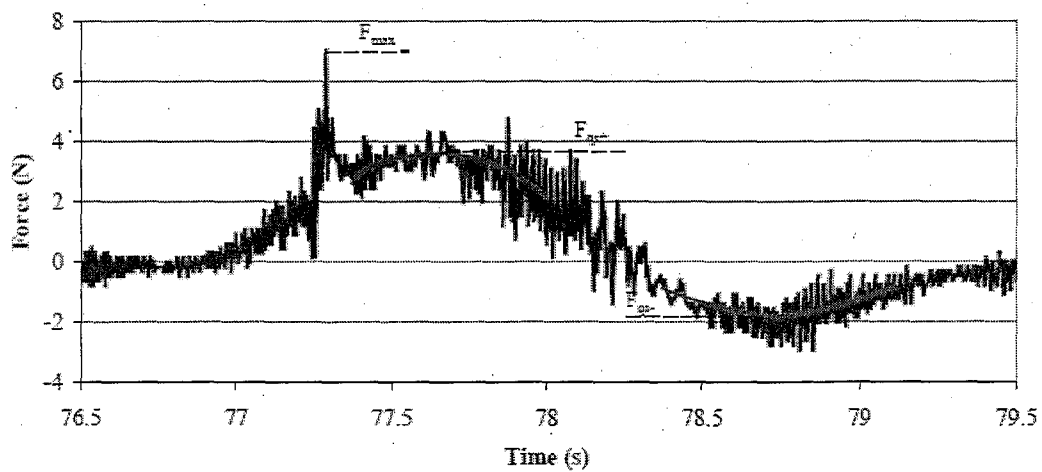
Figure 3.21   Definition of force parameters (model units)
(McConnell et al., 2004)

A subset of the most pertinent (for the case of coastal bridges) of McConnell, et al.

results are presented and discussed below. To render the results more general in

application, the results were presented in a dimensionless format. To do this, two basic

wave forces, F_v^* and F_h^*, were first defined as shown in Fig. 3.22. In each case it is

assumed that there is no water/pressure on the reverse side of the element, and a predicted

maximum wave crest elevation, η_{max}, is required in both cases.
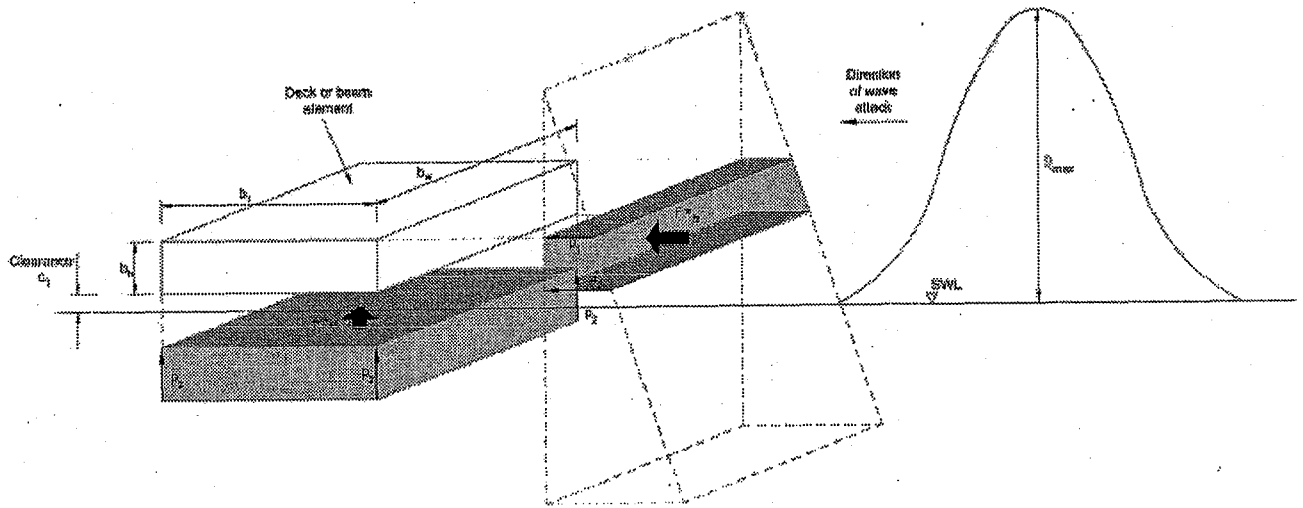
**Figure 3.22   Definition of 'basic wave forces' F_v^* and F_h^*
(from McConnell, et al.)**

As indicated in Fig. 3.22, F_v^* is defined by a simplified pressure distribution using

hydrostatic pressures, p_1 and p_2, at the top and bottom of the particular element being

considered, and F_h^* is calculated assuming a uniform pressure p_2 over the base of the

element. F_v^* and F_h^* can be calculated as follows:

$$F_v^* = \int_{b_w} \int_{b_l} p_2 \cdot dA \cong b_w \cdot b_l \cdot p_2 \qquad (3.5)$$

$$F_h^* = \int_{b_w} \int_{c_l}^{\eta_{max}} p_{hyd} \cdot dA = b_w \cdot (\eta_{max} - c_l) \cdot \frac{p_2}{2} \qquad \text{for } \eta_{max} \le c_l + b_h \qquad (3.6)$$

$$F_h{}^* = \int_{b_w} \int_{c_i}^{c_i+b_h} p_{hyd} \cdot dA = b_w \cdot b_h \cdot \frac{(p_1+p_2)}{2} \qquad \text{for } \eta_{max} > c_i + b_h \qquad (3.7)$$

where

$$p_1 = [\eta_{max} - (b_h + c_i)] \cdot \rho g \qquad\qquad (3.8)$$

$$p_2 = (\eta_{max} - c_i) \cdot \rho g \qquad\qquad (3.9)$$

and

p_{hyd}	hydrostatic pressure
p_1, p_2	pressures at top and bottom of the element
b_w	element width (perpendicular to direction of wave attack)
b_h	element depth
b_i	element length (in direction of wave attack)
c_i	clearance (distance between soffitt level and still water level, SWL)
η_{max}	maximum wave crest elevation (relative to SWL)
ρ	mass density of water

Note in the above equations that in order to estimate the maximum wave crest elevation, η_{max}, the maximum wave height, H_{max}, must be estimated. Methods of doing this are given by Goda (1985) for a range of conditions and by Battjes & Groenendijk (2000) for shallow foreshores. The maximum wave crest elevation, η_{max}, can then be estimated from H_{max} using various non-linear wave theories, e.g., $\eta_{max} = 0.78 H_{max}$ for shallow water conditions.

In presenting the wave flume testing results, McConnell et. al. present plots of the dimensionless forces F_{qs}/F^*, plotted against the dimensionless parameter $(\eta_{max} - c_i)/H_s$, which describes the incident wave conditions and geometry. When written as $(\eta_{max}/H_s) - (c_i/H_s)$, this parameter describes the relative elevation of the wave crest (η_{max}/H_s), often between 1.0 and 1.3, minus the relative excess of the wave over the clearance (c_i/H_s). The following subset of McConnell's results/forces are presented and discussed below:

- vertical upward acting force, F_{vqs+} caused by wave hitting the underside of the deck or beam/girder

- horizontal landward force, F_{hqs+} caused by the wave hitting the face of the beam/girder

It should be noted that McConnell's paper concentrates on the slowly-varying or quasi-static forces (F_{qs}). Shorter duration impact forces, F_{max}, as defined in Figure 3.21, were also processed and are briefly discussed in the paper.

Vertical quasi-static forces on the seaward beam elements and deck elements were found to be relatively unaffected by the configuration of the test structure, and were similar in magnitude for both element types. These were therefore considered together, see Figure 3.23 for upward-acting forces. It is worth noting that the smooth deck tended to give lower element loads than the deck with downstanding beams. Conditions for the internal elements are more complex, with the deck and beam elements showing different trends. The results for upward loads on the internal deck element are shown in Figure 3.24. Upward loads were not obviously influenced by 3-d effects. The following general observations can be made for vertical forces for all of the test elements:

- For $(\eta_{max} - c_i)/H_s > 0.8$, F_v^* seems to give a safe estimation of F_{vqs+}

- For $(\eta_{max} - c_i)/H_s < 1$, F_{vqs+} forces increase relative to F_v^*

  as $(\eta_{max} - c_i)/H_s$ decreases

- For $(\eta_{max} - c_i)/H_s < 1$, relative forces show significant scatter.

The horizontal quasi-static forces on beams, seaward and internal beam elements, are considered separately as the loads on internal beams are influenced by the deck structure, while loads on the seaward beam are unaffected by the structure configuration. Positive forces, acting in the direction of wave attack, i.e., landward, F_{hqs+} are presented in Figures 3.25 and 3.26 for seaward and internal beams, respectively, plotted against $(\eta_{max} - c_i)/H_s$. The scatter for these data is much less than for vertical loads for almost all of the data, with scatter increasing for smaller values of $(\eta_{max} - c_i)/H_s$.
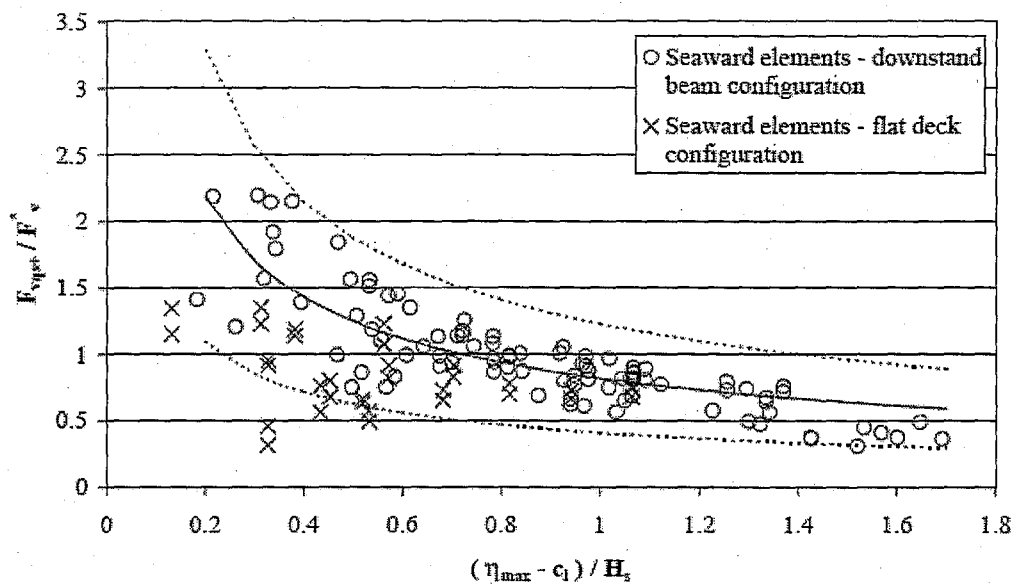
Figure 3.23 Vertical (upward) forces on seaward elements (from McConnell, et al.)
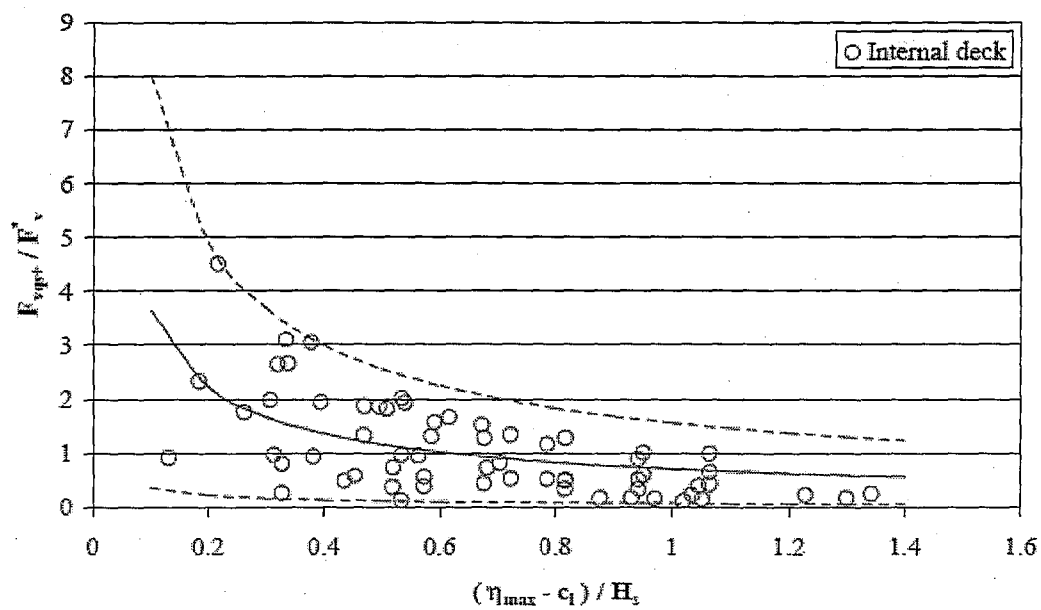
Figure 3.24 Vertical (upward) forces on internal deck (from McConnell, et al.)
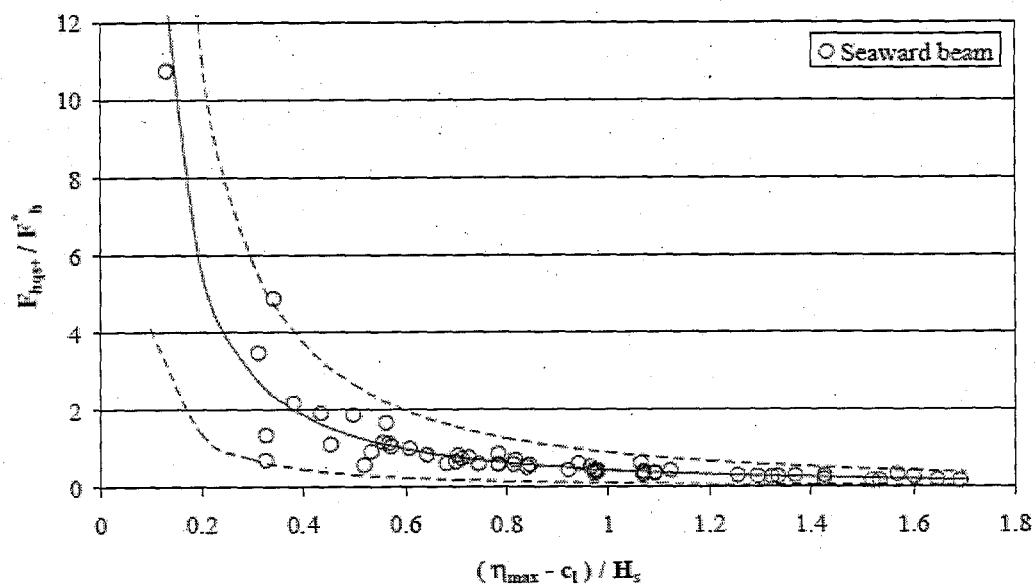
Figure 3.25   Horizontal (shoreward) forces on seaward beams (from McConnell, et al.)
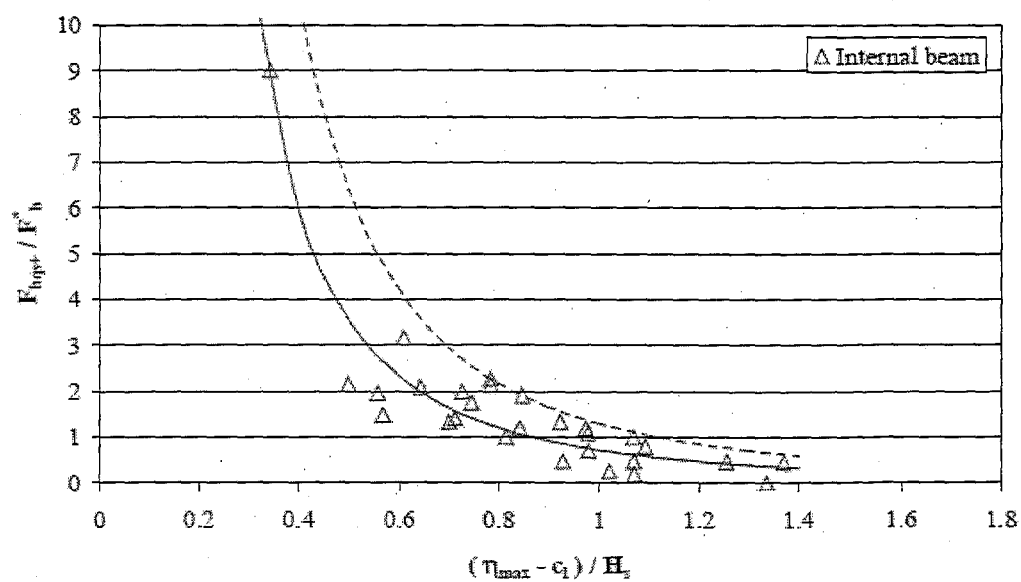
Figure 3.26   Horizontal (shoreward) forces on internal beams (from McConnell, et al.)

Short duration wave impact forces on beam and deck elements were also measured in the tests. In order to fully assess the importance of impact forces, information is necessary on their duration and also on the dynamic response characteristics for the structure in question. Wave impact forces were not examined and discussed in detail, however, a comparison is given of vertical impact forces and quasi-static impact forces for each test, where F_{max} is the largest impact force recorded in a test and F_{vqs+} is the associated quasi-static force. The results are presented in Figure 3.27 where it can be seen that none of the impact forces measured exceed their quasi-static component by more than 4 times.
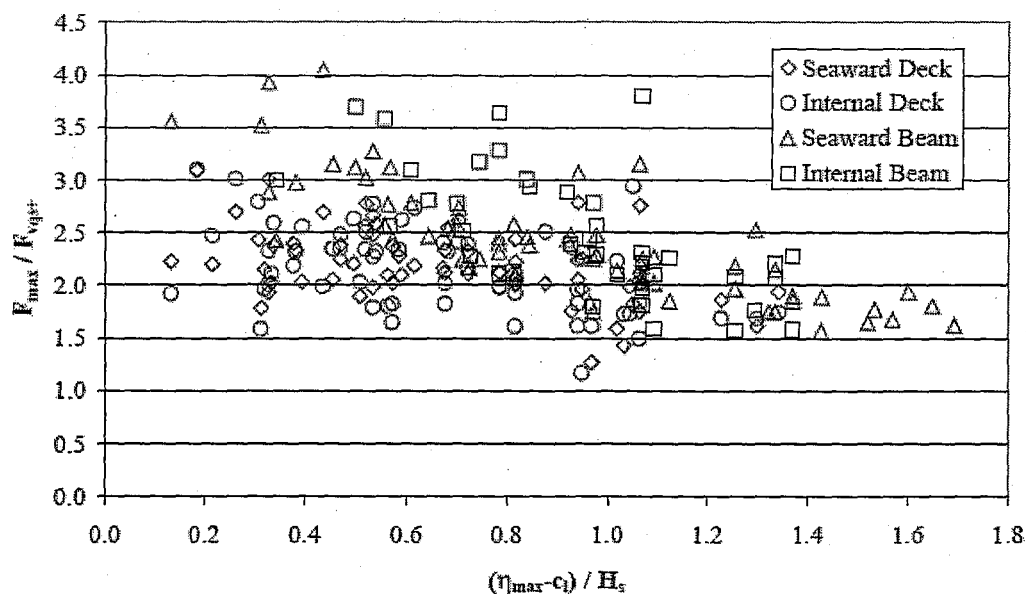
Figure 3.27   Ratio of vertical impact forces to quasi-static forces (from McConnell, et al.)

The select data sets from the wave flume model tests are presented in graphical form in Figures 3.23 to 3.26 for both vertical and horizontal quasi-static forces. Best fit regression lines fitted to each data set are shown by a solid line on the graphs (the dotted lines show upper and lower bound envelopes). The general form of the regression lines are:

$$\frac{F_{qs}}{F^*} = \frac{a}{\left[\dfrac{(\eta_{max} - c_l)}{H_s}\right]^b}$$

(3.10)

where

F_{qs} quasi-static force of interest (F_{vqs+} or F_{hqs+})

F^* 'basic wave force', either $F_v{}^*$ or $F_h{}^*$ defined in Equations (3.5) to (3.7)

c_l clearance (distance between soffit level and still water level, SWL)

η_{max} maximum wave crest elevation (relative to SWL)

a,b   coefficients

Coefficients a and b for the various configurations are given below in Table 3.1 for

upward vertical forces and for shoreward horizontal forces.

Table 3.1   Coefficients for calculation of upward vertical wave forces and shoreward horizontal forces using Equation 3.10

Wave load and configuration	EQN (3.10) Coefficients	
	a	b
Upward vertical forces (seaward beam & deck)	0.82	0.61
Upward vertical forces (internal beam only)	0.84	0.66
Upward vertical forces (internal deck, 2 and 3-d effects)	0.71	0.71
Shoreward horizontal forces, F_{hqs+} (seaward beam)	0.45	1.56
Shoreward horizontal forces, F_{hqs+} (internal beam)	0.72	2.30

Example Application. An example application of McConnell et al. Eqn (3.10) for an

assumed deck-girder bridge, as shown in Fig. 3.28a, is presented below. An assumed

storm sea state is as shown in Fig. 3.28a where

$c_l = 4.0$ ft (for deck) and $c_l = 1.0$ ft (for girders)
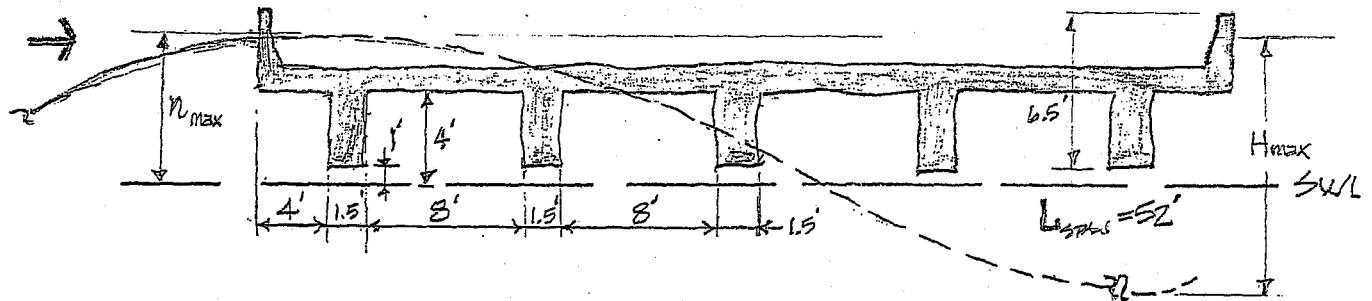
a. Assumed Bridge and Storm Wave Geometry
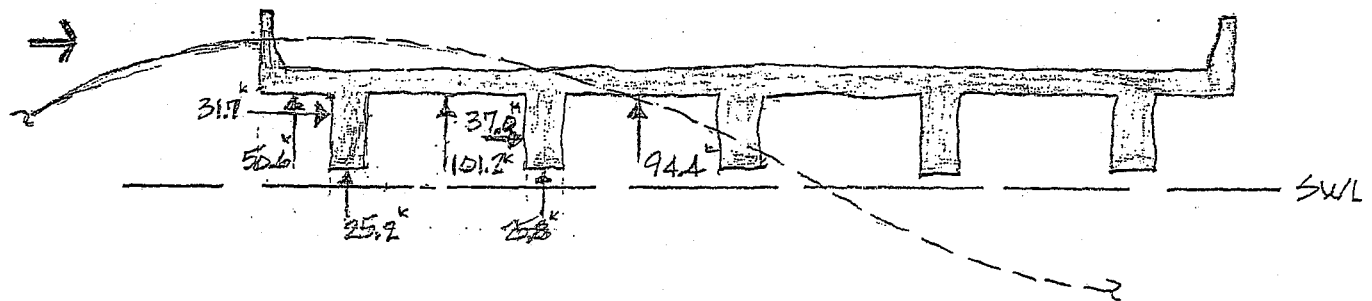
b. Vertical and Horizontal Storm Wave Element Forces
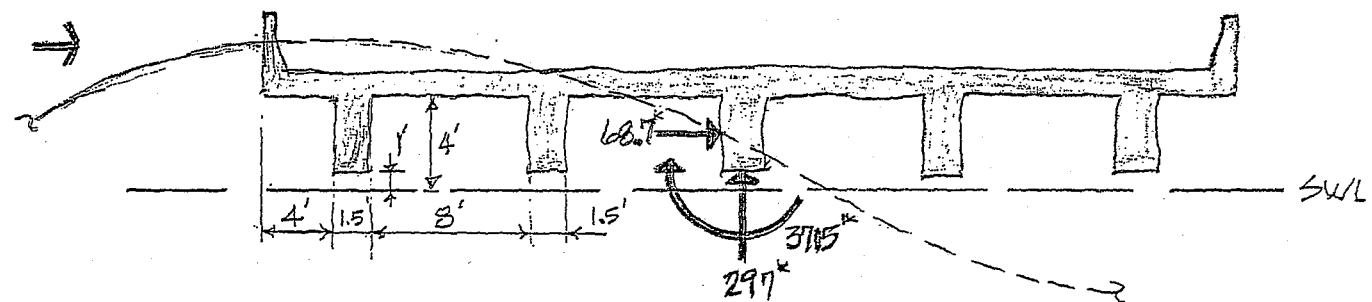
c. Resultant Storm Wave Forces

Figure 3.28   Example Bridge Superstructure and Storm Wave Geometry, Vertical
and Horizontal Storm Wave Forces on Elements, and Resultant
Storm Wave Forces

and assuming,

H_s = 6.3 ft

H_{max} = 1.4H_s = 1.4 x 6.3' = 8.8 ft

η_{max} = 0.78H_{max} = 0.78 x 8.8' = 6.86 ft

Vertical Force on Seaward Elements:

$$\frac{F_{vqs+}}{F_V{}^*} = \frac{a}{\left[\dfrac{(\eta_{max} - c_i)}{H_s}\right]^b}$$

$$F_{vqs+} = F_V{}^* \frac{a}{\left[\dfrac{(\eta_{max} - c_i)}{H_s}\right]^b}$$

where from Table 3.1,
$a = 0.82$
$b = 0.61$ } for Deck and Girder

For Deck:

$$F_{vqs+} = F_{VD}{}^* \frac{0.82}{\left[\dfrac{(6.86 - 4.0)}{6.3}\right]^{0.61}} = 1.33\ F_{VD}$$ (See also Fig. 3.23)

where $F_{VD}{}^* = b_w \cdot b_l \cdot p_2$

$p_2 = (\eta_{max} - c_i)\ \gamma = (6.86 - 4.0)64 = 183$ psf

Assuming a bridge superstructure as shown in Fig. 3.28a,

On overhang deck portion, b_w = 4.0' and b_l = 52'

$F_{VD}{}^* = 183$ psf x 4' x 52' = 38.1^k

$F_{vqs+} = 1.33$ x 38.1^k = 50.6^k

3-47

On deck inward from exterior girder, $b_w = 8.0'$ and $b_l = 52'$

$$F_{VD}{}^* = 183 \text{ psf} \times 8' \times 52' = 76.12^k$$

$$F_{vqs+} = 1.33 \times 76.12^k = 101.2^k$$

For Girder:

$$F_{vqs+} = F_{VG}{}^* \frac{0.82}{\left[\dfrac{6.86 - 1.0}{6.3}\right]^{0.61}} = 0.86 \, F_{VG}{}^*$$

where $F_{VG}{}^* = b_w \cdot b_l \cdot p_2$

$$p_2 = (\eta_{max} - c_l)\gamma = (6.86 - 1.0)64 = 375 \text{ psf}$$

$$F_{VG}{}^* = 1.5' \times 52' \times 375 \text{ psf} = 29.25^k$$

$$F_{vqs+} = 0.86 \times 29.25^k = 25.2^k$$

Vertical Force on Internal Elements:

$$F_{vqs+} = \frac{a}{\left(\dfrac{\eta_{max} - c_l}{H_s}\right)^b}$$

where from Table 3.1,
  a = 0.71, b = 0.71 for Deck
  a = 0.84, b = 0.66 for Girder

For Deck:

$$F_{vqs+} = F_{VD} * \frac{0.71}{\left[\dfrac{6.86 - 4.0}{6.3}\right]^{0.71}} = 1.24 F_{VD}^* \quad \text{(See also Fig. 3.24)}$$

where $F_{VD}^* = b_w \cdot b_l \cdot p_2$

$p_2 = (\eta_{max} - c_i)\gamma = (6.86 - 4.0)64 = 183 \text{ psf}$

$F_{VD}^* = 8' \times 52' \times 183 \text{ psf} = 76.12^k$

$F_{vqs+} = 1.24 \times 76.12^k = 94.4^k$

For Girder:

$$F_{vqs+} = F_{VG} * \frac{0.84}{\left[\dfrac{6.86 - 1.0}{6.3}\right]^{0.66}} = 0.88 \, F_{VG}^*$$

where $F_{VG} = b_w \cdot b_l \cdot p_2$

$p_2 = (\eta_{max} - c_i)\gamma = (6.86 - 1.0)64 = 375 \text{ psf}$

$F_{VG}^* = 1.5' \times 52' \times 375 = 29.25^k$

$F_{vqs+} = 0.88 \times 29.25^k = 25.8^k$

Thus, the estimated vertical storm wave forces on the example bridge superstructure elements would be as shown in Fig. 3.28b, and the resultant vertical force and overturning moment would be as shown in Fig. 3.28c. Note in Figure 3.28, that the maximum wave forces do not act on all elements of the deck and all of the girders simultaneously.

Horizontal Force on Seaward Beams/Girders:

$$\frac{F_{hqs+}}{F_h{}^*} = \frac{a}{\left(\dfrac{\eta_{max} - c_l}{H_s}\right)^b} \implies \text{from Table 3.1,}$$

a = 0.45
b = 1.56

η_{max} = 6.86'
c_l = 1.0 (on girder)
H_s = 6.3'

$$\therefore F_{hqs+} = \frac{0.45\, F_h{}^*}{\left(\dfrac{6.86-1.0}{6.3}\right)^{1.56}} = 0.50\, F_h{}^*$$

where $F_h{}^* = b_w \times b_h \times \left(\dfrac{p_1 + p_2}{2}\right)$

$p_1 = [\eta_{max} - (b_h + c_l)]\gamma = [6.86 - (6.50 + 1.0)]64 = -41$ psf

$\therefore$ Take $p_1 = 0$

$p_2 = [\eta_{max} - c_l]\gamma = [6.86 - 1.0]64 = 375$ psf

$$F_h{}^* = 52' \times 6.50' \times \left(\frac{0+375}{2}\right) = 63.4^k$$

$F_{hqs+} = 0.50 \times 63.4 = 31.7^k$

Horizontal Force on Interior Beam/Girder:

$$\frac{F_{hqs+}}{F_h{}^*} = \frac{a}{\left(\dfrac{\eta_{max} - c_l}{H_s}\right)^b} \implies \text{from Table 3.1,}$$

a = 0.72
b = 2.30

$$F_{hqs+} = \frac{0.72\, F_h{}^*}{\left(\dfrac{6.86-1.0}{6.3}\right)^{2.30}} = 0.85\, F_h{}^*$$

where $F_h^* = b_w \times b_h \times \left(\dfrac{p_1 + p_2}{2}\right)$

$p_1 = [\eta_{max} - (b_h + c_i)]\gamma$

$p_1 = [6.86 - (3.0 + 1.0)]64 = 183 \text{ psf}$

$p_2 = [\eta_{max} - c_i]\gamma$

$p_2 = [6.86 - 1.0]64 = 375 \text{ psf}$

$F_h^* = 52' \times 3' \times \left(\dfrac{183 + 375}{2}\right) = 43.5^k$

$F_{hqs+} = 0.85 \times 43.5 = 37.0^k$

The above estimate horizontal forces are shown acting on the seaward girder and first interior girder in Fig. 3.28b. The resultant of these two horizontal forces are shown in Fig. 3.28c. In that figure, the resultant moment of $3715^{k'}$ is assumed to come only from the vertical wave force components.

Example Application – Determine the maximum wave forces and moment on a 52 ft long I-10 ramp span in Mobile Bay when Hurricane Katrina hit, using McConnell, et al. equations.

A partial sketch of the ramp span geometry and elevations and the maximum sea state at the ramp when Katrina hit are shown in Fig. 3.29.

Fig. 3.29 Partial sketch of Mobile, AL I-10 ramp span geometry and sea state during Hurricane Katrina

In performing the analysis the following pertinent parameter values were extracted from the storm data or were assumed:

SWL$_{local}$ = at top of bent cap = SWL$_{storm}$ + 2' (assumed for Example)

SWL_{storm} = at bottom of bent cap

$h_c = 0.78H_b$

$h_t = 0.22H_b$

Significant Wave Ht. = H_s = 6.1'

Max Wave Ht. = H_b = $1.4H_s$ = 8.5'

$h_c = \eta_{max}$ = 0.78 x 8.5' = 6.6' $\Longrightarrow$ Use 6.5' (top of rail)

d_b = Initial Depth + Max Storm Surge = Elev. Of Bottom of Bent Cap

d_b = 4' +12' = 16'

Span Length = 52'

Elev Bay Bottom = 0'

Elev MWL = 4'

Elev. Bottom of Bent Cap = 16'

Elev. Top of Bent Cap = 18'

Elev. Bottom of Girders = 18'

Elev. Top of Guardrail = 24.5'

Girder Spacing = s_g = 8.0'

Clearance = c_i = 0' (on girders); c_i = 3' (on deck)

Analysis:

Use McConnell's Eqns with H_s = 6.1' c_i = 0 (on girders)

                                  η_{max} = 6.5' c_i = 3' (on deck)

3-53.

Vertical Force:

$$\frac{F_{vqs+}}{F_V^*} = \frac{a}{\left[\dfrac{(\eta_{max} - c_I)}{H_s}\right]^b} \implies F_{vqs+} = F_V^* \frac{a}{\left[\dfrac{(\eta_{max} - c_I)}{H_s}\right]^b}$$

For Seaward Elements: $\implies$ From McConnell's Table,

$$\left.\begin{array}{l} a = 0.82 \\[6pt] b = 0.61 \end{array}\right\} \text{For deck and girder}$$

For Deck:

$$F_{vqs+} = F_{VD}^* \frac{0.82}{\left[\dfrac{(6.5 - 3.0)}{6.1}\right]^{0.61}} = 1.15\, F_{VD}^*$$

where $F_{VD}^* = b_w \cdot b_I \cdot p_2$

$$p_2 = (\eta_{max} - c_I)\, \gamma = (6.5 - 3.0)64 = 224 \text{ psf}$$

Assuming a bridge superstructure as shown in Fig. 3.29,

On overhang deck portion, $b_w = 3.5'$ and $b_I = 52'$

$$F_{VD}^* = 224 \text{ psf} \times 3.5' \times 52' = 40.77^k$$

$$F_{vqs+} = 1.15 \times 40.77^k = 46.9^k$$

On deck inward from exterior girder, $b_w = 6.5'$ and $b_I = 52'$

$$F_{VD}^* = 224 \text{ psf} \times 6.5' \times 52' = 75.71^k$$

$$F_{vqs+} = 1.15 \times 75.71^k = 87.1^k$$

For Girder:

$$F_{vqs+} = F_{VG}^* \frac{0.82}{\left[\dfrac{6.5-0}{6.1}\right]^{0.61}} = 0.79\, F_{VG}^*$$

where $F_{VG}^* = b_w \cdot b_l \cdot p_2$

$p_2 = (\eta_{max} - c_l)\gamma = (6.5 - 0)64 = 416 \text{ psf}$

$F_{VG}^* = 1.5' \times 52' \times 416 \text{ psf} = 32.45^k$

$F_{vqs+} = 0.79 \times 32.45^k = 25.6^k$

For Internal Elements:

$$F_{vqs+} = \frac{a}{\left(\dfrac{\eta_{max}^i - c_l}{H_s}\right)^b}$$

From McConnell's Table,
a = 0.71, b = 0.71 for Deck
a = 0.84, b = 0.66 for Girder

For Deck:

$$F_{vqs+} = F_{VD}^* \frac{0.71}{\left[\dfrac{6.5-3.0}{6.1}\right]^{0.71}} = 1.05\, F_{VD}^*$$

where $F_{VD}^* = b_w \cdot b_l \cdot p_2$

$p_2 = (\eta_{max} - c_l)\gamma = (6.5 - 3.0)64 = 224 \text{ psf}$

$F_{VD}^* = 6.5' \times 52' \times 224 \text{ psf} = 75.71^k$

$F_{vqs+} = 1.05 \times 75.71^k = 79.5^k$

For Girder:

$$F_{vqs+} = F_{VG} * \frac{0.84}{\left[\frac{6.5-0}{6.1}\right]^{0.66}} = 0.81 \, F_{VG}{}^*$$

where $F_{VG} = b_w \cdot b_l \cdot p_2$

$$p_2 = (\eta_{max} - c_i) \, \gamma = (6.5 - 0)64 = 416 \text{ psf}$$

$$F_{VG}{}^* = 1.5' \times 52' \times 416 = 32.45^k$$

$$F_{vqs+} = 0.81 \times 32.45^k = 26.3^k$$

Thus, the estimated vertical storm wave forces on the example bridge superstructure elements would be as shown in Fig. 3.30b and the resultant vertical force and overturning moment would be as shown in Fig. 3.30c. Note in Figure 3.30, that the maximum wave forces do not act on all elements of the deck and all of the girders simultaneously.

Horizontal Force:

$$\frac{F_{hqs+}}{F_h{}^*} = \frac{a}{\left(\dfrac{\eta_{max} - c_i}{H_s}\right)^b} \qquad \Longrightarrow \qquad F_{hqs+} = F_h{}^* \frac{a}{\left[\dfrac{\eta_{max} - c_i}{H_s}\right]^b}$$

Seaward Beams/Girders: $\Longrightarrow$ From McConnell's Table,
$a = 0.45$
$b = 1.56$
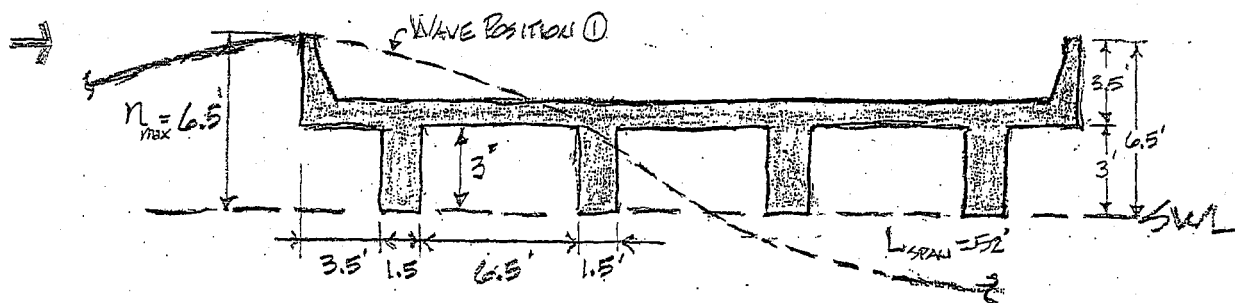
a. Assumed Bridge and Storm Wave Geometry
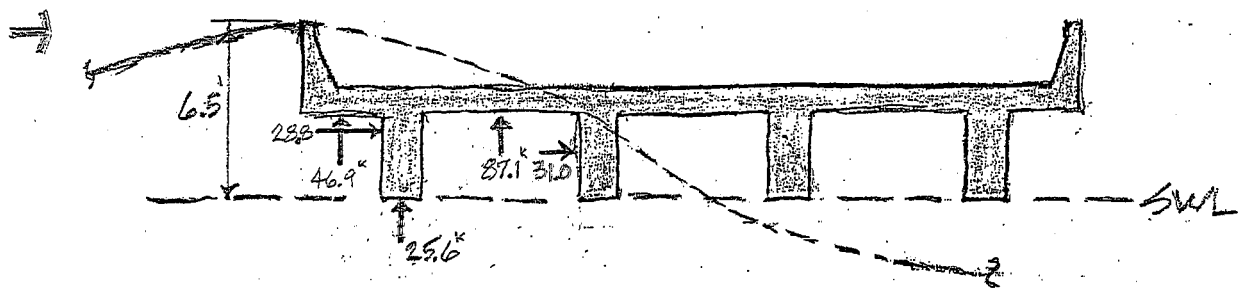
b. Vertical and Horizontal Storm Wave Element Forces
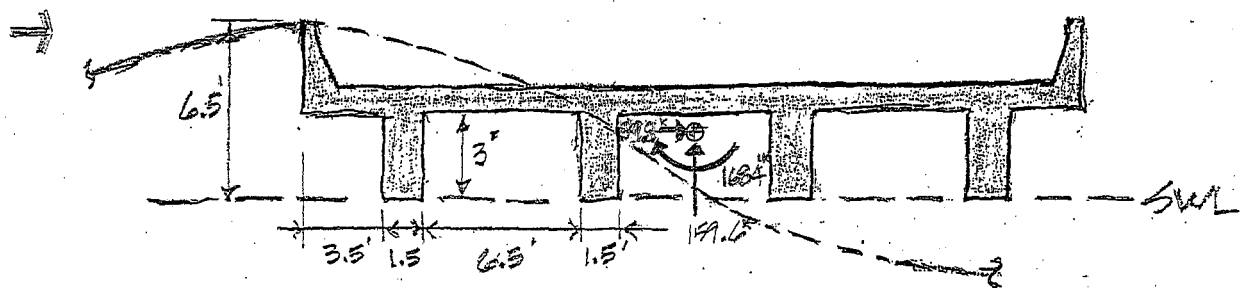
c. Resultant Storm Wave Forces

Figure 3.30   I-10 On-Ramp Bridge Superstructure and Storm Wave Geometry, Vertical and Horizontal Storm Wave Forces on Elements, and Resultant Storm Wave Forces For Wave Position ①

$$\therefore F_{hqs+} = \frac{0.45\,F_h{}^*}{\left(\dfrac{6.5-0}{6.1}\right)^{1.56}} = 0.41\,F_h{}^*$$

where $F_h{}^* = b_w \times b_h \times \left(\dfrac{p_1 + p_2}{2}\right)$

$p_1 = [\eta_{max} - (b_h + c_l)]\gamma = [6.5 - (6.50 + 0)]64$

$p_1 = 0$

$p_2 = [\eta_{max} - c_l]\gamma = [6.5 - 0]64 = 416$ psf

$$F_h{}^* = 52' \times 6.50' \times \left(\frac{0+416}{2}\right) = 70.3^k$$

$F_{hqs+} = 0.41 \times 70.3 = 28.8^k$

Interior Beam/Girder:

$$\frac{F_{hqs+}}{F_h{}^*} = \frac{a}{\left(\dfrac{\eta_{max} - c_l}{H_s}\right)^b} \qquad \Longrightarrow \qquad \begin{array}{l}\text{from McConnell's Table} \\ a = 0.72 \\ b = 2.30\end{array}$$

$$F_{hqs+} = \frac{0.72\,F_h{}^*}{\left(\dfrac{6.5-0}{6.1}\right)^{2.30}} = 0.62\,F_h{}^*$$

where $F_h{}^* = b_w \times b_h \times \left(\dfrac{p_1 + p_2}{2}\right)$

$p_1 = [\eta_{max} - (b_h + c_l)]\gamma$

$p_1 = [6.5 - (3.0 + 0)]64 = 224$ psf

$p_2 = [\eta_{max} - c_l]\gamma$

$$p_2 = [6.5 - 0]64 = 416 \text{ psf}$$

$$F_h{}^* = 52' \times 3' \times \left(\frac{224 + 416}{2}\right) = 49.9^k$$

$$F_{hqs+} = 0.62 \times 49.9 = 31.0^k$$

The above estimate horizontal forces are shown acting on the seaward girder and first interior girder in Fig. 3.30b. The resultant of these two horizontal forces are shown in Fig. 3.30c, where in that figure the resultant moment of 1684^{kr} is assumed to come only from the vertical wave force components.

It should be noted from the large vertical forces on the deck element that the wave position causing the maximum uplift force on the bridge span would probably be wave position ② shown in Fig. 3.31. Also shown on this figure are the element and resultant forces on a bridge span for wave position ② .
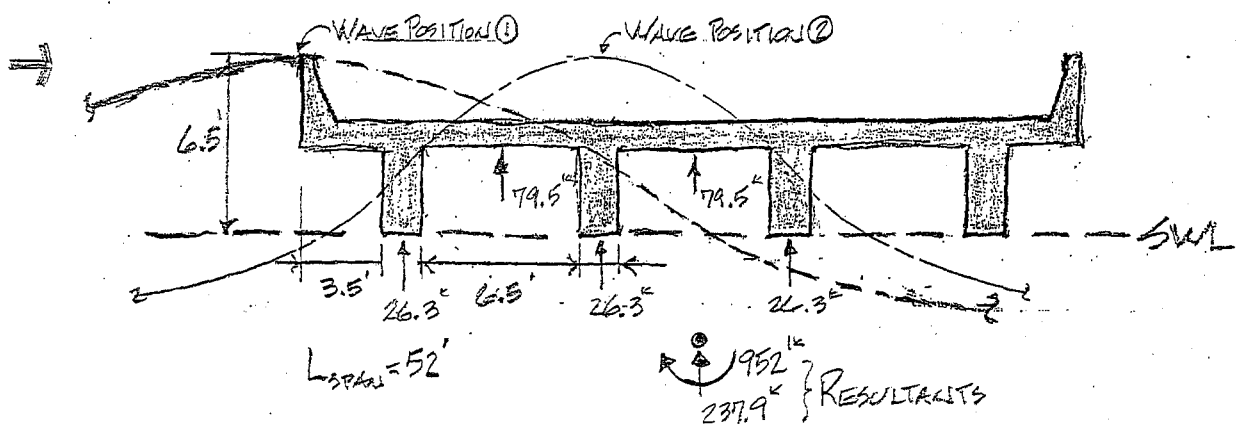
Fig. 3.31 Storm wave forces on elements and resultant forces
for wave positions ②

3.7 Douglass, et al. Equations for Wave Forces on Coastal Bridges

Douglass, et al. bridge-specific simplification of McConnell's equations for estimating ocean wave loads on elevated jetty heads/docks are given below. Their equations were developed to specifically estimate the vertical and horizontal wave load components on elevated deck-girder coastal bridge superstructures, and are as follows:

$$F_v = c_{v\text{-}va} \, F_v^*$$ (3.11)

and

$$F_h = [1 + c_r (N\text{-}1)] c_{h\text{-}va} \, F_h^*$$ (3.12)

where:

F_v	=	the estimated, vertical, wave-induced load component
F_h	=	the estimated, horizontal, wave-induced load component
F_v^*	=	a "reference" vertical load defined by Eq (3.13)
F_h^*	=	a "reference" horizontal load defined by Eq (3.14)
$c_{v\text{-}va}$	=	an empirical coefficient for the vertical "varying" load
$c_{h\text{-}va}$	=	an empirical coefficient for the horizontal "varying" load
c_r	=	a reduction coefficient for reduced horizontal load on the internal (i.e. not the waveward-most) girders (recommended value is $c_r = 0.4$)
N	=	the number of girders supporting the bridge span deck

$$F_v^* = \gamma \, (\Delta z_v) A_v$$ (3.13)

where:

A_v	=	the area the bridge contributing to vertical uplift, i.e., the projection of the bridge deck onto the horizontal plane
Δz_v	=	difference between the elevation of the crest of the maximum wave and the elevation of the underside of the bridge deck (see Figure 3.32 for definition sketch)
γ	=	unit weight of water (64 lb/ft^3 for saltwater)

$$F_h^* = \gamma\,(\Delta z_h)A_h \tag{3.14}$$

where:

A_h = the area of the projection of the bridge superstructure onto the vertical plane

Δz_h = difference between the elevation of the crest of the maximum wave and the elevation of the centroid of A_h (see Figure 3.32 for definition sketch)

γ = unit weight of water (64 lb/ft³ for saltwater)

When the wave crest elevation does not exceed the top of the bridge, a reduced area and lowered centroid corresponding to the area below the wave crest elevation can be used in Equation (3.14). The wave crest elevation used in Δz_v and Δz_h should be that corresponding to a very large wave height estimated in the design sea state, η_{max}.
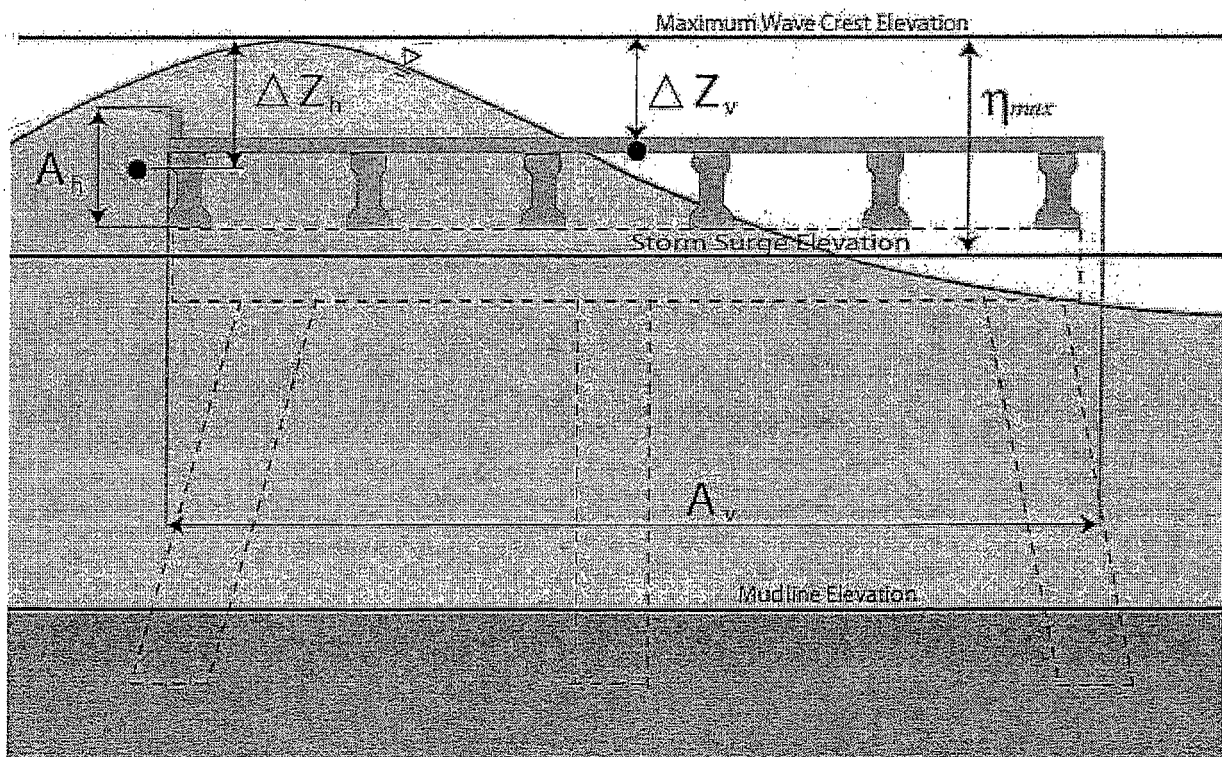
Fig. 3.32 Definition sketch for Δz_h, Δz_v, A_h, and η_{max} used in force prediction equations (from Douglass, et al.)

Given a design sea state with a significant wave height (H_s), this elevation can be estimated as:

$$\eta_{max} \approx (0.8)(1.67)\ H_s = 1.3\ H_s \tag{3.15}$$

as measured from the design storm surge elevation (see Figure 3.32).

The recommended value of each of the empirical coefficients $c_{v\text{-}va}$ and $c_{h\text{-}va}$ is given here as 1. Given the uncertainties involved in application of the above equations for estimating wave loads on bridges, Douglass, et al. recommend doubling these loads (i.e. using a factor-of-safety = 2). It is assumed that the two components (horizontal and vertical) of the wave-induced loads given above act in phase. Thus, a maximum resultant load can be resolved as usual from the two components. This resultant load can be assumed to be acting through the centroid of the cross-section.

Example Application – Determine the maximum wave forces and moment on a 52 ft long I-10 ramp span in Mobile Bay when Hurricane Katrina hit, using Douglass, et al. equations.

A partial sketch of the ramp span geometry and elevations and the maximum sea state at the ramp when Katrina hit are shown in Fig. 3.33.

Fig. 3.33 Partial sketch of Mobile, AL I-10 ramp span geometry and sea state during Hurricane Katrina

In performing the analysis the following pertinent parameter values were extracted from the storm data or were assumed:

SWL_{local} = at top of bent cap = SWL_{storm} + 2' (assumed for Example)

SWL_{storm} = at bottom of bent cap

$h_c = 0.78H_b$

$h_t = 0.22H_b$

Significant Wave Ht. = H_s = 6.1'

Max Wave Ht. = H_b = 1.4H_s = 8.5'

h_c = η_{max} = 0.78 x 8.5' = 6.6' $\Longrightarrow$ Use 6.5' (top of rail)

d_b = Initial Depth + Max Storm Surge = Elev. Of Bottom of Bent Cap

d_b = 4' +12' = 16'

Span Length = 52'

Elev Bay Bottom = 0'

Elev MWL = 4'

Elev. Bottom of Bent Cap = 16'

Elev. Top of Bent Cap = 18'

Elev. Bottom of Girders = 18'

Elev. Top of Guardrail = 24.5'

Girder Spacing = s_g = 8.0'

Δz_v = 3.5' (see Fig. 3.33)

Δz_h = 3.25' (see Fig. 3.33)

Analysis:

Use Douglass Eqns with $\qquad$ H_s = 6.1'

η_{max} = 6.5'

Δz_v = 3.5'

Δz_h = 3.25'

Vertical Force:

$$F_v = c_{v\text{-}va} \, F_V^*$$

where $c_{v\text{-}va} = 1.0$

$$F_V^* = \gamma \, (\Delta z_v) A_v$$

↘ Horizontal Projection of Bridge Deck

$$F_V^* = 64 \text{ lb/ft}^3 \times 3.5' \times 32.5' \times 52'$$

$$F_V^* = 379^k$$

$$\therefore F_v = 1.0 \times 379^k = 379^k$$

Horizontal Force:

$$F_h = [1 + c_r (N-1)] c_{h\text{-}va} \, F_h^*$$

where $c_r = 0.4$

$N = 4$

$c_{h\text{-}va} = 1.0$

$$F_h^* = \gamma \, (\Delta z_h) A_h$$

↘ Vertical Projection of Bridge
Superstructure

$$F_h^* = 64 \text{ lb/ft}^3 \times 3.25' \times 6.5' \times 52'$$

$$F_h^* = 70.3^k$$

$$\therefore F_h = [1 + 0.4(4-1)] 1.0 \times 70,300 = 154.7^k$$

$$F_h = 155^k$$

Resultant Max Wave
Loading:
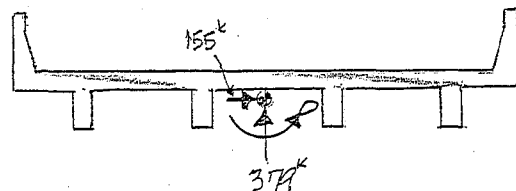
3.8　Modified Douglass, et al. Wave Force Equations

In reviewing the Douglass, et al. force prediction equations, it appears that the equations are based on the best theoretical thinking and wave flume experimental work in the literature. However, it also appears that some of the equation parameter values adopted by Douglass, et al. are overly conservative, while others may be under-conservative. For example, in defining Δz_v to the bottom of the deck, Douglass, et al. are not allowing for entrapped air in the girder-deck-girder cells and this is probably in error and underestimates the vertical force, while defining A_v as the horizontal projection of the total bridge deck that the upward water pressure acts on is probably in error (see Fig. 3.32) and this overestimates the vertical force.

Keeping the same simplified approach, the authors have modified the Douglass, et al. equations, and the modified equations are presented below. A definition sketch of parameters used in the modified force equations is shown in Fig. 3.34.
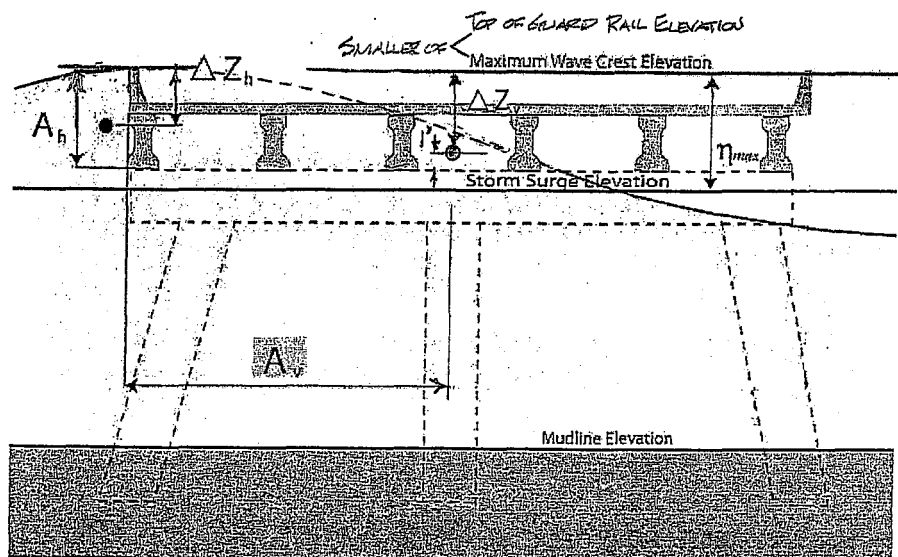
Fig. 3.34　Modified definition sketch for Δz_h, Δz_v, A_h, A_v and η_{max} used in the modified force equations

Vertical Wave Force:

$$F_v = c_v^{mc} \, F_v^*$$ (3.16a)

where, c_v^{mc} = an empirical coefficient from McConnell's work

$$c_v^{mc} \approx 1.0$$

$$F_v^* = \gamma \, (\Delta z_v) A_v$$ (3.16b)

where Δz_v = difference between the elevation of the crest of the maximum wave and the elevation of the bottom of the end diaphragms (to be taken as 1 ft. higher than thebottom of the girders)

or,

the difference between the elevation of the top of the solid portion of the guard rail and the bottom of the end diaphragms (to be taken as 1 ft. higher than the bottom of the girders),

whichever is smaller.

$$\eta_{max} = 0.78 H_{max} = 0.78 \times 1.4 \times H_s = 1.1 H_s$$

$$A_v \; = \text{bridge span length} \times \frac{\text{bridge width}}{2} \quad \text{(for widths > 20 ft)}$$
$$A_v \; = \text{bridge span length} \times \text{bridge width} \quad \text{(for widths} \leq 20 \text{ ft)}$$

Horizontal Wave Force:

$$F_h = \left[1 + c_r \frac{(N-1)}{2} \right] c_h^{mc} \, F_h^*$$ (3.17a)

where, c_r = a reduction coefficient for reduced horizontal load on half of the girders beyond the seaward girder.

$$c_r \approx 0.33$$

N = the number of span girders

c_h^{mc} = an empirical coefficient from McConnell's work (≈ 1.0)

$$F_h^* = \gamma\,(\Delta z_h)A_h \qquad\qquad\qquad (3.17b)$$

where Δz_h = the difference between the elevation of the crest of the maximum wave and the elevation of the centroid of A_h

or,

the difference between the elevation of the top of the solid portion of the guard rail and the elevation of the centroid of A_h,

whichever is smaller.

$$\eta_{max} = 0.78 H_{max} = 0.78 \times 1.4 \times H_s = 1.1 H_s$$

A_h = the bridge span length $\times$ the vertical projection of the superstructure from the girder bottoms up to the top of the solid portion of the guard rail

Moment from Wave:

We will neglect any contribution to moment from the horizontal wave force component and consider only the vertical component.
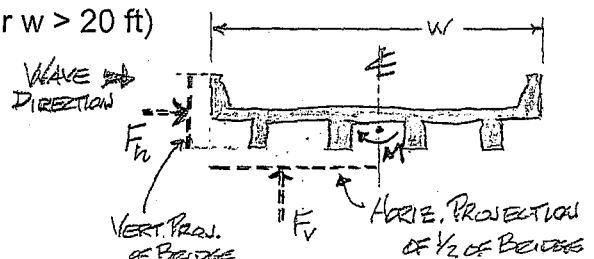
$$M = F_v \times \frac{w/2}{2}$$

$$M = F_v \times \frac{w}{4}$$

(for w > 20 ft)

$$M = 0 \text{ (for } w \le 20 \text{ ft)}$$

Resultant Wave Forces:

The resultant of the above wave forces are shown on the figure at the right, where

$$F_v = c_v^{mc} \times \gamma \times \Delta z_v \times A_v$$

$$F_h = \left[1 + c_r\left(\frac{N-1}{2}\right)\right] c_h^{mc} \times \gamma \times \Delta z_h \times A_h$$

$$M = F_v \times \frac{\text{Bridge Width}}{4}$$
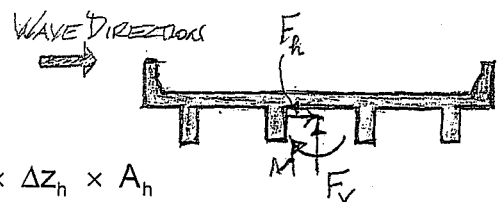
Example Application - Determine the maximum wave forces and moment on a 52 ft long I-10 ramp span in Mobile Bay when Hurricane Katrina hit using the Modified Douglass, et al. equations.

This is the same example application as was used for the Douglass, et al. equations in the previous section. See Fig. 3.33 in the previous section for a partial sketch of the ramp span geometry and elevations and the maximum sea state at the ramp when Katrina hit.

Analysis:

Use the Modified Douglass, et al. Eqns with

H_s = 6.1'

η_{max} = 6.5' (top of guard rail)

Δz_v = 5.5'

Δz_h = 3.25'

W = 32.5'

Vertical Force:

$$F_v = c_v^{mc} \ F_v^*$$

where c_v^{mc} = 1.0 (Use 1.0 to allow better comparison with Douglass' results)

$$F_v^* = \gamma \, (\Delta z_v) A_v$$

Horizontal Projection of Half of Bridge Deck (for W > 20 ft, or projection of full deck for W ≤ 20 ft)

$$F_v^* = 64 \ lb/ft^3 \times 5.5' \times \frac{32.5'}{2} \times 52' = 297.4^k$$

$$F_v^* = 298^k$$

$$\therefore F_v = 1.0 \times 298^k = 298^k$$

Horizontal Force:

$$F_h = \left[1 + c_r \frac{(N-1)}{2} \right] c_h^{mc} \; F_h^*$$

where c_r = 0.33

N = 4

c_h^{mc} = 1.0 (Use 1.0 to allow better comparison with Douglass' results)

$$F_h^* = \gamma \, (\Delta z_h) A_h$$

$\searrow$ Vertical Projection of Bridge Superstructure

$$F_h^* = 64 \; lb/ft^3 \times 3.25' \times 6.5' \times 52'$$

$$F_h^* = 70.3^k$$

$$\therefore F_h = \left[1 + 0.33 \left(\frac{4-1}{2} \right) \right] 1.0 \times 70{,}300 = 105.1^k$$

$$F_h = 105^k$$

Moment:

$$M = F_v \times \frac{\text{Bridge Width}}{4}$$

$$= 298^k \times \frac{32.5'}{4} = 2420^{k\text{-}ft}$$
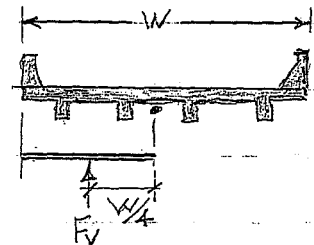
Resultant Max Wave Loading:
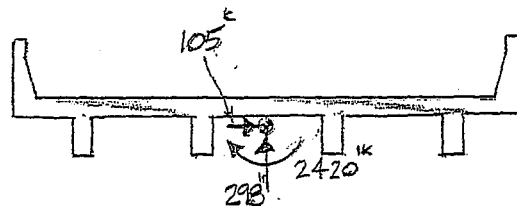
3.9 AASHTO/FHWA Pooled Project Wave Force Equations

The AASHTO/FHWA have established a Bridge Wave Task Force and they, in conjunction with ten coastal states, are currently funding a research project, "Development of Guide Specifications for Bridges Vulnerable to Coastal Storms and Handbook of Retrofit Options for Bridges Vulnerable to Coastal Storms." The 17 month project is about half-way done and the investigators have tentatively identified the following equations for ocean wave hydrostatic and hydrodynamic vertical forces on coastal bridges:

Quasi-Static Vertical Force:

$$\frac{F_z}{F^*} = a\left(\frac{W}{\lambda}\right)^b \tag{3.18a}$$

in which:

$$a = c_{z1}\left(\frac{z_c}{\eta}\right) + c_{z2} \tag{3.18b}$$

$$b = \begin{cases} c_{z3}\left(\dfrac{z_c}{\eta}\right) + c_{z4} & \text{for } \left(\dfrac{z_c}{\eta}\right) \geq 0 \\[3mm] c_{z6}\left(\dfrac{z_c}{\eta}\right) + c_{z4} & \text{for } \left(\dfrac{z_c}{\eta}\right) < 0 \end{cases} \tag{3.18c}$$

$$F^* = \gamma_w W \beta \tag{3.18d}$$

$$\beta = \begin{cases} 0 & \text{for } (\eta - z_c) \leq 0 \\[1mm] (\eta - z_c) & \text{for } 0 < (\eta - z_c) \leq t \\[1mm] t & \text{for } (\eta - z_c) > t \end{cases} \tag{3.18e}$$

where:

F_z = vertical quasi-static hydrostatic and hydrodynamic force per unit length of the span

t = girder height + deck thickness (ft)

λ = wave length (ft)

c_{z1}-c_{z6} = coefficients for vertical wave forces specified in tables (partially developed)

W = bridge width (ft)

z_c = vertical distance from bottom of cross-section to the storm water level, positive if storm water level is below the bottom of the cross-section (ft)

η = distance from the storm water level to design wave crest (ft)

γ_w = unit weight water taken as 0.064 (k/ft^3)

The investigators plan to include an equation to estimate a vertical slamming force and add this to the above value of F_z to obtain the total design/retrofit vertical force. They also plan to include equations for an associated horizontal force and moment that act simultaneously with the total vertical force. Equations for these forces are under development. It appears that the equations will use a 2% highest wave crest, i.e., $\eta_{0.02}$ in their design force equations.

Below is an application of their vertical combined hydrostatic/hydrodynamic vertical force equation to the Example I-10 Ramp Span considered in the other prediction equations in this chapter.

Example Application - Determine the maximum vertical wave force (excluding the slamming force) on a 52 ft long I-10 ramp span in Mobile Bay when Hurricane Katrina hit, using the AASHTO/FHWA Pooled Project equations.

A partial sketch of the ramp span geometry and elevations and the maximum sea state at the ramp when Katrina hit are shown in Fig. 3.35.
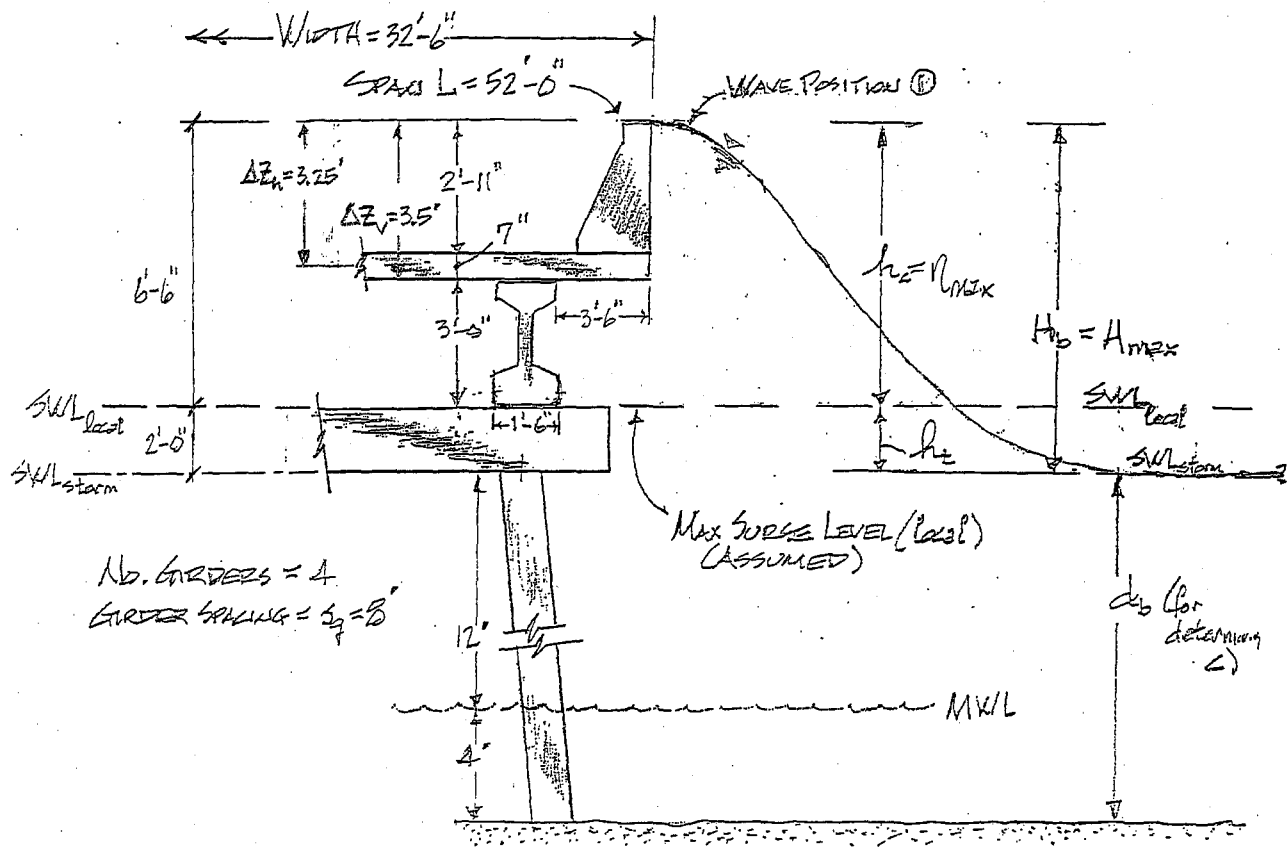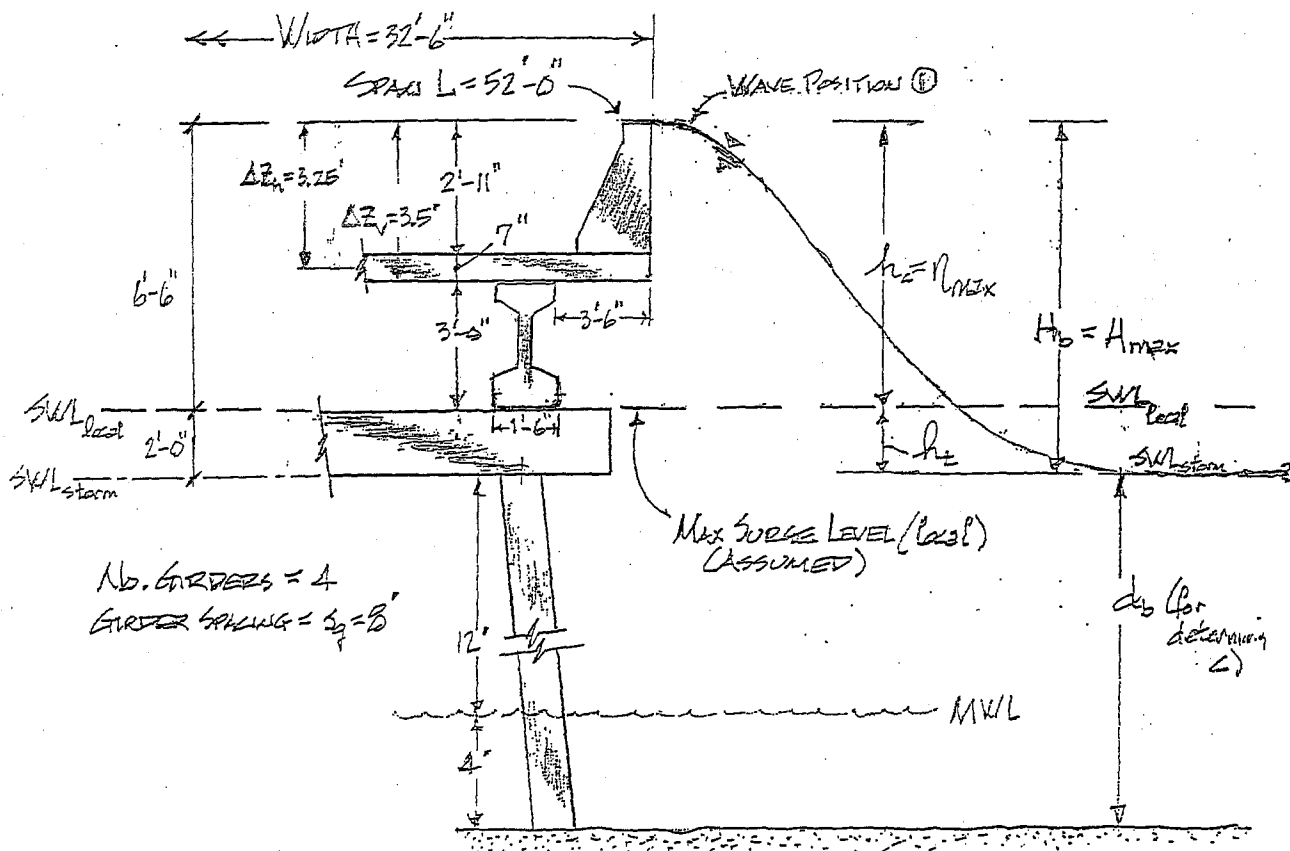

Fig. 3.35 Partial sketch of Mobile, AL I-10 ramp span geometry and sea state during Hurricane Katrina

In performing the analysis, the following pertinent parameter values were extracted from the storm data or were assumed:

SWL_{local} = at top of bent cap = SWL_{storm} + 2' (assumed for Example)

SWL_{storm} = at bottom of bent cap

$h_c = 0.78 H_b$

$h_t = 0.22 H_b$

Significant Wave Ht. = H_s = 6.1'

Max Wave Ht. = H_b = 1.4 H_s = 8.5'

$h_c = \eta_{max}$ = 0.78 x 8.5' = 6.6' $\Longrightarrow$ Use 6.5' (top of rail)

d_b = Initial Depth + Max Storm Surge = Elev. Of Bottom of Bent Cap

d_b = 4' +12' = 16'

Span Length = 52'

Elev Bay Bottom = 0'

Elev MWL = 4'

Elev. Bottom of Bent Cap = 16'

Elev. Top of Bent Cap = 18'

Elev. Bottom of Girders = 18'

Elev. Top of Guardrail = 24.5'

Girder Spacing = s_g = 8.0'

Wave Length $\approx$ 60-70 ft

Analysis:

Use AASHTO/FHWA Eqns with
H_s = 6.1'

η_{max} = 6.5'

λ = 70'

Vertical Hydrostatic/Hydrodynamic Wave Force:

$$\frac{F_z}{F^*} = a\left(\frac{W}{\lambda}\right)^b \quad \Longrightarrow \quad F_z = F^* \times a \times \left(\frac{W}{\lambda}\right)^b$$

where,

$$F^* = \gamma_w W \beta$$

where, parameters a, b, W, λ, γ_w, and β are identified in Eqns

(3.18) and where,

$c_{z1} = -0.306$

$c_{z2} = 0.406$

$c_{z3} = 0.228$ } from partially developed Tables in AASHTO/FHWA Progress Report

$c_{z4} = -0.963$

$c_{z6} = -0.271$

Thus,

$$\left(\frac{z_c}{\eta}\right) = \frac{0}{6.5} = 0$$

$$a = c_{z1}\left(\frac{z_c}{\eta}\right) + c_{z2} = -0.306(0) + 0.406 = 0.406$$

$$b = c_{z3}\left(\frac{z_c}{\eta}\right) + c_{z4} = 0.228(0) + (-0.963) = -0.963$$

W = 32.5'

$\lambda \approx 60' < \lambda < 70' \quad \Longrightarrow \quad \lambda = 70'$ yields larger F_t

$\therefore$ Use $\lambda = 70'$

$$F_z = F^* \times 0.406 \times \left(\frac{32.5}{70}\right)^{-0.963} = 0.850 \, F^*$$

where,

$$F^* = \gamma_w \times W \times \beta$$

$$\beta = \begin{cases} 0 & \text{for } (\eta - z_c) \leq 0 \\ (\eta - z_c) & \text{for } 0 < (\eta - z_c) \leq t \\ t & \text{for } (\eta - z_c) > t \end{cases}$$

$$\therefore \beta = t = 3.5 \text{ ft}$$

$$F^* = 0.064 \text{ k/ft}^3 \times 32.5' \times 3.5' = 7.28 \text{ k/ft}$$

$$\therefore F_z = 0.850 \times 7.28 \text{ k/ft} = 6.19 \text{ k/ft}$$

$$F_z^{span} = F_z \times 52' = 322^k$$

It should be noted that a vertical slamming force will be added to this value of F_z in the final version of the AASHTO/FHWA equations.

3.10 Comparison of Wave Force Predictions

A summary of resultant F_h^{max}, F_v^{max}, and M^{max} forces on the Example 52 ft long

I-10 ramp span in Mobile Bay when Katrina hit, for various assumed wave types and

modellings, is presented in Table 3.2. These same resultant forces are shown in

graphical form for convenience of comparison in Figs. 3.36 and 3.37. All of the forces

for the AASHTO/FHWA equations under development are not included in Table 3.2 and

Figs. 3.36 and 3.37 as these equations are not yet fully developed. However, it should

be noted in Fig. 3.36 that the maximum vertical hydrostatic/hydrodynamic force

predicted by the AASHTO/FHWA equation is close to that predicted by the McConnell,

et al., Douglass, et al., and the Modified Douglass equations. Also note in that figure

that the Douglass, et al. equation predicts the largest F_v^{max}, and the F_v^{max} predicted by

the Modified Douglass, et al. and the AASHTO/FHWA Pooled Project equations are

quite close to each other and are the second largest F_v^{max}. Figures 3.36 and 3.37 also

show that the Corps of Engineers Breaking Wave equation gives the largest horizontal

force, F_h, by far, and the Corps of Engineers Broken Wave equation gives the second

largest F_h force by far. Thus, if one were quite conservative and wanted to design for a

worst case scenario, he/she would use the Douglass, et al. equation to calculate F_v^{max}

and the Corps of Engineers Breaking Wave equation to calculate F_h^{max} and assume that

these forces act simultaneously on the bridge superstructure.

Table 3.2 Summary and Comparison of Resultant Wave Forces From Katrina on Example 52 ft Long I-10 Ramp Span in Mobile Bay

Assumed Wave Type/Modelling	F_h^{max} (kips)	F_v^{max} (kips)	M^{max} (ft-kips)	Max Simultaneous Acting F_h, F_v, M (kips and ft-kips)	
Corps of Engineers Unbroken Wave Forces	70.3	206	1648	$F_h = 70.3$ $F_v = 73.2$ or $M = 983$	$F_h = 0$ $F_v = 206$ $M = 1648$
Corps of Engineers Broken Wave Forces	243	134	1943	$F_h = 243$ $F_v = 134$ $M = 1943$	
Corps of Engineers Breaking Wave Forces	345	170	2465	$F_h = 345$ $F_v = 170$ $M = 2465$	
FEMA Equation	136	-	-	$F_h = 136$	
McConnell et al. Equations	60	238	1684	$F_h = 60$ $F_v = 160$ $M = 1684$	
Douglass et al. Equations	155	379	0	$F_h = 155$ $F_v = 379$ $M = 0$	
Modified Douglass et al. Equations	105	298	2420	$F_h = 105$ $F_v = 298$ $M = 2420$	
AASHTO/FHWA Pooled Project Equations	-	322	-	$F_h = -$ $F_v = 322$ $M = -$	

Recorded or Assumed Bridge Span Geometry and Sea State:

3-78
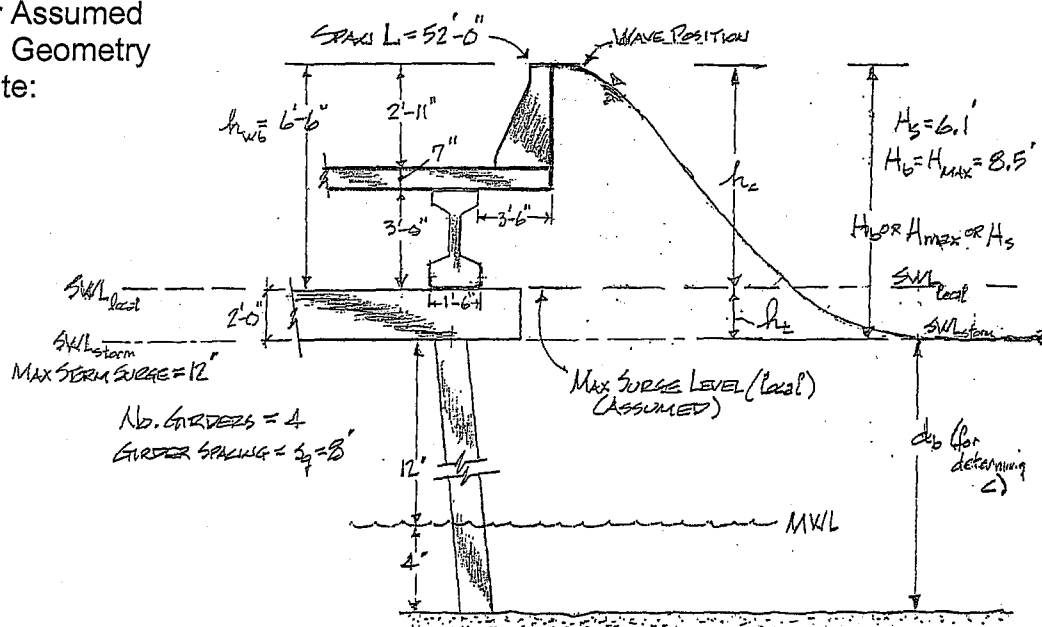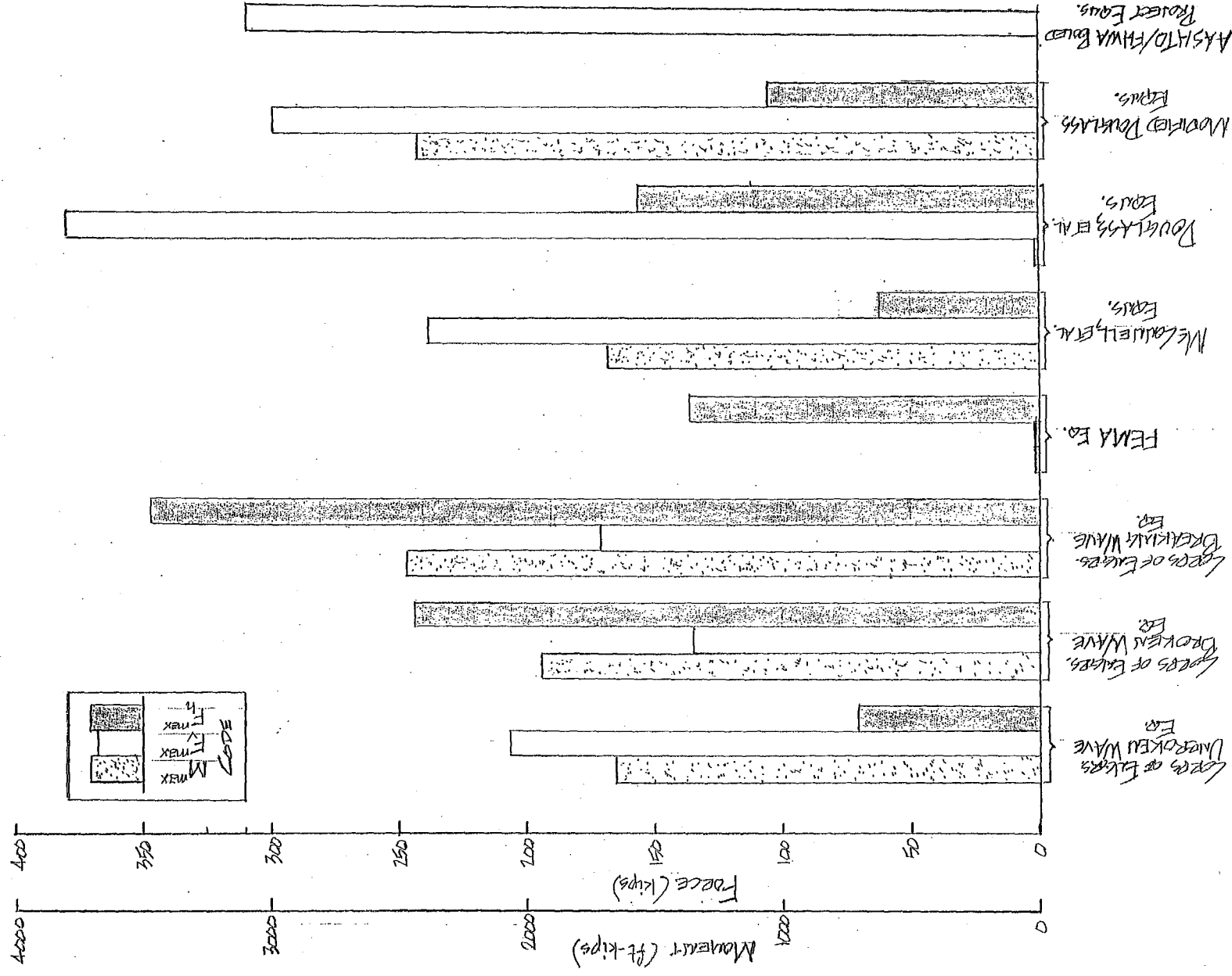
Fig. 3.36 Bar graph showing M^{max}, F_v^{max}, F_h^{max} forces acting on 52 ft long I-10 ramp span in Mobile Bay as predicted by eight sets of wave force equations (forces not necessarily acting simultaneously).

3-79
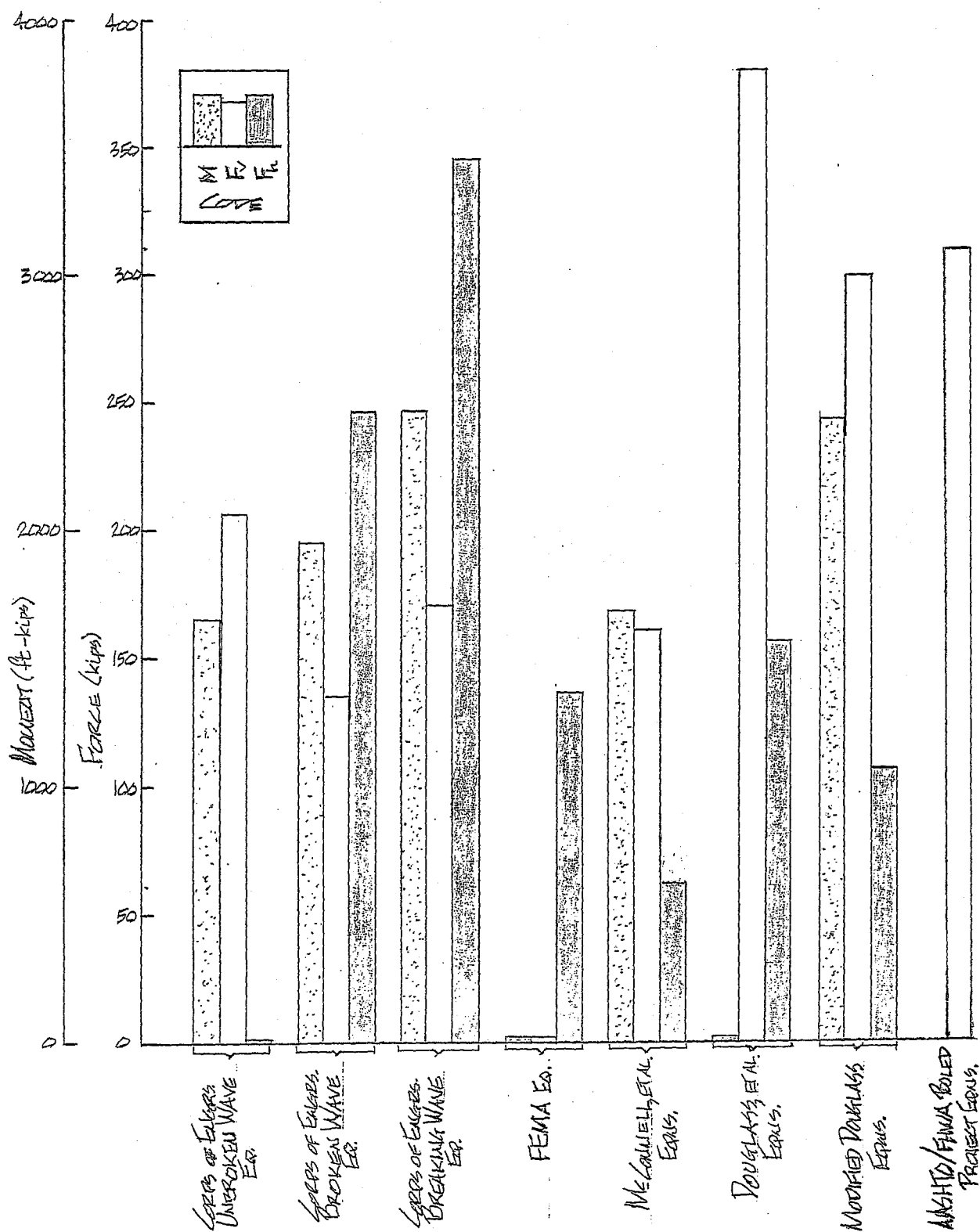
Fig. 3.37 Bar graph showing simultaneously acting M, F_v , F_h forces on 52 ft
long I-10 ramp span in Mobile Bay as predicted by eight sets
of wave force equations.

3.11 Case Study of CSX Biloxi Railroad Bridge

As indicated in Chapter 2, a number of coastal highway and railroad bridges were badly damaged when Hurricane Katrina came ashore in August 2005. At the Bay of Biloxi and Back Bay of Biloxi (see Fig. 3.38) there are five concrete bridge crossings and Hurricane Katrina's surge wave height at this location was measured to be approximately 22 feet.
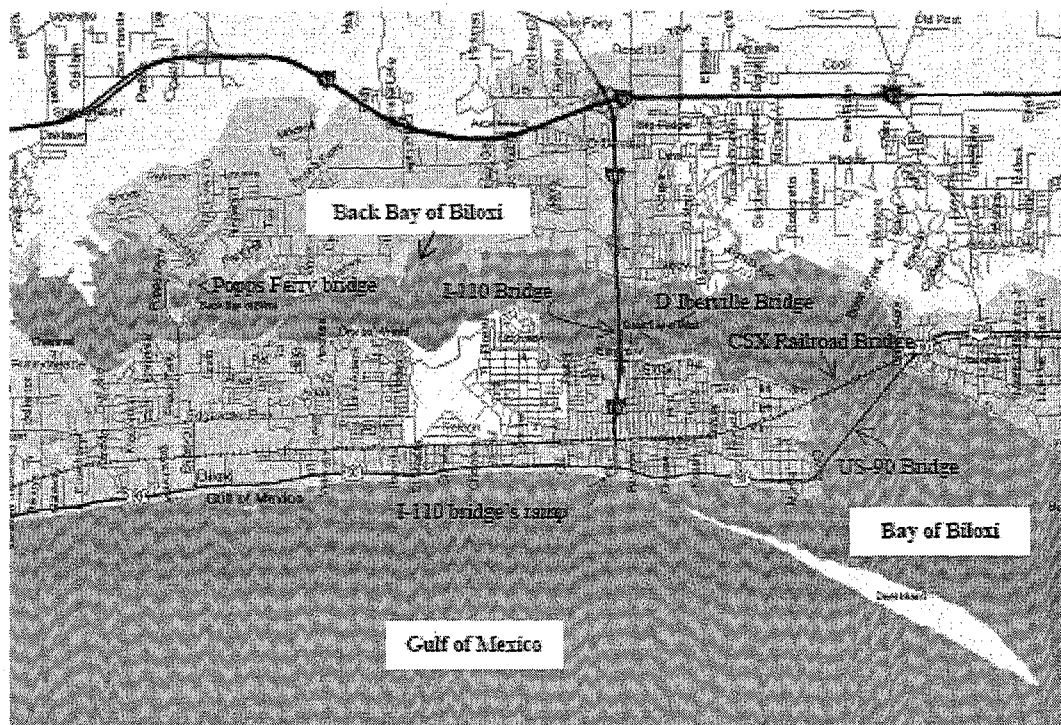
Fig. 3.38 Bridges over Bay and Back Bay of Biloxi, Mississippi (© Copyright 2006 Garmin Ltd. or its subsidiaries. All rights reserved. Map data © 2002 NAVTEQ. All rights reserved. Enhancement by NIST)

The US-90 bridge between Biloxi and Ocean Springs is a 1.6 mile long, four lane, concrete bridge. Most of the bridge has low elevation except for the segment toward the middle of Biloxi Bay at the navigation channel where the superstructure was gradually raised higher to allow passage of boat traffic. The superstructure is comprised of simply supported spans with 42 feet long pre-stressed concrete I-girders, and the substructure consists of multiple bents (concrete piers and cap beams). Each superstructure span was supported on the pier through steel bearing plates, which were bolted on top of the cap beam of the pier and cast into the bottom of the bridge girder. The steel bearing plate on top of the pier has low-rise steel shear keys (½ inch thick) at each end to provide restraint against lateral displacement (see Fig. 3.40 (b)). There is no provision for restraint against vertical displacement except for gravity.

The superstructure of the US-90 Biloxi-Ocean Springs bridge was subjected to direct surge and wave actions and sustained significant structural damage. The lack of positive connection between the superstructure and the supporting piers allowed many individual superstructure spans to be lifted up and displaced transversely northward (in the direction of the waves) and either partially or completely dropped into the water (see Fig. 3.39). The ½ inch low-rise steel shear keys on the bearing plates were clearly unable to provide restraint against the combined uplift and lateral wave forces. The superstructure spans that were constructed at a higher elevation near the navigation channel, i.e., spans above an elevation of approximately 22 feet, were apparently high enough to avoid direct surge and wave actions and survived intact (see Fig. 3.40 (a)).
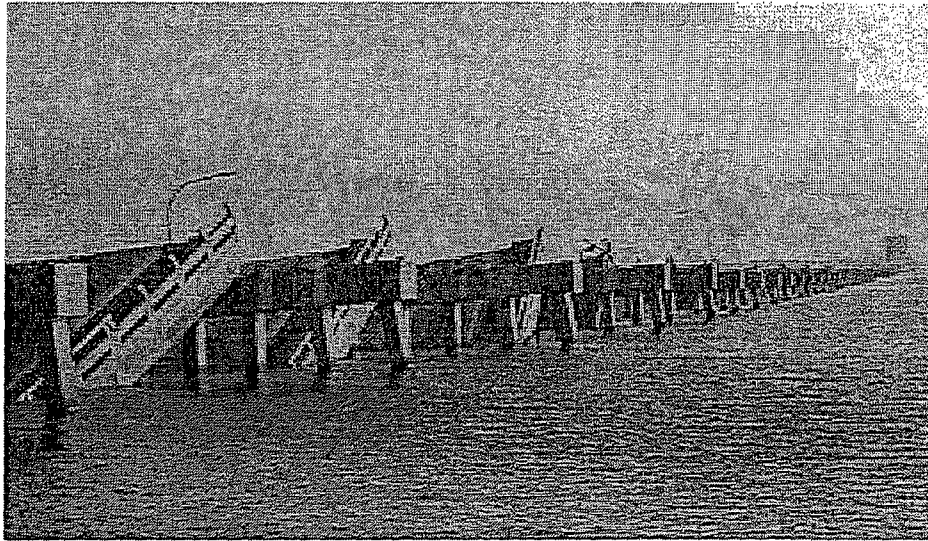
Fig. 3.39 Looking west toward Biloxi from the east shore, many superstructure spans of US-90 Biloxi-Ocean Springs bridge were displaced north off their piers (photo credit: J. O'Connor, MCEER).

(a)

(b)

½" x 3" steel shear keys on bridge bearing plate

Neoprene pad
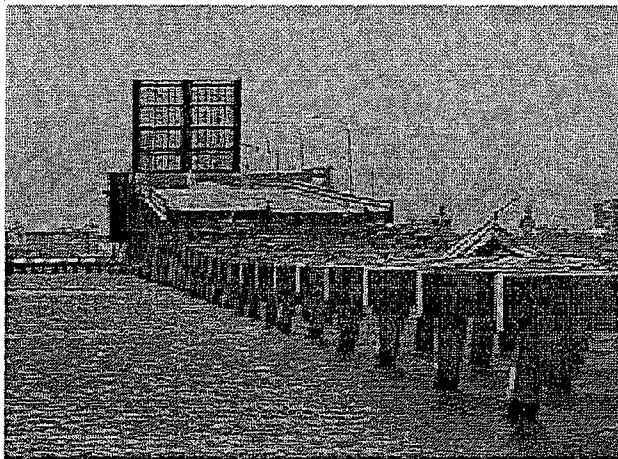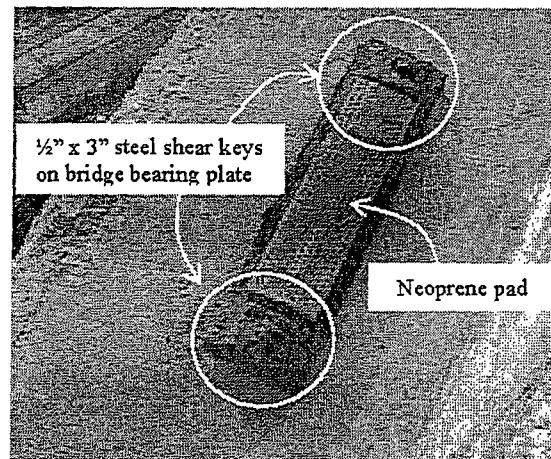
Fig. 3.40 (a) Looking west toward Biloxi, spans above the surge line near the navigation channel survived but the superstructure in the foreground was dropped off the piers (photo credit: J. O'Connor, MCEER), (b) A typical bearing plate from the US-90 bridge with ½ in. thick shear keys (photo credit: NIST).

The CSX Biloxi-Ocean Springs railroad bridge (see Fig. 3.41) successfully survived Hurricane Katrina's surge and wave actions with only minor structural damage, despite being a lower elevation crossing and subjected to approximately the same sea-state and water forces that destroyed the US-90 bridge slightly to its south. Its superstructure is comprised of simply supported spans, each consisting of a 9 in. thick, 17 feet wide concrete bridge deck cast on top of four 4 ft-10 in. deep pre-stressed concrete girders with I-sections. The four girders are further tied together to perform as a unit using 1¼ in. diameter threaded bars (see Fig. 3.41).
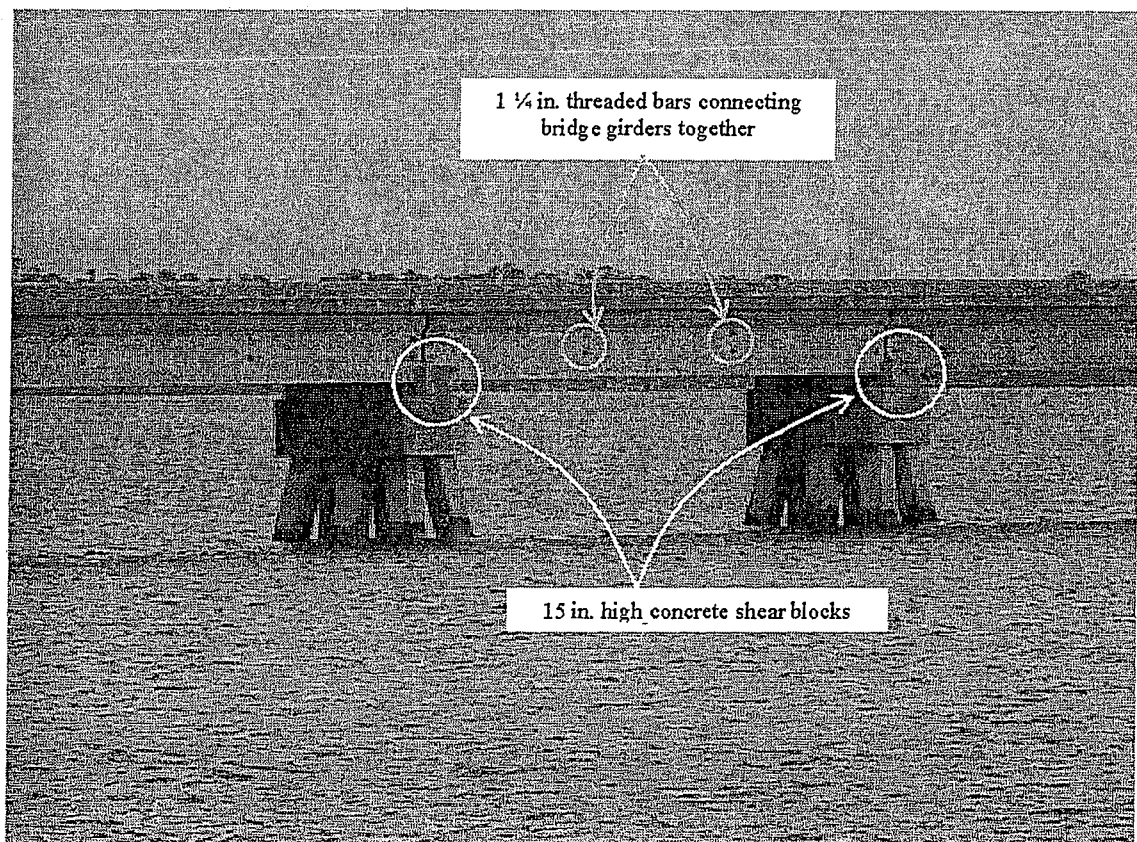
Fig. 3.41 The CSX railroad bridge survived with minor damage, most likely due to the presence of high shear blocks (photo credit: LA DOTD).

Each CSX bridge superstructure span rests on the cap beam of the bridge piers, with vertical uplift resisted only by gravity. On both ends of the cap beam there are two 15 in. high concrete shear blocks to provide restraint against lateral displacement of the superstructure spans which are estimated to be 32.5 ft long. The Biloxi CSX bridge had its railroad tracks and ties completely washed off by wave forces, but the superstructure remained largely intact and connected to the supporting bridge piers. The successful performance of the Biloxi CSX bridge is in stark contrast with the adjacent US-90 bridge, which was almost completely destroyed.

Approximately 30 miles west of the Biloxi CSX bridge is a CSX railroad bridge over St. Louis Bay (near Bay St. Louis, MS). This is a concrete box girder bridge. Each span is a monolithically cast unit comprised of a 17 ft.-6 in. wide concrete deck and a 10 ft-2 in. wide rectangular concrete box girder. Each individual superstructure span is simply supported, with one end simply resting on one concrete pier, while the other end simply resting on the adjacent pier, is further restrained against longitudinal and transverse displacements by capping over three reinforcing bars protruding about 8 in. from the piers and acting as dowels. Further restraint against transverse lateral displacement of the superstructure span is provided by 4 in. high concrete shear keys on the cap beam.

Despite the restraint against lateral displacements provided by the 4 in. concrete shear keys and the 8 in. dowel bars, many of the superstructure spans of the CSX railroad bridge were displaced and dropped into the Bay due to surge-induced wave actions (see Fig. 3.42). This suggests that the uplift wave forces were able to overcome any restraint against vertical displacement and lift the spans high enough (over 8 in.) for

them to move off the piers and drop into the water. Most of the bridge piers appeared to have sustained no damage from wave actions, with a few piers sustaining minor damage probably due to impact by the displaced superstructure spans. Fig. 3.42 shows the piers of the CSX railroad bridge with missing superstructure spans.

The successful performance of the CSX Biloxi bridge, in contrast with the CSX Bay St. Louis and US-90 Biloxi bridges, was attributed in the literature to be largely due to the presence of the high (15 in.) concrete shear blocks at the ends of the bent caps on the CSX Biloxi bridge. The fact that some of these shear blocks sustained damage indicate that they indeed were providing some horizontal restraint to the bridge superstructure. However, the authors believe that the major cause of differences in performance of the bridges were that the CSX Biloxi bridge did not appear to have any end or intermediate diaphragms between the span girders and thus no significant hydrostatic uplift or buoyant forces acted on the spans. In contrast, the US-90 Biloxi bridge appeared to have end (and probably intermediate) diaphragms and the CSX Bay St. Louis bridge was a fairly deep box girder bridge and consequently both of these bridges probably had quite large hydrostatic uplift/buoyant forces acting.

Known information about the size and geometry of the CSX Biloxi bridge and about the surge water level at that location allow us to estimate the probable maximum surge/surface wave horizontal and vertical forces on this bridge using some of the wave force prediction equations presented earlier. This in turn can provide a partial test of the validity of the prediction equations. This analysis/testing is given below.
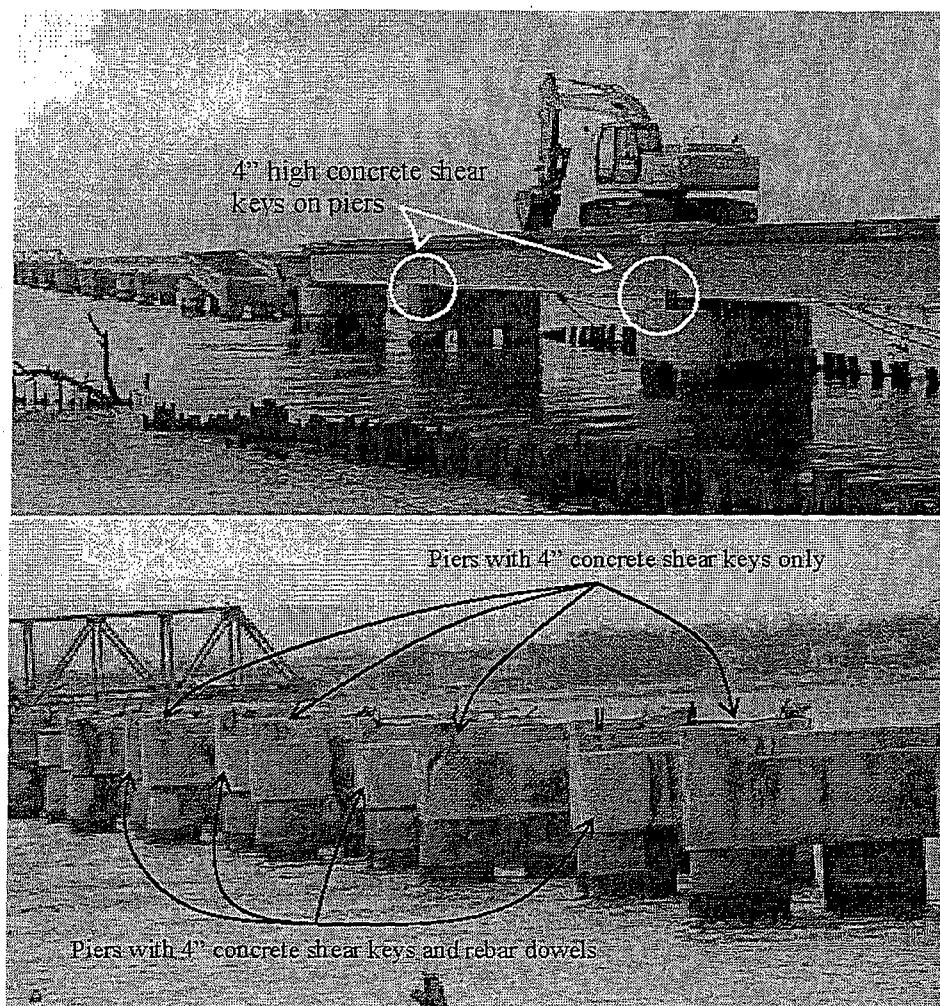
Fig. 3.42 CSX railroad bridge at Bay St. Louis, MS with remaining spans (top) and the supporting piers (bottom) (photos credit: NIST).

Estimates of Applied and Resisting Forces on CSX Biloxi Bridge:

<u>Span DL:</u> Estimated span length = 32.5 ft

    Girders - Four 4'-10" deep prestressed concrete I-girders

    Deck - Concrete 9" thick x 17' wide x 32.5' long

    AASHTO Highway I-girders $\left\{ \begin{array}{l} \text{4'-6" Type IV} \rightarrow \quad w = 822 \text{ lb/ft} \\ \text{5'-3" Type V} \rightarrow \quad w = 1055 \text{ lb/ft} \end{array} \right.$

    Estimate CSX girders $w \approx 930$ lb/ft

    $\therefore$ I-Girder Wt. = $0.930^{k/ft}$ x 32.5' x 4   = 120.9^k

    Deck Wt. = $\dfrac{9'}{12}$ x 17' x 32.5' x $0.150^{k/ft^3}$ = $\underline{62.1^k}$

               Total Wt. = 183.0^k

<u>Surge/Surface Wave Forces:</u>

  Using Douglass, et al. Eqns:

    Vertical Wave Force: $F_v = c_v^{mc} F_v^*$

      where $c_v^{mc} \approx 1.0$

        $F_v^* = \gamma \Delta z_v A_v$

           17' x 32.5'

           (4'-10")+9" = 5'-7" (assuming spans
                have full depth end diaphragms)

           9" (assuming spans have no diaphragms)
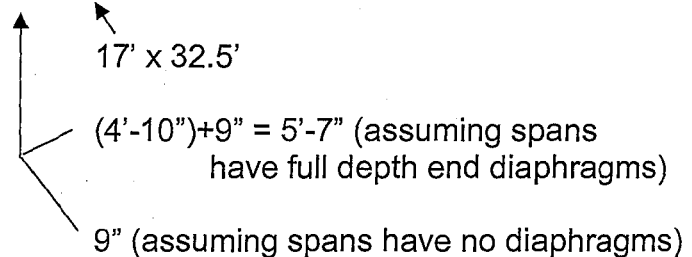
  $\therefore F_v = 1.0$ x 64 lb/ft^3 x 5.58' x 17' x 32.5' = 197.3^k $\uparrow$
               (assuming diaphragms)

  $F_v = 1.0$ x 64 lb/ft^3 x 0.75' x 17' x 32.5' = 26.5^k $\uparrow$
               (assuming no diaphragms)

Horizontal Wave Force:

$$\gamma(\Delta z_h)A_h$$

$$F_h = [1 + c_r(N-1)]\, c_{h\text{-}va}\, F_h^*$$

$$= \underbrace{[1 + 0.4(4-1)]}_{2.2}\, 1.0 \times 64\ \text{lb/ft}^3 \times \frac{5.58'}{2} \times 32.5' \times 5.58'$$

$$= 71{,}240\ \text{lb} = 71.2^k \;\rightarrow$$

Using Modified Douglass, et al. Eqns:

Vertical Wave Force: $F_v = c_v^{mc}\, F_v^*$

where $c_v^{mc} \approx 1.0$

$$F_v^* = \gamma \Delta z_v A_v$$

Bridge Width ≤ 20 ft

$\therefore A_v = 17' \times 32.5'$

(4'-10") + 9" - 1' = 4'-7" (assuming spans have
diaphragms)

9" (assuming spans have no diaphragms)

$$F_v = 1.0 \times 64\ \text{lb/ft}^3 \times 4.58' \times 17 \times 32.5' = 162^k$$
(assuming diaphragms)

$$F_v = 1.0 \times 64\ \text{lb/ft}^3 \times 0.75' \times 17 \times 32.5' = 26.5^k$$
(assuming no diaphragms)

Horizontal Wave Force:

$$F_h = \left[1 + c_r \frac{(N-1)}{2}\right] c_h^{mc}\, F_h^*$$

3-89

where, $c_r \approx 0.33$

N = number of girders = 4

$c_h^{mc} \approx 1.0$

$F_h^* = \gamma \Delta z_h A_h$

      (4'-10" + 9") x 32.5'

      5.58' x 32.5' = 181.4 ft²

2.22 ft

$$F_h = \left[1 + 0.33 \frac{(4-1)}{2} \right] 1.0 \times 64 \text{ lb/ft}^3 \times 2.22' \times 181.4 \text{ ft}^2$$

$= 38.5^k \rightarrow$

Moment: $M \approx 0$ since bridge width < 20 ft

Using Corps of Engineers Breaking Wave Eqn:

  Alternatively, for a probable upper bound horizontal force estimate, use the Corps of Engineers Breaking Wave Force Eqns, ie,

$$\tilde{p}_m = 10.1 w \frac{H_b}{L_D} \cdot \frac{d_s}{D} (D + d_s)$$

  where $H_b \approx 7.5'$

    $d_s \approx 15.0'$

    $L_D \approx 75'$ Estimated Values

    $D \approx 15'$

$$\tilde{p}_m = 10.1 \times 64 \text{ lb/ft}^3 \times \frac{7.5'}{7.5'} \times \frac{15'}{15'} \,(15'+15')$$

$$0.1 \qquad 1 \qquad 30'$$

$$= 1940 \text{ lb/ft}$$

$$\tilde{R}_m = \frac{\tilde{p}_m \times \Delta z_v}{3} = \frac{1940 \times 5.58'}{3} = 3608 \text{ lb/ft}$$

$$R_s = \frac{w(\Delta z_v)^2}{2} = \frac{64 \times 5.58^2}{2} = 996 \text{ lb/ft}$$

$$R_t = \tilde{R}_m + R_s = 3608 + 996 = 4604 \text{ lb/ft}$$

$$F_h = R_t \times 32.5 = 4604 \text{ lb/ft} \times 32.5' = 149.6^k$$

Therefore, the maximum applied forces were approximately as shown below.
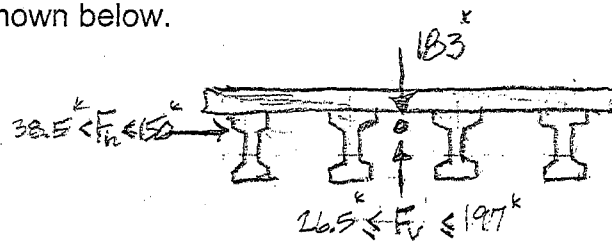
Bridge Bent Shear Block Capacity:

Estimated Shear Block Dimensions ⟹
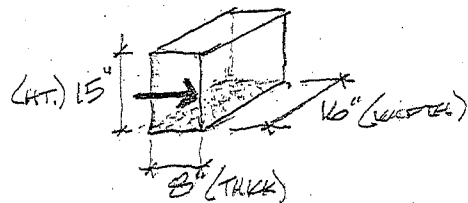
Assume Block $f_c' = 4000$ psi

3-91
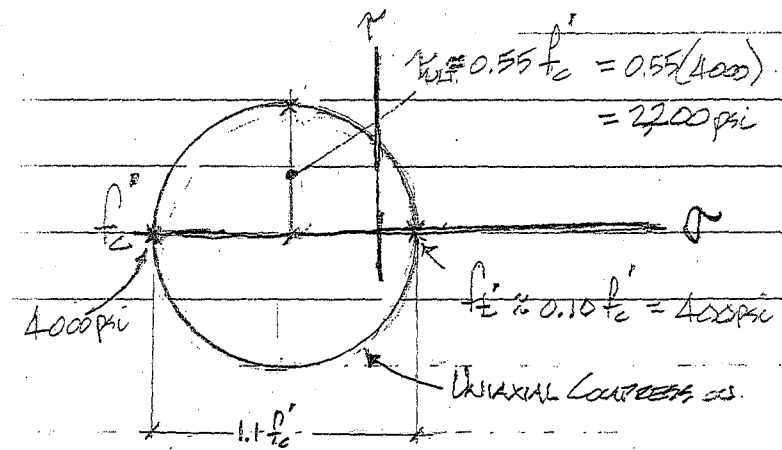
It is difficult to measure concrete strength in pure shear.

According to Mohr Failure Theory,

τ_0 = shear strength in pure shear

= where Mohr rupture envelope crosses the τ-axis (σ = zero), as indicated in Fig. 3.43

$\approx 0.20\ f_c' \approx 0.20(4000) = 800$ psi
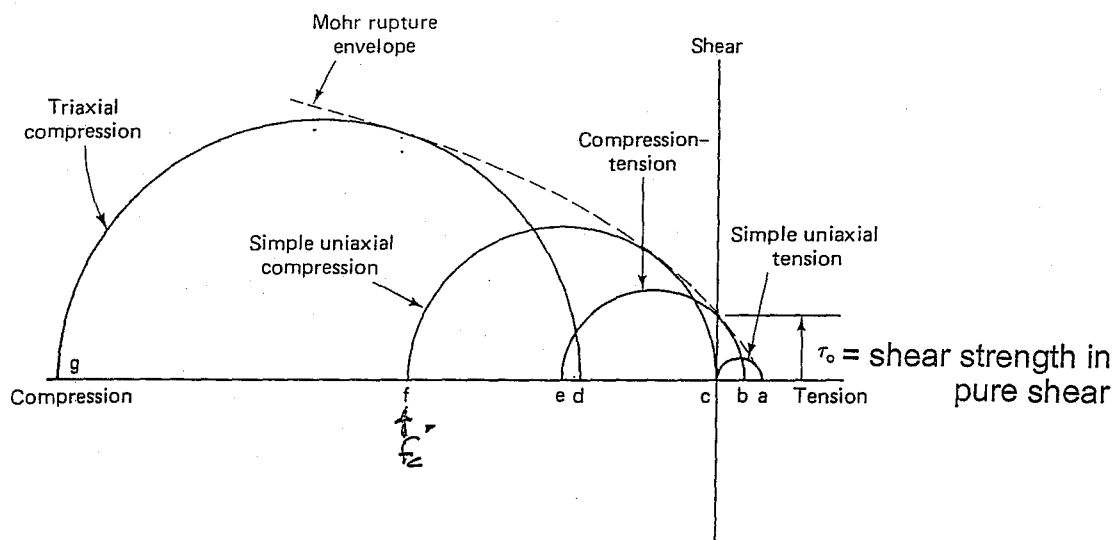
Fig. 3.43 Typical Mohr rupture diagram for concrete

$$\therefore \; F_v^{failure} \approx \tau_o A_{shear} = 800 \text{ psi} \times 16" \times 8" = 102.4^k$$

Note from Fig. 3.41 that a half shear block at each end of a span resists the horizontal wave force on the span.

Based on the above horizontal forces/capacity, i.e.,

$$38.5^k < F_h^{max\ applied} < 150^k \qquad vs \qquad F_h^{capacity} \approx 102^k$$

it appears that the $F_h^{max\ applied} < 102^k$.

Also, based on the above analysis, it appears that

$$26.5^k \le F_v^{applied\ by\ waves} \le 197^k$$

depending on the span diaphragming.

Note that the upper limit of 197^k is for full-depth end diaphragms and is larger than F_v^{weight}. If this is indeed the diaphragm situation, then the spans were being lifted vertically as surface waves moved through the bridge but not high enough to be lifted over the blocks.

Also note in Fig. 3.42 (the CSX bridge with the short 4" high blocks) it appears that the 4" concrete blocks are in place, and thus the bridge spans were probably lifted over the blocks by the vertical force and then moved laterally by the horizontal force. Some spans appear to have moved longitudinally once adjacent spans were out of the way.

3.12 Closure

It was indicated earlier that limiting or conservative hurricane surge/surface wave design forces would be to use the Douglass, et al. equation to determine the force F_v^{max} and to use the Corps of Engineers Breaking Wave equation to determine the force, F_h^{max}, and then to assume that these forces act simultaneously on the bridge superstructure. However, both of these equations appear to provide overly-

conservative forces. The Douglass, et al. equation is overly-conservative because it assumes maximum vertical wave pressures act on the full-width of the bridge, and the Corps of Engineers Breaking Wave equation because it assumes a maximum height wave breaks against the side of the bridge as if it were a seawall with no where for the breaking water to flow/escape underneath, which is certainly not the case for a coastal bridge in a 20-30 ft deep (due to the storm surge) sea. Also, these forces would not act simultaneously.

The modification made in the Douglass, et al. equations to arrive at the Modified Douglass, et al. equations are based on rational physics, hydraulics and statics considerations, and are felt to be reasonable and realistic modifications. Because of the basic science and ocean engineering background included in the original equations, and the further sound and realistic modifications made, it is recommended that the Modified Douglass, et al equations be used to estimate maximum hurricane surge/surface wave forces on coastal deck-girder type bridges. In using these equations, the local storm surge elevation at the bridge site should be increased 1 ft above the maximum storm surge elevation to allow for interference of the bridge with surface wave propagations on the seaward face of the bridge.

4. I-10 BRIDGE ACROSS MOBILE BAY

4.1 General

The U.S. Interstate 10 (I-10) bridge across the north end of Mobile Bay is a part of the southernmost major east-west roadway corridor across the U.S. A portion of this corridor is shown in Fig. 4.1, and obviously includes many coastal bridges that may be subjected to hurricane loadings. The I-10 Mobile Bay twin bridges are in this group, and were built in the mid 1960's using prefabricated prestressed girder-deck superstructure construction. Each bridge is two lanes wide and consists of 65 foot long prefabricated simple spans that were barged to the site and set in place via crane on on-site constructed pile support bents. The top of deck level stands at 21.45 feet above mean sea level. Pertinent bridge elevations, dimensions, properties, connection details, and estimated maximum hurricane surge and surface wave elevations at the I-10 Mobile Bay bridge site are given in the following sections.
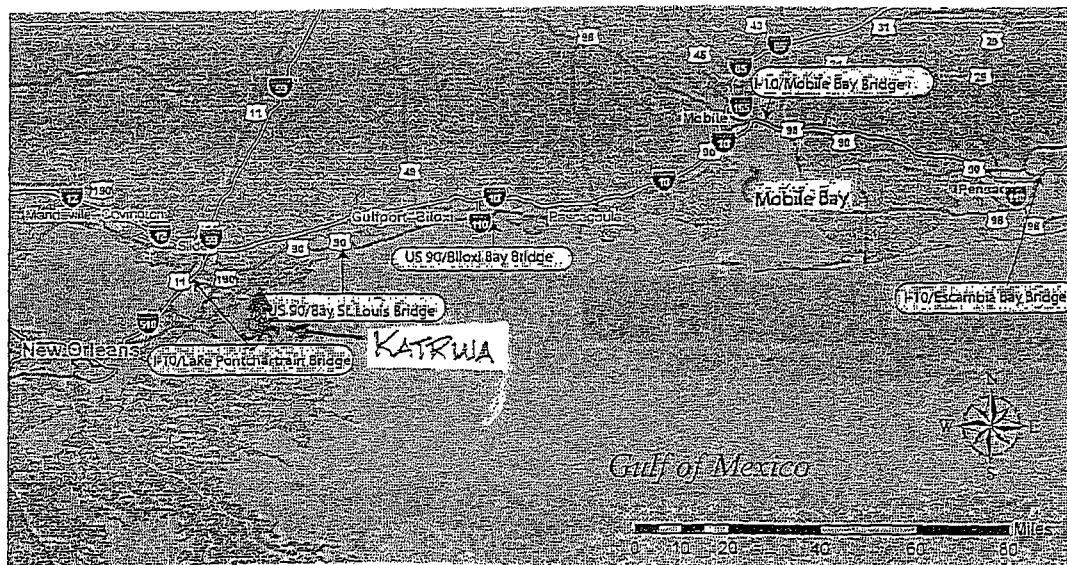
Fig. 4.1 Portion of I-10 Corridor Near Mobile, AL

4-1

4.2 Bridge Elevations, Dimensions, Weights, and Properties

As stated previously, each span is constructed of a prefabricated prestressed concrete girder-deck superstructure. Each span was poured monolithically to enhance strength and durability and to reduce on-site construction time. The superstructure cross-section was designed to mimic the construction of AASHTO Type III girders with a 7" deck cast-in-place as can be shown in Fig. 4.2. Original Alabama Department of Transportation (ALDOT) plans show that the intent was to build the superstructure with open-style guard rails, but a change in legislation/FHWA requirements resulted in the design being changed to use Alabama Standard Safety Rails or "Jersey Barriers". This design changed the original open-style to a safer (for the traveling public) closed-style rail.
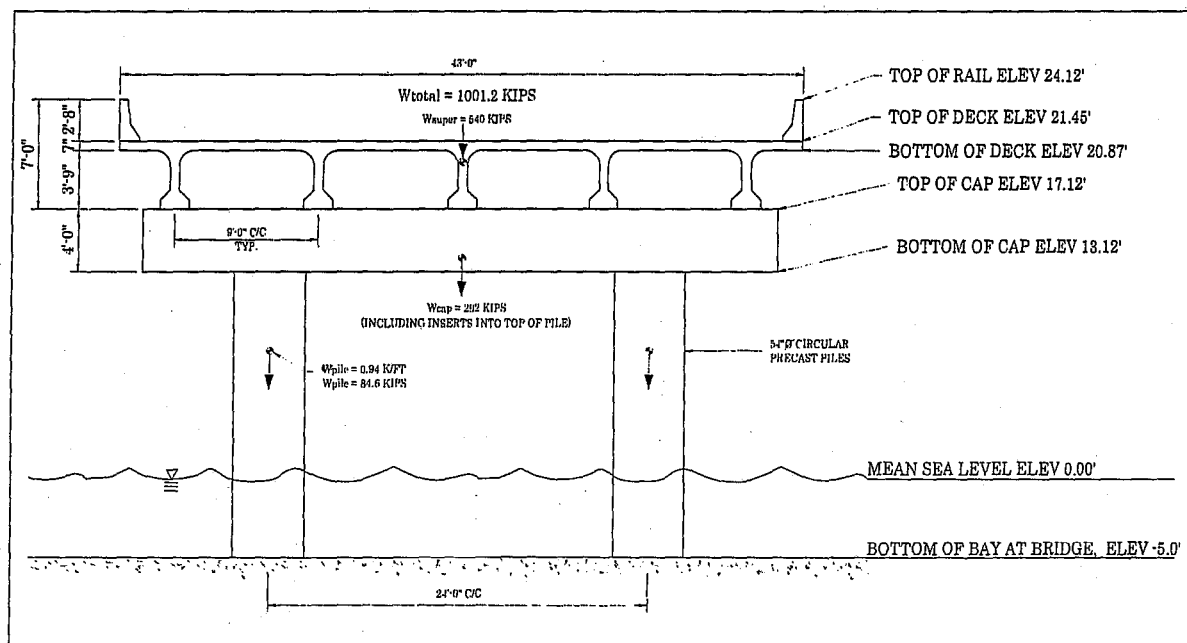
Fig. 4.2 Typical Span Cross-Section Showing Pertinent Component Elevations Relating to MSL

Bridge span elevations were taken from ALDOT plans and are measured from Mean Seal Level (MSL). A representative cross-section of a typical span is shown in Fig. 4.2 and denotes all pertinent elevations. As shown in Fig. 4.2, during normal sea state, the elevation to the top of the deck is 21.45' above MSL. Top of Guard Rail elevation is 24.12', Bottom of Deck/Top of Girders elevation is 20.87', Top of Cap/Bottom of Girders elevation is 17.12', and Bottom of Cap elevation is 13.12' using the assumed 4'-0" minimum thickness given in the plans. Plan and elevation/profile views of the I-10 bridge are shown in Fig. 4.3. This figure shows the fixed and expansion bearings at each end of the 65 ft simple spans, the horizontal and vertical clearances of the bridge, the approximate mean water depths and other pertinent dimensions and elevations.

The bridge superstructure consists of five girders evenly spaced 9'-0" apart, a 7" deck on top, and typical 32" high "Jersey" type barrier rails all monolithically precast. These girders share similar cross-sectional geometry, section properties, and weight with standard AASHTO Type III Prestressed Girders (unit weight = 583 lbs/ft). Each span is 65'-0" in length with a section width of 42'-11", a total height of the span superstructure including the guard rail, deck, and girders is 7'-0", and has a weight of approximately 274 tons. The transverse slope for each span varies but an assumed value of 0.015625'/ft. will be considered typical for these applications. Figure 4.4 shows a plan view and typical section view of an I-10 span. Note in these views the originally planned open-style guard rails are shown. However, Detail A in Fig. 4.4 shows the revised guard rail as well as 4"$^\phi$ gutter drains at 5 ft on center on the low gutter side of the deck. These drains were designed to provide rain water drainage for the deck;

however, they also act to provide some air venting to help avoid excessive surface wave slamming pressures in the event of a hurricane. Nonslamming wave air pressures will be mostly vented longitudinally along the bridge for the regions outboard of the exterior girders where the gutter drains are located. Figure 4.4 also shows that each span has four diaphragms (two end and two intermediate diaphragms) with the bottom elevation of these diaphragms being approximately 1 ft higher than the bottom of girder elevations.

Each span of the I-10 bridge rests on a substructure consisting of a pile cap and two cylindrical piles as shown in Fig. 4.5. Each pile cap has a length of 40'-0", a minimum thickness of 4'-0" up to about 4'-6" to account for the superelevation of the span, and a width of 5'-0" at the bottom tapering to 4'-0" at the top. This cap is positively connected to two 54" diameter hollow cylindrical precast prestressed concrete piles of length approximately 90' and transversely spaced 24' apart via 5' deep poured-in-place concrete plugs at the top of the piles as indicated in Fig. 4.5. Photos of typical I-10 spans and support bents over Mobile Bay are shown in Figs. 4.6 and 4.7.
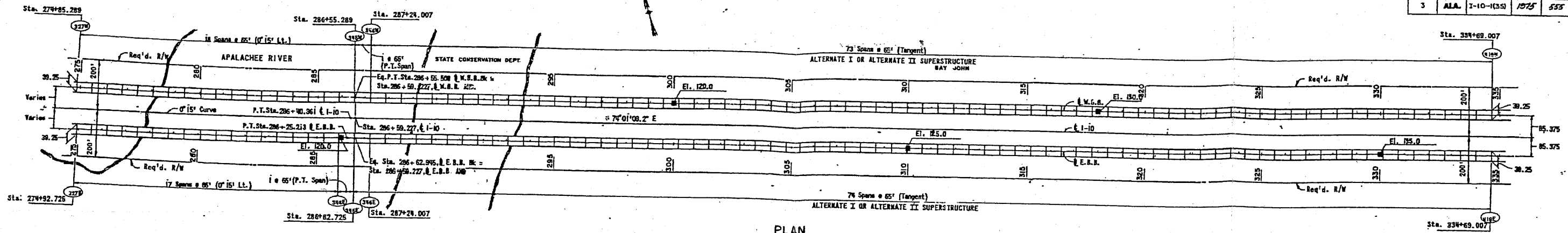
PLAN
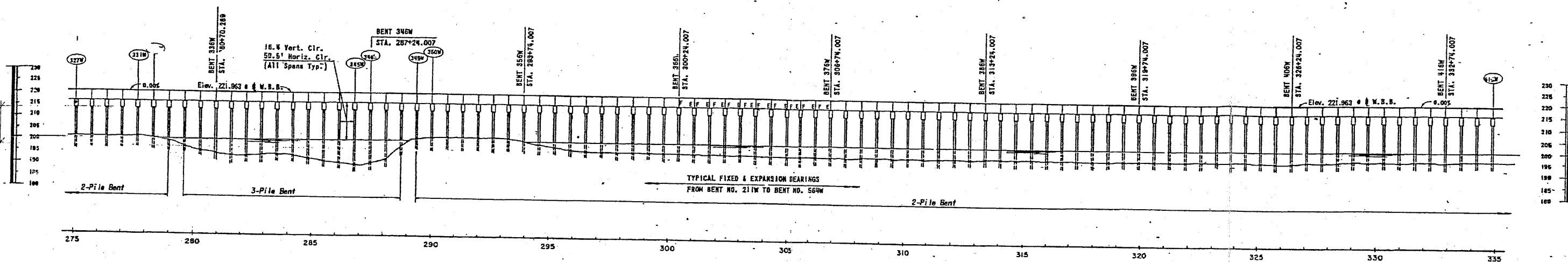
SCALE: 1" = 200'

ELEVATION & PROFILE – W.B.B.

SCALE: 1" = 200' Horiz.
1" = 20' Vert.
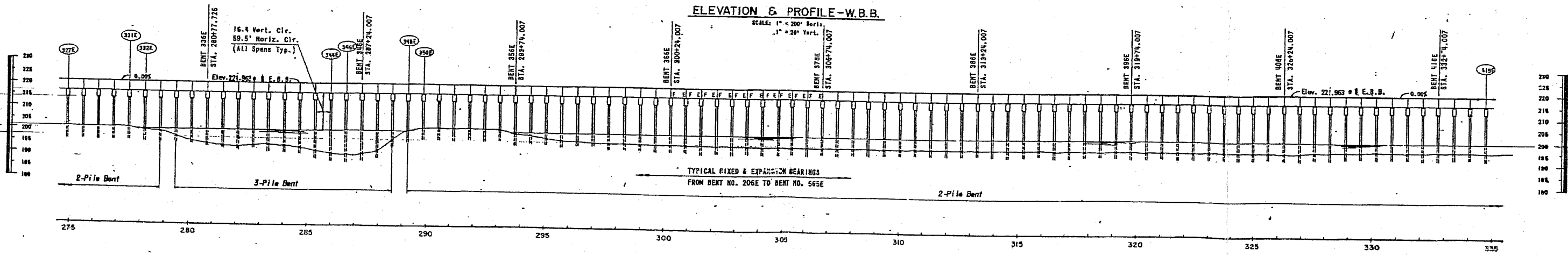
ELEVATION & PROFILE – E.B.B.

SCALE: 1" = 200' Horiz.
1" = 20' Vert.

Notes:
1. Fixed and expansion bearings at ends of 65 ft simple spans.
2. Mean water depth in bay region is ± 5 ft
3. Mean vertical clearance (mean water level to underside of girders) of 16.4 ft
4. Horizontal clearance between pile bents of 59.5 ft
5. 54"⌀ cylindrical pipe piles used for bents
6. Two-pile bents used in bay regions and three-pile bents at river mouths.

LEGEND

AASHO GIRDER SUPERSTRUCTURE
Superstructure to be cast-in-place concrete deck on Precast Prestressed AASHO Girders

ALTERNATE I OR ALTERNATE II SUPERSTRUCTURE
Superstructure to be either cast-in-place concrete deck on Precast Prestressed AASHO Girders or Precast Prestressed Nonolithic spans with deck and girders cast integrally

Superstructure to be cast-in-place concrete deck on welded steel Plate Girders

54"⌀ CYLINDER PILE SUBSTRUCTURE ALT. C

STATE OF ALABAMA HIGHWAY DEPARTMENT

PROJECT NO. I-10-1(35)
INTERSTATE ROUTE I-10
MOBILE BAY CROSSING
MOBILE-BALDWIN COUNTIES, ALABAMA

GENERAL PLAN & ELEVATION

DAVID VOLKERT & ASSOCIATES
CONSULTING ENGINEERS

DATE June 1974

DWG. NO. 5

Fig. 4.3. Plan and Elevation/Profile of I-10 Bridge Across Mobile Bay
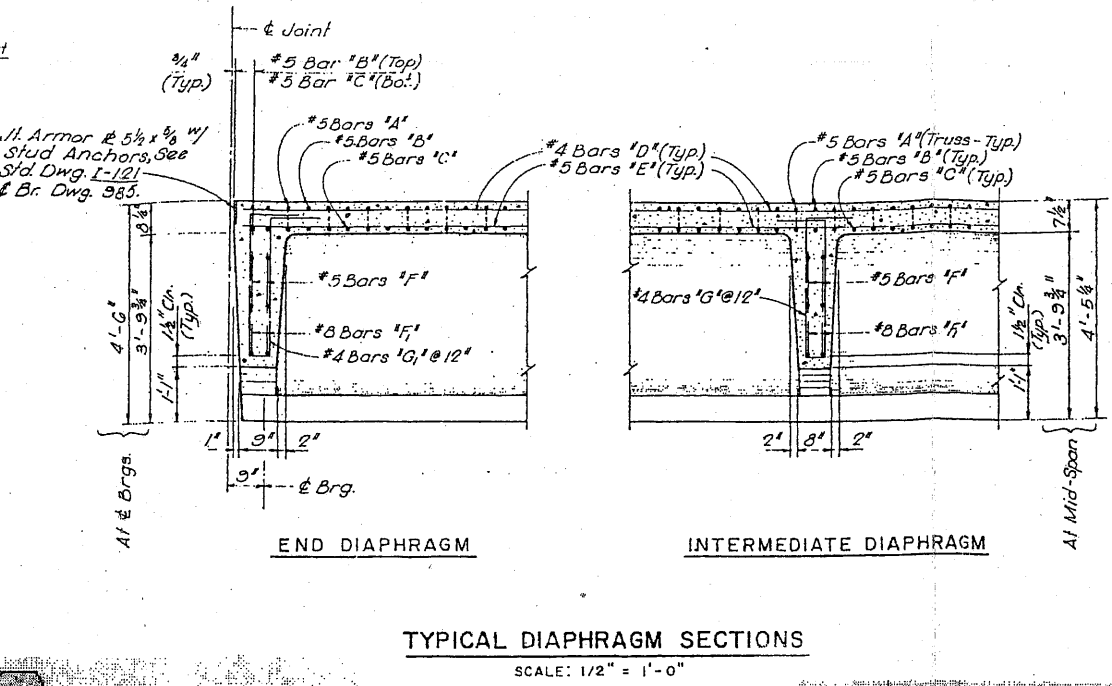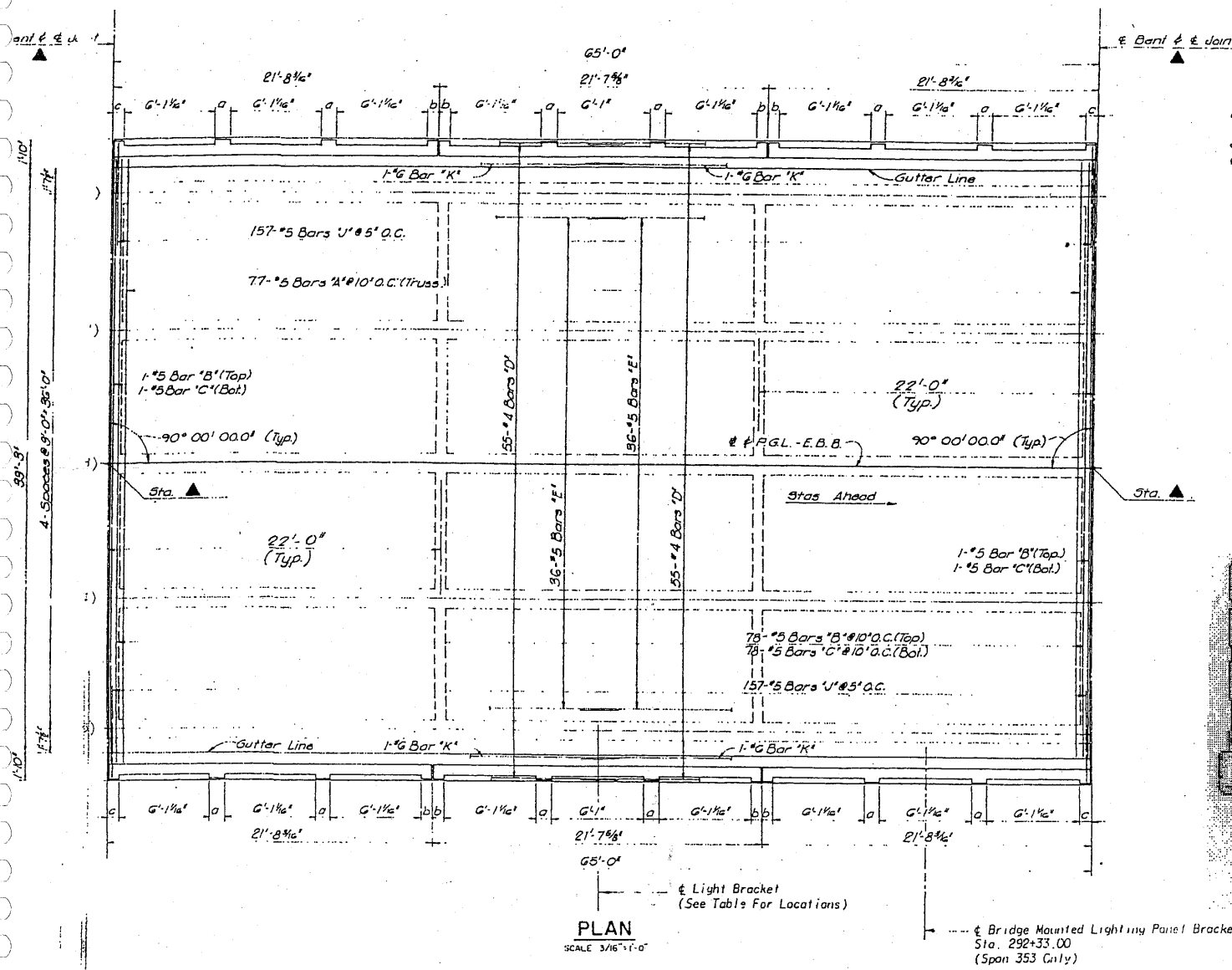
Notes:

1. Deck is flat with a transverse slope of 0.015625 ft/ft.
2. No scupper drains at the gutter lines.
3. No openings in end or intermediate diaphragms.
4. Height of end and intermediate diaphragms from underside of deck to bottom of diaphragm is 2'-9".
5. Diaphragms at 21'-8" longitudinally.
6. Guard rail was changed from an open post-and-rail to a solid Jersey barrier rail.

PLAN
SCALE 3/16"=1'-0"

TYPICAL DIAPHRAGM SECTIONS
SCALE: 1/2" = 1'-0"

END DIAPHRAGM   INTERMEDIATE DIAPHRAGM

DETAIL Ⓐ – GUARD RAIL / CURB DRAIN CHANGE

TYPICAL GIRDER END DETAILS

CONNECTION ANGLE DETAILS

SWEDGE BOLT DETAIL

TYPICAL SECTION
SCALE 3/8"=1'-0"

39'-3" Clear Roadway

19'-7½"   19'-7½"

See Detail Ⓐ
Reinf. Sym. About ₵ Bridge
₵ ₵ P.G.L.-E.B.B.

Const. Joint (Typ.)
Optional Const. Joint

8¼" Slab At ₵ Brgs.
7½" Slab At Mid-Span

Slope With Roadway

Intermediate Diaphragms   End Diaphragms

4 Spaces @ 9'-0" = 36'-0"

⊗ ESTIMATED QUANTITIES (ONE SPAN)			
ITEM	UNIT	QUANTITY
Bridge Concrete (Class A) *	Cu. Yds.	127.10
Steel Reinforcement *	Lbs.	21,405
Structural Steel	Lbs.	962

* Includes Concrete & Reinforcement for Handrail

APPROVED:

STATE OF ALABAMA HIGHWAY DEPARTMENT
PROJECT NO. I-10-1(35)
INTERSTATE ROUTE I-10
MOBILE BAY CROSSING
MOBILE-BALDWIN COUNTIES, ALABAMA
MONOLITHIC SPANS 345 THRU 476

DAVID VOLKERT & ASSOCIATES
CONSULTING ENGINEERS

DESIGNED	ARL	DETAILED	SMB	TRACED	MATHAM
CHECKED	TL	CHECKED	TL	CHECKED	

REVISIONS
DATE JUNE, 1974

10/23/74 △ Added Safety Rail Note DV&A

Fig. 4.4. Superstructure Plan and Section of I-10 Bridge

4-6

PLAN
SCALE: 3/8"=1'-0"

40'-0"
4 Girder Spaces @ 9'-0" = 30'-0"
2'-0"
18'-0"
2'-0"
$\mathbb{C}$ $\mathbb{C}$ P.G.L.
80°00'00.0' (To Local Tangent)
Stas. Ahd

El. A1   El. B1   El. C1   El. D1   El. E1
El. A   El. B   El. C   El. D   El. E

90°09'45.0' (Typ.)
90°09'45.0' (Typ.)

5'(Typ.)
$\mathbb{C}$ Bent & Jt.

2' Chamfer (Typ.)

6'-0"   3 Step Spaces @ 9'-0" = 27'-0"   6'-0"

Dimensional View of Pile Cap

5'-0"
2'-6"   2'-6"
2'-0"   2'-0"
4'-0" (MIN.)
(5) #11 BARS TYP.
PRECAST CONCRETE BENT CAP
C.I.P. CONCRETE TO ANCHOR BENT CAP TO PILES
6" PLUG DEPTH
3"   3"
6" WALL THICKNESS
54" Ø CYLINDRICAL PILE

SECTION THRU PILE PLUG AND CAP

ELEVATION
SCALE: 3/8"=1'-0"

Reinf. Sym. About $\mathbb{C}$
8-#11 Bars A
1-#6 Bar B, Ea. Fa.
A   B
El. F
Level
El. G (Typ.)
5-#11 Bars C
4-#11 Bars C1
1-#6 Bar N, Ea. End
1-#6 Bar N1, Ea. End
2-#11 Bars F
2-#11 Bars F1
1-#11 Bar F2
8 Spaces @ 12"   5 Spaces @ 12"
#4 Bars D & E Spacing
54" Ø Precast Prestressed Concrete Pile (Typ.)
8'-0"   24'-0"   8'-0"

END ELEVATION
SCALE: 3/8"=1'-0"

6'-0"
2'-0"   2'-0"
2'-0"   2'-0"
4'-0" (Min.)
#6 Bar N
#6 Bar N1
3'   3'

NEOPRENE PAD DETAILS

SECTION A-A
SCALE: 1 1/2"=1'-0"

#11 Bars A
#4 Bars E
#4 Bars D
#6 Bars B
#11 Bars C
#11 Bars C1
3'-8" O.C.
3" Clr (Typ.)

SECTION B-B

#11 Bars A
#4 Bars E
#4 Bars D
#6 Bars B
#11 Bars C
3'-8" O.C.
3" Clr (Typ.)

54" ALTERNATE

ESTIMATED QUANTITIES (ONE BENT)		
ITEM	UNIT	QUANTITY
Bridge Concrete (Class A)	Cu. Yds.	32.50
Steel Reinforcement	Lbs.	5962
Structural Steel	Lbs.	149

Fig. 4.5. Substructure Plan and Elevation of I-10 Bridge

4-7

4.3   Bridge Connections and Connection Details

Each bridge superstructure is positively connected to the bent caps by clip

angles as shown in the photo of Fig. 4.7. This connection consists of two clip angles at

each end of the two exterior girders as well as the middle girder, in this case, girders 1,

3, and 5. Each clip angle setup is comprised of an L8x6x1" bolted to the bottom flange

of the girder by two 7/8" dia. x 3" galvanized cap screws in threaded inserts. The girder

is attached to the bent cap by two 1¼" dia. x 1'-3" galvanized swedge bolts embedded

into the concrete 11". Details of this connection can be seen in Fig. 4.4. The load path

travels through these clip angles into the precast bent cap which, in turn, is positively

connected to the piles by a reinforced concrete "plug". This plug is cast 5' into the pile

and connects the pile cap to the piles by a series of #11 bars as shown in Fig. 4.5
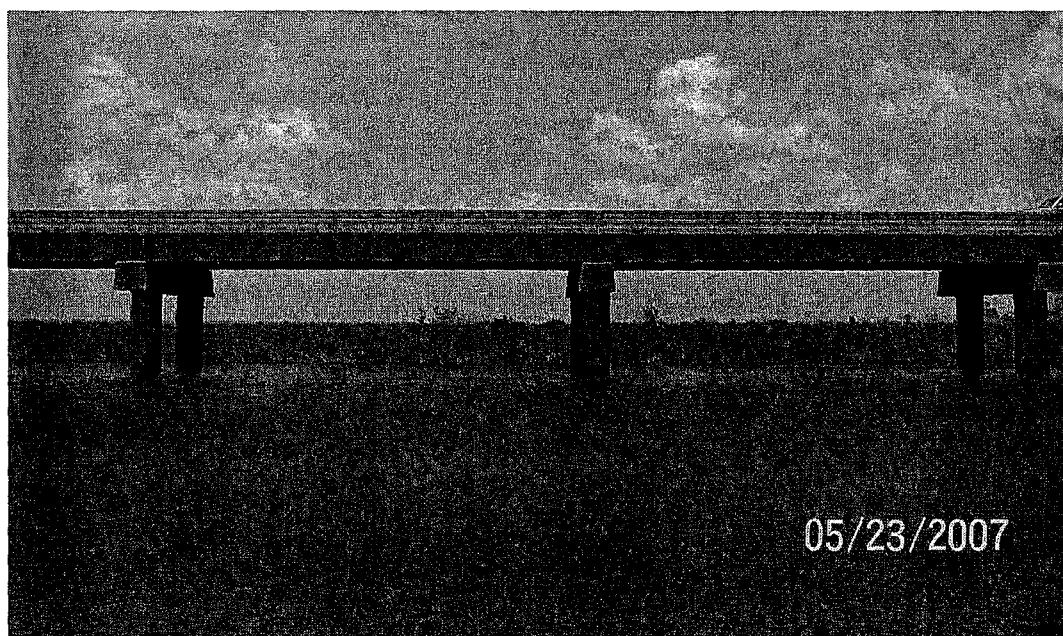
Fig. 4.6. Typical I-10 Spans Over Mobile Bay

Fig. 4.7. Photo of Typical Clip Angle Connection

4.4 Estimated "Design Hurricane" Sea State at Mobile Bay I-10 Bridge

The worst-case storm surge/surface wave sea states at Mobile, AL in the last 75 years appear to have been due to Hurricane Frederic in 1979 and Hurricane Katrina in 2005. Thus, for purposes of this research, when determining the maximum surge wave forces on the Mobile Bay I-10 bridge superstructure and substructure, we will consider the following three cases.

Case A. Hurricane Frederic (1979) - A Category 3 Hurricane that made landfall near Pascagoula, MS (≈ 35 miles west of Mobile, AL) that produced wind gusts of 145 mph, resulting in a storm surge of 9 - 15 feet above MSL. At the Mobile Bay I-10 Bridge the maximum storm surge appeared to have been 11.7 feet.

Case B. Hurricane Katrina (2005) - A Category 3 Hurricane that made landfall near Slidell, LA (≈ 105 miles west of Mobile, AL) that produced wind gusts of 155 mph, resulting in a maximum storm surge of 25 - 28 feet above MSL. At the north end of Mobile Bay, the maximum storm surge was approximately 12.0 - 12.4 feet above MSL, and we will use 12.4 feet.

Case C. Mock-Hurricane Katrina - A Category 3 Hurricane at time of a theoretical landfall near Biloxi, MS ($\approx$ 45 miles west of Mobile, AL) that would produce wind gusts of 155 mph resulting in a maximum storm surge of 25 - 28 feet above MSL. At the U.S. 90 Biloxi Bay Bridge the maximum storm surge was estimated to be 21.5 feet above MSL, and this coupled with the anticipated decrease in surge elevation going to the north end of Mobile Bay, we will use a maximum storm surge of 21.5 feet at the I-10 Bridge for **Case C**.

Case C represents the estimated maximum surge/surface wave heights if Hurricane Katrina's track had been shifted approximately 70 miles to the east (or 45 miles west of Mobile) of where it hit. It should be noted that this would place it approximately along the track of Hurricane Frederic. To estimate the maximum sea state condition for **Case C**, the best available data appears to be the maximum sea state at Biloxi Bay when Katrina hit in August 2005. This maximum condition was assumed to also be possible in the future at Mobile Bay. Thus this sea state condition was considered along with **Cases A** and **B** in estimating an appropriate design sea state at the Mobile Bay I-10 Bridge site. Estimated maximum sea state conditions, i.e., surge and surface wave heights, for these three hurricanes at the north end of the Mobile Bay I-10 bridge site are discussed and summarized below.

Case A. Based on maximum storm surge/surface wave elevations found in the literature (see Section 2.2.3) and adjusting for the 35 mile northerly position of the I-10 bridge from the Gulf of Mexico coastline, the estimated maximum sea state condition for Hurricane Frederic at the north end of Mobile Bay I-10 Bridge site is shown in Fig. 4.8.
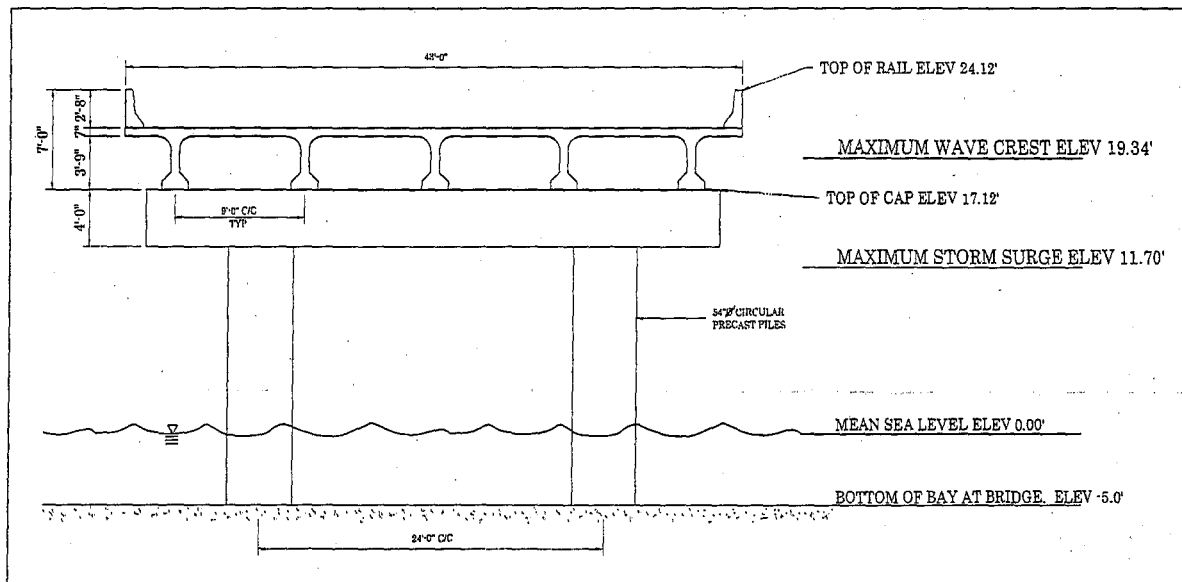
**Fig. 4.8 Case A - Estimated Maximum Sea State Elevations
at I-10 Bridge During Hurricane Frederic**

Case B. Based primarily on Douglass, et al work [1] on damage to the I-10

Ramp in Mobile Bay during Hurricane Katrina (see Section 2.2.2 - Damage to I-10

Ramp in Mobile Bay) the estimated maximum sea state condition during Hurricane

Katrina at the north end of Mobile Bay I-10 bridge site is shown in Fig. 4.9.
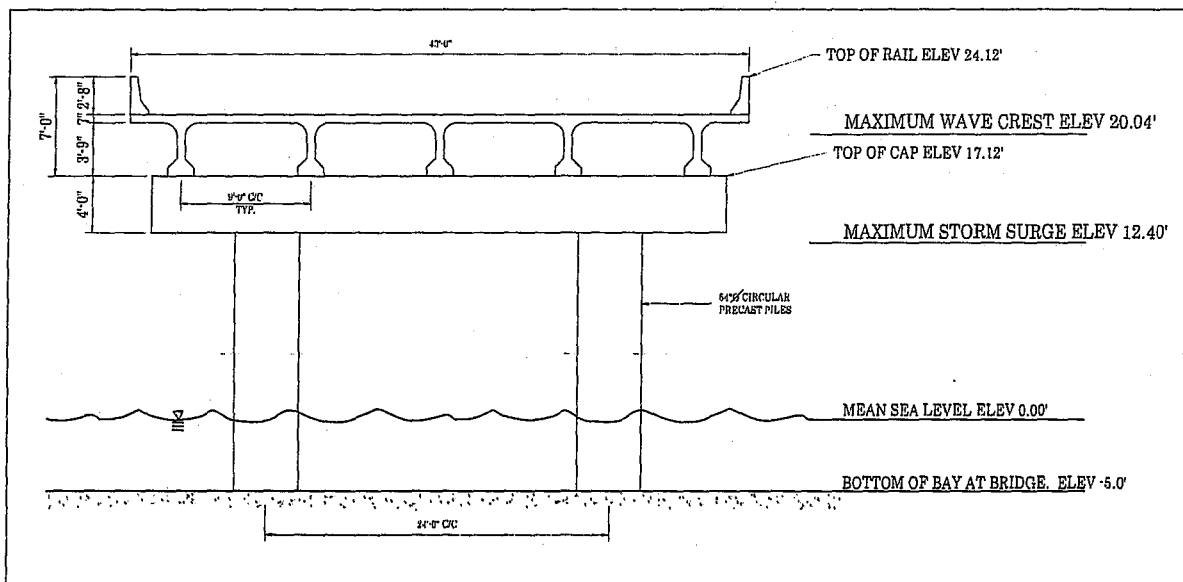
**Fig. 4.9   Case B - Estimated Maximum Sea State Elevations
at I-10 Bridge During Hurricane Katrina**

Case C. Maximum sea state conditions at the Mobile Bay I-10 bridge site for a mock Hurricane Katrina hitting just west of Mobile, i.e., approximately along the path of Hurricane Frederic, were estimated based on the maximum sea state occurring at the U.S. 90 Biloxi Bay Bridge during Hurricane Katrina.

When Hurricane Katrina made landfall on August 29, 2005 (see Fig. 4.10), a number of locations experienced storm surge heights greater than 20 feet. NOAA's NHC estimated a storm surge of up to 27 feet. NOAA, in their advisories prior to landfall of Hurricane Katrina, predicted "coastal storm surge flooding of 18 to 22 ft above normal tide levels...locally as high as 28 ft along with large and dangerous battering waves... can be expected near and to the east of where the center makes landfall". An estimated surge height of 27 feet was reported by the Hancock, Mississippi Emergency Operation Center. Observations by a post-storm NIST reconnaissance team also suggested that, in some locations between Biloxi and Long Beach, Mississippi, the surge reached as high as 28 feet. It was reported [8] that Hurricane Katrina's large horizontal size likely contributed to its exceptionally high storm surge.
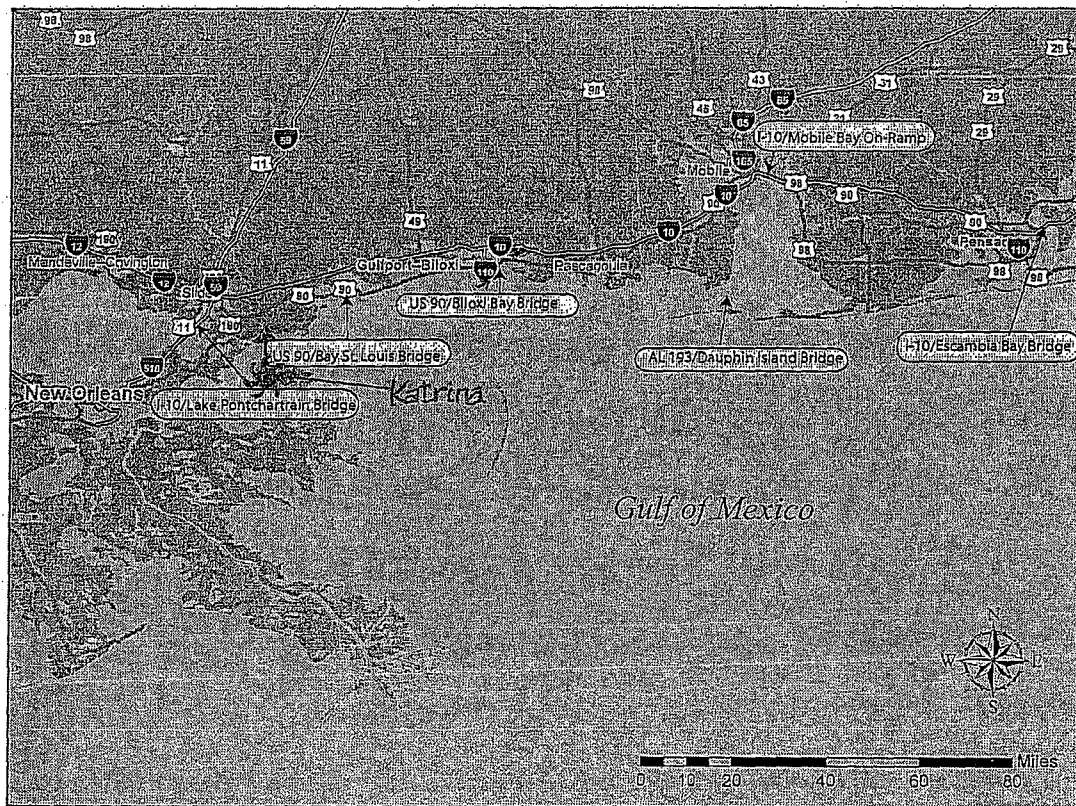
Fig. 4.10 Location map of Hurricane Katrina and US90/Biloxi Bay Bridge

The water depth across the mouth of Biloxi Bay are very shallow being around 2 to 3 feet for most of the bridge, with a typical tide range of about 1.75 feet (-0.55 ft (NGVD) to +1.20 ft (NGVD)). Figures 4.11 - 4.14 show Katrina damages to the U.S. 90 Biloxi Bay Bridge and Fig. 4.15 shows a typical bridge span. Figure 4.16 shows estimated peak storm surge and surface wave heights at the bridge, and Table 4.1 gives the top of bent/bottom of girder elevations along the bridge as well as identifying the bridge spans that were and were not removed by Katrina.
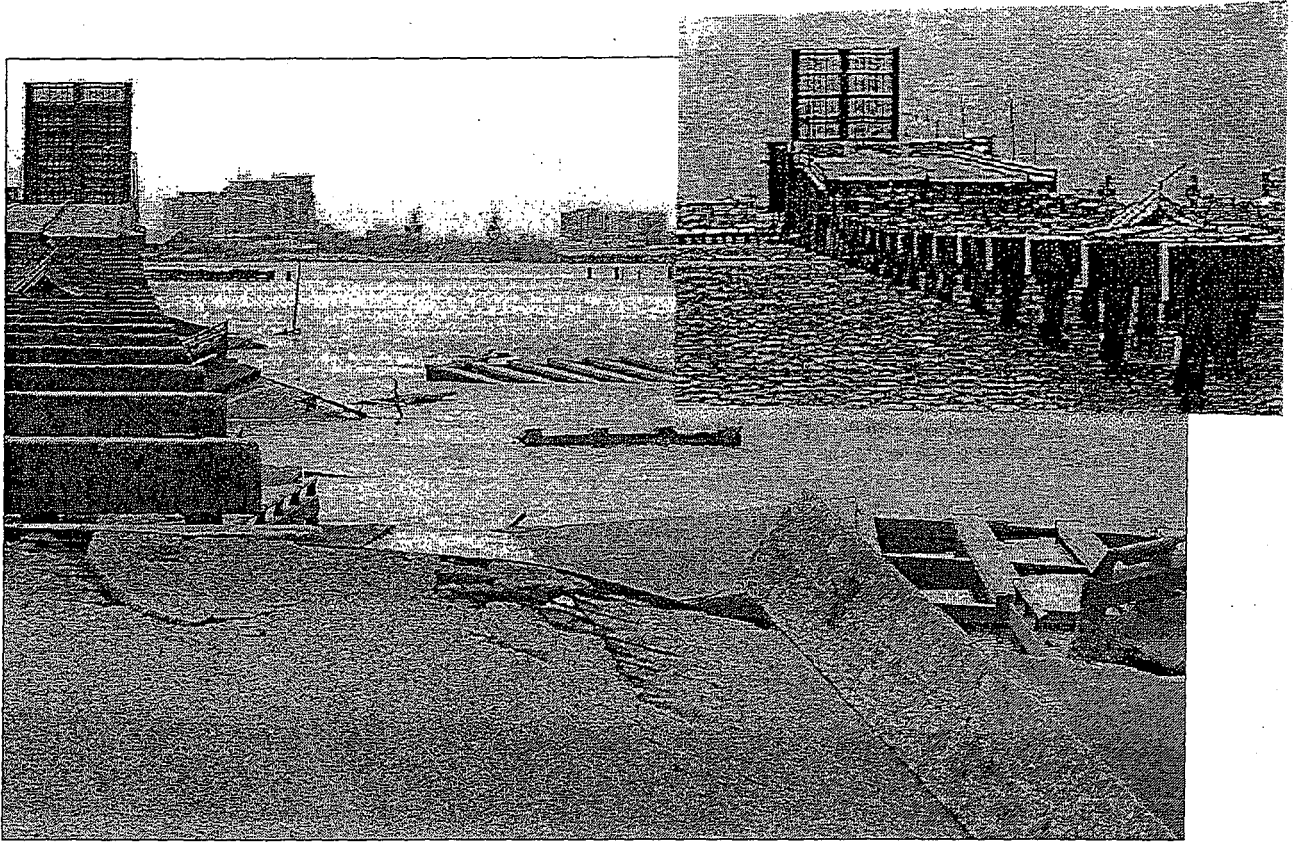
Fig. 4.11. Photo looking west toward Biloxi of Hurricane Katrina damage
to U.S. 90 Bridge over Biloxi Bay [1].

Fig. 4.12. Photograph of the damage to the U.S. 90 Biloxi Bay bridge caused by
Hurricane Katrina. Photo was taken looking northeast
from Biloxi 9/21/05 (Katrina Hit 8/29/05).
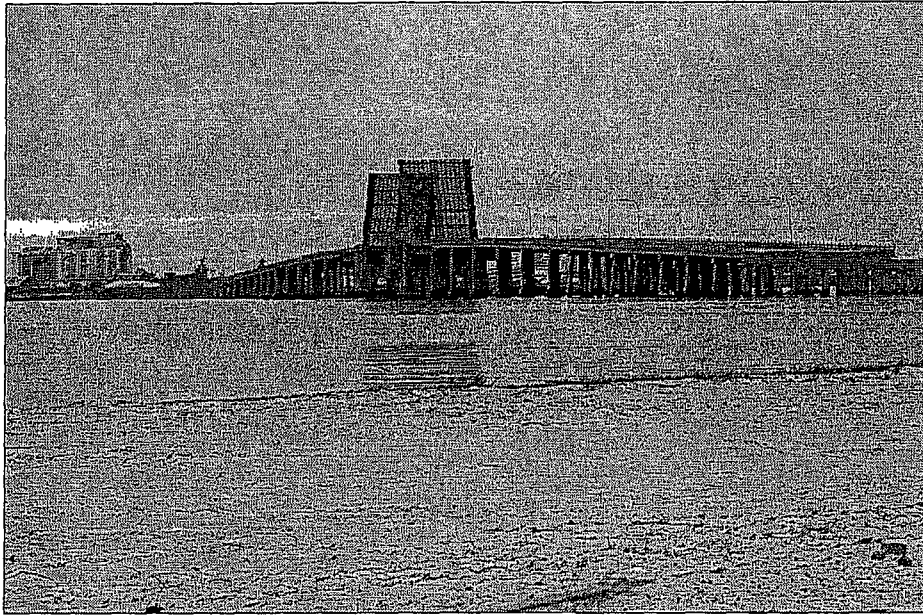
Fig. 4.13. Photograph of U.S. 90 bridge over Biloxi Bay showing high spans which were not knocked off pile cap bents during Hurricane Katrina (This photo was taken 2/19/06 looking west from Ocean Springs.)
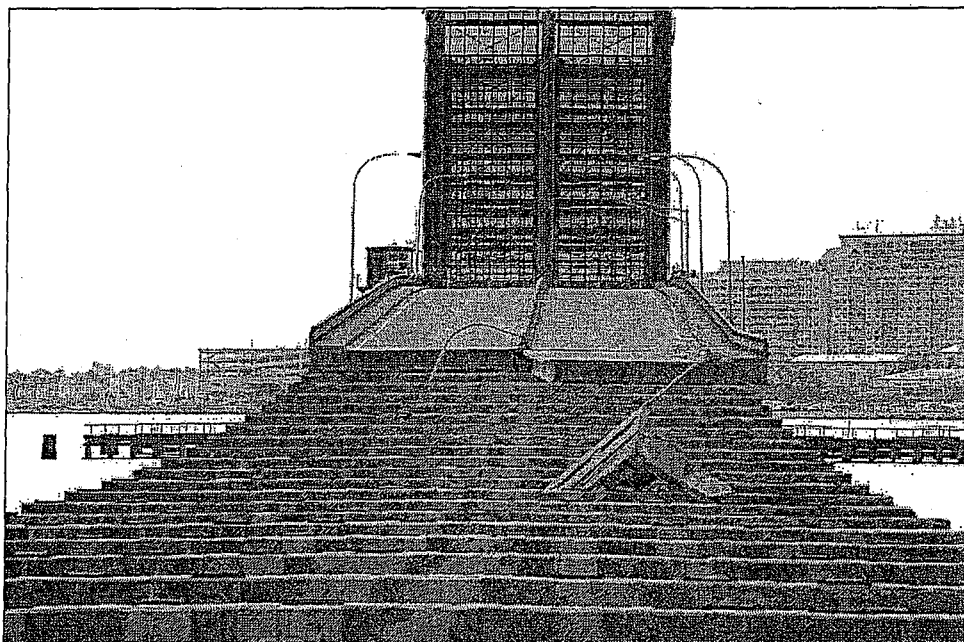
Fig. 4.14. Photograph of U.S. 90 bridge over Biloxi Bay showing the westbound half-span #100 that is still on pile caps but rotated and displaced to the landward side. The eastbound half-span was knocked completely off. The spans at higher elevations, beginning with span #99, were not knocked off the pile caps by the storm. (This photo was taken 2/19/06 looking southwest from Ocean Springs towards Biloxi.)
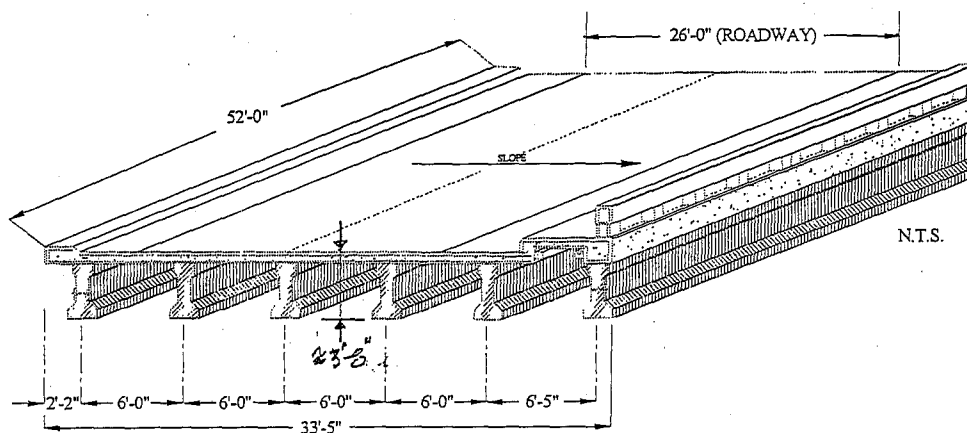
Fig. 4.15 Details of the typical span design on the U.S. 90 bridge across Biloxi Bay, Mississippi, that was destroyed by Hurricane Katrina. This sketch shows one-half the total width of the bridge.
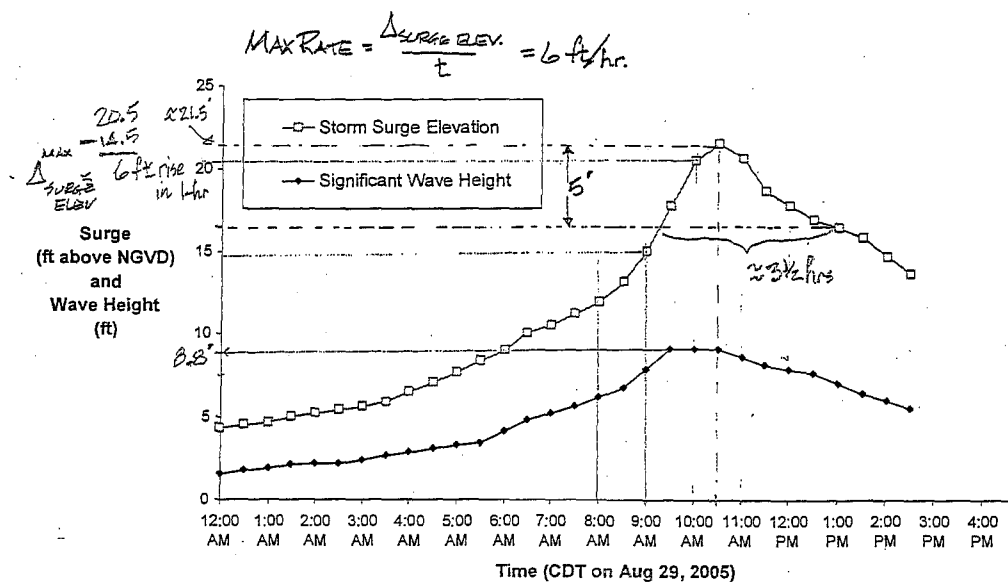
Fig. 4.16 Estimated storm surge and wave heights at the U.S. 90 bridge across Biloxi Bay during landfall of Hurricane Katrina. These estimates are hindcast data at the location of the high-span of the bridge based on ADCIRC modeling of surge and SWAN modeling of waves.

4-18

Table 4.1   Elevations of U.S. 90 Bridge Across Biloxi Bay[+]

Bent Number	Low-chord Elevation at Bent (ft)	Bent Number	Low-chord Elevation at Bent (ft)	Bent Number	Low-chord Elevation at Bent (ft)	Bent Number	Low-chord Elevation at Bent (ft)
1	10.1	32	11.4	63	14.6	94	33.1 [*]
2	10.1	33	11.5	64	14.7	95	31.5
3	10.1	34	11.6	65	14.8	96	29.9
4	10.1	35	11.7	66	14.9	97	28.4
5	10.1	36	11.8	67	15.0	98	26.8
6	10.1	37	11.9	68	15.1	99	25.3
7	10.1	38	12.0	69	15.2	100	23.7
8	10.1	39	12.1	70	15.3	101	22.1
9	10.1	40	12.2	71	15.4	102	20.6
10	10.1	41	12.3	72	15.5	103	19.0
11	10.1	42	12.4	73	15.6	104	17.5
12	10.1	43	12.5	74	15.7	105	16.2
13	10.1	44	12.6	75	15.8	106	15.0
14	10.1	45	12.7	76	15.9	107	13.9
15	10.1	46	12.8	77	16.0	108	13.0
16	10.1	47	12.9	78	16.2	109	12.2
17	10.1	48	13.0	79	16.6	110	11.5
18	10.1	49	13.1	80	17.0	111	10.9
19	10.2	50	13.2	81	17.6	112	10.5
20	10.2	51	13.3	82	18.3	113	10.3
21	10.3	52	13.4	83	19.2	114	10.2
22	10.3	53	13.5	84	20.1	115	10.1
23	10.4	54	13.6	85	21.2	116	10.1
24	10.5	55	13.8	86	22.4	117	10.1
25	10.6	56	13.9	87	23.8	118	10.1
26	10.7	57	14.0	88	25.3	119	10.1
27	10.8	58	14.1	89	26.8	120	10.1
28	10.9	59	14.2	90	28.4	121	10.1
29	11.0	60	14.3	91	29.9	122	10.1
30	11.2	61	14.4	92	31.5	123	10.1
31	11.3	62	14.5	93	33.1 [*]	124	10.1
						125	10.1

[+]Elevations are estimates of the low-chord (bottom of the girders) elevations (NGVD). Bents, piles with pile caps, are numbered from west to east. The highest bents, those near the drawbridge, are between bents #93 and #94, are designated by a different lettering nomenclature, and are not included in this table. (adapted Ref [1] from design plans provided by Mississippi D.O.T.)

*Highest bents. Spans in shaded region were not removed.

Looking at Figs. 4.11 - 4.14, it appears that about half way up the rise in elevation from the flat spans to the top spans (i.e., the draw spans), is where the transition between spans being removed and spans staying in place occurred. This is in agreement with Table 4.1, where bent elevations go from 10.1' to 33.1' with (10.1 + 33.1)/2 = 21.6' being the average and this is the approximate bent elevation where the spans remained in place. This approximate elevation is consistent with the estimated peak storm surge elevation at the bridge shown in Fig. 4.16. Based on this, it appears that when the hurricane peak storm surge elevation reached the level of the bottom of the bridge span girders, the buoyant and hydrodynamic forces from the hurricane surface waves, superimposed on top of the peak storm surge, were sufficient to lift and push the bridge spans from their positions on the bridge bents.

Hence, at the U.S. 90/Biloxi Bay Bridge, it is estimated that the peak storm surge height was approximately 21.5 ft above NGVD, with a significant wave height of approximately 8.8 ft. This sea state condition is shown in Fig. 4.16 superimposed on the Mobile Bay I-10 Bridge elevations. Since Katrina was such a large hurricane, it seems rational to use these surge and wave heights as the "design hurricane" for the design of new coastal bridges along the southern Gulf of Mexico coastline. However, for older existing coastal bridges, such as the I-10 bridge across the north end of Mobile Bay, it seems rational to retrofit the bridges for less severe hurricane surge/surface waves and associated forces. This is discussed further in a later section.

MAXIMUM WAVE CREST ELEV 31.10'

TOP OF RAIL ELEV 24.12'

MAXIMUM STORM SURGE ELEV 21.50'

TOP OF CAP ELEV 17.12'

CIRCULAR PRECAST PILES

MEAN SEA LEVEL ELEV 0.00'

BOTTOM OF BAY AT BRIDGE, ELEV -5.0'
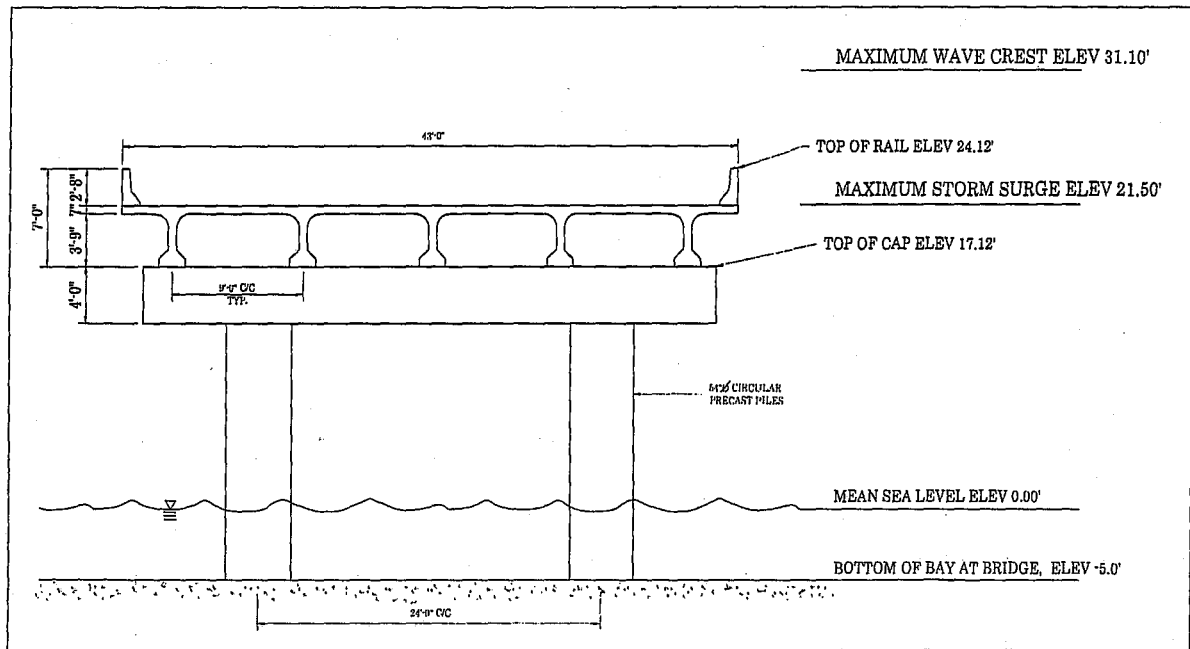
Fig. 4.16   Case C - Estimated Maximum Sea State Elevations at I-10 Bridge During Mock-Hurricane Katrina

4.5 Closure

Considering mean sea level at the Mobile Bay I-10 bridge site to be elevation 0 ft, the bottom of the bay at the bridge is approximately at elevation - 5.0 ft at the site, and the I-10 bridge components are at approximately elevations,

Bottom of bent cap = 13.1 ft

Top of bent cap/ = 17.1 ft
bottom of girders

Top of deck = 21.4 ft

Top of guard rail = 24.1 ft

Continuing to use mean sea level at the site as elevation 0 ft, any hurricane with a maximum storm surge greater than 17 ft would move the existing I-10 bridge superstructure and cause significant bridge damage. Due to a somewhat higher surge height at the bridge due to interference of the bridge with surface wave propagations, the effective surge height at the bridge may be 0.5 - 1.0 ft higher than the storm surge height. Thus, any hurricane with a maximum storm surge greater than 16 ft may move the bridge superstructure and cause bridge damage.

The maximum storm surge elevations at the Mobile Bay I-10 Bridge shown in Figs. 4.8 and 4.9 for Hurricane's Frederic and Katrina, respectively, did not exceed the above critical values, and these hurricanes did not damage the Mobile Bay Bridge. However, had Hurricane Katrina's track been located approximately 70 miles to the east, the maximum storm surge elevation shown in Fig. 4.16 would probably have occurred at the north end of Mobile Bay, and this would have probably destroyed the Mobile Bay I-10 Bridge superstructure. Hurricane surge/surface wave forces that could,

in the future, act on the Mobile Bay Bridge, and retrofit actions recommended for this bridge are presented in the ensuing chapters.

5. HURRICANE SURGE/SURFACE WAVE FORCES ON I-10 MOBILE BAY BRIDGE AND RESPONSE OF BRIDGE TO THESE FORCES

5.1 General

As indicated in Chapter 3, the hurricane storm surge simply raises the sea state still water level (SWL) to an elevation where

- vertical buoyant forces resulting from the SWL may act on all or part of the bridge superstructure

- vertical buoyant forces from the storm surface waves that are super-imposed on the storm SWL may act on all or part of the superstructure

- the storm surface waves can apply large periodic hydrodynamic horizontal and vertical forces on the superstructure.

All of the above forces can be large and are important, and their magnitudes, directions, and time and duration of application should be considered.

Chapter 3 presented commonly used surface wave force prediction equations and proposed modifications to the equations by Douglass, et al. by the authors. Comparisons of the resulting forces from application of these equations to a common bridge span were made and discussed in Chapter 3. The "best" of these equations appears to be the Modified Douglass, et al. equations, and these are the equations that were used in predicting hurricane surge/surface wave forces on the I-10 Mobile Bay Bridge.

From the above, and from the discussions in Chapter 3, a hurricane's peak surge height and significant surface wave height, relative to the height of a coastal bridge's

superstructure, are the dominant parameters of importance in assessing hurricane wave induced forces on a coastal bridge. These critical hurricane sea state parameters were estimated for the I-10 Bridge site across the north end of Mobile Bay in Chapter 4, and these estimates along with the known geometry of the I-10 Bridge and along with the surface wave force prediction equations given in Chapter 3, allow us to make a reasonable estimate of the maximum anticipated hurricane surge/surface water forces that could act on a typical span of the I-10 Bridge over Mobile Bay. These forces, along with the bridge DL, allow us to estimate the response of the I-10 bridge superstructure and substructure as a hurricane moves through the bridge. This is the purpose of this chapter and is presented in the sections below.

5.2 Assumed Retrofit Hurricane Sea State for Mobile Bay I-10 Bridge

Based on the facts that the I-10 Bridge spans across the north end of Mobile Bay

1. are approximately 43 years old and probably only have a remaining service life of approximately 17 years,
2. have never experienced hurricane surge/surface wave water elevations and forces of the level needed to produce catastrophic bridge damage in their 43-year lifetime (excluding the lower elevation ramps),
3. are at a site that has never (as best as can be determined) experienced water elevations to the level to cause catastrophic bridge damage (excluding the lower elevation ramps), and
4. knowing that the winds (Category 5 just prior to landfall) and storm surge elevations of Hurricane Katrina are probably those associated with a 100-year hurricane,

it is not recommended that the Case C (Mock-Hurricane Katrina) sea state discussed in Chapter 4 and shown in Fig. 4.16 be used as the basis for possible retrofit actions on the I-10 Bridge. The Case C sea state would be appropriate for the design of any future new bridges that may be constructed at the north end of Mobile Bay site.

For the existing I-10 Bridge over Mobile Bay, it seems appropriate to retrofit the bridge as needed for a sea state associated with a direct hit of a hurricane smaller than Katrina Hurricane, such as Hurricane Frederic, i.e., for Case A in Chapter 4, or for a near-miss for a large hurricane such as Hurricane Katrina, i.e., for Case B in Chapter 4. Since Case B gives the more severe loading condition, it is recommended that the Mobile Bay I-10 Bridge be retrofitted to sustain the hurricane forces associated with the Case B hurricane sea-state. This sea-state is repeated below in Fig. 5.1 for convenience and completeness.
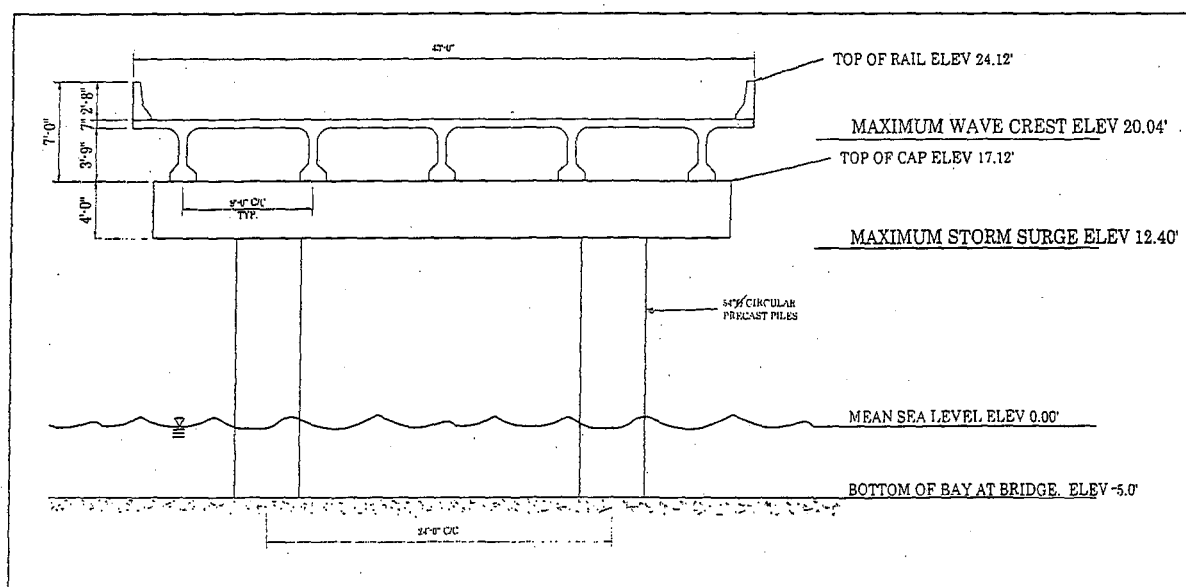
**Fig. 5.1 Recommended Retrofit Sea State Elevations
at I-10 Bridge for Hurricane Loadings**

5-3

5.3 Estimated Maximum Hurricane Surge/Surface Wave Forces on I-10 Bridge

In order to quantify the forces due to surge/surface waves at the I-10 Bridge site, the Modified Douglass et al. equations were used to calculate the vertical and horizontal forces due to the three hurricane cases stated previously, i.e., Frederic, Katrina, and Mock-Katrina. All three cases were considered initially to gain an appreciation of the range of wave forces that may act on the I-10 bridge in the future. Necessary bridge parameters for calculating these wave forces include the bridge elevations and geometry, as well as storm parameters such as surge height and significant wave height. The bridge elevations and geometry were taken from construction plans provided by ALDOT, and the storm surge elevations were obtained from the storm data near the site during Hurricanes Frederic and Katrina given in Chapters 2 and 4, and from assumptions made for the Mock-Katrina hurricane, i.e., to use storm data at Biloxi, MS during Hurricane Katrina. Some other estimates of maximum surge elevations, significant wave heights, and wave crest elevations from the literature are shown in Table 5.1.

Table 5.1 Estimates of Maximum Wave Height and Crest Elevations (from Ref. 9)

Hydraulic/Wave Parameter	Simulation		
	Hurricane Ivan	100-year Design Storm	500-year Design Storm
Maximum Surge Water Surface Elevation (WSE$_{max}$, m-NAVD88)	+3.27 (+10.72 ft)	+2.87 (+9.4 ft)	−3.77 (+12.36 ft)
Significant Wave Height (m)	1.98 (6.51 ft)	1.83 (5.99 ft)	2.17 (7.12 ft)
Associated Wave Peak Period (sec)	3.19	3.09	3.31
Associated Wave Mean Direction (degrees from North)	345	345	344
Maximum Wave Height (H$_{max}$, m)	3.97 (13.01 ft)	3.65 (11.98 ft)	4.34 (14.25 ft)
Maximum Crest Elevation (m-NAVD88) (WSE$_{max}$ + 0.8*H$_{max}$)	+6.44 (+21.13 ft)	+5.79 (+18.98 ft)	−7.24 (−23.76 ft)

An assumed significant wave height of 7.0' was assumed for the **Cases A** and **B** (Hurricanes Frederic and Katrina storm data). For **Case C**, the Mock-Katrina hurricane, a value of 8.8' was used for the significant wave height and 21.5' for the storm surge, based on Fig. 5.2.
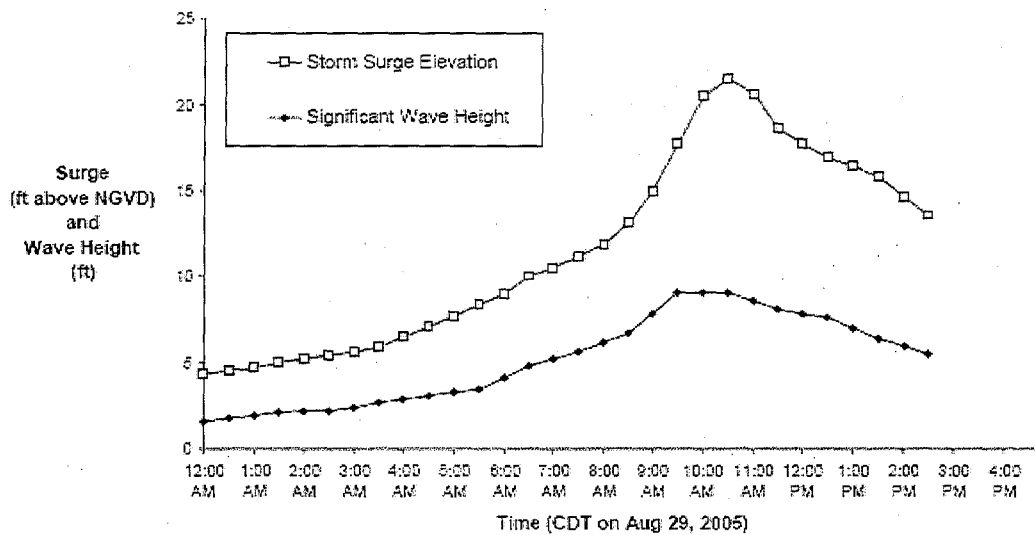
Fig. 5.2 Significant Wave Height During Hurricane Katrina Near Biloxi Bay, MS (Douglass et al.)

The Modified Douglass et al. equations used to estimate the vertical and horizontal wave load components are as follows:

Vertical Force

$$F_v = c_v^{mc} F_v *$$

Horizontal Force

$$F_h = \left[1 + c_r \frac{(N-1)}{2} \right] c_h^{mc} F_h *$$

where:

F_V = estimated vertical wave force
F_h = estimated horizontal wave force
F_V^* = a "reference" vertical load
F_h^* = a "reference" horizontal load
c_V^{mc} = an empirical coefficient from McConnell's work (to be taken as 1.0)
c_h^{mc} = an empirical coefficient from McConnell's work (to be taken as 1.0)
c_r = a reduction coefficient for reduced horizontal load on the internal (i.e. not the waveward-most) girders (to be taken as 0.33)
N = the number of girders supporting the bridge span deck

The "reference" loads can be determined by the following equations:

$$F_v^* = \gamma(\Delta z_v) A_v$$

$$F_h^* = \gamma(\Delta z_h) A_h$$

where:

Δz_v = difference between the elevation of the crest of the maximum wave and the elevation of the bottom of the end diaphragms (to be taken as 1 ft. higher than the bottom of the girders)

or

the difference between the elevation of the top of the solid portion of the guard rail and the bottom of the end diaphragms (to be taken as 1 ft. higher than the bottom of the girders),

whichever is smaller,

Δz_h = difference between the elevation of the crest of the maximum wave and the elevation of the centroid of A_h

or

the difference between the elevation of the top of the solid portion of the guard rail and the elevation of the centroid of A_h,

whichever is smaller,

5-6

A_v = bridge span length x ½ bridge width (for widths > 20 ft)

= bridge span length x bridge width (for widths ≤ 20 ft)

A_h = the bridge span length x the vertical projection of the superstructure from the girder bottoms up to the top of the solid portion of the guard rail

γ = unit weight of water (64 pcf for saltwater).

The above equations were used to estimate the maximum surge/surface wave forces on a typical I-10 bridge span during Hurricanes Frederic, Katrina, and Mock-Katrina. Calculations of the resultant wave forces are presented below along with figures showing the combined wave and DL forces acting on a typical bridge span.

Estimated Wave Forces During Hurricane Frederic, Case A

Assumptions:

- MSL = 0.00'
- Mudline = -5.00'
- 11.70' Storm Surge
- 7.00' Significant Wave Height
- Elevation of Centroid of Deck = 20.62' (3.5' Above Top of Cap)

Calculations:

η_{max} = 0.78 * (1.4*7.00') = 7.64'
Maximum Wave Crest Elevation = 11.70' + 7.64' = 19.34'
A_h = 65' x 7' = 455 ft^2
A_v = 65' x (43'/2) = 1397.5 ft^2
Δz_v = smaller of   19.34' – 18.12' = 1.22'
                             or
                             24.12' – 18.12' = 6.00'

Δz_v = 1.22'

Δz_h = smaller of   19.34' – 20.62' = 0.00'
                             or
                             24.12' – 20.62' = 3.50'

∴ Take Δz_h = 0.00'

Vertical Force:

F_v* = (64pcf)(1.22')(1397.5 ft^2) = 109.1 kips
F_v = (1.0)(109.1 kips) = **109.1 kips**

Horizontal Force:

F_h* = (64 pcf)(0.00')(455 ft^2) = 0.00 kips
F_h = [1+ (0.33)((5-1)/2)](1.0)(0.00 kips) = **0.00 kips**

Overturning Moment:
*Assume Vertical Force Acts at a Location of ¼ Span Width

M = Fv * ¼ Span Width
M = (109.1 kips)(43'/4) = **1172.8 kip-ft**

F_v = **109.1 kips**	
F_h = **0.0 kips**	
M = **1172.8 kip-ft**	

These resultant wave forces along with the span DL forces and the combined

DL plus wave forces are shown in Fig. 5.3.

SPAN DEAD LOAD

108k   108k   108k   108k   108k

SPAN WAVE LOAD

26k   13k   13k   26k   DUE TO MOMENT
OF 1172.8 K-FT

DUE TO UPLIFT
OF 109.1 K

21.8k   21.8k   21.8k   21.8k   21.8k

SPAN DEAD + WAVE LOAD

112.2k   99.2k   86.2k   73.2k   60.2k
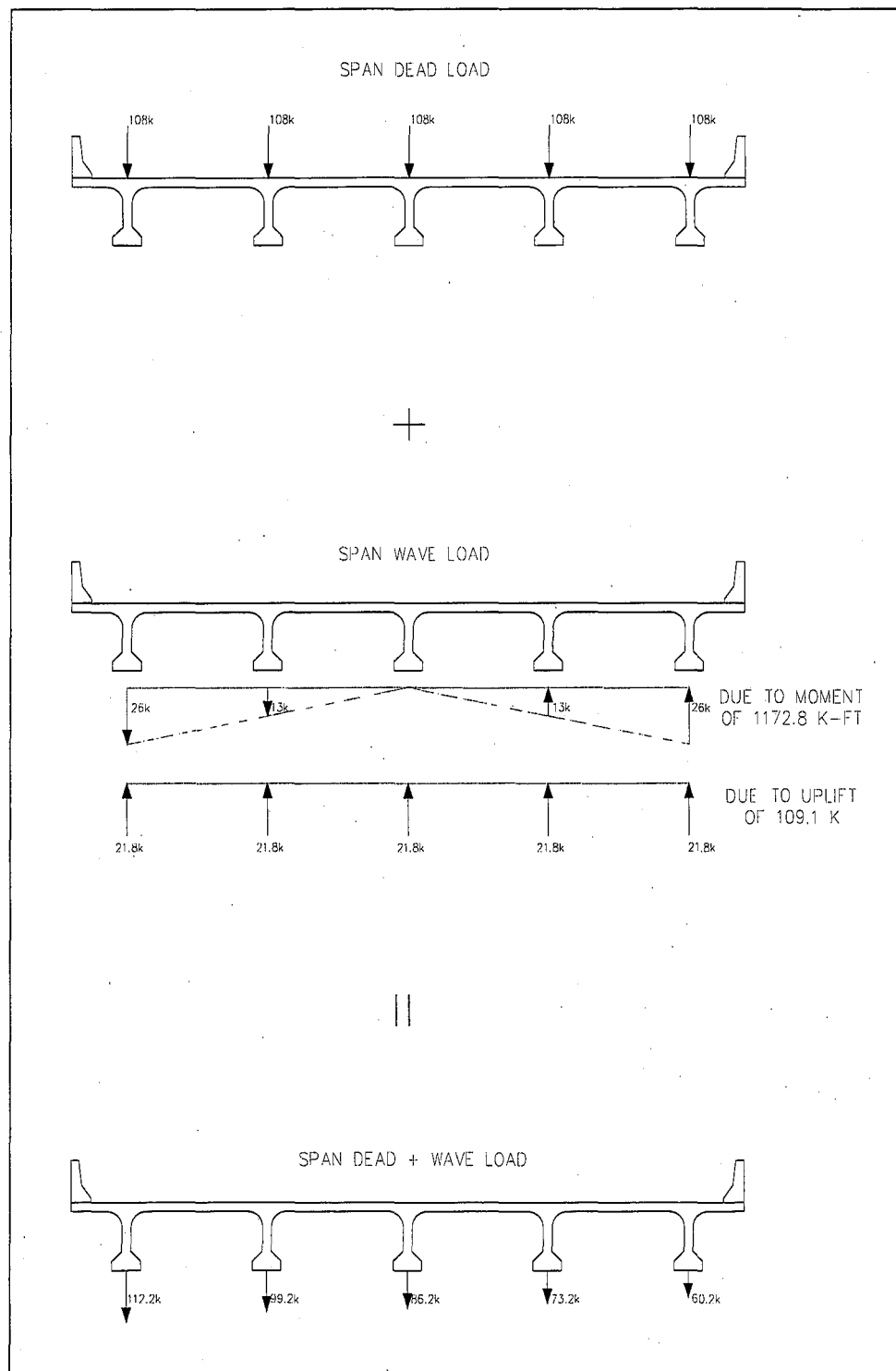
Fig. 5.3   Estimated Maximum Forces on a Typical Mobile Bay I-10
Span During Hurricane Frederic, Case A

5-9

Estimated Wave Forces During Hurricane Katrina, Case B

Assumptions:

- MSL = 0.00'
- Mudline = -5.00'
- 12.40' Storm Surge
- 7.00' Significant Wave Height
- Elevation of Centroid of Deck = 20.62' (3.5' Above Top of Cap)

Calculations:

η_{max} = 0.78 * (1.4*7.00') = 7.64'
Maximum Wave Crest Elevation = 12.40' + 7.64' = 20.04'
A_h = 65' x 7' = 455 ft^2
A_v = 65' x (43'/2) = 1397.5 ft^2
Δz_v = smaller of   20.04' − 18.12' = 1.92'
                                             or
                                             24.12' − 18.12' = 6.00'
Δz_v = 1.92'

Δz_h = smaller of   20.04' − 20.62' < 0.00'
                                             or
                                             24.12' − 20.62' = 3.50'
∴ Take Δz_h = 0.00'

Vertical Force:

F_v* = (64pcf)(1.92')(1397.5 ft^2) = 171.7 kips
F_v = (1.0)(171.7 kips) = **171.7 kips**

Horizontal Force:

F_h* = (64 pcf)(0.00)(455 ft^2) = 0.00 kips
F_h = [1+ (0.33)((5-1)/2)](1.0)(0.00 kips) = **0.00 kips**

Overturning Moment:
*Assume Vertical Force Acts at a Location of ¼ Span Width

M = Fv * ¼ Span Width
M = (171.7 kips)(43'/4) = **1845.8 kip-ft**

F_v = 171.7 kips
F_h = 0.0 kips
M = 1845.8 kip-ft

These resultant wave forces along with the span DL forces and the combined

DL plus wave forces are shown in Fig. 5.4.

SPAN DEAD LOAD

108k   108k   108k   108k   108k

+

SPAN WAVE LOAD

41k   20.5k   20.5k   41k   DUE TO MOMENT
                               OF 1845.8 K-FT

34.3k   34.3k   34.3k   34.3k   34.3k   DUE TO UPLIFT
                                        OF 171.7 K

||

SPAN DEAD + WAVE LOAD

114.7k   94.2k   73.7k   53.2k   32.7k
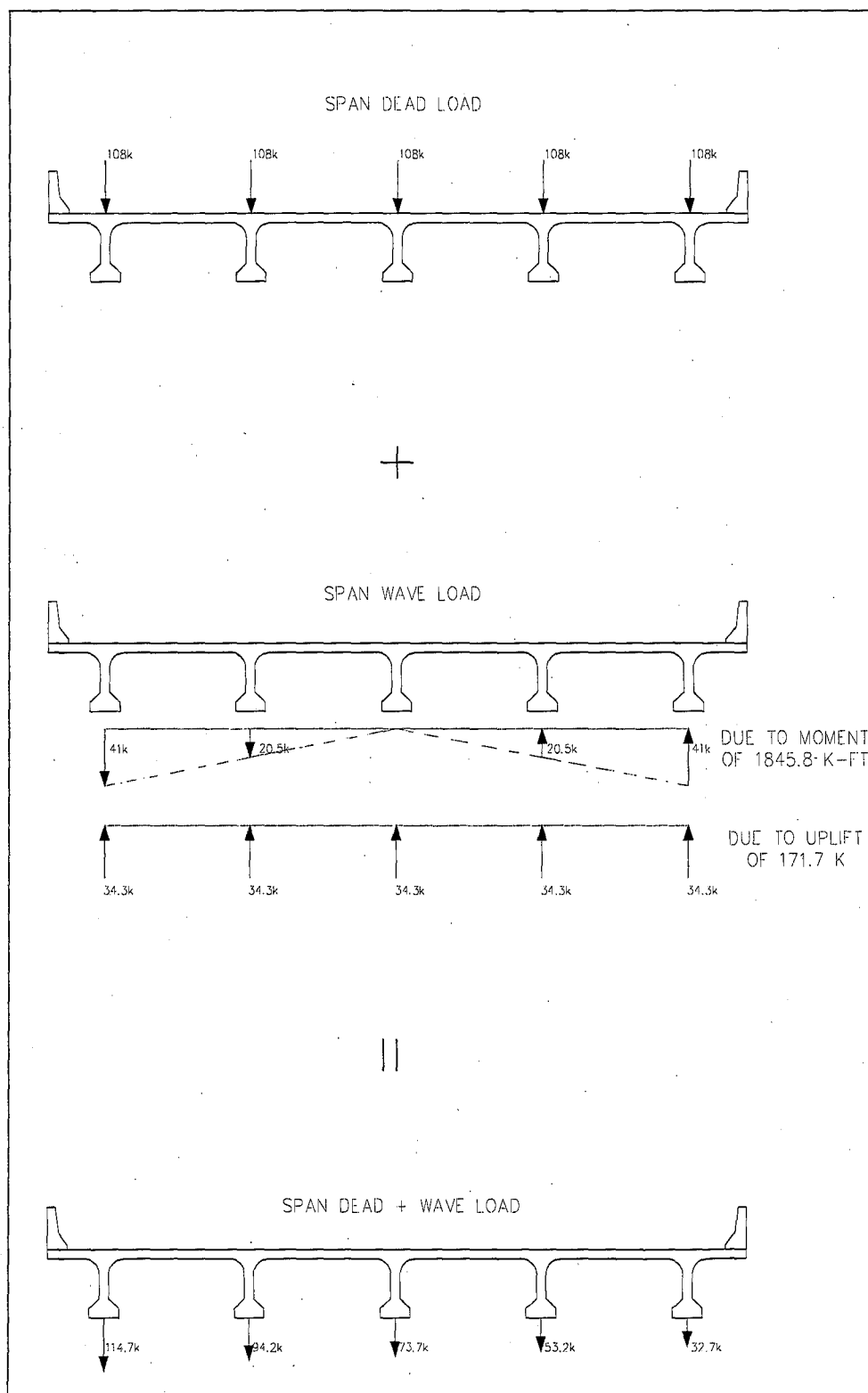
Fig. 5.4   Estimated Maximum Forces on a Typical Mobile Bay I-10 Span During Hurricane Katrina, Case B

5-11

Estimated Wave Forces on I-10 Bridge During Mock Hurricane Katrina, Case C

Assumptions:

- MSL = 0.00'
- Mudline = -5.00'
- 21.50' Storm Surge
- 8.80' Significant Wave Height
- Elevation of Centroid of Deck = 20.62' (3.5' Above Top of Cap)

Calculations:

η_{max} = 0.78 * (1.4*8.80') = 9.61'
Maximum Wave Crest Elevation = 21.50' + 9.61' = 31.10'
A_h = 65' x 7' = 455 ft^2
A_v = 65' x (43'/2) = 1397.5 ft^2
Δz_v = smaller of   31.10' – 18.12' = 12.98'
                         or
                         24.12' – 18.12' = 6.00'

Δz_v = 6.00'

Δz_h = smaller of   31.10' – 20.62' = 10.48'
                         or
                         24.12' – 20.62' = 3.50'

Δz_h = 3.50'

Vertical Force:

$F_v{}^*$ = (64pcf)(6.00')(1397.5 ft^2) = 536.6 kips
F_v = (1.0)(536.6 kips) = **536.6 kips**

Horizontal Force:

$F_h{}^*$ = (64 pcf)(3.50')(455 ft^2) = 101.9 kips
F_h = [1+ (0.33)((5-1)/2)](1.0)(101.9 kips) = **169.2 kips**

Overturning Moment:
*Assume Vertical Force Acts at a Location of ¼ Span Width

M = Fv * ¼ Span Width
M = (536.6 kips)(43'/4) = **5768.9 kip-ft**

F_v	=	**536.6 kips**
F_h	=	**169.2 kips**
M	=	**5768.9 kip-ft**

These resultant wave forces along with the span DL forces and the combined

DL plus wave forces are shown in Fig. 5.5.
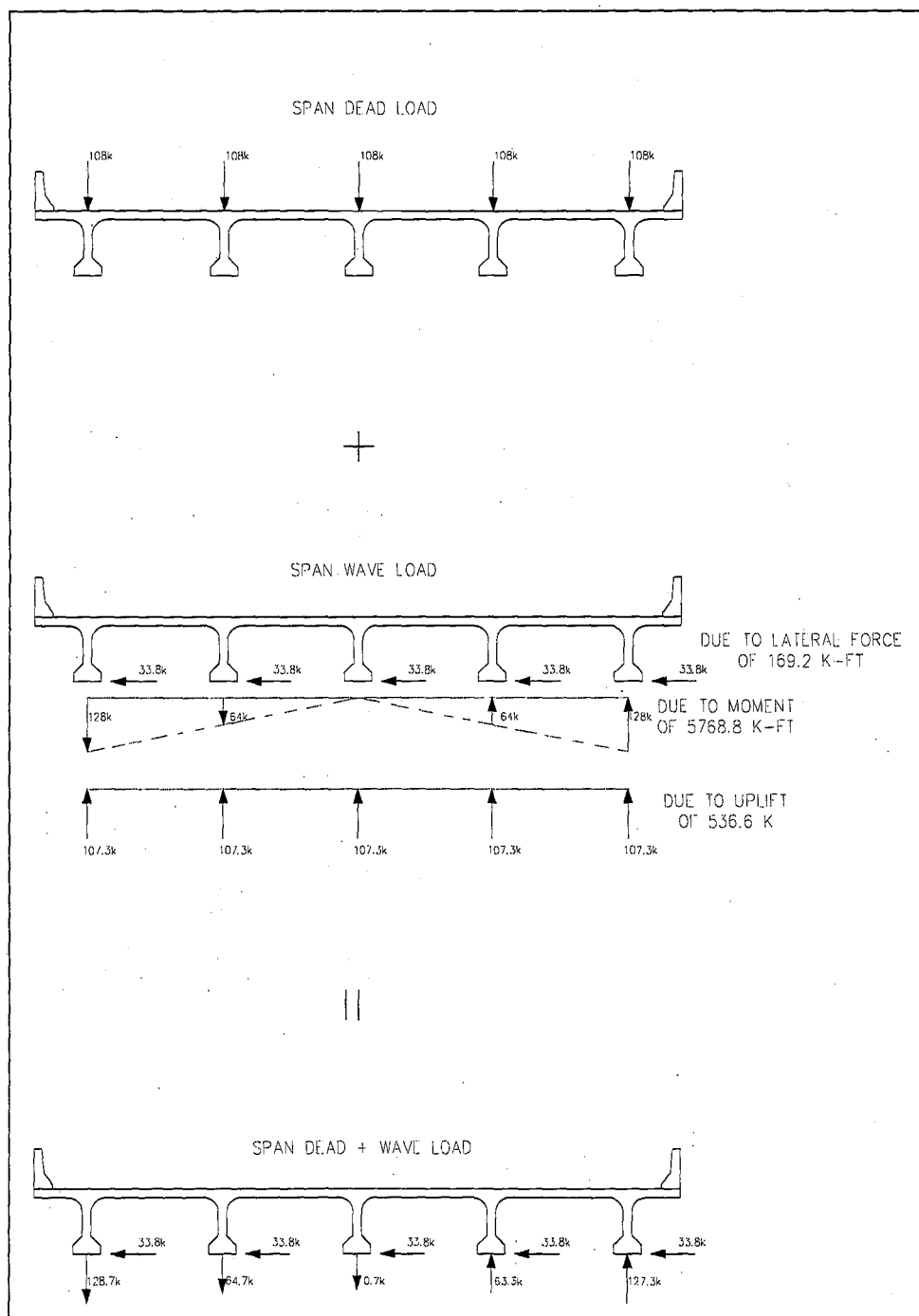
Fig. 5.5   Estimated Maximum Forces on a Typical Mobile Bay I-10 Span During a Mock-Katrina Hurricane, Case C

5.4 Response of I-10 Bridge Superstructure to Hurricane Wave Plus Dead Loadings

Upon calculating the wave forces associated with each of the three hurricane cases stated earlier, we then determined the response of the I-10 bridge superstructure and substructure to the vertical and horizontal forces as well as the moment of each hurricane to gain an appreciation of the range of possible responses of the I-10 Bridge in future hurricanes. This section will focus on the response of the bridge superstructure to the estimated wave plus dead loadings presented in Section 5.3.

Response to Hurricane Frederic Loading:

Estimated Hurricane Frederic wave plus DL forces for a typical I-10 span are given in Fig. 5.3 and are summarized in Fig. 5.6 below.
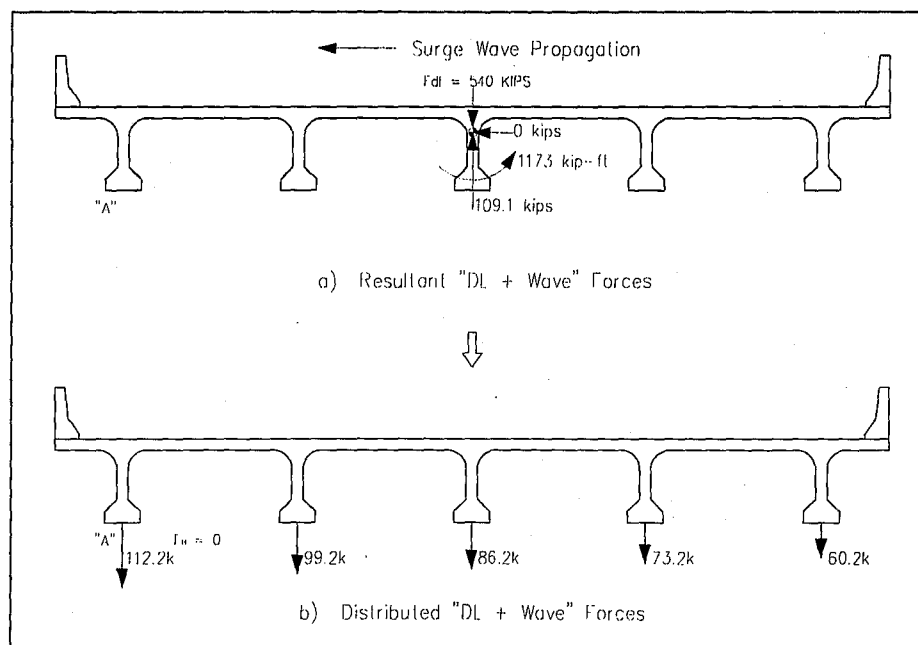
Fig. 5.6 Estimated 'DL + Wave' Forces on a Typical Mobile Bay I-10 Span During Hurricane Frederic, Case A

Note in Fig. 5.6 that the net horizontal force is zero so the span would not have been expected to slide off of its support bents. The net vertical force is 431^k down so the span would not be expected to have been lifted, and there is no net moment about point "A" trying to tip/rotate the span counterclockwise about point "A". Thus, for Hurricane Frederic wave forces, the I-10 span was expected to be stable and would not have experienced rigid body motion, even if the span was not attached to the bent caps. It should be noted that the above estimated forces and the superstructure response to these forces are consistent with the apparent response of the spans as no spans (excluding the ramp spans) were moved or connection's damaged during Hurricane Frederic.

Response to Hurricane Katrina Loading:

Estimated Hurricane Katrina wave plus DL forces for a typical I-10 span are given in Fig. 5.4 and are summarized in Fig. 5.7 below.
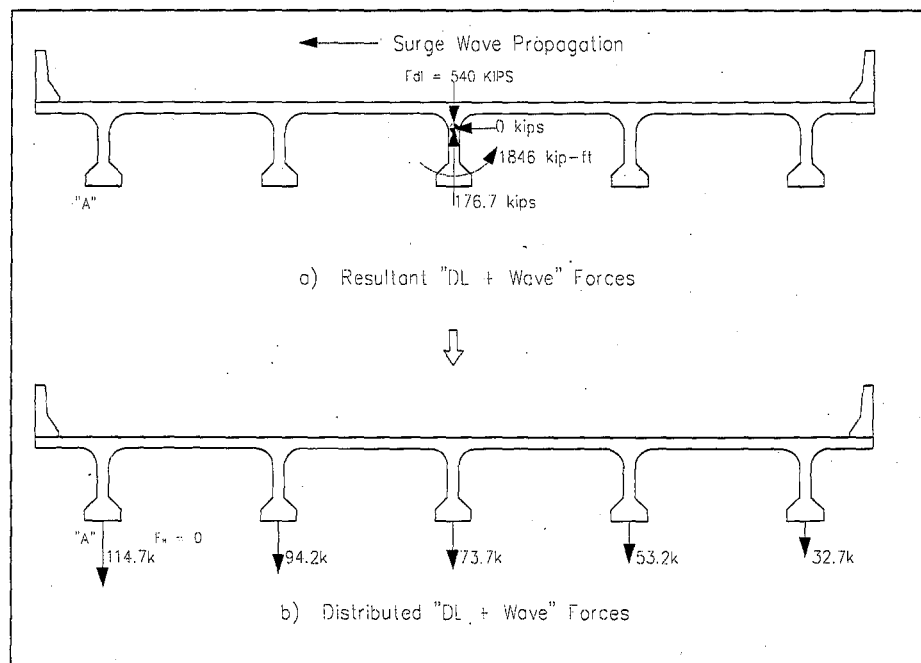
Fig. 5.7   Estimated 'DL + Wave' Forces on a Typical Mobile Bay I-10 Span During Hurricane Katrina, Case B

5-15

Note in Fig. 5.7 that the net horizontal force, F_H, is zero and thus the span does not try to slide off its support bents, the net vertical force, F_v, is 368^k down and thus the span does not try to be lifted, and there is not net moment, M, about point "A" trying to tip/rotate the span counterclockwise about point "A". Therefore, for Hurricane Katrina (making landfall 130 miles west of Mobile Bay) wave forces, the I-10 span is stable and would not have experienced rigid body motion even if the span was not attached to the bent caps. It should be noted that the above estimated forces and the superstructure response to these forces are consistent with the apparent response of the spans since no spans (excluding the ramp spans) were moved or connections damaged during Hurricane Katrina.

Response to a Mock-Katrina Hurricane:

Estimated Mock-Katrina Hurricane wave plus DL forces for a typical I-10 span are given in Fig. 5.5 and are summarized in Fig. 5.8 below.
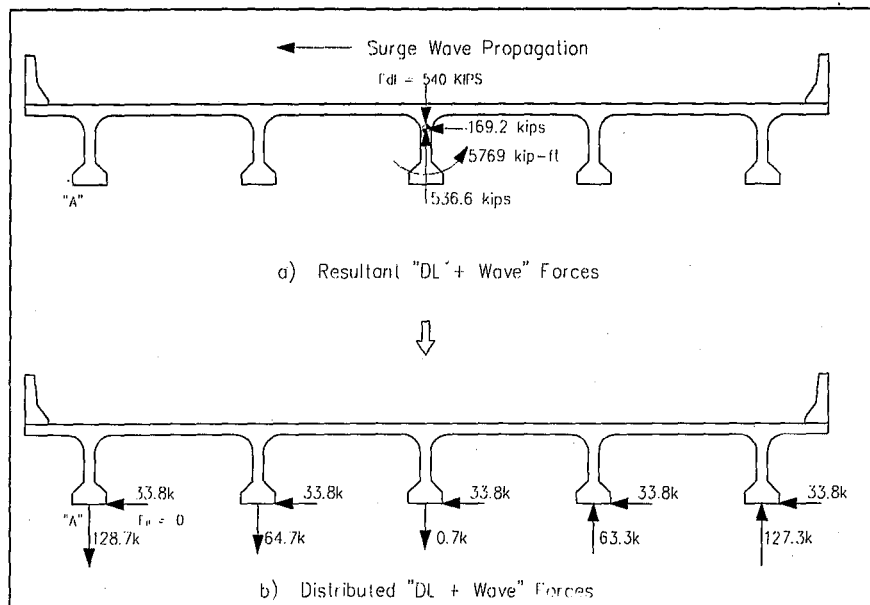
Fig. 5.8   Estimated 'DL + Wave' Forces on a Typical Mobile Bay I-10 Span During a Mock-Katrina Hurricane, Case C

Note in Fig. 5.8 that there is a significant net horizontal force of $F_H = 169^k$ acting on the span, and thus the span needs to be positively connected to the bent substructure with sufficient capacity to resist this horizontal shearing or sliding force. Note further in Fig. 5.8b that the three girders on the ocean side of the span have zero friction resistance capacity due to the vertical forces at those locations being upward or nearly zero. The two landside girders can resist some horizontal forces via friction; however, not to a level of 169^k. Thus, shear lugs or shear bolts or equivalent will be needed at the superstructure girder-to-bent cap connection to safely transmit the 169^k horizontal wave loading to the bridge substructure.

Note in Fig. 5.8a that the net vertical force on the span is almost zero and thus the span is very close to being lifted. Thus, hold-down anchor bolts should be used but their size would need to be minimal to prevent rigid body uplift. However, in looking at Fig. 5.8a we see that there is a net counterclockwise tipping moment about point "A" of approximately $5770^{\text{ft-kips}}$ that must be designed for to prevent rigid body rotation of the span about point "A". Looking at Fig. 5.8b, one can see that the most severe super-to-substructure connection will be at the oceanmost girder where an uplift anchor force of 127.3^k must be designed for as well as all of the 33.8^k shear force (none will be resisted by friction at this location). As can be seen in Fig. 5.8b, the girder-to-cap connection of the next most seaward girder will require an uplift anchorage of 63.3^k and a bolt shear capacity of 33.8^k. However, as stated in Chapter 4, only the two outer girders and the centerline girder are bolted to the bridge bent cap, and consequently, the second-most seaward girder has no uplift or shear anchorage. Thus there is nothing to resist the 63.3^k uplift and 33.8^k shear forces shown in Figs. 5.5c and 5.8b on the second-most

seaward girder. It should be noted that the forces on the second-most landward girder can probably be resisted by direct bearing and friction even though it is not positively connected to the bent cap. Because of the missing girder-to-cap connection on the second-most seaward girder, the forces on the most seaward girder-to-cap connection in Figs. 5.5c and 5.8b will be increased to approximately 143^k vertically and 42.3^k horizontally and the forces on the second-most seaward girder connection will be zero. The connection at the most seaward girder location can probably resist the 42.3^k horizontal shearing force; however, the 143^k vertical force would probably fail the four horizontal $7/8"^\phi$ cap screws (or the adjacent concrete) at that location (see Fig. 4.4).

The four $1\frac{1}{4}"^\phi$ swedge bolts used to connect the most seaward girder to the bent cap would probably be adequate to resist the 143^k vertical force. Also, the applied horizontal loading of 169.2^k will be resisted by the total number of $1\frac{1}{4}"^\phi$ swedge bolts connecting the superstructure to the substructure, in this case, twelve bolts. These bolts have a shear capacity of ≈ 43 kips each as per AISC, giving a total shear resistance of 516 kips. This should be more than adequate to resist the horizontal wave induced loading. However, Figs. 2.30 and 2.31 in Chapter 2, which are for a lower elevation ramp span, speak to the inadequacy of the span girder-to-cap connections.

5.5 Response of I-10 Bridge Substructure to Hurricane Wave Plus Dead Loadings

Assuming that the superstructure is adequately connected to the substructure, the total loads sustained by the superstructure will be transferred to the substructure. For each bridge span, the vertical loads will be resisted by the total dead weight of the superstructure, one pile cap, and two piles. This is due to the fact that the bridge deck

is essentially being supported by half of a pile cap at each end, since there are two span ends connected to each pile cap. The same effect is accounted for in the number of piles. Therefore, the total dead weight of a bridge span to resist uplift is 1001.2 kips. This can be seen in Figure 5.9.
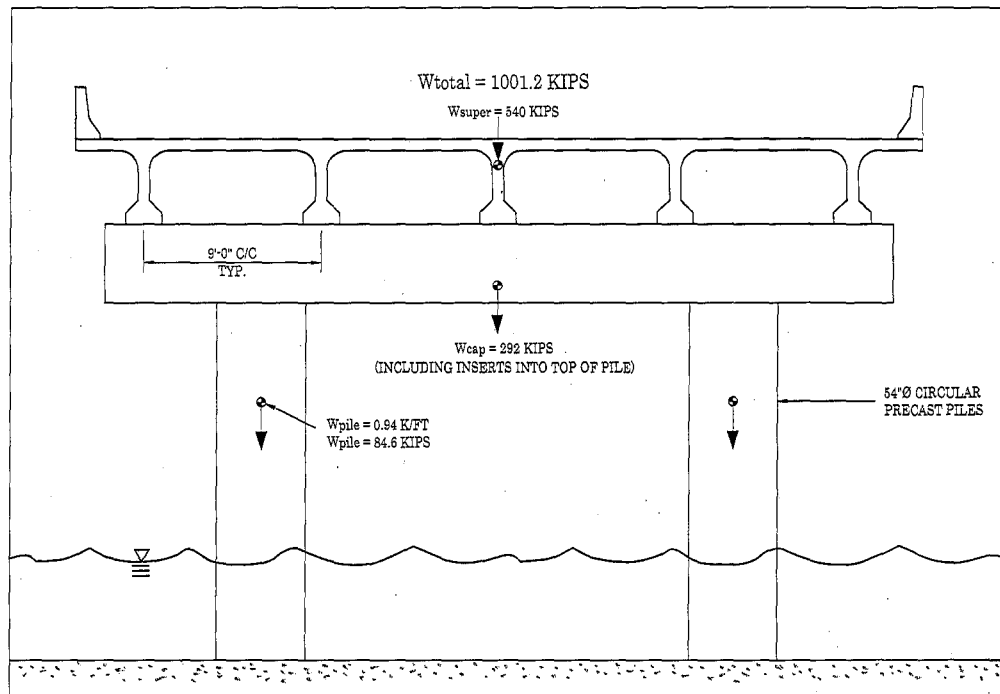
Figure 5.9 Total Dead Weight of Super+Substructure Spans

The loadings on the substructure for each of the three cases of hurricanes were modeled in RISA 2-D using two different pile length models corresponding to the pile lengths above the mud-line plus 5 feet and 10 feet, respectively, below the mud-line to model a "fixed connection" for the piles. Substructure member forces were extracted from the RISA 1-D analyses and a general analysis of the pile cap and the piles was conducted to evaluate their performance during each hurricane. The RISA 2-D model results can be seen in Appendix D.

A general moment capacity of the pile cap was calculated in order to compare the results of the RISA model. This moment capacity was calculated as follows:

$$M_n = A_s f_y \left(d - \frac{a}{2} \right)$$

The reinforcing pattern and geometry for the pile caps is shown in Figure 4.5, and consists of nine (9) #11 reinforcing bars top and bottom. This corresponds to an A_s of 14.04 in^2. Given a height of cap of 48", a value of d is determined to be 44.3", based on an assumption of 3", cover as shown in the plans. The height of the compression block, a, was calculated using the following formula:

$$a = \frac{A_s f_y}{0.85 f'_c b}$$

Using a value of b equal to 48" to be conservative and a value of the compressive strength of the concrete, f'$_c$, to be 5000 psi, the height of the compression block was calculated to be 4.13". Plugging these values into the moment equation above, the unfactored moment capacity of the pile cap was determined to be 2668.4 kip-feet.

The pile capacity for each hurricane scenario was checked by comparing stresses on the prestressed piles for cracking as well as the ultimate moment capacity of the section. ALDOT plans specify that each pile was prestressed with sixteen strands composed of twelve-0.192" diameter wires prestressed to 140 ksi, correlating to a compressive stress on the cross section of each pile of 862 psi. The moments taken from the model were then equated to bending stresses, based on the equation $\sigma = My/I$, with y being 27" and I being the gross moment of inertia of the cylindrical pile, 264,648 in^4. The moment capacity of the prestressed piles was computed by the same methods as for the pile cap above. The moment capacity for the piles was calculated to be

2263.8 kip-ft. Calculations can be seen in Appendix D. For each hurricane case, the maximum moments occurred in the piles when using a bent modelling length of pile of 10 feet below the mud-line, i.e., a pile length of 28' above the assumed "fixity" point. The response of the substructure for each case is given below.

In the case of Hurricane Frederic, the total loads acting on the superstructure as calculated in Section 5.4 were as follows:

$$F_v = 109.1 \text{ kips}$$
$$F_h = 0.0 \text{ kips}$$
$$M = 1172.8 \text{ kip-ft}$$

These loads are then imparted onto the substructure as show in Figure 5.10.

As for the cases of Hurricane Katrina and Mock-Hurricane Katrina, the total loads acting on the superstructure calculated in Section 5.4 were:

Hurricane Katrina	Mock-Hurricane Katrina
$F_v = 171.7$ kips	$F_v = 536.6$ kips
$F_h = 0.0$ kips	$F_h = 169.2$ kips
$M = 1845.8$ kip-ft	$M = 5768.8$ kip-ft

The net loads imparted on the substructure from the superstructure can be seen in Figures 5.11 and 5.12 respectively.

SPAN DEAD LOAD

108k 108k 108k 108k 108k

+

SPAN WAVE LOAD

26k 13k 13k 26k DUE TO MOMENT
OF 1172.8 K-FT

21.8k 21.8k 21.8k 21.8k 21.8k DUE TO UPLIFT
OF 109.1 K

||

SPAN DEAD + WAVE LOAD

112.2k 99.2k 86.2k 73.2k 60.2k
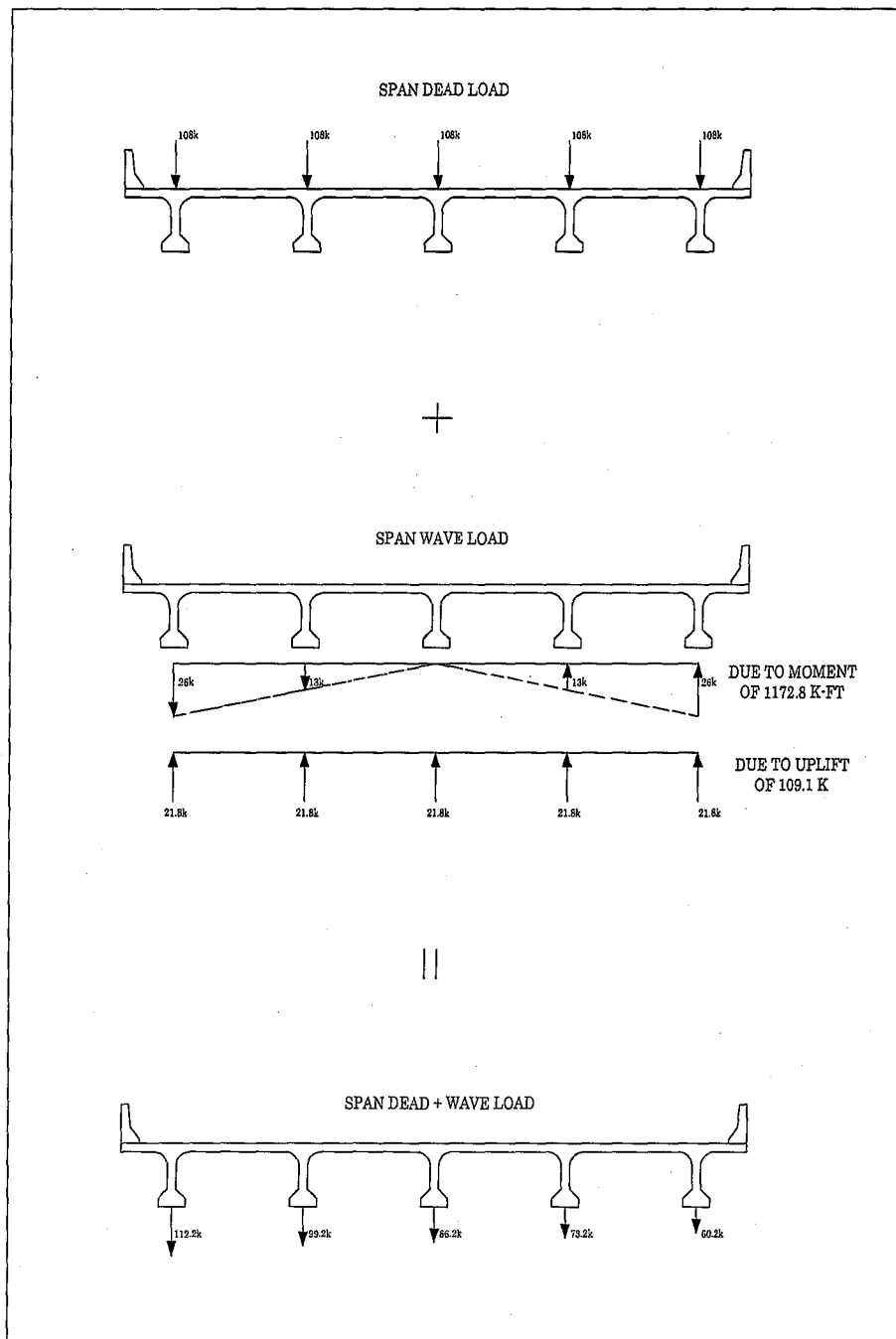
Figure 5.10   Substructure Loading Due to Hurricane Frederic, Case A

SPAN DEAD LOAD

108k   108k   108k   108k   108k

+

SPAN WAVE LOAD

41k   30.5k   20.5k   41k   DUE TO MOMENT OF 1845.8 K-FT

DUE TO UPLIFT OF 171.7 K

34.3k   34.3k   34.3k   34.3k   34.3k

||

SPAN DEAD + WAVE LOAD

114.7k   94.2k   73.7k   53.2k   32.7k
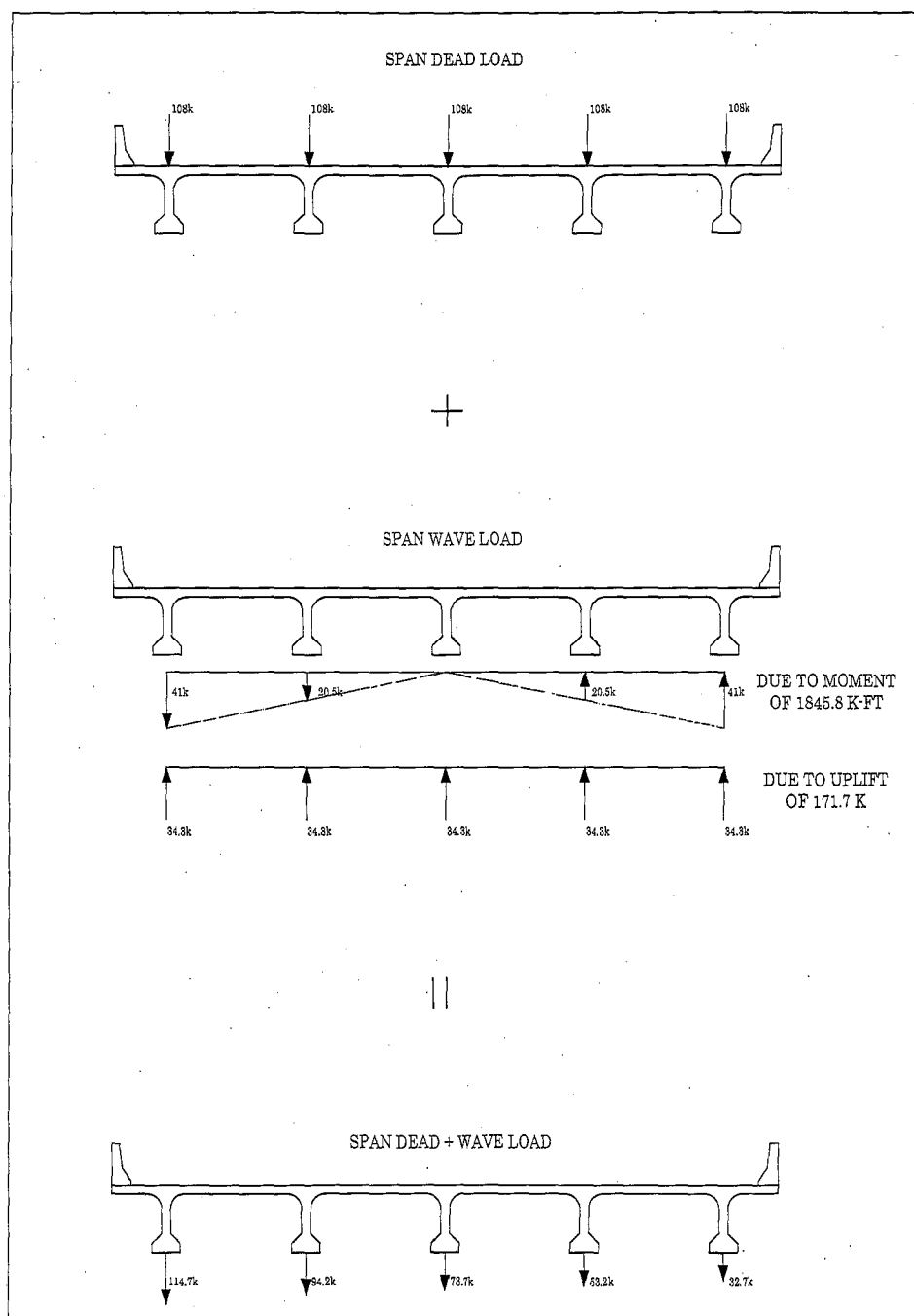
Figure 5.11   Substructure Loading Due to Hurricane Katrina, Case B

SPAN DEAD LOAD

108k   108k   108k   108k   108k

+

SPAN WAVE LOAD

33.8k   33.8k   33.8k   33.8k   33.8k   DUE TO LATERAL FORCE
                                            OF 169.2 K-FT

128k   64k   64k   128k   DUE TO MOMENT
                                        OF 5768.8 K-FT

DUE TO UPLIFT
OF 536.6 K

107.3k   107.3k   107.3k   107.3k   107.3k

||

SPAN DEAD + WAVE LOAD

33.8k   33.8k   33.8k   33.8k   33.8k

128.7k   64.7k   0.7k   63.3k   127.3k
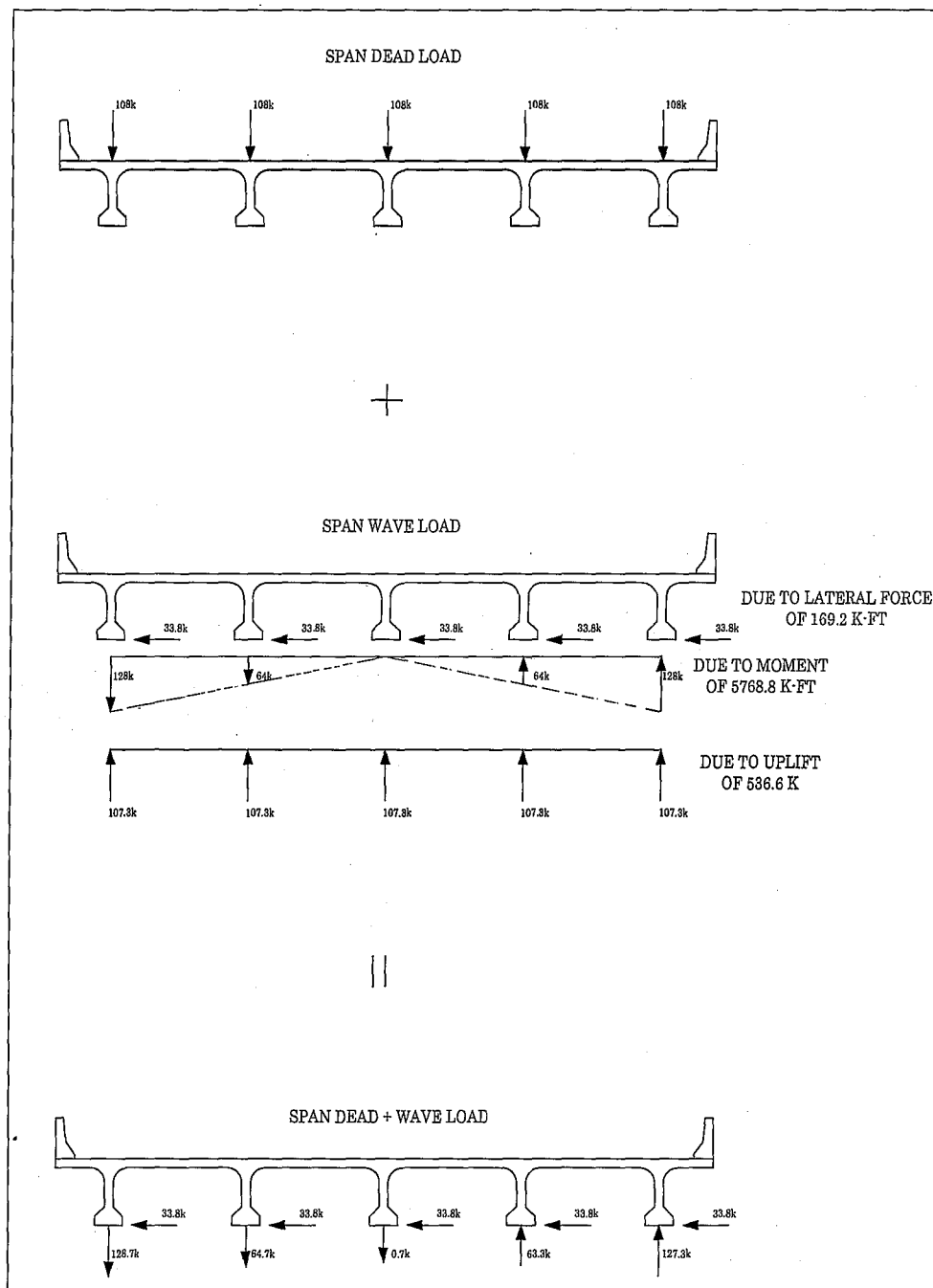
Figure 5.12   Substructure Loading Due to Mock-Hurricane Katrina, Case C

5-24

The maximum unfactored moment in the pile cap for the Hurricane Frederic load case was determined to be 759.6 kip-feet. This value is much less than the moment capacity of 2668.4 kip-feet, and therefore there should be no moment failure of the pile cap. The maximum unfactored moment and minimum axial force acting on the piles was calculated to be 42.4 kip-feet and 224 kips respectively. This corresponds to a maximum bending stress of 51.9 psi and compressive stress of 247 psi. Summing these values with their respective signs with the compressive stress of 862 psi yields compressive stresses of ≈ 1161 psi on the compressive face and ≈ 1057 psi on what would be the tensile face but this face would remain in compression throughout the storm event. The ultimate moment capacity of the piles, calculated to be 2263.8 kip-ft, far exceeds the demand of 42.4 kip-ft. These effects are consistent with the assessment that there was no damage to the I-10 Bridge substructure during Hurricane Frederic.

The maximum unfactored moment in the pile cap for the Hurricane Katrina case was determined to be 774.6 kip-feet. This value is much less than the moment capacity of 2668.4 kip-feet; therefore there should be no moment failure of the pile cap. The maximum unfactored moment and minimum axial force acting on the piles was calculated to be 65.6 kip-feet and 165.9 kips respectively. This corresponds to a maximum bending stress of 80.3 psi and compressive stress of 183 psi. Summing these values with their respective signs with the compressive stress of 862 psi yields compressive stresses of ≈ 1126 psi on the compressive face and ≈ 966 psi on what would be the tensile face but this face would remain in compression throughout the storm event. The ultimate moment capacity of the piles, calculated to be 2263.8 kip-ft,

far exceeds the demand of 65.6 kip-ft. Again, these effects are consistent with the assessment that there was no damage to the I-10 Bridge substructure during Hurricane Katrina.

For the Mock-Katrina scenario, the maximum unfactored moment in the pile cap for this case was determined to be 1642.2 kip-feet. This value is also less than the moment capacity of 2668.4 kip-feet and therefore there should be no moment failure of the pile cap. The maximum unfactored moment and minimum axial force acting on the piles were calculated to be 1629.8 kip-feet and 246.9 kips uplift respectively. This corresponds to a maximum bending stress of 1994 psi and tensile stress of 273.2 psi. Summing these values with their respective signs with the compressive stress of 862 psi yields compressive stresses of $\approx$ 2583 psi on the compressive face and $\approx$1405 psi on the tensile face. This tensile stress far exceeds the upper limit of $12\sqrt{f_c}$ (849 psi) for Class C prestressed concrete in ACI 318-05 Section 18.3.3. However, the ultimate moment capacity of the piles, calculated to be 2263.8 kip-ft, exceeds the moment demand of 1629.8 kip-ft. In this case, the pile would be predicted to crack but not to fail structurally. The cracking would allow saltwater to reach the strands, but this one-time exposure should not create a corrosion problem.

5.6   Closure

When using the storm surge and wave height elevations given in Chapter 4, the Modified Douglass Equations were used to calculate the anticipated hurricane surge/surface wave forces on the I-10 Mobile Bay Bridge. The surge elevations were taken from post-hurricane records, and the significant wave height was estimated based

on a study done by OEA based on Hurricane Ivan's landfall near Pensacola, FL. It was

decided to use 7.0' as this wave height for Case A and Case B based on the similarities

between the Pensacola Bay Bridge site and the I-10 Mobile Bay Bridge site and the

intensities of both hurricanes at landfall. The significant wave height for Case C was

taken as 8.8' using the surge/wave height analysis performed by Douglass et al. for the

Biloxi Bay Bridge site during Hurricane Katrina on August 29th, 2005. These criteria

were used in the Modified Douglass Equations, and the following vertical, horizontal,

and moment loadings were calculated for each of the three cases:

Case A – Hurricane Frederic
$$F_v = 109 \text{ kips}$$
$$F_h = 0.0 \text{ kips}$$
$$M = 1173 \text{ kip-ft}$$

Case B – Hurricane Katrina
$$F_v = 172 \text{ kips}$$
$$F_h = 0.0 \text{ kips}$$
$$M = 1846 \text{ kip-ft}$$

Case C – Mock-Hurricane Katrina
$$F_v = 537 \text{ kips}$$
$$F_h = 169 \text{ kips}$$
$$M = 5769 \text{ kip-ft}$$

These loadings were then used to evaluate the response of the superstructure

alone, as well as the response of the superstructure/substructure acting monolithically

to these applied uplift, lateral, and moment forces. The net loads acting on the structure

were analyzed using two RISA-2D models and these results were compared to the

flexural analysis of the capacity of both the pile cap and the piles. The analyses results

were as follows:

Hurricane Frederic, Case A:

Pile Cap Flexural Capacity –	2668 kip-ft.
Pile Flexural Capacity –	2264 kip-ft.
Maximum Flexural Demand on Pile Cap –	760 kip-ft.
Maximum Flexural Demand on Pile –	42.4 kip-ft.
Maximum Stress on Pile –	1161 psi (Compression)
	1057 psi (Compression)
Pile Bent Poststorm Status -	Good
Superstructure Adequacy -	Good
Super-to-Substructure Connections -	Good

Hurricane Katrina, Case B:

Pile Cap Flexural Capacity –	2668 kip-ft.
Pile Flexural Capacity –	2264 kip-ft.
Maximum Flexural Demand on Pile Cap –	775 kip-ft.
Maximum Flexural Demand on Pile –	65.6 kip-ft.
Maximum Stress on Pile –	1126 psi (Compression)
	966 psi (Compression)
Pile Bent Poststorm Status -	Good
Superstructure Adequacy -	Good
Super-to-Substructure Connections -	Good

Mock-Hurricane Katrina, Case C:

Pile Cap Flexural Capacity –	2668 kip-ft.
Pile Flexural Capacity –	2264 kip-ft.
Maximum Flexural Demand on Pile Cap –	1642 kip-ft.
Maximum Flexural Demand on Pile –	1630 kip-ft.
Maximum Stress on Pile –	2583 psi (Compression) 1405 psi (Tension)
Pile Bent Poststorm Status -	Piles crack during storm but are capable of supporting loads and cracks are closed by prestressing forces after the storm event.
Superstructure Adequacy -	Good
Super-to-Substructure Connections -	Not adequate. Connections need to be improved.

6. RETROFIT OPTIONS/ACTIONS FOR MOBILE BAY I-10 BRIDGE

6.1 General

Since retrofitting is simply modifying an original design to enhance its performance, original and retrofit design philosophies, priorities and actions are very closely related. For coastal bridges, appropriate and recently recognized and widely being accepted design and/or retrofit priorities are as follows:

1. Do not allow bridge substructure components to fail or to be significantly damaged, i.e., damaged to a level of requiring after-the-storm strengthening or replacement.

2. Do not allow bridge superstructure to become disconnected from the substructure. Note, the superstructure may have some limited movement relative to the substructure.

3. Minimize the number of bridge superstructure spans requiring significant after-the-storm repairs and thus minimize after-the-storm lane closure time.

When retrofitting an existing coastal bridge to improve its performance during major hurricane events, an effective philosophy appears to be to retrofit to simultaneously achieve the following:

1. a reduced level of surge/surface wave forces on a span and/or on a support bent,

2. a distribution of some of the reduced surge/surface wave forces on a span to adjacent bridge spans and bents,

3. superstructure-to-substructure connections which can yield/move/sustain damage, but not fail, and thus not allow the bridge superstructure to slip off or be dumped into the bay/ocean.

Specific design and retrofit actions to meet the above priorities and design philosophies for coastal bridges are presented in the following sections.

6.2   Typical Deck-Girder Coastal Bridge Design/Retrofit Options

Design actions to render new coastal bridges adequate or safe for the high storm surge/surface waves associated with strong hurricanes (Category 4 and 5 hurricanes) should be as follows:

1. Elevate the superstructure so that storm peak surge level and surface waves do not impinge on the superstructure.

2. Near bridge ends, if highway grade elevations do not allow (1) above, have bridge end span cross-section geometry be such that air cannot get entrapped on the underside, and ensure that the "aerodynamics" of the end span cross-section geometry be such that minimal uplift and horizontal forces will be developed from the storm surge/surface waves.

3. If (1) cannot be accomplished, then design all of the superstructure in the manner of (2) above.

4. If (1) cannot be accomplished, then make the bridge superstructure continuous for horizontal and vertical (downward and upward) loads in the regions where storm peak surge/surface waves do impinge on the superstructure.

5. If (1) cannot be accomplished, then design the bridge barrier rails to be open rails, or be open in the regions where waves can impinge on the superstructure.

6. If (1) and/or (2) and (3) cannot be accomplished, then design adequate venting in all regions of the superstructure where air could possibly get entrapped.

7. If (1) cannot be accomplished, then design the superstructure-to-substructure connections to safely transmit the storm surge/surface wave forces.

8. If (1) cannot be accomplished, then design the bridge substructure to safely transmit the forces coming from the superstructure down to the supporting soil.

Design actions to <u>retrofit existing coastal bridges</u> where storm surge/surface wave elevations do impinge on the superstructure, such as the I-10 Twin Bridges over Mobile Bay, to make them more resistant to the surge/surface waves of major hurricanes coming ashore, should be enacted as follows:

1. Vent the superstructure wherever air can get entrapped on the underside. Especially vent the region under the deck overhang on the seaward side via additional grated scupper openings, and the region in the most seaward girder-deck-girder cell.

2. Make the superstructure continuous for horizontal and vertical upward surge/surface wave forces via installation of $3"^{\phi}$ shear pins in the span end diaphragms.

3. Connect superstructure to substructure in a positive manner via a combination of shear blocks, shear pins and strapping/cable tie-downs that will allow very limited superstructure movement and good connection ductility and energy absorption capacity. The positive connection needs to have adequate force capacity to transmit the calculated "sustained wave forces", where sustained means 1 - 2 seconds or greater duration. The connection needs to also be able to transmit short duration (0.1 – 0.5 secs) forces or slamming forces at a diminished level via allowing some small relative movements between the super and substructures. This movement will allow energy dissipation, but it should not be a progressive movement.

4.   Verify that the force capacity of the coastal bridge substructure can safely withstand the maximum "sustained wave forces" coming from the bridge superstructure. Slamming forces applied to the superstructure do not need to be considered in checking the substructure, as they are of very short duration, and energy dissipation in the superstructure, the super-to-substructure connection, and in the substructure, will be sufficient to render these forces harmless to the substructure. If the substructure does not have adequate force capacity, then modify the superstructure to reduce the maximum forces going to the substructure, or strengthen the substructure.

Some interesting observations made when Hurricane Katrina hit New Orleans in August 2005 regarding some of the above actions were made in Ref [8] and are presented below.

- At the Lake Pontchartrain Bridge in Louisiana, 14,000 feet of parapet were broken off. This suggest that the use of a sacrificial parapet that would respond inward in a sacrificial manner, while still providing the proper traffic barrier resistance outward, could reduce the amount of area exposed to the waves. This would also promote inundation which reduces the total wave uplift force to be resisted.

- Calculated estimates of the effect on entrapped air on the vertical wave forces on the Lake Pontchartrain I-10 Bridge and the Escambia Bay I-10 Bridge in Florida have shown that the vertical force can be substantially reduced if the amount of air entrapped between the

girders can be reduced. Calculations based on venting the cavities formed by girders and diaphragms on selected spans from those two bridges indicated that it was not practical to drill deck holes to vent air entrapped by waves. The use of large holes in concrete diaphragms, framed cross-frames and end diaphragms, or concrete partial depth diaphragms can create large openings which can be effective in venting entrapped air and in allowing the exchange of trapped air between spans. Figure 6.1 shows the area of opening necessary to permit evacuation of a volume of air in one second, a time period short enough to represent wave attack. It should be noted that air venting equations and figures developed by the authors for use in determining underneath-bridge venting requirements are given in Appendix A.

- Continuous superstructures appear to have benefits due to the three-dimensionality of the waves, because storm waves have finite crest lengths, and the chance of multiple spans being struck by design size waves at the same time is small. Thus, the ability of the structure to resist vertical and horizontal forces are increased through continuous spans.

- The use of slab bridges may be especially appropriate for those spans that cannot be raised sufficiently to avoid wave forces, such as those near the ends of bridges which have grade constraints.
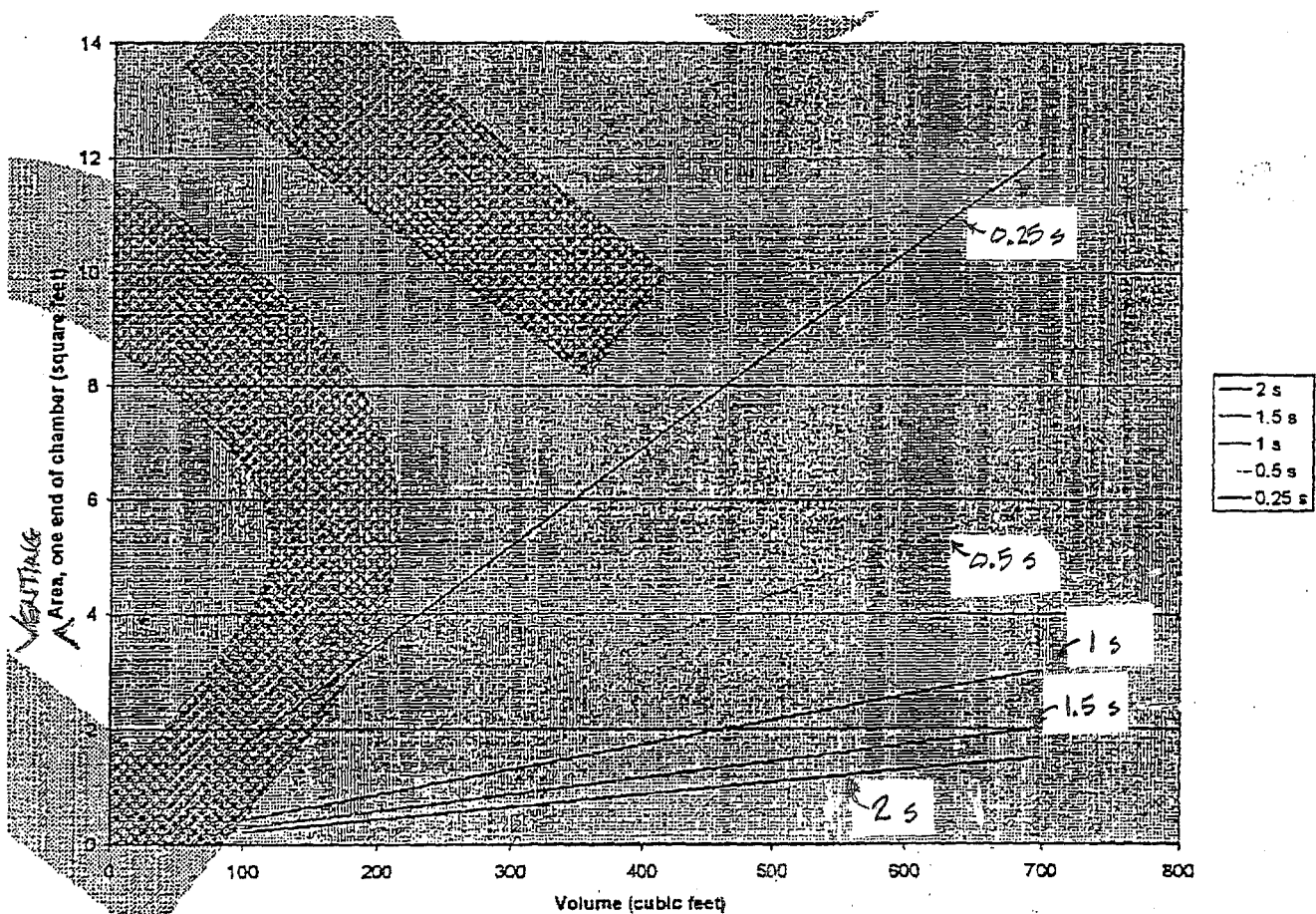
Fig. 6.1 Venting Area Required for Escape of Air of a Given Volume [Ref. (14)]

The AASHTO/FHWA and ten coastal state DOT's have an ongoing Pooled Fund

Research Project underway entitled "Development of Guide Specifications for Bridges

Vulnerable to Coastal Storms and Handbook of Retrofit Options for Bridges Vulnerable

to Coastal Storms" [14]. The project contractor is Modjeski and Masters, Inc., and at

this time it appears that they have identified 30 – 40 retrofit options for coastal bridges.

Some of the options would not be applicable to the I-10 Bridges over Mobile Bay, and

some, while applicable, are not too attractive. The most viable and attractive options for

the I-10 Mobile Bay Bridges are actions to

1. reduce buoyancy forces resulting from high peak storm surge elevations being higher than the bottom of span girder elevations, and from storm surface waves impinging on the bridge superstructure,

2. reduce surface wave hydrodynamic forces on the bridge superstructure,

3. reduce wave uplift forces on bridge super-to-substructure connections and on the bridge substructure components via connection of simply supported spans to adjacent spans,

4. increase DL resisting forces of bridge super and substructure via connection of simply supported spans to adjacent spans,

5. increase the vertical holdown and lateral force capacity of super-to-substructure connections, and

6. increase the ductility, control the limits of relative movement, and maintain the connectivity of bridge super-to-substructure connections.

These options are briefly summarized in Figs. 6.2 – 6.8 below:
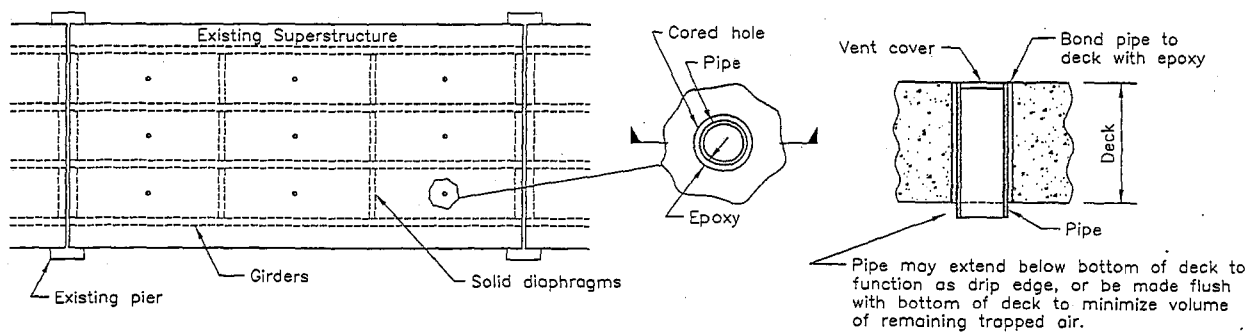
a. Cored Deck Vents
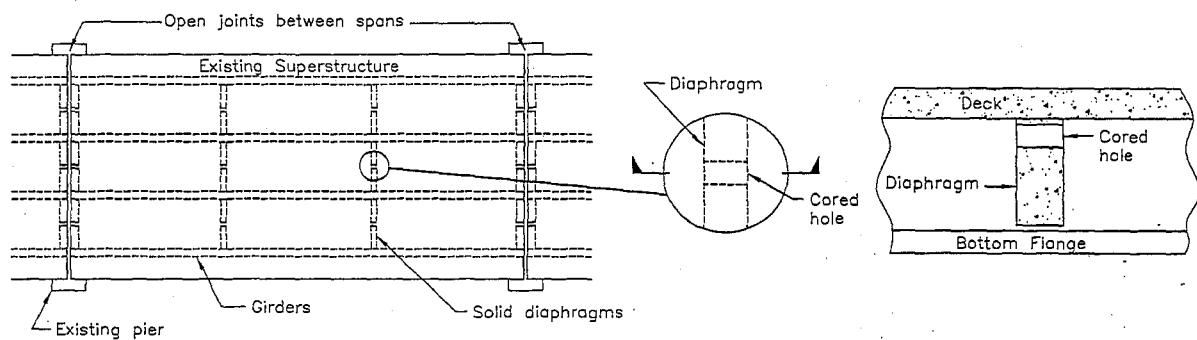
b. Diaphragm Vents
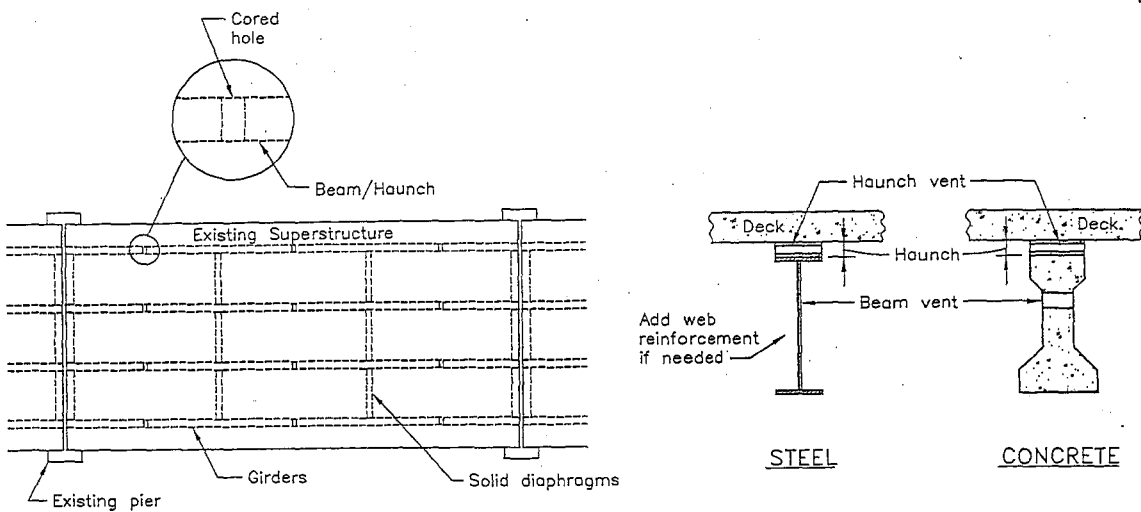
c. Girder/Haunch Vents

Fig. 6.2 Retrofit Actions to Reduce Buoyancy Forces on Superstructure-Venting
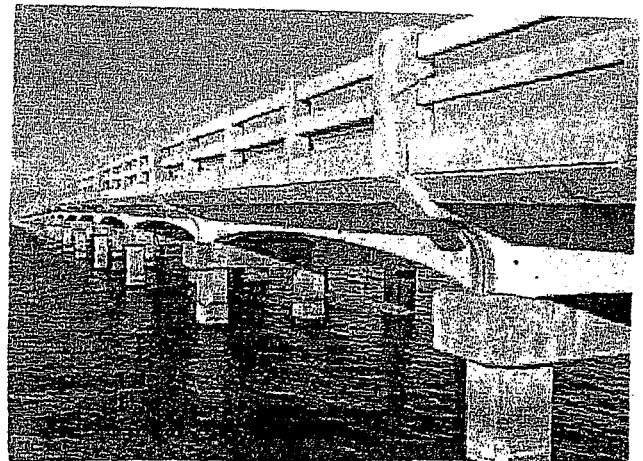
a. Replace Solid Barrier with Open Barrier (Photos not in Modjeski and Masters Report)

Fully developed reinforcement
provided from barrier to deck
on inside face of barrier

Reinforcement not
provided from barrier
into deck on outside
face of barrier

Construction joint
(smooth or rough as required)

Bolt on inside
face of barrier
transmits tension

Zero gap

Shear block
if required

Bolt on outside
face of barrier
does not transmit
tension

Use through bolts for
retrofits or where bolt
replacement may be required

Precast Jersey
barrier

Zero gap

Alternate
shear block
detail

Use J—bolt on new
construction where
bolt replacement
is not anticipated

b. Break-Away Barrier

Shield plate
(fasten to superstructure)

Brace as needed to prevent
damage of the shield under
wave loads

c. Overhang Shield

Fig. 6.3 Retrofit Actions to Reduce Wave Forces on Superstructure

Drilled hole
(chip concrete typ.)

Splice

Deck

Girder bottom flange

Cable

Drilled hole

NOTE: Place neoprene sponge between
ends of beams to minimize spalling when
contact is made, if desired
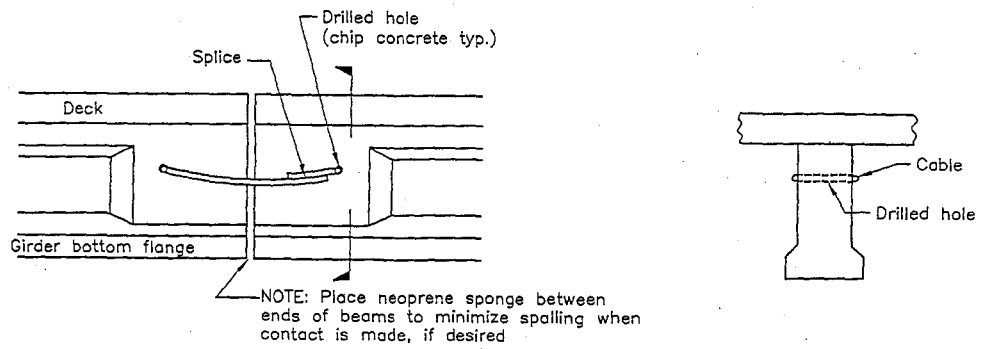
a. Girder to Girder Cable Ties

Girder

Deck

Steel plate
fastened with
expansion anchors

Girder bottom flange

End diaphragm

Concrete filled
steel pipe

Cored hole

NOTE: Place neoprene sponge between ends of beams
to minimize spalling if contact is made, if desired.
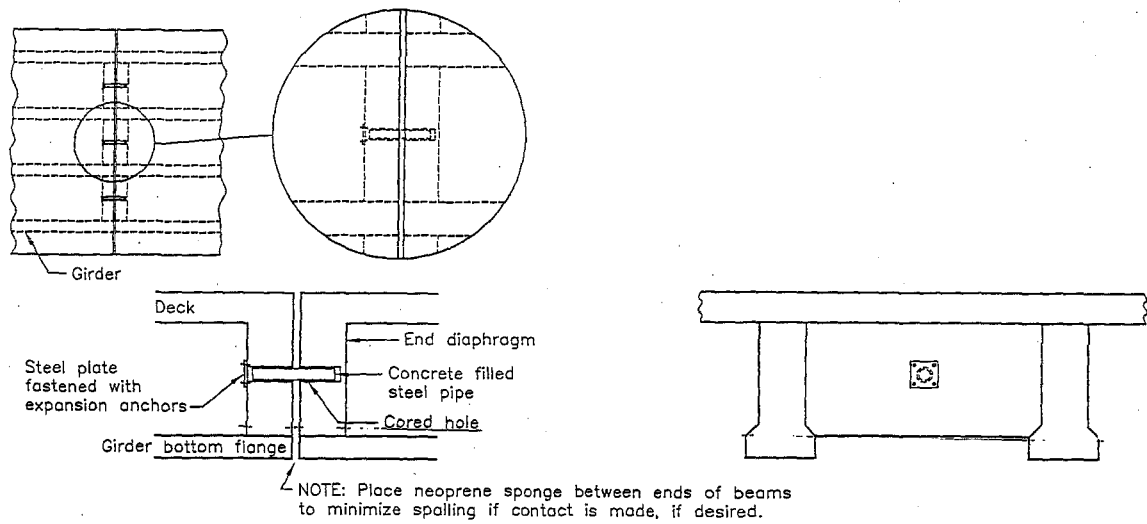
b. End Diaphragm Shear Pins

Slotted holes permit free expansion
and rotation under normal conditions

NOTE: Place neoprene sponge between
ends of beams to minimize spalling if
contact is made, if desired

STEEL WEB PLATE ELEVATION

PLATES ON BOTH
SIDES OF BEAM
(No end diaphragms)

PLATES ON ONE
SIDE OF BEAM
(Facia beams with end diaphragms)
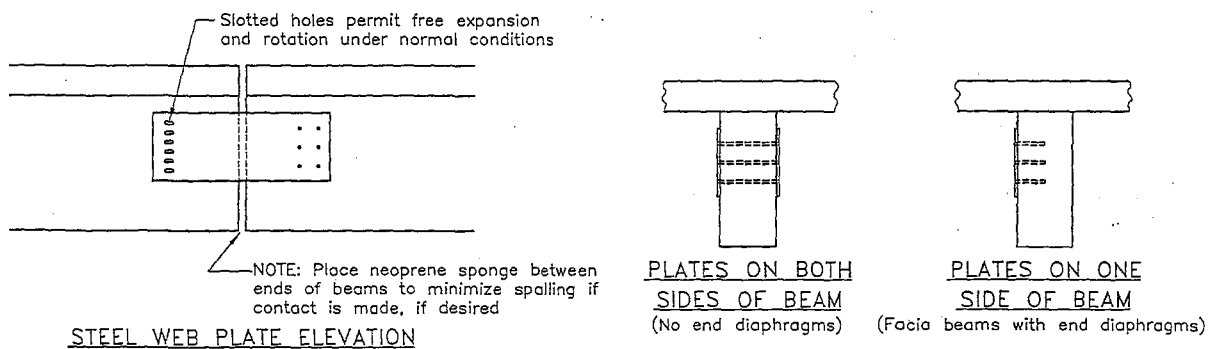
c. Girder Steel Web Plates

**Fig. 6.4   Retrofit Actions to Reduce Forces on Super-to-Sub Connections and on
Bents – Tie SS Spans Together**

6-11

Modify existing end
diaphragms as needed
to facilitate shear
block installation and
air venting

New
shear block

New
shear block

Existing
pier cap

Dowels or U—bars drilled and grouted
or drilled and swedged, verify constructibility
in confined area

Existing
pier cap

Fasten with nuts
and washers or
nuts and plates

Dowels or U—bars
placed in holes drilled
through pier cap

a. Low-Shear Blocks

Appropriate corbel reinforcing
as needed (typ.)

Neoprene sheet (typ.)

Modify existing end
diaphragms as needed
to facilitate shear
block installation and
air venting

New
shear block

New
shear block

Existing
pier cap

Dowels drilled and grouted or drilled and
swedged, verify constructibility in confined area

Existing
pier cap

Fasten with nuts
and washers or
nuts and plates

Dowels placed in holes
drilled through pier cap

b. High Shear Blocks with Protrusions

Modify existing end
diaphragms as needed
to facilitate shear
block installation
and air venting

Taper faces slightly to reduce binding
of the superstructure during uplift

New shear
block

New
shear block

Dowels placed
in holes drilled
through pile cap

Existing
pier cap

Dowels drilled and grouted or drilled and swedged,
verify constructability in confined area

Existing
pier cap

Fasten with nuts and
washers or nuts and plates

c. High Shear Blocks without Protrusions

Fig. 6.5   Retrofit Actions to Improve Bridge Span-to-Bent Connections Via Concrete Shear Blocks

a. Concrete Shear Blocks with Steel Hold-Downs
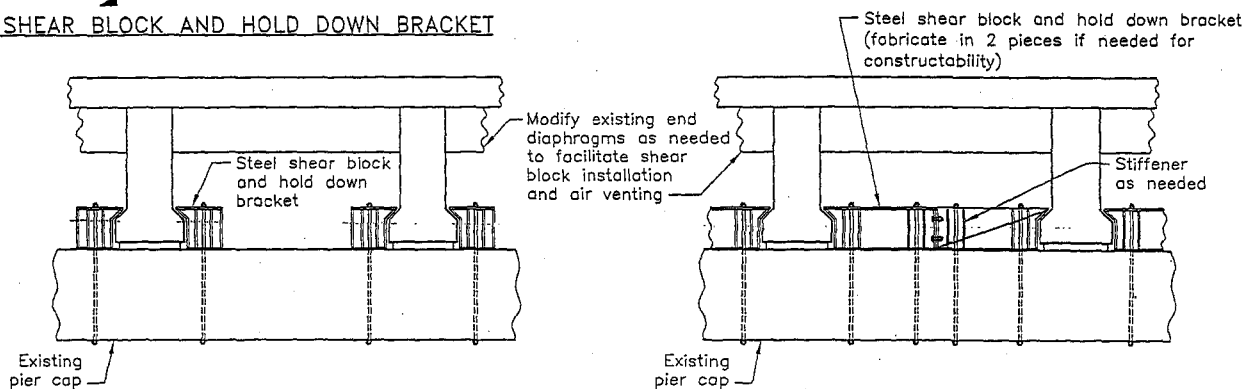
b. Steel Shear Blocks and Hold-Downs
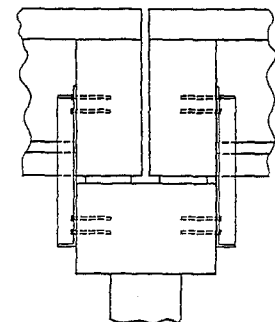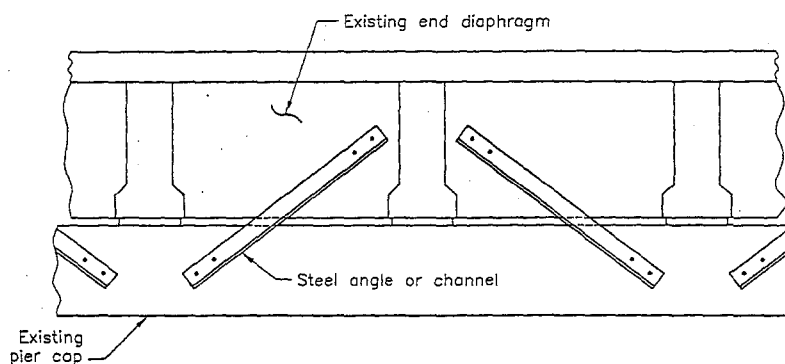
c. Steel Angles/Channels

Fig. 6.6 Retrofit Actions to Improve Bridge Span-to-Bent Connections Via Steel Shear Blocks and Angles

a. Steel Bars

CONCRETE   STEEL
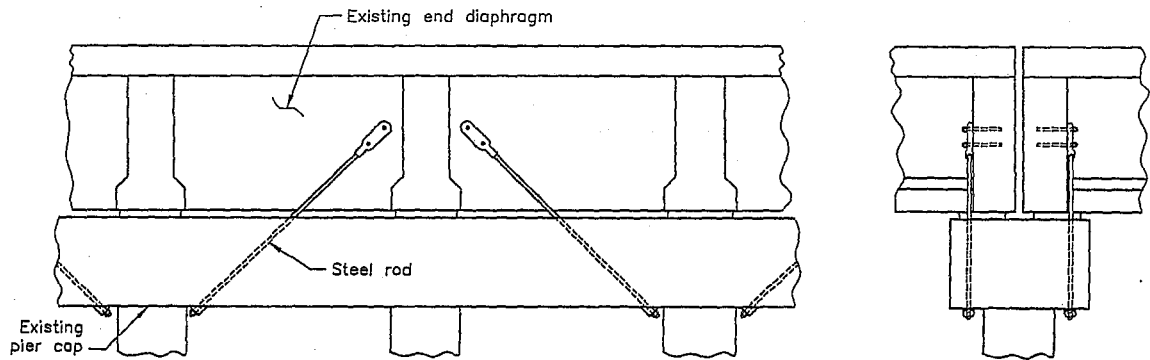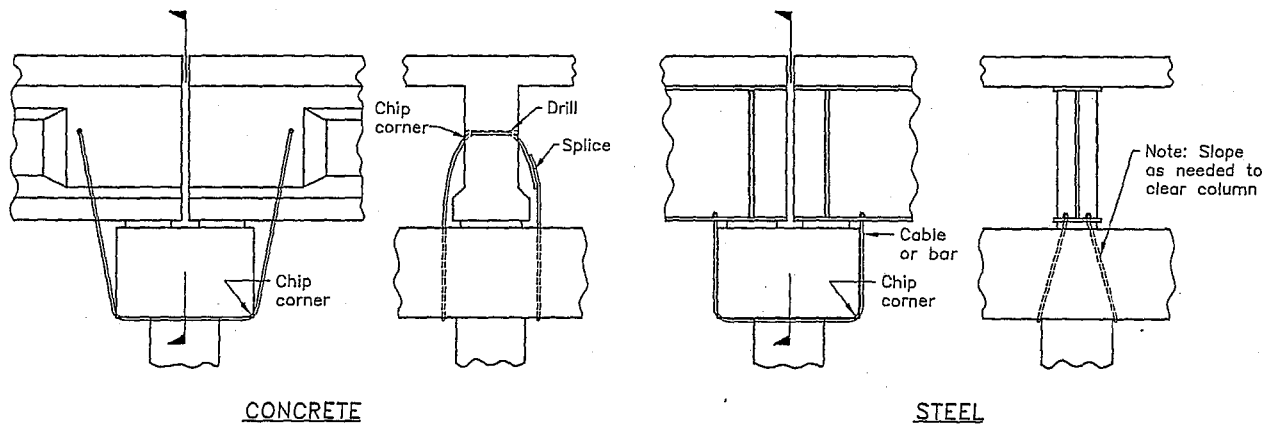
b. Straps or Cables Through Girders
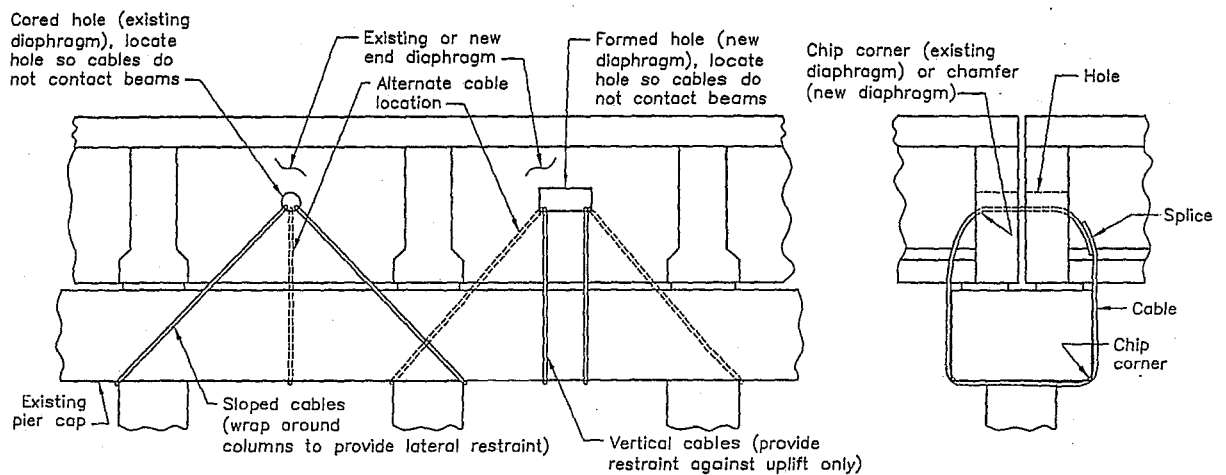
c. Straps or Cables Through Diaphragms

Fig. 6.7 Retrofit Actions to Improve Bridge Span-to-Bent Connections Via Steel Bars, Cables, Straps
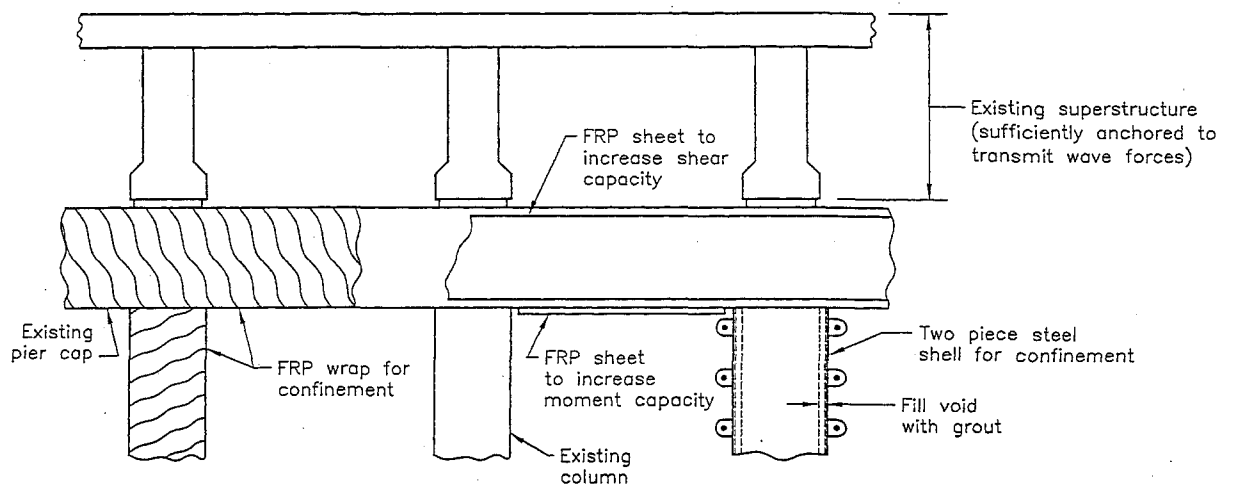
a. Strengthen Pile Bent Components
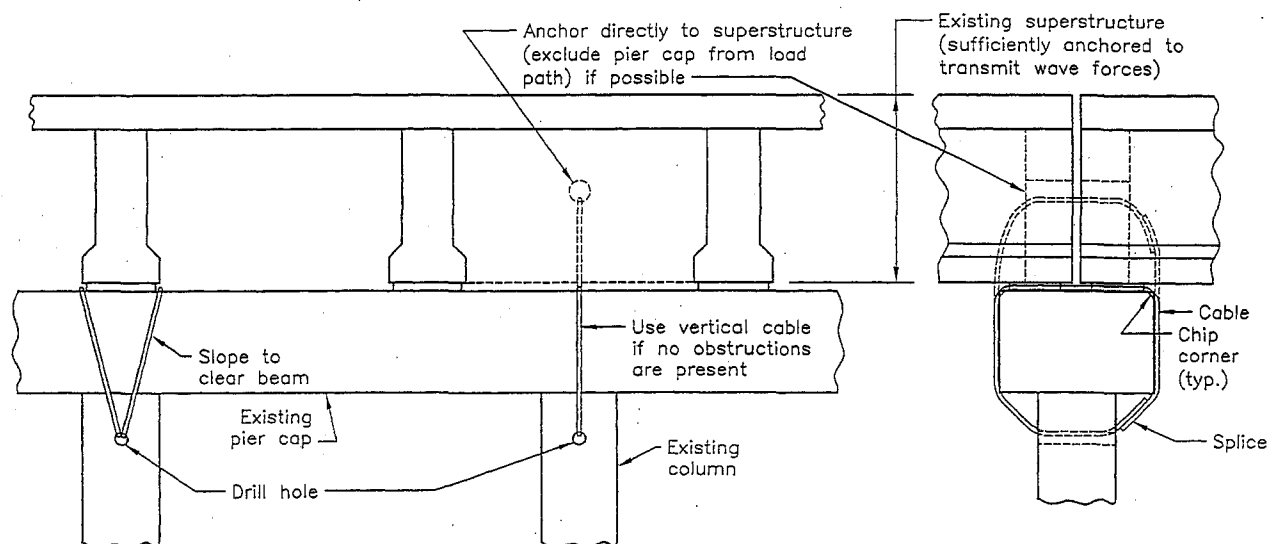
b. Strengthen Cap-to-Pile Connection or Anchor Superstructure Directly to Piles

Fig. 6.8   Retrofit Actions to Strengthen Existing Substructure Via Strengthening Pile Cap/Top of Pile/Pile-to-Cap Connection

6-15

6.3   Viable Retrofit Options for I-10 Twin Bridges Over Mobile Bay

Listed below are retrofit options that the authors feel are the most viable, practical, and effective for initial consideration for use on the I-10 twin bridges over Mobile Bay. These are the options that the authors initially identified as the most viable, and that should be examined more closely to estimate their bridge performance benefits, ease/difficulty in implementing, and costs, if it is later determined that major retrofitting of the I-10 Twin Bridges is needed. The final recommended retrofit actions for the I-10 Bridges are presented in Chapter 7.

Retrofit options:

- Selective weakening of Jersey barriers on seaward side to have them fail inward under high wave loadings. This will reduce the vertical projection of the bridge and thus the horizontal forces, and it will allow water to spill onto the deck and will reduce the vertical buoyant forces.

- Improve venting of underneath regions of bridge superstructure to reduce buoyant forces. Do this via selective deck coring and the creation of large holes in span end diaphragms to allow exchange of trapped air between spans (see Fig. 6.9).

- Use large grated scupper opening on the seaward deck edge (even if water drainage is on the other edge of deck) to allow enhanced venting of deck overhang portion of bridge (see Fig. 6.9). Note that this region is almost self-venting in the longitudinal direction.

- Install two solid shear pins in span end diaphragms (probably two 3"ϕ pins per diaphragm) to render the bridge continuous for wave uplift and lateral forces to increase the reactive force capacity of individual spans (see Fig. 6.9 – Section A).

- Install span connection plates and/or angle irons as shown in Figs. 6.10 and 6.11 to render the bridge continuous for wave uplift and lateral forces and thereby increase the reactive force capacity of individual spans and reduce the maximum forces on span-to-bent cap connections and on a given bridge bent.

- Install cable ties as indicated in Fig. 6.12, tying span ends to the bent cap as a belt-and-suspenders philosophy, along with shear pins, to provide greater ductility and energy absorption capacity to the span-to-bent connection.

WAVE ACTION

SECTION A

PLAN VIEW
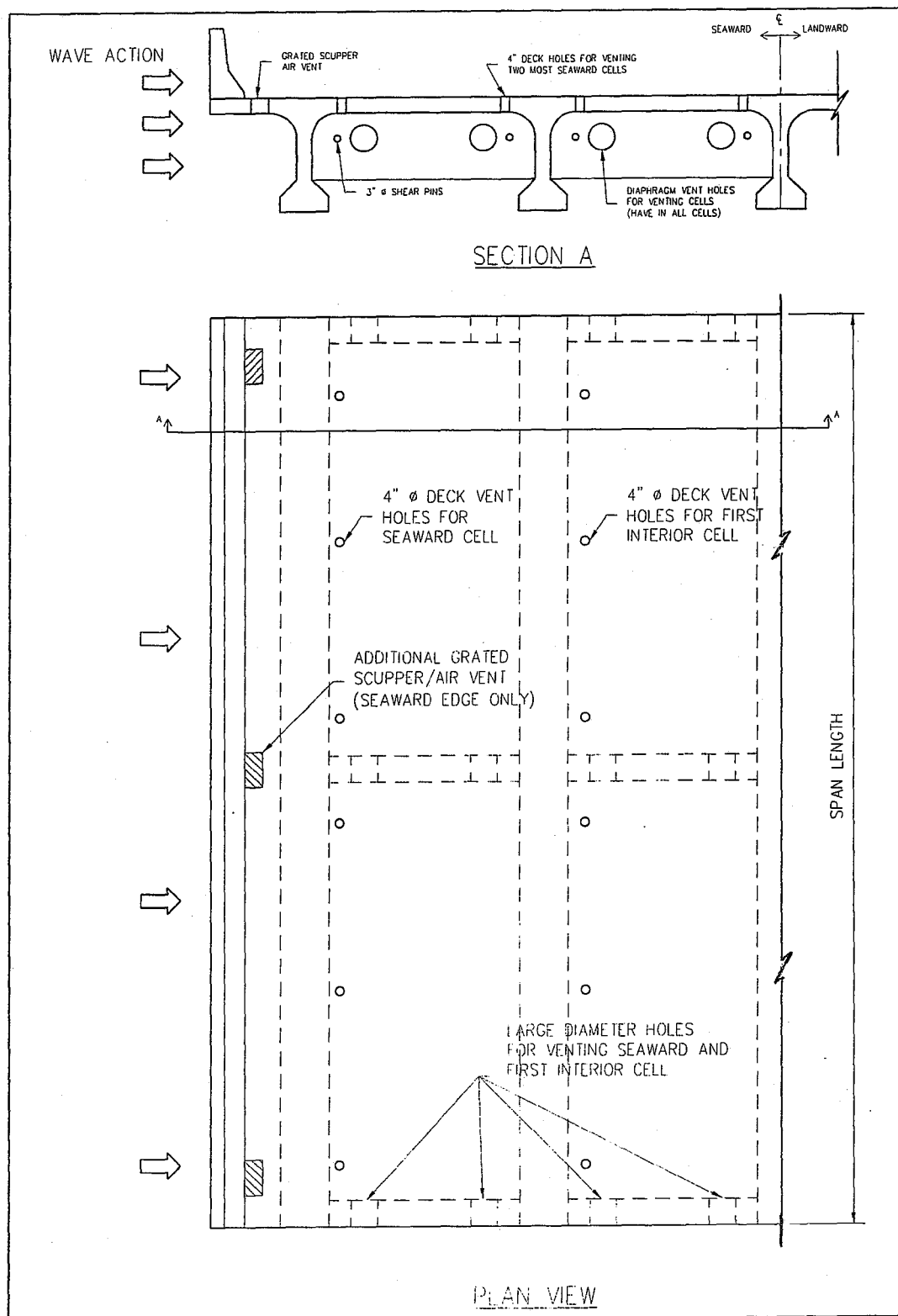
Fig. 6.9 Superstructure Partial Venting Plan to Reduce Buoyant and Slamming Forces

6-18

8"x17"x TAPER THICKNESS
STEEL WEDGE PLATE
EPOXIED ON INSIDE
FACE OF RAIL

JERSEY BARRIER
RAIL

8"X36"X1" STEEL PLATE
EACH FACE OF BARRIER
RAIL, BOLT HOLES SLOTTED
ON ONE SPAN FOR THERMAL
EXPANSION/CONTRACTION

SECTION A

*NOTE – DO THIS FOR BARRIER
RAIL ON EACH SIDE OF BRIDGE

ADJACENT SPANS

DECK

JERSEY
BARRIER
RAIL

TAPERED WEDGE PLATE

8"x36"x1" STEEL PLATE

A

A

PLAN VIEW
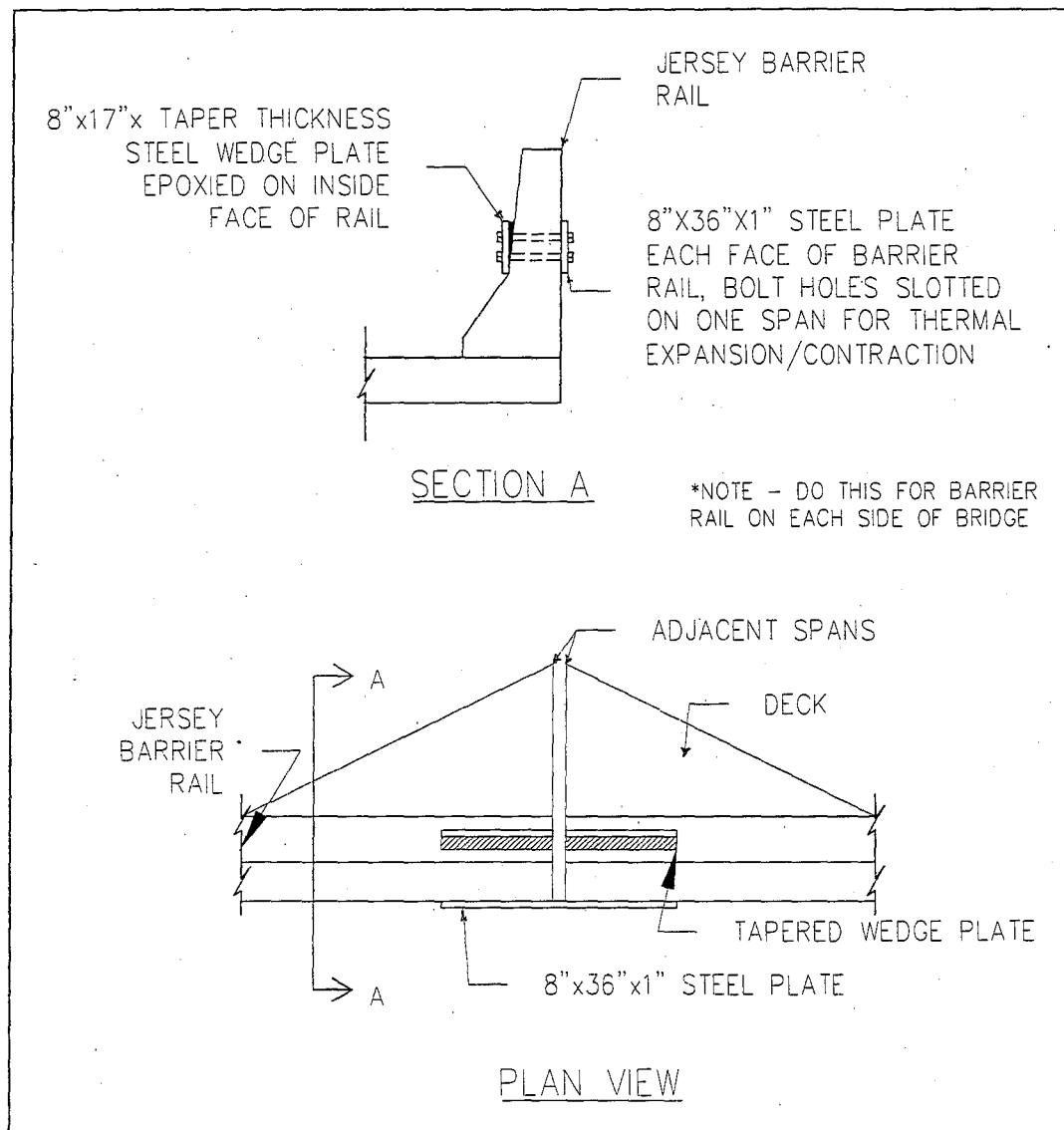
Fig. 6.10   Detail Showing Jersey Barrier Rail Connection to Transmit Vertical and Transverse Shear Forces to Adjacent Spans

6-19

JERSEY BARRIER

L 6"x4"X¾"
WITH BOLT HOLES
SLOTTED ON ONE SPAN

DECK OVERHANG

L 6"x4"X¾"
WITH BOLT HOLES
SLOTTED ON ONE SPAN

ON EACH SIDE OF BRIDGE
EXTERIOR GIRDERS
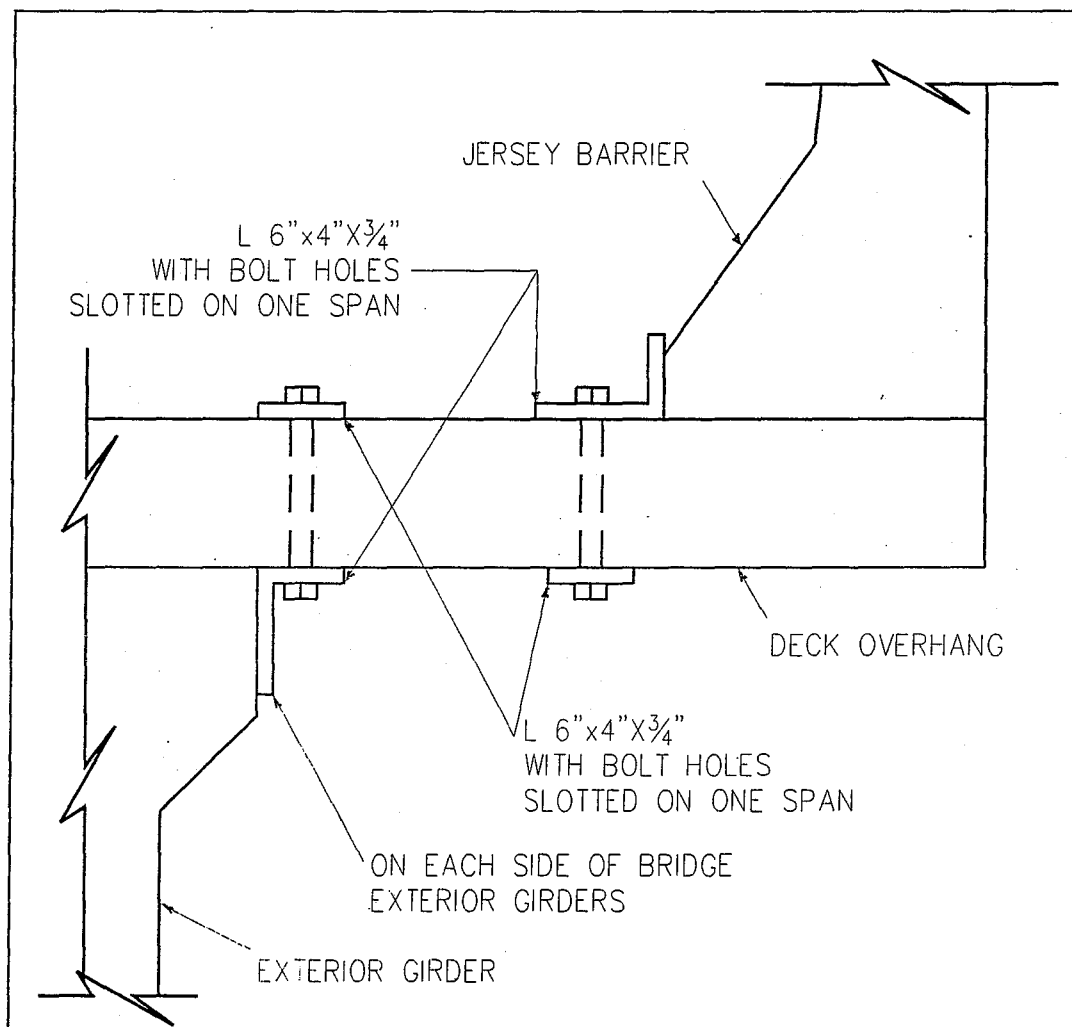
EXTERIOR GIRDER

Fig. 6.11 Partial Section Showing Connecting of Spans at Exterior Girders and
Barrier Rails to Transmit Vertical and Transverse Shear
Forces to Adjacent Span

Cored hole (existing
diaphragm), locate
hole so cables do
not contact beams

Existing or new
end diaphragm

Alternate cable
location

Formed hole (new
diaphragm), locate
hole so cables do
not contact beams

Chip corner (existing
diaphragm) or chamfer
(new diaphragm)

Hole

Splice

Cable

Chip
corner

Existing
pier cap

Sloped cables
(wrap around
columns to provide lateral restraint)

Vertical cables (provide
restraint against uplift only)

**Fig. 6.12 Tie Superstructure to Substructure Via Straps or Cables
Through Diaphragms**
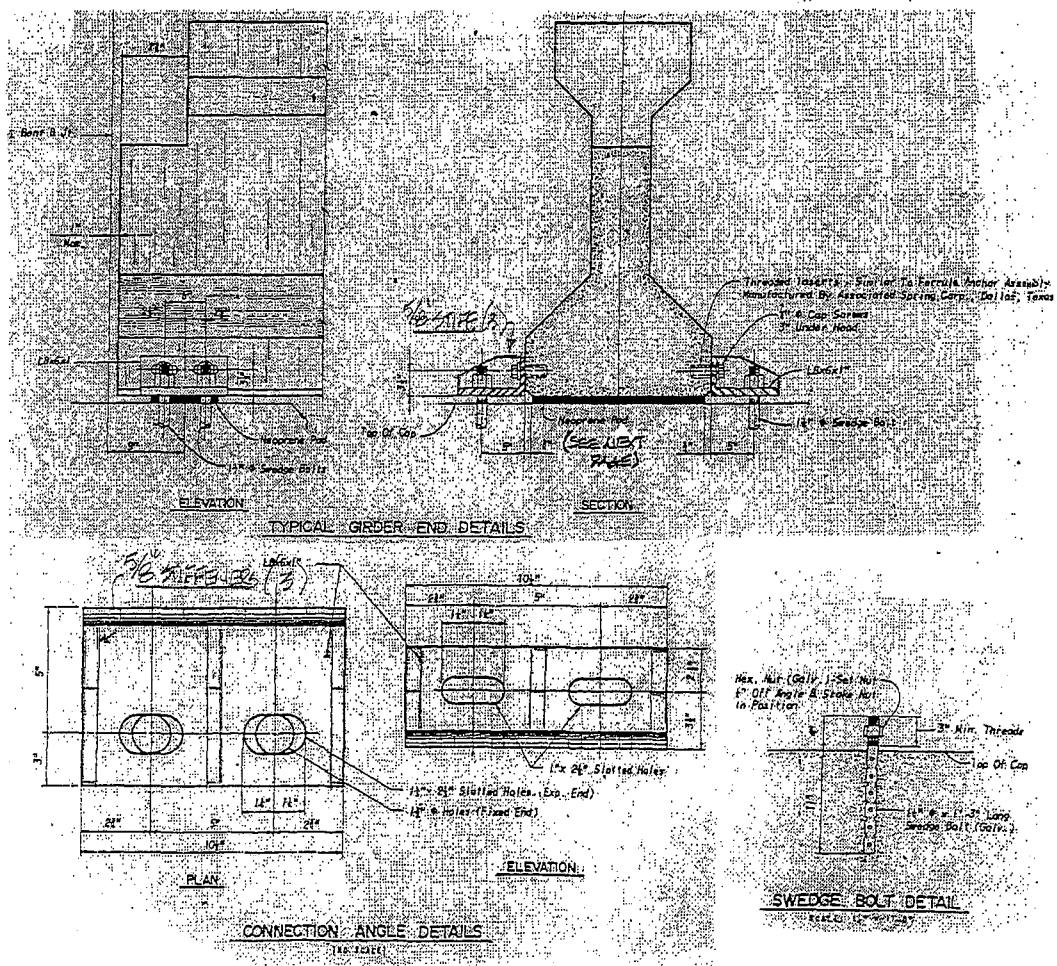
Fig. 6.13 Stiffen Angle Iron connection to Act as Shear Lugs Via Adding Stiffeners

6-21

It should be noted that if ALDOT desires to retrofit the I-10 bridge to resist a

Mock-Katrina Hurricane loading, one only needs to study the photos of Figs. 2.30 and

2.31, which are of a lower elevation Mobile Bay I-10 ramp span after Hurricane Katrina,

to see the inadequacy of the current I-10 span connections, if Katrina had directly hit the

bridge spans. Note in these photos the failure of the girder concrete below the

horizontal cap screws and the bending over of the swedge bolts and connection angle

iron. Thus, for the Mobile Bay I-10 Bridge to survive a direct hit by a Katrina-size

hurricane, the superstructure-to-substructure connection should be strengthened via

a. the addition of stiffened angle iron connections to the second-most
    seaward girder to the bent cap in the same manner as the present
    three girder connections (it may be good to also add connections to
    the second-most landward girder but this is not essential),

b. stiffen the angle iron connections by adding stiffeners as indicated in
    Fig. 6.13, so that they will act as horizontal shear lugs in resisting
    horizontal loading and movement,

c. add two cable ties tying the superstructure end diaphragms to the
    bent cap at each end of each span, as indicated in Fig. 6.12.

6.4   Mount Pole and Bracket Supports for VSE Equipment on I-10 Ramp

Mount video surveillance camera and equipment (VSE) at two select locations on the I-10 bridge ramp at the north end of Mobile Bay to capture hurricane surge/surface waves approaching, inundating (or partially inundating), and moving/displacing spans of the ramp superstructure (see Fig. 6.14). Prior to hurricane season, identify the two select locations for mounting of the VSE and construct a pole/shelf/bracket for later mounting the VSE's. Later, when the NWS declares that there is a high probability of a significant size hurricane (Category 3, 4, or 5) making landfall near Mobile, ALDOT personnel should contact the VSE provider (such as OxBlue ARM Systems) to come and install two of their wireless construction webcams (see Appendix A) at the two prepared stations. This contact should be made several days prior to the hurricane making landfall. The webcam system provides high resolution images taken every 1 or 2 minutes from the site, and these are uploaded onto an OxBlue server that can be accessed by personnel for review. The OxBlue Construction Webcam System includes all hardware, software, and services.

The webcam system images can provide design information related to,

- the hurricane surge/surface wave forces (magnitudes and locations)

- the rate of surge wave height build-up

- the significant wave height of surface waves

- the wavelength of significant surface waves relative to that of the bridge superstructure width
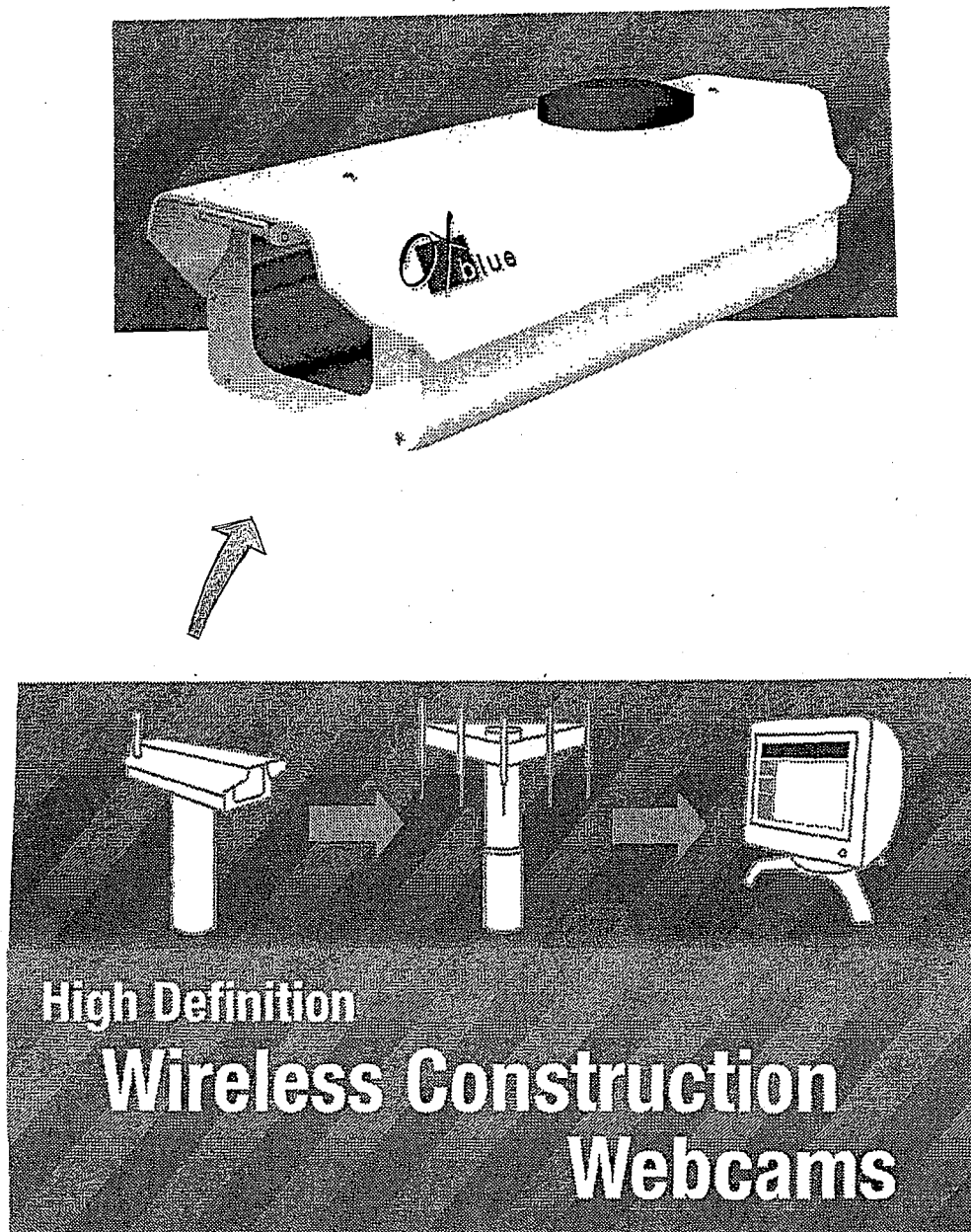
Fig. 6.14 Video Surveillance Webcam and Equipment (VSE)

- the feasibility of venting or partially venting the underside of the bridge superstructure

- the wave height relative to that of the bridge superstructure when the superstructure begins to move/displace

- the wave height (relative to the span height) when spans actually fail or are lifted/pushed from their support bents

- the time and wave height sequence of failure of bridge ramp spans

The above information can, in turn, be used to better design a retrofit underside venting system and a superstructure tie-down (to substructure) system to help prevent the loss/significant damage to coastal bridges in future hurricanes.

The wireless construction webcams should be removed from their bridge site stations after the hurricane and stored for the next major hurricane event. After recording the landfalling of several major hurricanes at the site, ALDOT may choose to dispense with such recordings for future hurricanes.

6.5 Closure

As indicated in Chapter 5, based on the facts that the Mobile Bay I-10 Bridges are 43 years old, have never experienced hurricane surge/surface wave elevations to the level of the bridge superstructure, and are at a site that has never experienced water elevations to the level of the bridge superstructure, it is recommended that only minimal retrofit actions be taken at this time for these bridges. These actions include:

1. Tying adjacent spans together longitudinally to allow spans to better distribute wave loads to adjacent spans and bents. Ties should have good ductility

2. Tying spans to the bent caps and/or piles to better transmit vertical and horizontal surge/surface wave forces. Ties should be ductile.

3. Performing select superstructure coring on the south side of each bridge to allow greater venting and to reduce uplift hydrostatic/buoyant forces and possible slamming forces.

4. Making all ramp spans continuous for uplift and transverse horizontal forces, and tied together for longitudinal forces. The ties should allow for thermal expansion/contraction in the longitudinal direction, and should have good ductility.

5. Venting ramp spans (longitudinally and vertically through the deck on the south overhang and southernmost cavity) to reduce hydrostatic/buoyant forces and possible slamming forces on these spans.

6. Install two video surveillance cameras (VSEs) at two select locations on the I-10 bridge ramp to capture actual hurricane surge/surface wave sea states and the responses of I-10 spans to these sea states. Information gathered will allow the design of better future bridge retrofit systems, and better future replacement alternatives and better new coastal bridges.

7. CONLUSIONS AND RECOMMENDATIONS

7.1 General

Determining the appropriate design hurricane sea state at the I-10 bridges across the north end of Mobile Bay, and the surge/surface wave forces that this sea state would apply to the bridge superstructure and substructure was the purpose of this research. To assist in doing this, an attempt was made to locate some video footage of past hurricane surge/surface waves approaching, inundating, and displacing one or more coastal bridges. Unfortunately this attempt was in vain. Thus, the investigation was limited to a review of the literature, discussions with state DOT bridge engineers, and discussions with coastal engineering experts to determine the mode and sequence of failure of coastal bridges as hurricane surge/surface waves pass through these bridges. Using these same sources of information, a design hurricane sea state and its associated design storm surge/surface wave forces were estimated for the I-10 bridges. An analytical assessment of the adequacy of the as-is I-10 Mobile Bay bridge, as well as of an appropriately retrofitted I-10 bridge for the estimated design hurricane passing directly through the bridge was performed. Conclusions and recommendations resulting from the investigation are presented below.

7.2 Conclusions

The objectives of this research were to determine the surge/surface wave forces that large hurricanes (Categories 3-5) subject coastal bridges to as they make landfall, and more specifically what are magnitudes of these forces for the I-10 bridge at the

north end of Mobile Bay. The objective was also to determine the adequacy of the Mobile Bay I-10 bridge for these forces and to identify retrofit actions if the bridge can not sustain these forces. Based on a literature review, information on the I-10 bridge elevations and anticipated hurricane surge/surface wave elevation at the bridge site, and analytical structural analyses of the bridge super and substructures, the following conclusions have been drawn.

1. Maximum storm surge elevation and significant surface wave height along with bridge substructure and superstructure elevations/heights are critical parameters in the performance of a coastal bridge when hurricanes pass through the bridge.

2. Ocean/bay buoyant, hydrostatic, and hydrodynamic forces can all be very significant forces.

3. Slamming forces from breaking waves entrapping air against a bridge can be quite large; however these forces are so sensitive to wave direction and breaking conditions that large areas of a bridge are not subjected to these pressures/forces concurrently. A good design philosophy for these forces are to vent the bridge in the areas where waves may break against the structure and to have ductile super-to-substructure connections.

4. Because of the mitigation of slamming/impact forces with spatial distance, it is not necessary to assume transmittal of these forces to the bridge substructure.

5. Current I-10 span superstructure-to-substructure connections are not adequate to avoid catastrophic bridge failure if a large hurricane, such as Hurricane Katrina, were to follow a northerly path approximately 30 miles west of Mobile, i.e., around Pascagoula, MS. as evident from the I-10 ramp span connections shown in Figs. 2.30 and 2.31 in Chapter 2. It should be noted that a hurricane would need to be large enough for the storm surge/surface waves to significantly impinge on the bridge superstructure for the current connections not to be adequate (see Numbers 9 and 10 below).

6. The Modified Douglass et al. wave force prediction equations presented in Chapter 3 are felt to be fairly accurate in estimating hurricane induced surge/surface wave forces on coast bridge superstructures.

7. Analyses indicate that both the super and substructure of the I-10 bridge, as well as the connections between the two, are adequate for Hurricane Cases A and B, i.e., a direct hit by a Hurricane Frederic and a near miss (approximately 100 miles) by a Hurricane Katrina.

8. Analyses indicate that both the super and substructure of the I-10 bridge are adequate for Hurricane Case C, i.e., a Mock-Katrina Hurricane. However, the I-10 bridge super-to-substructure connections are not adequate for a Mock-Katrina Hurricane.

9. Considering mean sea level at the Mobile Bay I-10 bridge site to be elevation 0 ft, the bottom of the bay and pertinent bridge component elevations for the Mobile Bay I-10 bridges are approximately as follows:

    Bottom of Bay   = -5.0 ft

    Bottom of bent cap = 13.1 ft

    Top of bent cap/   = 17.1 ft
    bottom of girders

    Top of deck   = 21.4 ft

    Top of guard rail   = 24.1 ft

10. Considering mean sea level at the site as elevation 0 ft, any hurricane with a maximum storm surge greater than 17 ft would probably move the existing Mobile Bay I-10 bridge superstructure and cause significant bridge damage. Furthermore, due to a somewhat higher surge height at the bridge due to interference of the bridge with surface wave propagations, the effective surge height at the bridge may be 0.5 - 1.0 ft higher than the storm surge height. Thus, any hurricane with a maximum storm surge greater than 16 ft may move the Mobile Bay I-10 bridge superstructure and cause bridge damage.

11. The maximum storm surge elevations at the I-10 bridge during Hurricane's Frederic and Katrina did not exceed the above critical values, and these hurricanes did not damage the Mobile Bay Bridge.

12. Had Hurricane Katrina's track been located approximately 50 miles to the east, the maximum storm surge elevation at the I-10 bridge site would probably have exceeded the above critical values, and because the super-to-substructure connections are not sufficiently strong, this would have probably destroyed the Mobile Bay I-10 Bridge superstructure.

13. Using the storm surge elevations and significant wave heights estimated in Chapter 4, the Modified Douglass Equations estimated the maximum surge/surface wave forces on a typical I-10 Mobile Bay Bridge span shown below during Hurricanes Frederic, Katrina, and a Mock-Katrina.

Case A – Hurricane Frederic
F_v = 109 kips
F_h = 0.0 kips
M = 1173 kip-ft

Case B – Hurricane Katrina
F_v = 172 kips
F_h = 0.0 kips
M = 1846 kip-ft

Case C – Mock-Hurricane Katrina
F_v = 537 kips
F_h = 169 kips
M = 5769 kip-ft

14. Analyses of the response of a typical Mobile Bay I-10 bridge span super and substructure to the hurricane forces in No. 13 plus the bridge DL yielded the following results:

Hurricane Frederic:

Pile Cap Flexural Capacity –	2668 kip-ft.
Pile Flexural Capacity –	2264 kip-ft.
Maximum Flexural Demand on Pile Cap –	760 kip-ft.
Maximum Flexural Demand on Pile –	42 kip-ft.
Maximum Stress on Pile –	1161 psi (Compression) 1057 psi (Compression)
Pile Bent Poststorm Status -	Good
Superstructure Adequacy -	Good
Super-to-Substructure Connections -	Good

Hurricane Katrina:

Pile Cap Flexural Capacity –	2668 kip-ft.
Pile Flexural Capacity –	2264 kip-ft.
Maximum Flexural Demand on Pile Cap –	775 kip-ft.
Maximum Flexural Demand on Pile –	66 kip-ft.
Maximum Stress on Pile –	1126 psi (Compression) 966 psi (Compression)
Pile Bent Poststorm Status -	Good
Superstructure Adequacy -	Good
Super-to-Substructure Connections -	Good

Mock-Hurricane Katrina:

Pile Cap Flexural Capacity –	2668 kip-ft.
Pile Flexural Capacity –	2264 kip-ft.
Maximum Flexural Demand on Pile Cap –	1642 kip-ft.
Maximum Flexural Demand on Pile –	1630 kip-ft.
Maximum Stress on Pile –	2583 psi (Compression) 1405 psi (Tension)

7-6

Pile Bent Poststorm Status -   Piles crack during
                                                storm but are
                                                capable of supporting the
                                                loads and cracks are
                                                closed by prestressing
                                                forces after the storm
                                                event.

Superstructure Adequacy -   Good

Super-to-Substructure Connections -   Not adequate.
                                                Connections need
                                                to be improved.

7.3   Recommendations

As indicated in Chapter 5, based on the facts that the Mobile Bay I-10 Bridges are 43 years old, have never experienced hurricane surge/surface wave elevations to the level of the bridge superstructure, and are at a site that has never experienced water elevations to the level of the bridge superstructure, it is recommended that only minimal retrofit actions be taken at this time for these bridges. These actions include:

1. Tying adjacent spans together longitudinally to allow spans to better distribute wave loads to adjacent spans and bents. Ties should have good ductility.

2. Typing spans to the bent caps and/or piles to better transmit vertical and horizontal surge/surface wave forces. Ties should be ductile.

3. Performing select superstructure coring on the south side of each bridge to allow greater venting and reduce uplift hydrostatic/buoyant forces and possible slamming forces.

4. Making all ramp spans continuous for uplift and transverse horizontal forces and tied together for longitudinal forces. The ties should allow for thermal expansion/contraction in the longitudinal direction and should have good ductility.

5. Venting ramp spans (longitudinally and vertically through the deck on the south overhang and southernmost cavity) to reduce hydrostatic/buoyant forces and possible slamming forces on these spans.

6. See Section 6.3 in Chapter 6 for more specific details and sketches of the actions recommended in 1-5 above, and for other viable retrofit options if a more conservative retrofit program is desired.

7. When and where necessary to quantify hurricane surge/surface wave forces on a coastal deck-girder bridge, it is recommended that the Modified Douglass et al. equations, presented in No. 8 below, be used. Then, use the resulting uplift force, F_v, horizontal force, F_h, and overturning moment, M, acting on the bridge superstructure spans, design or check the adequacy of the bridge superstructure, superstructure-to-substructure connections, and substructure.

8. The Modified Douglass, et al. Equations are recommended for quantifying hurricane surge/surface wave forces on deck-girder bridge superstructures. These equations, with their parameter definitions and recommended coefficient values are shown below.

Vertical Wave Force:

$$F_v = c_v^{mc} \, F_v^*$$

where, c_v^{mc} = an empirical coefficient from McConnell's work

$$c_v^{mc} \approx 1.0$$

$$F_v^* = \gamma \, (\Delta z_v) A_v$$

where Δz_v = difference between the elevation of the crest of the maximum wave and the elevation of the bottom of the end diaphragms (to be taken as 1 ft. higher than the bottom of the girders)

or,

the difference between the elevation of the top of the solid portion of the guard rail and the bottom of the end diaphragms (to be taken as 1 ft. higher than the bottom of the girders),

whichever is smaller,

$$\eta_{max} = 0.78 H_{max} = 0.78 \times 1.4 \times H_s = 1.1 H_s$$

A_v = bridge span length x $\dfrac{\text{bridge width}}{2}$ (for widths > 20 ft)

A_v = bridge span length x bridge width (for widths $\leq$ 20 ft)

Horizontal Wave Force:

$$F_h = \left[1 + c_r \frac{(N-1)}{2}\right] c_h^{mc} F_h^*$$

where, c_r = a reduction coefficient for reduced horizontal load on half of the girders beyond the seaward girder,

$c_r \approx 0.33$,

N = the number of span girders,

c_h^{mc} = an empirical coefficient from McConnell's work,

$c_h^{mc} \approx 1.0$

$F_h^* = \gamma (\Delta z_h) A_h$

where Δz_h = the difference between the elevation of the crest of the maximum wave and the elevation of the centroid of A_h,

or,

the difference between the elevation of the top of the solid portion of the guard rail and the elevation of the centroid of A_h, whichever is smaller.

A_h = the bridge span length x the vertical projection of the superstructure from the girder bottoms up to the top of the solid portion of the guard rail

Moment from Wave:

Any contribution to moment from the horizontal wave force component is neglected and only moment from the vertical component is considered.
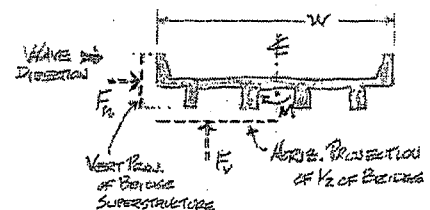
$$M = F_v \times \frac{w/2}{2}$$

$$M = F_v \times \frac{w}{4}$$

(for w > 20 ft)

$M = 0$ (for $w \leq 20$ ft)

Resultant Wave Forces:

The resultant of the above wave forces are shown on the figure at the right, where
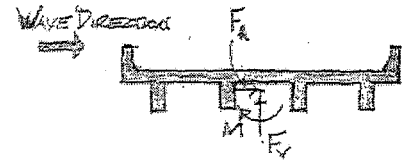
$$F_v = c_v^{mc} \times \gamma \times \Delta z_v \times A_v$$

$$F_h = \left[1 + c_r\left(\frac{N-1}{2}\right)\right] c_h^{mc} \times \gamma \times \Delta z_h \times A_h$$

$$M = F_v \times \frac{\text{Bridge Width}}{4}.$$

9. Mount video surveillance camera and equipment (VSE) at two select locations on the I-10 bridge ramp at the north end of Mobile Bay to capture hurricane surge/surface waves approaching, inundating (or partially inundating), and moving/displacing spans of the ramp superstructure. The webcam system images can provide design/retrofit information related to,

- the hurricane surge/surface wave forces (magnitudes and locations)

- the rate of surge wave height build-up

- the significant wave height of surface waves

- the wave length of significant surface waves relative to that of the bridge superstructure width

- the feasibility of venting or partially venting the underside of the bridge superstructure

- the wave height relative to that of the bridge superstructure when the superstructure begins to move/displace

7-11

- the wave height (relative to the span height) when spans actually fail or are lifted/pushed from their support bents

- the time and wave height sequence of failure of bridge ramp

The above information can in turn be used in the future to design a retrofit underside venting system and a superstructure tie-down (to substructure) system to help prevent the loss/significant damage to coastal bridges in future hurricanes. Additionally, the information can be used in making design elevation and connection decisions for any future new or replacement bridges at the north end of Mobile Bay site.

REFERENCES

1. Douglass, S.L., Chen, Q., Olsen, J.M., Edge, B.L., and Brown, D.A., "Wave Forces on Bridge Decks," <u>Draft Report</u>, U.S. Department of Transportation, Federal Highway Administration, Office of Bridge Technology, Washington, D.C., April 2006.

2. FEMA 550, "Recommended Residential Construction for the Gulf Coast," July 2006.

3. FEMA 55, "Coastal Construction Manual," Edition 3, August 2005.

4. FEMA 499, "Home Builder's Guide to Coastal Construction," August 2005.

5. McConnell, K.J., Allsop, W., Cuomo, G., and Cruikshank, I.C. (2003) New Guidance for Wave Forces on Jetties in Exposed Locations. *Proceedings of the Sixth Conference on Coastal and Port Engineering Developing Countries (COPEDEC VI)*, Colombo, Sri Lanka, 20 pp.

6. McConnell, K., Allsop, W., and Cruickshank, I. (2004) *Piers, jetties, and related structures exposed to waves: Guidelines for hydraulic loadings.* Thomas Telford Press, London. 148 pp.

7. National Weather Service (2005) Extremely Powerful Hurricane Katrina leaves a Historic Mark on the Northern Gulf Coast, report on website <u>www.srh.noaa.gov/mob</u> posted by the Mobile Forecast office, Aug. 5, 2005.

8. NIST Technical Note 1476, "Performance of Physical Structures in Hurricane Katrina and Hurricane Rita: A Reconnaissance Report," National Institute of Standards and Technology, Gaithersburg, MD, June 2006.

9. Ocean Engineering Associates (2005) Hurricane Impact Analysis and Development of Design Criteria for the I-10 Bridges over Escambia Bay Escambia County, Florida, report to Florida Department of Transportation Drainage Design Office, January, 77 pp.

10. OxBlue, <u>http://oxblue.com/product/?c=ui</u>, Accessed August 24, 2007.

11. US Army (1984) *Shore Protection Manual*, Coastal Engineering Research Center, US Army Engineers Waterways Experiment Station, 2 volumes, US Government Printing Office.

12. US Army Engineer District, Mobile (1981) Hurricane Frederic Post Disaster Report: 30 August - 14 September 1979, February 1981.

13. Horikawa, Kiyoshi, (1927, 1978), *Coastal Engineering - An Introduction to Ocean Engineering*, John Wiley & Sons, New York, 402 pp.

14. Modjeski and Masters, Inc., (2007), "Development of Guide Specifications for Bridges Vulnerable to Coastal Storms and Handbook of Retrofit Options for Bridges Vulnerable to Coastal Storms", Transportation Pooled Fund Program - Federal Highway Administration Contract No. DTFH61-06-T-70006.

15. Tedesco, J.W., McDougal, W.G., and Ross, C.A. (1999), *Structural Dynamics Theory and Applications*, Addison-Wesley, Menlo Park, California.

Appendix A

Entrapped Air Venting Equations and Calculations

Analysis Assumptions:
T = 80°F
ρ = 0.00228 slugs/ft^3
γ = 0.0735 lb/ft^3
V_s = 1139 ft/sec (speed of sound)
p_{atm} = 2117 lb/ft^2 = 14.7 psi
v = 1.69x10^{-4} ft^2/sec = kinematic viscosity of air

So long as the air flow velocity, V, does not exceed ~0.3 V_s , Bernoulli's equation can be applied under the assumption of steady state incompressible flow.

$$p_o = p_{atm} + \frac{\rho V_j^2}{2}$$

$$\Delta p = p_o - p_{atm}$$

$$V_j = \sqrt{\frac{2\Delta p}{\rho}}$$

Then defining the area contraction coefficient $A_j = C_c A$ (where A = $\pi D^2/4$ and $A_j = \pi D_j^{\,2}/4$), the average velocity through the orifice is

Fig. A1. Contracted Air Jet

$$V = C_c\sqrt{\frac{2\Delta p}{\rho}}$$

and the volumetric flow rate is

$$Q = \frac{\pi D^2}{4} C_c \sqrt{\frac{2\Delta p}{\rho}} \ .$$

For an example calculation, using C_c = 0.72 which is experimentally determined for the orifice geometry defined in Fig. A1,

D = 3 in = ¼ ft
Δp = $^1/_{10}\, p_{atm}$ = 211.7 lb/ft^2 = 1.47 psi

then

$$V = C_c\sqrt{\frac{2\Delta p}{\rho}}$$

$V = 310$ ft/sec

and

$Q = 15.2$ ft^3/sec = volumetric flow rate through a single vent.

This value for the velocity is at approximately the upper limit necessary for the incompressible flow assumption and gives a relatively large Reynolds number, Re = $VD/\nu = 4.59 \times 10^5$.

Now consider $V = L\,W\,d$ = volume of air to be vented. If all of this V is to be vented in the time required for the wave to traverse the width, W, then the time required for venting is

$$t = \frac{W}{c}$$

where c = 25 ft/sec = the approximate wave propagation velocity.

The average rate of the vented volume is then V/t.

For the volume shown in Fig. A2,
$$V/t = L\,W\,d\,/t$$
$$= 3,900 \text{ ft}^3/\text{sec.}$$
$$= \text{Average venting rate}$$

$V = L W d = 1248$ ft^3
$t = W/c = 0.32$ sec
V / t = venting rate
$= 3,900$ ft^3/sec
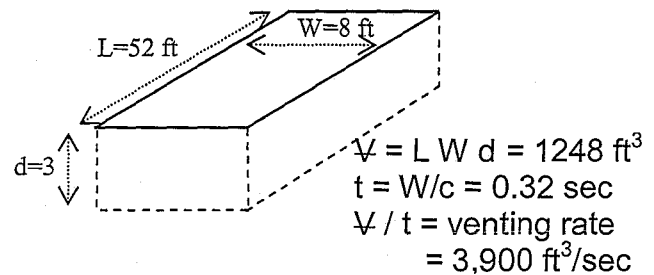
Fig. A2. Volume to be Vented, V

Then if N = the number of vents then $NQ = V / t$. For an example with D = 3 in = ¼ ft and
$Q = 15.2$ ft^3/sec , N = 256 is the number of 3" vents required.

The number of vents for fixed volumes to be vented, V, of 1248 ft^3 and 624 ft^3 and a range of values for $\Delta p = p_{atm}/50$ to $\Delta p = p_{atm}/10$ are shown plotted in Figs. A3 and A4 respectively. If one assumes the full cell cavity shown in Fig. A2 needs to be vented then the curves of Fig. A3 are applicable. However, if one assumes that half of the cavity air gets vented under the adjacent girders and end diaphragms as the water surface rises, or if we assume we can accept partial (half) venting, then the curves of Fig. A4 would be applicable.

A-2
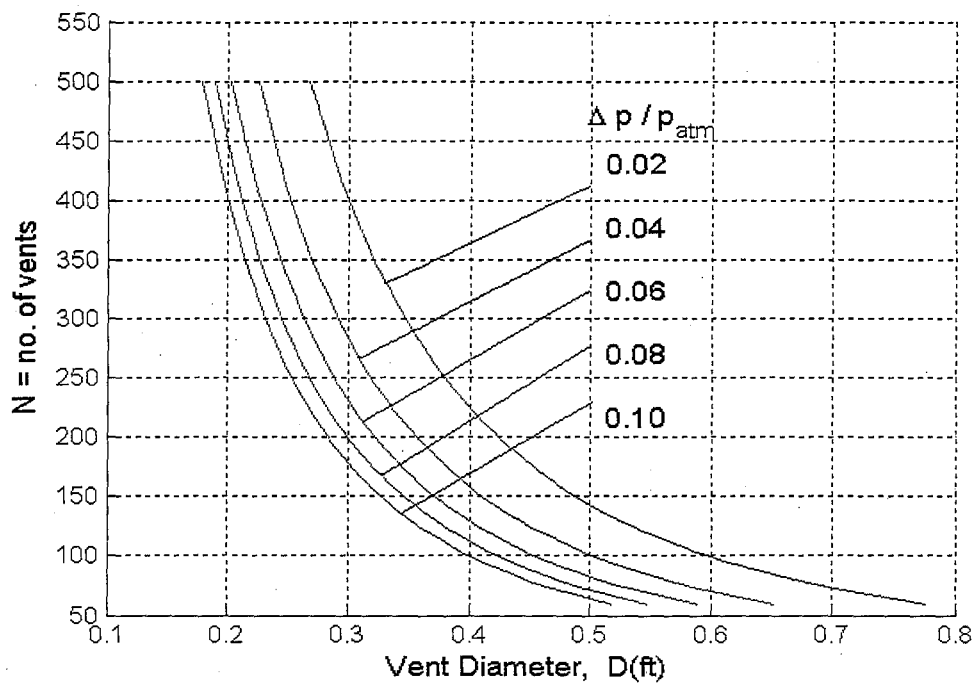
Fig. A3. $\forall$ = 1248 ft^3 and $\forall$ / t = 3900 ft^3/sec
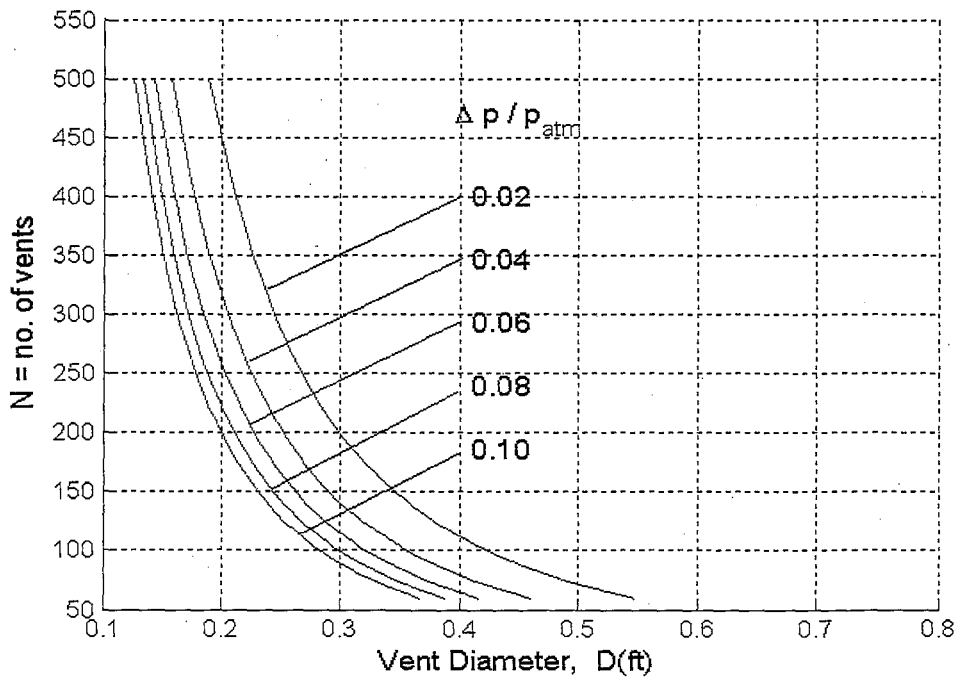
Fig. A4. $\forall$ = 624 ft^3 and $\forall$ / t = 1950 ft^3/sec

Appendix B

OxBlue Construction Webcams

OxBlue Construction Webcams (see Ref. 10) can provide video documentation of hurricane surge/surface waves approaching, inundating (or partially inundating), and displacing coastal bridge superstructures. OxBlue Construction Webcams offer standardized turnkey systems that include all hardware/software/services that can provide high resolution images taken every 2, 5, 10, 20, 30 (or whatever) minutes from a coastal bridge site which are uploaded onto an OxBlue server which can be accessed by personnel for review. This would allow ALDOT to visually observe the performance of one of its coatal bridges as a hurricane approached and moved through the bridge.

Table B1 below provides a pricing summary of multiple configurations of the Integrated OxBlue systems available.

Table B1. Pricing Summary for Integrated OxBlue System (Hardware and Recurring Monthly Service Fee)

Integrated OxBlue System	1 Unit Price	2 to 5 Unit Price	6 to 10 Unit Price
3 Megapixel Hardware Service	$3,850 system $495/month	$3,650 system $475/month	$3,465 system $445/month
6 Megapixel Hardware Service	$4,750 system $650/month	$4,500 system $615/month	$4,250 system $585/month
OxBlue Pro®	$95/month	$70/month	$40/month

OxBlue construction webcams provide two versions of the user interface: (1) OxBlue Standard, and (2) OxBlue Pro. OxBlue Standard is the interface that can be used for "general monitoring and light project management" (OxBlue, 2007). OxBlue Pro provides a more comprehensive interface allowing for in depth analyses for "intensive project management controls, productivity improvements, claims/dispute resolution, and warranty management" (OxBlue, 2007). Table B2 below provides a summary of key features each version of the software contains.

Table B2. Feature Comparison of OxBlue User Interface Versions

Features	OxBlue Standard	OxBlue Pro
Calendar Based Navigation	●	●
Image Select by Time of Day	●	●
Zoom In/Out	●	●
Image Emailing	●	●
Visual Calendar	●	●
Time-Lapse Playback	●	●
Interactive Slideshow Mode	●	●
Project Dashboard for Viewing All Projects from One Location	●	●
Image Overlay Mode		●
Split Screen Mode		●
Quad View by Day, Week, or Month for Detailed Project Analysis		●

High Definition
Wireless Construction Webcams
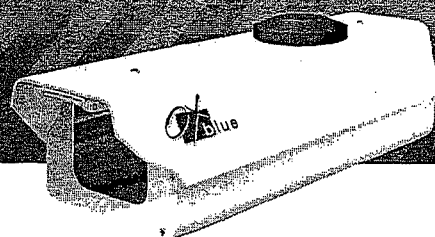
OxBlue ARM Systems are powerful, highly reliable systems tested, optimized and built to run 24/7, indoors or outdoors, in the harshest conditions. The ARM System is a turnkey solution that runs on the OxBlue network independently of any additional hardware or software.

OXBLUE ARM SYSTEM

Camera Resolution	2048 x 1536 (3 megapixel) 2816 x 2112 (6 megapixel)	Surge Supression	140v RMS clamping/ 600 joules/ 48,000 amps
			0.0 ns surge response time w/ continuous power
Memory	Unlimited Remote Storage		
Data Connection	Wireless (Cellular GPRS) Ethernet (Cat5 Network Cable) Dialup (RJ11 Analog Phone Line)	Operating Environment	-10 to 120 degrees F -23 to 49 degrees C
		Focus System	Dual autofocus; contrast and phase difference detection systems
Power Connection	120 / 240 VAC, 75 watts max		
Controller	Proprietary OxBlue System Embedded Industrial Computer	White Balance System	iESP2 Auto
		Meter Modes	Digital ESP, spot, and center-weighted metering systems
Dimensions	21" L (53.34 cm) 5.5" W (13.97 cm) 4.25" H (10.795 cm)	Optics	Aspherical glass 4x zoom lens 6.3 mm - 63 mm (38 - 380 mm equivalent in 35mm photography) 0.66x wide angle lens, standard option
Weight	17.5 lb (4.42 kg) installed		
Construction	Die-cast aluminum - extruded and sheet; gray polyester powder coat	Field of View	78 degrees standard remotely adjustable
Mounting	Fixed to pole or wall Hardware included		

SPECIFICATIONS SUBJECT TO CHANGE

Have A Question?

TOLL FREE:	ON THE WEB:	EMAIL:
888-849-BLUE	www.oxblue.com	info@oxblue.com

High Definition
Wireless Construction Webcams

The OxBlue solution is a standardized turnkey offering that includes all hardware, software and services. Pricing is simple and all-inclusive. Monthly service may be suspended or discontinued at any time.
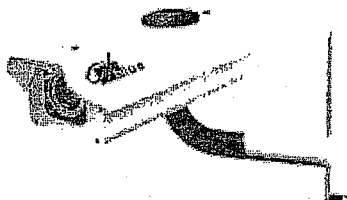
Hardware

✓ High definition camera
✓ Cellular transmission hardware
✓ Embedded controller
✓ OxBlue system software
✓ Weatherproof outdoor enclosure
✓ Auto-sensing heater and blower
✓ Mounting equipment
✓ Free installation support
✓ Lifetime warranty
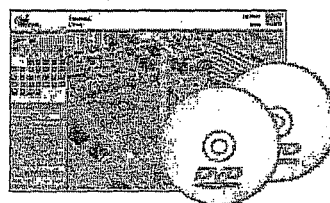
Monthly Service

✓ Secure, <u>unlimited</u> image storage
✓ OxBlue image viewing software
✓ Cellular jobsite transmission service
✓ Image quality optimization technology
✓ Backup and archive services
✓ Proactive connection monitoring
✓ Hosted project web page
✓ 24 x 7 x 365 live tech support
✓ Rock solid reliability

Pricing for the Integrated OxBlue System consists of:
One time, all-inclusive hardware cost + Recurring monthly service fee

	1 UNIT PURCHASE	2-5 UNIT PURCHASE	6-10 UNIT PURCHASE
3 Megapixel Hardware Service	$3,850 system $495/month	$3,650 system $475/month	$3,465 system $445/month
6 Megapixel Hardware Service	$4,750 system $650/month	$4,500 system $615/month	$4,250 system $585/month
OxBlue Pro°	$95/month	$70/month	$40/month

OxBlue Pro° includes enhanced features and services. Ask for details.
Enterprise pricing available for larger purchases.
Dial-up and Ethernet systems also available.

VISA MasterCard AMERICAN EXPRESS

Have A Question?

PHONE: 888-849-2583
ON THE WEB: www.oxblue.com
EMAIL: contact@oxblue.com

Appendix C

Hurricanes Having Largest Storm Surge at Mobile Bay I-10 Bridge During Past 60-Years

Name	Year	Category	Landfall Location	Maximum Storm Surge* (ft)
Katrina	2005	5→ 3	East New Orleans, LA	12.4
Frederic	1979	3	Dauphin Island/AL-MS Border	11.7
Georges	1998	3	Biloxi, MS	9.4
Camille	1969	5	Bay St. Louis, MS	7.4
Ivan	2004	3	Gulf Shores, AL	4.9

*Near I-10 tunnel/bridge

Appendix D

Bridge Pile Bent Modelling and Analysis Via RISA 2-D Analysis for 23' and 28' Bent Heights for Hurricane Frederic, Katrina and Mock-Katrina Loadings

Triple Sawyer	Frederic 23' Piles	January 29, 2008
		8:00 PM
		RISA Frederic 23' Piles.r2e

Global

Display Sections for Member Calcs	5

Joint Coordinates

Joint Label	X Coordinate (ft)	Y Coordinate (ft)
N1	8	0
N2	32	0
N3	0	23
N4	8	23
N5	32	23
N6	40	23

Boundary Conditions

Joint Label	X Translation (k/in)	Y Translation (k/in)	Rotation (k-ft/rad)
N1	Reaction	Reaction	Reaction
N2	Reaction	Reaction	Reaction

Member Data

Member Label	I Joint	J Joint	Area in^2	Moment of Inertia in^4	Elastic Modulus ksi	End Releases I-End	End Releases J-End	Length ft
PILE1	N4	N1	904.78	264648	4030			23
PILE2	N5	N2	904.78	264648	4030			23
BENTCAP1	N3	N4	2592	138263	4030			8
BENTCAP2	N4	N5	2592	138263	4030			24
BENTCAP3	N5	N6	2592	138263	4030			8

Member Point Loads

Member Label	I Joint	J Joint	Direction	Magnitude (k, k-ft)	Location (ft or %)
BENTCAP1	N3	N4	Y	-134	2
BENTCAP2	N4	N5	Y	-121	3
BENTCAP2	N4	N5	Y	-108	12
BENTCAP2	N4	N5	Y	-95	21
BENTCAP3	N5	N6	Y	-82	6

Member Distributed Loads

Member Label	Direction	Start Magnitude (k/ft, F)	End Magnitude (k/ft, F)	Start Location (ft or %)	End Location (ft or %)
BENTCAP1	Y	-2.7	-2.7	0	0
BENTCAP2	Y	-2.7	-2.7	0	0
BENTCAP3	Y	-2.7	-2.7	0	0

Joint Displacements

Joint Label	X Translation (in)	Y Translation (in)	Rotation (radians)
N1	0	0	0
N2	0	0	0
N3	-.016	-.088	8.003e-4
N4	-.016	-.028	1.174e-4
N5	-.016	-.021	1.208e-4
N6	-.016	-.041	-3.202e-4

D-2

Reactions

Joint Label	X Force (k)	Y Force (k)	Moment (k-ft)
N1	.14	369.554	-39.425
N2	-.14	278.446	-37.282
Totals:	0	648	

Member Section Forces

Member Label	Section	Axial (k)	Shear (k)	Moment (k-ft)
PILE1	1	369.554	-.14	-36.197
	2	369.554	-.14	-37.004
	3	369.554	-.14	-37.811
	4	369.554	-.14	-38.618
	5	369.554	-.14	-39.425
PILE2	1	278.446	.14	-40.511
	2	278.446	.14	-39.704
	3	278.446	.14	-38.896
	4	278.446	.14	-38.089
	5	278.446	.14	-37.282
BENTCAP1	1	0	0	0
	2	0	-139.4	-5.4
	3	0	-144.8	-289.6
	4	0	-150.2	-584.6
	5	0	-155.6	-890.4
BENTCAP2	1	.14	213.954	-854.203
	2	.14	76.754	17.92
	3	.14	-47.446	429.843
	4	.14	-63.646	96.566
	5	.14	-174.646	-616.911
BENTCAP3	1	0	103.6	-578.4
	2	0	98.2	-376.6
	3	0	92.8	-185.6
	4	0	5.4	-5.4
	5	0	0	0

D-3
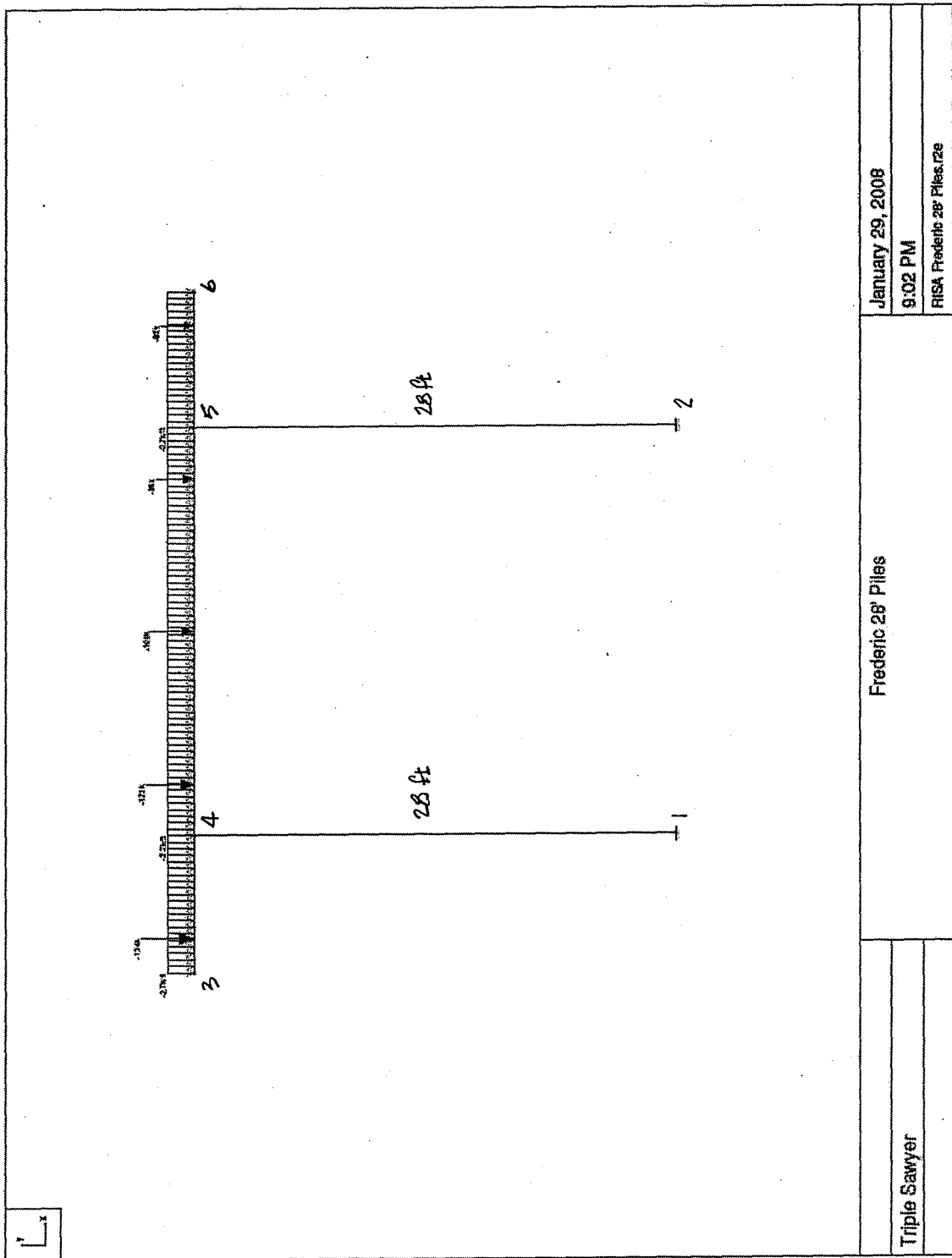
Triple Sawyer

Frederic 28' Piles

January 29, 2008
9:02 PM
RISA Frederic 28' Piles.r2e

D-4

Global

Display Sections for Member Calcs	5

Joint Coordinates

Joint Label	X Coordinate (ft)	Y Coordinate (ft)
N1	8	0
N2	32	0
N3	0	28
N4	8	28
N5	32	28
N6	40	28

Boundary Conditions

Joint Label	X Translation (k/in)	Y Translation (k/in)	Rotation (k-ft/rad)
N1	Reaction	Reaction	Reaction
N2	Reaction	Reaction	Reaction

Member Data

Member Label	I Joint	J Joint	Area in^2	Moment of Inertia in^4	Elastic Modulus ksi	End Releases I-End	End Releases J-End	Length ft
PILE1	N4	N1	904.78	264648	4030			28
PILE2	N5	N2	904.78	264648	4030			28
BENTCAP1	N3	N4	2592	138263	4030			8
BENTCAP2	N4	N5	2592	138263	4030			24
BENTCAP3	N5	N6	2592	138263	4030			8

Member Point Loads

Member Label	I Joint	J Joint	Direction	Magnitude (k, k-ft)	Location (ft or %)
BENTCAP1	N3	N4	Y	-134	2
BENTCAP2	N4	N5	Y	-121	3
BENTCAP2	N4	N5	Y	-108	12
BENTCAP2	N4	N5	Y	-95	21
BENTCAP3	N5	N6	Y	-82	6

Member Distributed Loads

Member Label	Direction	Start Magnitude (k/ft, F)	End Magnitude (k/ft, F)	Start Location (ft or %)	End Location (ft or %)
BENTCAP1	Y	-2.7	-2.7	0	0
BENTCAP2	Y	-2.7	-2.7	0	0
BENTCAP3	Y	-2.7	-2.7	0	0

Joint Displacements

Joint Label	X Translation (in)	Y Translation (in)	Rotation (radians)
N1	0	0	0
N2	0	0	0
N3	-.022	-.095	8.099e-4
N4	-.022	-.034	1.27e-4
N5	-.022	-.026	1.309e-4
N6	-.022	-.045	-3.101e-4

Reactions

Joint Label	X Force (k)	Y Force (k)	Moment (k-ft)
N1	.111	369.908	-35.134
N2	-.111	278.092	33.074
Totals:	0	648	

Member Section Forces

Member Label	Section	Axial (k)	Shear (k)	Moment (k-ft)
PILE1	1	369.908	-.111	-32.036
	2	369.908	.111	-32.811
	3	369.908	-.111	-33.585
	4	369.908	.111	-34.36
	5	369.908	-.111	-35.134
PILE2	1	278.092	.111	-36.172
	2	278.092	.111	-35.397
	3	278.092	.111	-34.623
	4	278.092	.111	-33.848
	5	278.092	.111	-33.074
BENTCAP1	1	0	0	0
	2	0	-139.4	54
	3	0	-144.8	-289.6
	4	0	-150.2	-584.6
	5	0	-155.6	-890.4
BENTCAP2	1	.111	214.308	858.364
	2	.111	77.108	15.884
	3	.111	-47.092	429.932
	4	.111	-63.292	98.78
	5	.111	-174.492	-614.572
BENTCAP3	1	0	103.6	-578.4
	2	0	98.2	-376.6
	3	0	92.8	-185.6
	4	0	54	-54
	5	0	0	0

D-6

Katrina 23' Piles

Triple Sawyer

January 29, 2008

9:06 PM

RISA Katrina 23' Piles.r2e

Global

| Display Sections for Member Calcs | 5 |

Joint Coordinates

Joint Label	X Coordinate (ft)	Y Coordinate (ft)
N1	8	0
N2	32	0
N3	0	23
N4	8	23
N5	32	23
N6	40	23

Boundary Conditions

Joint Label	X Translation (k/in)	Y Translation (k/in)	Rotation (k-ft/rad)
N1	Reaction	Reaction	Reaction
N2	Reaction	Reaction	Reaction

Member Data

Member Label	I Joint	J Joint	Area in^2	Moment of Inertia in^4	Elastic Modulus ksi	End Releases I-End	End Releases J-End	Length ft
PILE1	N4	N1	904.78	264648	4030			23
PILE2	N5	N2	904.78	264648	4030			23
BENTCAP1	N3	N4	2592	138263	4030			8
BENTCAP2	N4	N5	2592	138263	4030			24
BENTCAP3	N5	N6	2592	138263	4030			8

Member Point Loads

Member Label	I Joint	J Joint	Direction	Magnitude (k, k-ft)	Location (ft or %)
BENTCAP1	N3	N4	Y	-149	2
BENTCAP2	N4	N5	Y	-128.5	3
BENTCAP2	N4	N5	Y	-108	12
BENTCAP2	N4	N5	Y	-87.5	21
BENTCAP3	N5	N6	Y	-67	6

Member Distributed Loads

Member Label	Direction	Start Magnitude (k/ft, F)	End Magnitude (k/ft, F)	Start Location (ft or %)	End Location (ft or %)
BENTCAP1	Y	-2.7	-2.7	0	0
BENTCAP2	Y	-2.7	-2.7	0	0
BENTCAP3	Y	-2.7	-2.7	0	0

Joint Displacements

Joint Label	X Translation (in)	Y Translation (in)	Rotation (radians)
N1	0	0	0
N2	0	0	0
N3	-.026	-.102	9.388e-4
N4	-.026	-.05	1.861e-4
N5	-.026	-.019	1.895e-4
N6	-.026	-.028	1.817e-4

D-8

Reactions

Joint Label	X Force (k)	Y Force (k)	Moment (k-ft)
N1	.14	395.835	-61.553
N2	-.14	252.165	59.41
Totals:	0	648	

Member Section Forces

Member Label	Section	Axial (k)	Shear (k)	Moment (k-ft)
PILE1	1	395.835	-.14	-58.324
	2	395.835	-.14	-59.131
	3	395.835	-.14	-59.939
	4	395.835	-.14	-60.746
	5	395.835	-.14	-61.553
PILE2	1	252.165	.14	-62.638
	2	252.165	.14	-61.831
	3	252.165	.14	-61.024
	4	252.165	.14	-60.217
	5	252.165	.14	-59.41
BENTCAP1	1	0	0	0
	2	0	-154.4	-5.4
	3	0	-159.8	-319.6
	4	0	-165.2	-644.6
	5	0	-170.6	-980.4
BENTCAP2	1	.14	225.235	-922.076
	2	.14	80.535	-4.766
	3	.14	-43.665	429.843
	4	.14	-59.865	119.253
	5	.14	-163.565	-551.038
BENTCAP3	1	0	88.6	-488.4
	2	0	83.2	-316.6
	3	0	77.8	-155.6
	4	0	5.4	-5.4
	5	0	0	0

Triple Sawyer

Katrina 28' Piles

January 29, 2008

9:06 PM

RISA Katrina 28' Piles.r2e

Global

Display Sections for Member Calcs	5

Joint Coordinates

Joint Label	X Coordinate (ft)	Y Coordinate (ft)
N1	8	0
N2	32	0
N3	0	28
N4	8	28
N5	32	28
N6	40	28

Boundary Conditions

Joint Label	X Translation (k/in)	Y Translation (k/in)	Rotation (k-ft/rad)
N1	Reaction	Reaction	Reaction
N2	Reaction	Reaction	Reaction

Member Data

Member Label	I Joint	J Joint	Area in^2	Moment of Inertia in^4	Elastic Modulus ksi	End Releases I-End	J-End	Length ft
PILE1	N4	N1	904.78	264648	4030			28
PILE2	N5	N2	904.78	264648	4030			28
BENTCAP1	N3	N4	2592	138263	4030			8
BENTCAP2	N4	N5	2592	138263	4030			24
BENTCAP3	N5	N6	2592	138263	4030			8

Member Point Loads

Member Label	I Joint	J Joint	Direction	Magnitude (k, k-ft)	Location (ft or %)
BENTCAP1	N3	N4	Y	-149	2
BENTCAP2	N4	N5	Y	-126.5	3
BENTCAP2	N4	N5	Y	-108	12
BENTCAP2	N4	N5	Y	-87.5	21
BENTCAP3	N5	N6	Y	-67	6

Member Distributed Loads

Member Label	Direction	Start Magnitude (k/ft, F)	End Magnitude (k/ft, F)	Start Location (ft or %)	End Location (ft or %)
BENTCAP1	Y	-2.7	-2.7	0	0
BENTCAP2	Y	-2.7	-2.7	0	0
BENTCAP3	Y	-2.7	-2.7	0	0

Joint Displacements

Joint Label	X Translation (in)	Y Translation (in)	Rotation (radians)
N1	0	0	0
N2	0	0	0
N3	-.034	-.11	9.54e-4
N4	-.034	-.037	2.014e-4
N5	-.034	-.023	2.053e-4
N6	-.034	.03	-1.659e-4

Reactions

Joint Label	X Force (k)	Y Force (k)	Moment (k-ft)
N1	.111	396.393	-54.81
N2	.111	251.607	-52.749
Totals:	0	648	

Member Section Forces

Member Label	Section	Axial (k)	Shear (k)	Moment (k-ft)
PILE1	1	396.393	-.111	-51.712
	2	396.393	-.111	-52.486
	3	396.393	-.111	-53.261
	4	396.393	-.111	-54.035
	5	396.393	-.111	-54.81
PILE2	1	251.607	.111	-55.847
	2	251.607	.111	-55.073
	3	251.607	.111	-54.298
	4	251.607	.111	-53.524
	5	251.607	.111	-52.749
BENTCAP1	1	0	0	0
	2	0	-154.4	-5.4
	3	0	-159.8	-319.6
	4	0	-165.2	-644.6
	5	0	-170.6	-980.4
BENTCAP2	1	.111	225.793	-928.688
	2	.111	81.093	-8.028
	3	.111	43.107	429.932
	4	.111	-59.307	122.693
	5	.111	-163.007	544.247
BENTCAP3	1	0	88.6	-488.4
	2	0	83.2	-316.6
	3	0	77.8	-155.6
	4	0	5.4	-5.4
	5	0	0	0

3   4   5   6

23 ft   23 ft

1   2

	Mock-Katrina 23' Piles	January 29, 2008
Triple Sawyer		9:09 PM
		RISA Mock-Katrina 23' Piles.r2e

Global

Display Sections for Member Calcs	5

Joint Coordinates

Joint Label	X Coordinate (ft)	Y Coordinate (ft)
N1	8	0
N2	32	0
N3	0	23
N4	8	23
N5	32	23
N6	40	23

Boundary Conditions

Joint Label	X Translation (k/in)	Y Translation (k/in)	Rotation (k-ft/rad)
N1	Reaction	Reaction	Reaction
N2	Reaction	Reaction	Reaction

Member Data

Member Label	I Joint	J Joint	Area in^2	Moment of Inertia in^4	Elastic Modulus ksi	End Releases I-End	End Releases J-End	Length ft
PILE1	N4	N1	904.78	264648	4030			23
PILE2	N5	N2	904.78	264648	4030			23
BENTCAP1	N3	N4	2592	138263	4030			8
BENTCAP2	N4	N5	2592	138263	4030			24
BENTCAP3	N5	N6	2592	138263	4030			8

Joint Loads/Enforced Displacements

Joint Label	[L]oad or [D]isplacement	Direction	Magnitude (k, k-ft, in, rad)
N6	L	X	-169.2

Member Point Loads

Member Label	I Joint	J Joint	Direction	Magnitude (k, k-ft)	Location (ft or %)
BENTCAP1	N3	N4	Y	-236	2
BENTCAP2	N4	N5	Y	-172	3
BENTCAP2	N4	N5	Y	-108	12
BENTCAP2	N4	N5	Y	-44	21
BENTCAP3	N5	N6	Y	20	6

Member Distributed Loads

Member Label	Direction	Start Magnitude (k/ft, F)	End Magnitude (k/ft, F)	Start Location (ft or %)	End Location (ft or %)
BENTCAP1	Y	-2.7	-2.7	0	0
BENTCAP2	Y	-2.7	-2.7	0	0
BENTCAP3	Y	-2.7	-2.7	0	0

Joint Displacements

Joint Label	X Translation (in)	Y Translation (in)	Rotation (radians)
N1	0	0	0
N2	0	0	0
N3	-.326	-.26	2.515e-3
N4	-.326	-.046	1.358e-3
N5	-.326	-.003	1.371e-3

D-14

Joint Displacements

Joint Label	X Translation (in)	Y Translation (in)	Rotation (radians)
N6	-.33	.131	1.405e-3

Reactions

Joint Label	X Force (k)	Y Force (k)	Moment (k-ft)
N1	84.457	608.455	-1408.531
N2	84.743	39.545	-1416.154
Totals:	169.2	648	

Member Section Forces

Member Label	Section	Axial (k)	Shear (k)	Moment (k-ft)
PILE1	1	608.455	-84.457	533.985
	2	608.455	-84.457	48.356
	3	608.455	-84.457	-437.273
	4	608.455	-84.457	-922.902
	5	608.455	-84.457	-1408.531
PILE2	1	39.545	-84.743	532.93
	2	39.545	-84.743	45.659
	3	39.545	-84.743	-441.612
	4	39.545	-84.743	-928.883
	5	39.545	-84.743	-1416.154
BENTCAP1	1	0	0	0
	2	0	-241.4	-5.4
	3	0	-246.8	-493.6
	4	0	-252.2	-992.6
	5	0	-257.6	-1502.4
BENTCAP2	1	84.457	350.855	-2036.385
	2	84.457	162.655	-495.856
	3	84.457	38.455	431.472
	4	84.457	22.255	613.601
	5	84.457	-37.945	566.53
BENTCAP3	1	169.2	1.6	33.6
	2	169.2	-3.8	31.4
	3	169.2	-9.2	18.4
	4	169.2	5.4	-5.4
	5	169.2	0	0

D-15

Triple Sawyer

January 29, 2008

9:11 PM

RISA Mock-Katrina 28' Piles.r2e

Global

Display Sections for Member Calcs	5

Joint Coordinates

Joint Label	X Coordinate (ft)	Y Coordinate (ft)
N1	8	0
N2	32	0
N3	0	28
N4	8	28
N5	32	28
N6	40	28

Boundary Conditions

Joint Label	X Translation (k/in)	Y Translation (k/in)	Rotation (k-ft/rad)
N1	Reaction	Reaction	Reaction
N2	Reaction	Reaction	Reaction

Member Data

Member Label	I Joint	J Joint	Area in^2	Moment of Inertia in^4	Elastic Modulus ksi	End Releases I-End	End Releases J-End	Length ft
PILE1	N4	N1	904.78	264648	4030			28
PILE2	N5	N2	904.78	264648	4030			28
BENTCAP1	N3	N4	2592	138263	4030			8
BENTCAP2	N4	N5	2592	138263	4030			24
BENTCAP3	N5	N6	2592	138263	4030			8

Joint Loads/Enforced Displacements

Joint Label	[L]oad or [D]isplacement	Direction	Magnitude (k, k-ft, in, rad)
N6	L	X	-169.2

Member Point Loads

Member Label	I Joint	J Joint	Direction	Magnitude (k, k-ft)	Location (ft or %)
BENTCAP1	N3	N4	Y	-236	2
BENTCAP2	N4	N5	Y	-172	3
BENTCAP2	N4	N5	Y	-108	12
BENTCAP2	N4	N5	Y	-44	21
BENTCAP3	N5	N6	Y	20	6

Member Distributed Loads

Member Label	Direction	Start Magnitude (k/ft, F)	End Magnitude (k/ft, F)	Start Location (ft or %)	End Location (ft or %)
BENTCAP1	Y	-2.7	-2.7	0	0
BENTCAP2	Y	-2.7	-2.7	0	0
BENTCAP3	Y	-2.7	-2.7	0	0

Joint Displacements

Joint Label	X Translation (in)	Y Translation (in)	Rotation (radians)
N1	0	0	0
N2	0	0	0
N3	-.524	-.297	2.786e-3
N4	-.524	-.058	1.629e-3
N5	-.527	-.002	1.641e-3

Joint Displacements

Joint Label	X Translation (in)	Y Translation (in)	Rotation (radians)
N6	-.528	.158	1.674e-3

Reactions

Joint Label	X Force (k)	Y Force (k)	Moment (k-ft)
N1	84.544	626.666	-1614.448
N2	84.656	21.334	-1619.169
Totals:	169.2	648	

Member Section Forces

Member Label	Section	Axial (k)	Shear (k)	Moment (k-ft)
PILE1	1	626.666	-84.544	752.775
	2	626.666	-84.544	160.97
	3	626.666	-84.544	-430.836
	4	626.666	-84.544	-1022.642
	5	626.666	-84.544	-1614.448
PILE2	1	21.334	-84.656	751.208
	2	21.334	-84.656	158.614
	3	21.334	-84.656	-433.98
	4	21.334	-84.656	-1026.575
	5	21.334	-84.656	-1619.169
BENTCAP1	1	0	0	0
	2	0	-241.4	-5.4
	3	0	-246.8	-493.6
	4	0	-252.2	-992.6
	5	0	-257.6	-1502.4
BENTCAP2	1	84.544	369.066	-2255.175
	2	84.544	180.866	-605.379
	3	84.544	56.666	431.217
	4	84.544	40.466	722.612
	5	84.544	-19.734	764.808
BENTCAP3	1	169.2	1.6	33.6
	2	169.2	-3.8	31.4
	3	169.2	-9.2	18.4
	4	169.2	5.4	-5.4
	5	169.2	0	0

D-18